

UNIVERSITY OF  
BIRMINGHAM



**ERODIBILITY OF SOILS IN RURAL ROADS**

By

**Esdras Ngezahayo**

A thesis submitted to The University of Birmingham for the award of a degree of  
**DOCTOR OF PHILOSOPHY**

Department of Civil Engineering  
School of Engineering  
College of Engineering and Physical Sciences  
The University of Birmingham  
Edgbaston, Birmingham, B15 2TT  
United Kingdom

June 2020

UNIVERSITY OF  
BIRMINGHAM

**University of Birmingham Research Archive**

**e-theses repository**

This unpublished thesis/dissertation is copyright of the author and/or third parties. The intellectual property rights of the author or third parties in respect of this work are as defined by The Copyright Designs and Patents Act 1988 or as modified by any successor legislation.

Any use made of information contained in this thesis/dissertation must be in accordance with that legislation and must be properly acknowledged. Further distribution or reproduction in any format is prohibited without the permission of the copyright holder.

## Abstract

Rainfall is a significant factor in the erosion of unpaved roads. If inappropriate soils are used for construction, even a short rainfall duration can render poor conditions on unpaved roads. Rainfall has a twofold effect on the surface. The impact of raindrops can result in the dislodgement of soil particles; while subsequent water flow transports the loosened soils. A laboratory investigation was undertaken to study erodibility of granular and clayey soils that may be used for the construction of unpaved roads. The study aimed at identifying the suitability of soils that can be used for the construction of erosion resistant unpaved roads. Those roads are indispensable for sustainable growth of rural areas in developing countries. Compacted samples were subjected to simulated rainfall intensities of 30 mm/hr, 51 mm/hr and 68 mm/hr for 30 minutes over a two-day period. The eroded soil quantities contained in the run-off were measured at intervals of 5 minutes. The effect of erosion on the surface particles was assessed using photographs. Erodibility decreased with increases of both the clay fraction and the size of the granular particles. Moreover, erodibility increased with the increases of the rainfall intensity, slope gradient and length. Smaller particles eroded faster than coarser particles. At the surface, the number of soil particles reduced, whilst their size increased with the increasing rainfall duration. The runoff coefficients increased with the increasing clay content, slope gradient, and higher rainfall intensity. Both the erodibility and the runoff coefficients reduced in the second-day experiments.

## Dedications

To God and Humanity.

To my wife Dative, and our daughters Iley and Ileen: *For your immeasurable support, patience, and heart-warming words.*

To my late parents: Mr Jean and Mrs Eunice, sadly you left me. The helpless teenager has now grown up.

To my late aunt Mrs Eudie, you exceptionally replaced your sister, as my mother, for about twenty-five years.

To the ten years of hardship in my life. Only God knows. This is a peaceful, probably most wise, and perfect revenge. I could not be asked for more!

## Acknowledgements

I would like to sincerely thank my supervisors, Dr Gurmel Ghataora and Dr Michael Burrow, for whom without the success of this research would not have been possible. I am deeply appreciative of their time, inspiration, and support through both the highs and lows of the PhD journey. I will always feel indebted to them. Many thanks to my annual reviewers, Dr Mehran Eskandari Torbaghan and Prof David Chapman, for their invaluable inputs to my research. I proudly thank Mr Mark Carter, Mr James Guest, Mr David Allsop, Mr David Cope, Mr Navid Aslam and Mr James Glover, the technicians of the Civil Engineering Laboratory, and the Civil Engineering Department, University of Birmingham; for their support and humanity.

I would like to thank Mr Eric Kayisire and his family, for everything they have done to help me stay focussed on my PhD. A thank you is not enough. I must thank Mr Steve and Mrs Sue Sandys, for being the new grandparents to my daughters. Their love, affection, presents and particularly Sue's weekly book reading sessions to my daughters cannot be thanked enough. They have touched my heart and I will remember them all my life.

Lastly but importantly, my unlimited gratitude and thanksgiving go to the Commonwealth Scholarship Commission (CSC) in the UK, for financially funding this research. Without this support, it would have been impossible for my dream to come true. My programme officers at CSC, Miss Vanessa Worthington and Mr James Goldsmith are sincerely thanked for their timely assistance throughout the PhD journey.

## Table of Contents

Abstract .....	ii
Dedications.....	iii
Acknowledgements .....	iv
Table of Contents .....	v
List of Figures .....	x
List of Tables.....	xiv
Abbreviations .....	xv
1. INTRODUCTION.....	1
1.1. Background .....	1
1.2. Aim and Objectives of the Research .....	6
1.3. Outline Methodology .....	6
1.4. Novelty and Knowledge Contribution of the Research.....	7
1.5. Thesis Structure.....	8
1.6. Summary .....	10
2. LITERATURE .....	11
2.1. Introduction .....	11
2.2. Methodology for Systematic Analysis of Literature .....	11
2.3. Identification and Sourcing of Globally Published Data.....	11
2.4. Screening of Studies.....	12
2.4.1. Inclusion and Exclusion Criteria .....	13
2.4.2. Weight of Evidence .....	13
2.5. Globalization of Studies .....	14
2.6. Timeline of the Studies .....	16
2.7. Distribution of the Studies in terms of Themes.....	17
2.8. The 26 Key Studies .....	18
2.9. Distribution of Studies by Types.....	19
2.10. Sorting, Mining and Parking of Data .....	19
2.11. Analysing the Studies by the Fields of Application .....	21
2.12. Analysing the Studies by the Types of Erosion .....	22
2.13. Analysing the Studies by the Soils Used for Investigation .....	23
2.14. Use of the English China Clay (Kaolin) in Construction .....	26
2.15. Factors Affecting Erodibility of Unpaved Roads.....	28
2.16. Analysis of the Major Factors Affecting Erodibility of Unpaved Roads .....	34

2.16.1. Erodibility and Clay Content.....	34
2.16.2. Erodibility and Plasticity Index .....	39
2.16.3. Erodibility and Particle Size Distribution.....	42
2.16.4. Erodibility and Rainfall .....	47
2.16.5. Erodibility, Rainfall Duration and Vegetative Cover.....	48
2.16.6. Erodibility and Rainfall Intensity .....	49
2.16.7. Erodibility, Runoff Discharge and Slope Gradient .....	50
2.16.8. Erodibility, Road and Vehicular Traffic.....	53
2.17. Erosion Resistant Unpaved Roads .....	56
2.18. Summary .....	61
3. METHODOLOGY .....	63
3.1. Introduction .....	63
3.2. Methodology Flow Chart .....	63
3.3. Selection of Soils for Erosion Tests .....	65
3.4. Characterization of the Selected Soil Materials .....	66
3.4.1. Particle Size Distribution.....	66
3.4.2. Classification and Engineering Properties of Selected Mixes.....	67
3.5. Engineering Behaviour of Selected Soil Mixes .....	69
3.5.1. Infiltration Rate .....	69
3.5.2. Erosion Susceptibility Tests .....	70
3.5.2.1. Crumb Test.....	70
3.5.2.2. Double Hydrometer Test .....	72
3.5.2.3. Hole Erosion Test (HET) .....	72
3.6. Rainfall Simulator for Erodibility Tests.....	74
3.6.1. Overview on Rainfall Simulators .....	74
3.6.2. Design of the Rainfall Simulator.....	75
3.6.3. Design of the Simulated Rainfall Intensity .....	77
3.6.4. Determination of the Raindrops' Size .....	78
3.6.5. Flour Method for Raindrop Size Determination .....	79
3.7. Design of the Soil Test Container .....	81
3.8. Small-scale Testing of Erodibility.....	81
3.8.1. Moisture and Density Variations during Erodibility Tests.....	83
3.8.2. Data Collected During the Small-scale Erodibility Tests.....	84
3.9. Large-scale Testing of Erodibility.....	85

3.9.1. Enlargement of the Rainfall Simulator.....	86
3.9.2. Homogeneity of Compacted Samples .....	88
3.9.3. Data Collected During the Large-scale Erodibility Tests.....	89
3.10. Calibration of ImageJ Software.....	90
3.11. Sheet Erosion Tests .....	91
3.12. Correlating the Factors Affecting Erodibility .....	95
3.13. Summary .....	98
4. RESULTS .....	99
4.1. Introduction.....	99
4.2. Infiltration Rate Test Results.....	99
4.3. Erosion Susceptibility Tests .....	101
4.3.1. Crumb Test Results .....	101
4.3.2. Double Hydrometer Test Results .....	101
4.3.3. Hole Erosion Test Results .....	102
4.4. Flour Method Test Results .....	104
4.5. Determination of the Kinetic Energy from the Simulated Rainfall.....	106
4.6. Performance of the Rainfall Simulator.....	108
4.7. Key Outcomes from Material Selection and Rainfall Simulator Calibration.....	108
4.7.1. Quality of Selected Materials for Unpaved Roads’ Surface Soils.....	108
4.7.2. Quality of Selected Soils for Erodibility Tests.....	109
4.7.3. Detachment of Selected Soils due to Raindrops’ Kinetic Energy .....	110
4.7.4. Moisture Content Variation during Rainfalls .....	111
4.7.5. Strength Improvement due to Increased English China Clay Content .....	114
4.8. ImageJ Software Calibration Results .....	115
4.9. Sheet Erosion Test Results .....	116
4.9.1. Area and Depth of Erosion Damage after the first- and second-day Tests .....	117
4.9.2. Area and Depth of Erosion Damage after the tenth- and eleventh-day Tests .....	121
4.9.3. Effect of Glass Marbles in the Formation of Potholes .....	122
4.10. Simulated Rainfall Erodibility Test Results .....	123
4.10.1. Eroded Sediment from GS and VGS mixed with 20% ECC.....	125
4.10.2. Eroded Sediment from GS and VGS mixed with 15% ECC.....	127
4.10.3. Eroded Sediment from GS and VGS mixed with 10% ECC.....	128
4.10.4. Eroded Sediment from GS and VGS mixed with 5% ECC.....	130
4.10.5. Eroded Sediment from GS and VGS mixed with 0% ECC.....	131

4.10.6. Eroded Sediment from Subbase .....	134
4.11. Erosion Rate .....	136
4.11.1. Erosion Rate for GS and VGS mixed with 20% ECC.....	137
4.11.2. Erosion Rate for GS and VGS mixed with 15% ECC.....	140
4.11.3. Erosion Rate for GS and VGS mixed with 10% ECC.....	143
4.11.4. Erosion Rate for GS and VGS mixed with 5% ECC.....	146
4.11.5. Erosion Rate for GS and VGS mixed with 0% ECC.....	149
4.11.6. Erosion Rate for Subbase .....	152
4.12. Eroded Soil Materials Particle Size Distribution Changes.....	154
4.13. Surface Particle Size Changes.....	156
4.13.1. Surface Particle Size Changes Due to a 30 mm/hr Rainfall on GS + ECC mixes .....	158
4.13.2. Surface Particle Size Changes Due to a 51 mm/hr Rainfall on GS + ECC mixes .....	158
4.13.3. Surface Particle Size Changes Due to a 68 mm/hr Rainfall on GS + ECC mixes .....	159
4.13.4. Surface Particle Size Changes Due to a 68 mm/hr Rainfall on VGS mixes and Subbase.....	160
4.14. Runoff Coefficients .....	161
4.14.1. Influence of Various Rainfall Events on Runoff Coefficients .....	162
4.15. Summary .....	164
5. DISCUSSION .....	165
5.1. Introduction .....	165
5.2. Erodibility Due to Simulated Rainfall.....	165
5.2.1. Eroded Soil Materials (Sediment) Collection.....	166
5.2.2. Erosion Rate .....	169
5.2.2.1. Effect of ECC Content and Plasticity Index on Erosion Rate .....	169
5.2.2.2. Effect of Maximum Dry Density on Erosion Rate.....	171
5.2.2.3. Scale Factor for Erodibility Tests.....	172
5.2.2.4. Effect of Particle Size on Erosion Rate .....	175
5.3. Particle Size Distribution of Eroded Soils.....	176
5.4. Surface Particle Size Changes.....	177
5.5. Runoff Coefficients .....	178
5.5.1. Effect of Clay Content and Particle Size on Runoff Coefficients .....	179
5.5.2. Effect of Clay Content and Slope on Runoff Coefficients .....	180
5.5.3. Effect of Mean Particle Size on Runoff Coefficient .....	181
5.5.4. Effect of Cu and Cc on Runoff Coefficients .....	182
5.5.5. Effect of Percent of Fines and Density on Runoff Coefficients .....	184

5.6. Summary .....	185
6. CORRELATION OF FACTORS affecting ERODIBILITY IN UNPAVED ROADS .....	186
6.1. Introduction .....	186
6.2. Validation of the Predictive Models.....	186
6.3. Regression Equations .....	190
6.3.1. Small-scale, First-day Erodibility Tests .....	190
6.3.2. Small-scale, Second-day Erodibility Tests.....	190
6.3.3. Large-scale, First-day Erodibility Tests .....	193
6.3.4. Large-scale, Second-day Erodibility Tests.....	193
6.3.5. Combined Small- and Large-scale, First-day Erodibility Tests .....	196
6.3.6. Combined Small- and Large-scale, Second-day Erodibility Tests.....	196
6.4. Summary .....	199
7. CONCLUSIONS AND RECOMMENDATIONS.....	201
7.1. Conclusions .....	201
7.1.1. Rainfall Erosion.....	201
7.1.2. Sheet Erosion.....	204
7.2. Recommendations for Further Work.....	205
REFERENCES.....	207
APPENDICES.....	237

## List of Figures

Figure 1. 1. Rural transport systems and poverty connections (Adopted from Hine, 2014).....	3
Figure 1. 2. Poverty rate and accessibility within 2 km of all-weather road (Petts et al., 2006)	5
Figure 1. 3. The research flow chart.....	7
Figure 2. 1. Flow chart showing how the publications were searched and filtered to identify most suitable ones for detailed study.....	14
Figure 2. 2. Number and origin of the studies of the systematic analysis.....	15
Figure 2. 3. Distribution of studies in the continents.....	15
Figure 2. 4. Relationship between number of publication and percentage of unpaved roads ..	16
Figure 2. 5. Distribution of studies with time.....	17
Figure 2. 6. Schematic showing number of studies under the various themes.....	17
Figure 2. 7. Extract from spreadsheet showing the first stage of the data mining process .....	20
Figure 2. 8. Distribution of studies in areas of application.....	21
Figure 2. 9. Investigations shown in number and percentage for each type of erosion .....	23
Figure 2. 10. USDA' soil textural triangle (Fernandez-Illescas et al., 2001).....	24
Figure 2. 11. Level of investigation in various soils by studies .....	26
Figure 2. 12. Ideal layered structure of kaolinite (Sperinck et al., 2011).....	28
Figure 2. 13. Classification of factors that affect erosion.....	29
Figure 2. 14. Investigation of different factors that affect erodibility by studies .....	30
Figure 2. 15. Erosion rate as a function of shear stresses and clay content.....	35
Figure 2. 16. Erosion rate as a function of the plasticity of soils .....	37
Figure 2. 17. Gradient and plasticity index .....	37
Figure 2. 18. Plasticity and gradient of erodibility as functions of critical shear stress .....	38
Figure 2. 19. Mean erosion rate and critical shear stress. Plasticity index is in parentheses ...	39
Figure 2. 20. Critical shear stress as a function of the plasticity of soils .....	41
Figure 2. 21. Erosion rate, plasticity index and critical shear stress.....	42
Figure 2. 22. Threshold raindrop kinetic energy and critical erosion velocity versus mean particle size of the soil.....	43
Figure 2. 23. Critical shear stress versus mean particle size of soils.....	45
Figure 2. 24. Predicted soil loss versus average annual rainfall (Dubé et al., 2004).....	48
Figure 2. 25. Splash evolutions for three replicated simulations on silt loam and clay loam soils (Leguédois and Le Bissonnais, 2004) .....	48
Figure 2. 26. Sediment yield rate versus rainfall duration for road sections with different grass cover percentages (Liu et al., 2010) .....	49
Figure 2. 27. Soil loss as a function of rain intensity and duration (Cao et al., 2013) .....	50
Figure 2. 28. Erosion rate as a function of the road gradient, road type and surface flow discharge (Cao et al., 2009).....	51
Figure 2. 29. Erosion rate as a function of surface flow discharge, road type and gradient (Cao et al., 2009).....	52
Figure 2. 30. Sediment production as affected by traffic passes (Iverson, 1980) .....	55
Figure 2. 31. Detachment rate with time as of presence of rills (ruts) (Foltz et al., 2008).....	56
Figure 2. 32. Proposed envelope for soils that resist erosion in unpaved roads.....	60
Figure 2. 33. Allocation of the envelope into the South African diagram .....	60
Figure 3. 1. Summary map of the key steps of the methodology .....	64

Figure 3. 2. PSD of gravelly SAND soil mixed with English china clay.....	66
Figure 3. 3. PSD of subbase and very gravelly SAND mixed with English china clay .....	67
Figure 3. 4. Infiltration rate test setting .....	70
Figure 3. 5. Colloidal reaction of samples after 10 min (A); 1 hour (B); and 2 hours (C).....	71
Figure 3. 6. Hole erosion test set up (A); pre-drilled sample before test (B); tested sample with erosion hole (C); casting of wax into the erosion hole (D); and wax casts of erosion holes (E) .....	73
Figure 3. 7. Supplied nozzle (A), original nozzle bottom to be cut off (B) and modified nozzle inserted into new nylon pipe (bleu) bottom (C) .....	76
Figure 3. 8. A top view of the overturned rainfall simulator.....	77
Figure 3. 9. IDF curves from KARAMA, Rwanda (Demarreé and Van de Vyver, 2013).....	78
Figure 3. 10. Raindrops collection into the flour (A), separating air-dried pellets from the flour (B) and sieved oven-dried pellets (C).....	80
Figure 3. 11. Small-scale testing: sample placement after being compacted (A) and side view during testing (B).....	83
Figure 3. 12. Core cutters inserted into soil every 5 min (A), core cutters removed (B), samples into core cutters (C), and samples' extrusion from core cutters (D) .....	84
Figure 3. 13. Large-scale testing: rainfall simulator with flow control zone (CZ) and soil sample (A) and side view of the rain simulator during the test (B).....	87
Figure 3. 14. Detail of the flow control zone (CZ).....	87
Figure 3. 15. Calibration of rainfall intensities for large-scale rainfall simulator .....	88
Figure 3. 16. Mixing samples in electric mixer (A); compaction by electric hammer (B); collected runoff and sediment (C); oven-drying sediment (D); and sediment for sieving (E) .	89
Figure 3. 17. The VGS + 20% ECC sample with glass marbles before being embedded (A); glass marbles being embedded into the soil (B); and after sheet erosion test (C).....	92
Figure 3. 18. The GS + 20% ECC sample with glass marbles exposed to the surface before the sheet erosion test (A); and after the sheet erosion test (B) .....	93
Figure 3. 19. Locating the soils used for sheet erosion tests into envelopes by Carey and Simon, 1984 and Pham, 2008 .....	93
Figure 3. 20. Design of the model process .....	97
Figure 4. 1. Infiltration rate versus elapsed time for selected soils .....	100
Figure 4. 2. Pressure changes for erosion test on GS + 20% ECC.....	104
Figure 4. 3. Number of drops falling on 21 cm diameter pan in 3 seconds for different rain intensities .....	104
Figure 4. 4. Comparison of the simulated raindrops' sizes and the raindrops' sizes reported by other researchers .....	105
Figure 4. 5. Fall velocity due to the size and fall height of the raindrops (ASTM, 2015) .....	107
Figure 4. 6. Location of the soils used in the unpaved road soils' performance diagram (Paige-Green, 2006) .....	109
Figure 4. 7. Detachment of selected soils due to raindrops' kinetic energy.....	110
Figure 4. 8. Measured moisture content variations with depth for GS + 20% ECC soil tested using 30 mm/hr (A), 51 mm/hr (B), and 68 mm/hr (C) rainfall intensities.....	112
Figure 4. 9. Measured moisture content variations with depth for GS + 10% ECC (a), GS + 15% ECC (b), and GS + 20% ECC (c) soils tested using 51 mm/hr rainfall intensity .....	113
Figure 4. 10. CBR changes in GS + ECC mixes (Ngezahayo et al., 2019b).....	114

Figure 4. 11. CBR changes in VGS + ECC mixes and subbase.....	115
Figure 4. 12. Calibration of ImageJ software .....	116
Figure 4. 13. Sheet erosion on GS + 20% ECC without glass marbles: (A) first-day test, (A') second-day test; GS + 20% ECC + buried glass marbles: (B) first-day test, (B') second-day test; GS + 20% ECC + exposed glass marbles: (C) first-day test and (C') second-day test. Sheet erosion on VGS + 20% ECC without or with buried glass marbles: (D) first-day test, (D') second-day test; VGS + GS + 20% ECC + exposed glass marbles: (E) first-day test, (E') second-day test. Effect of exposed glass marbles on GS + 20% ECC (F) and on VGS + 20% ECC (F').....	118
Figure 4. 14. Areas of erosion damage and runoff duration.....	120
Figure 4. 15. Depths of erosion damage and runoff duration.....	121
Figure 4. 16. Areas of erosion damage due to time of runoff flow .....	122
Figure 4. 17. Depths of erosion damage due to time of runoff flow .....	122
Figure 4. 18. Sediment from small- and large-scale first-day experiments for GS + 20% ECC and VGS + 20% ECC .....	126
Figure 4. 19. Sediment from small- and large-scale second-day experiments for GS + 20% ECC and VGS + 20% ECC .....	127
Figure 4. 20. Sediment from small- and large-scale first-day experiments for GS + 0% ECC and VGS + 0% ECC .....	133
Figure 4. 21. Sediment from small- and large-scale second-day experiments for GS + 0% ECC and VGS + 0% ECC .....	134
Figure 4. 22. Sediment from small- and large-scale first-day experiments subbase.....	135
Figure 4. 23. Sediment from small- and large-scale second-day experiments subbase .....	136
Figure 4. 24. Erosion rate from small- and large-scale first-day experiments for GS + 20% ECC and VGS + 20% ECC .....	138
Figure 4. 25. Erosion rate from small- and large-scale second-day experiments for GS + 20% ECC and VGS + 20% ECC .....	139
Figure 4. 26. Erosion rate from small- and large-scale first-day experiments for GS + 15% ECC and VGS + 15% ECC .....	141
Figure 4. 27. Erosion rate from small- and large-scale second-day experiments for GS + 15% ECC and VGS + 15% ECC .....	142
Figure 4. 28. Erosion rate from small- and large-scale first-day experiments for GS + 10% ECC and VGS + 10% ECC .....	144
Figure 4. 29. Erosion rate from small- and large-scale second-day experiments for GS + 10% ECC and VGS + 10% ECC .....	145
Figure 4. 30. Erosion rate from small- and large-scale second-day experiments for GS + 5% ECC and VGS + 5% ECC .....	147
Figure 4. 31. Erosion rate from small- and large-scale second-day experiments for GS + 5% ECC and VGS + 5% ECC .....	148
Figure 4. 32. Erosion rate from small- and large-scale first-day experiments for GS + 0% ECC and VGS + 0% ECC.....	150
Figure 4. 33. Erosion rate from small- and large-scale second-day experiments for GS + 0% ECC and VGS + 0% ECC .....	151
Figure 4. 34. Erosion rate from small- and large-scale first-day experiments for subbase ....	152
Figure 4. 35. Erosion rate from small- and large-scale first-day experiments for subbase ....	153

Figure 4. 36. PSD of the sediment from a GS + 5% ECC soil (Ngezahayo et al., 2019a, e) .	154
Figure 4. 37. PSD and envelopes for the sediment eroded from 0 to 30 min of the rainfall for the first-day erosion experiments .....	155
Figure 4. 38. PSD and envelopes for the sediment eroded from 0 to 30 min of the rainfall for the second-day erosion experiments .....	156
Figure 4. 39. Surface particle size analysis during erodibility test at 10 <sup>th</sup> min of rainfall.....	157
Figure 4. 40. Surface particle size analysis during erodibility test at 25 <sup>th</sup> min of rainfall.....	157
Figure 4. 41. Surface particles reduction and increase in D <sub>50</sub> with increased 30 mm/hr rainfall duration for GS + ECC mixes based on image analysis.....	158
Figure 4. 42. Surface particles reduction and increase in D <sub>50</sub> with increased 51 mm/hr rainfall duration for GS + ECC mixes based on image analysis.....	159
Figure 4. 43. Surface particles reduction and increase in D <sub>50</sub> with increased 68 mm/hr rainfall duration for GS + ECC mixes based on image analysis.....	160
Figure 4. 44. Surface particles reduction and increase in D <sub>50</sub> with increased 68 mm/hr rainfall duration for VGS + ECC mixes and subbase based on image analysis .....	161
Figure 4. 45. Runoff coefficients, rainfall intensities and clay content.....	163
Figure 5. 1. Effect of ECC percentages on erosion rate .....	171
Figure 5. 2. Effect of plasticity on erosion rate .....	171
Figure 5. 3. Effect of maximum dry density on erosion rate.....	172
Figure 5. 4. Scale factor for eroded sediment.....	174
Figure 5. 5. Scale factor for erosion rate .....	174
Figure 5. 6. Runoff coefficients, clay content and particle size .....	180
Figure 5. 7. Runoff coefficients and clay content.....	181
Figure 5. 8. Runoff coefficients and mean grain size .....	182
Figure 5. 9. Runoff coefficients and coefficient of uniformity .....	183
Figure 5. 10. Runoff coefficients and coefficient of gradation .....	183
Figure 5. 11. Runoff coefficients and percent of fines in GS and VGS soils.....	184
Figure 5. 12. Runoff coefficients and maximum dry density .....	184
Figure 6. 1. Typical results from the processed data .....	189
Figure 6. 2. Small-scale testing correlation between measured and predicted eroded mass ..	191
Figure 6. 3. Validation of the small-scale testing correlations between measured and predicted eroded mass .....	192
Figure 6. 4. Large-scale testing correlations between measured and predicted eroded mass	194
Figure 6. 5. Validation of the large-scale testing correlations between measured and predicted eroded mass .....	195
Figure 6. 6. Small- and large-scale combined tests correlation between measured and predicted eroded mass .....	197
Figure 6. 7. Validation of small- and large-scale combined tests correlation between measured and predicted eroded mass.....	198

## List of Tables

Table 2. 1. Studies identified for the 20 key words used in searches .....	12
Table 2. 2. Top 15 countries that contributed about 88% of studies .....	15
Table 2. 3. The 26 key studies .....	18
Table 2. 4. Erosion types that affect unpaved roads .....	23
Table 2. 5. USDA' soil classification by percent of clay, silt and sand (Karamage et al., 2017) .....	24
Table 2. 6. Geological and geotechnical factors of erodibility .....	31
Table 2. 7. Environmental and climatic factors of erodibility .....	32
Table 2. 8. Road factors of erodibility .....	33
Table 2. 9. Composition of the soils in Figure 2.15 and the regression lines' equations .....	35
Table 2. 10. Typical coefficients of erodibility for different soil textures .....	46
Table 3. 1. Suitability of soils for erosion tests (ASTM, 2015; Ngezahayo et al., 2019a, e) ...	65
Table 3. 2. Classification of soils used in this study (BS 5930: 2015) .....	67
Table 3. 3. Summary table of the standards tests .....	68
Table 3. 4. Description of crumb test grades of reaction (Maharaj, 2011) .....	71
Table 3. 5. Double hydrometer test interpretation (Maharaj and Paige-Green, 2013) .....	72
Table 3. 6. A comparison between drop-forming and pressurized rainfall simulators .....	75
Table 3. 7. Schedule of small-scale erodibility tests .....	82
Table 3. 8. Schedule of large-scale erodibility tests .....	85
Table 3. 9. Average hand vane shear test results in compaction moulds and soil testing box .	89
Table 3. 10. Schedule of sheet erosion tests .....	91
Table 3. 11. Flow velocities during sheet erosion tests .....	92
Table 3. 12. Summary of erosion susceptibility and erodibility tests: repetitions and justifications.....	94
Table 3. 13. Typical spreadsheet of data preparation .....	96
Table 4. 1. Results of the crumb test .....	101
Table 4. 2. Results of the double hydrometer test .....	102
Table 4. 3. Hole Erosion Test results.....	102
Table 4. 4. Kinetic Energy (KE) embedded in raindrops .....	107
Table 4. 5. Eroded soil (g) during rainfall erosion tests for GS and VGS mixed with 20% ECC .....	124
Table 4. 6. Erosion rate (kg/m <sup>2</sup> /s) during rainfall erosion for GS and VGS mixed with 20% ECC .....	124
Table 6. 1. Evolution of modelling in developing the USLE (Lafren and Flanagan, 2003) ..	187
Table 6. 2. Rating of the factors' contribution to the predictive erosion model.....	199

## Abbreviations

ASCE: American Society of Civil Engineers

ASTM: American Society for Testing and Materials

ASANRA: Association of Southern African National Roads Agencies

CBR: California Bearing Ratio

$E_r$ : Erosion rate

GIS and RS: Geographical Information System and Remote Sensing

HET: Hole Erosion Test

HIV/AIDS: Human Immunodeficiency Virus/ Acquired Immunodeficiency Syndrome

ICE: Institution of Civil Engineers

IDF: Rainfall's Intensity-Duration-Frequency

IMT: Intermediate Means of Transport

$I_p$ : Plasticity Index

MDD: Maximum Dry Density

MLRRB: Minnesota Local Roads Research Board

OC: Organic Content

OMC (or  $W_{opt}$ ): Optimum Moisture Content

pH: Potential Hydrogen

PSD: Particle Size Distribution

(R)USLE: (Revised) Universal Soil Loss Equation

SDGs: Sustainable Development Goals

SA: South Africa

$\tau$ : Shear stress

$\tau_c$ : Critical shear stress

UCS: Uniaxial Compressive Strength

UK: United Kingdom

USA: United States of America

USDA: United States Department of Agriculture

WEPP: Water Erosion Prediction Project

$W_L$ : Liquid limit

$W_P$ : Plastic limit

## 1. INTRODUCTION

### 1.1. Background

The world's road network is currently estimated to be about 64.3 million kilometres of length. Only about 30% of these roads are paved with bituminous materials (flexible pavements) or with concrete materials (rigid pavements); while the remaining 70% are unpaved roads (Faiz, 2012; World Factbook, 2017). In some countries, unpaved roads can comprise 90% of the total road network (Burrow et al., 2014, 2016). Some of the unpaved roads have an upper layer of borrowed gravel but most of them are made with the local soils of the area. Unpaved roads are also known as unsealed roads, unsurfaced roads, uncovered roads, native and engineered earth roads, gravel roads, and dirt roads. Furthermore, these roads are called "Rural Roads" because of their role in connecting the rural communities.

A native earth road relies on the subgrade soil strength to withstand the traffic loadings and to deal with environmental stresses such as those caused by changes in weather and erosion. Some soils used in unpaved roads are very prone to water erosion leading to excessive loss of surface soils, formation of potholes and erosion rills in the road surface. Thus, unpaved roads may only be usable during dry seasons, although dust may be an issue; and then can be practically unusable in the rainy seasons. Unpaved roads can fail through rutting, formation of potholes and erosion, amongst several other modes of failure. Therefore, these roads require regular maintenance. Although unpaved roads are less expensive to build when compared to paved roads, which makes them a first choice to connect rural communities, their seasonal and regular maintenance schemes are an issue. Petts (2013) reported that the cost of unpaved road maintenance seems to be unaffordable for many developing countries, which can lead to poor transport of people and goods, with detrimental consequences on the overall development.

The unpaved roads are essential to socio-economic and growth of rural areas in developing countries. These roads can provide access to millions of communities, helping the populations to improve their well-being and development. Currently, only about 37% of the world's population can access an all-weather road within 2 kilometres, in other words, within a 30-minute walking distance in rural areas (World Bank, 2008). Petts (2013) defines an all-weather road as “the road constructed to an appropriate engineered standard with clear characteristics and technical details, passable by the local means of transport for 98% of the year, and with all justifiable routine and periodic maintenance met”. In Sub-Saharan Africa, a region in which about 80% of the roads are unpaved, only about 34% of the population can access a road (Riverson et al., 1991; Torero and Chowdhury, 2005; World Bank, 2008; Faiz, 2012; Ngezahayo et al., 2019b, f). Mostly, it is the women and children who suffer from the inadequate rural transport systems, as they cannot afford the increasing transport costs due to both the low density and the poor condition of rural roads.

Considering their importance, the poor condition of rural roads can be a major factor in the exacerbation of poverty. Hine (2014) explored the links between poverty and isolation on one hand, and low funds' allocation for rural roads on the other hand. The low funding encourages ineffective road network institutions, which poorly deliver their missions leading to an overall failed transport sector. Furthermore, a failed transport sector can lead to exacerbated poverty and isolation of rural areas. The poorer and isolated rural areas deplete the resources and contribute less to the funding for road construction, leading to a back and forth reciprocating situation between poverty and poor rural transport, as shown in Figure 1.1.

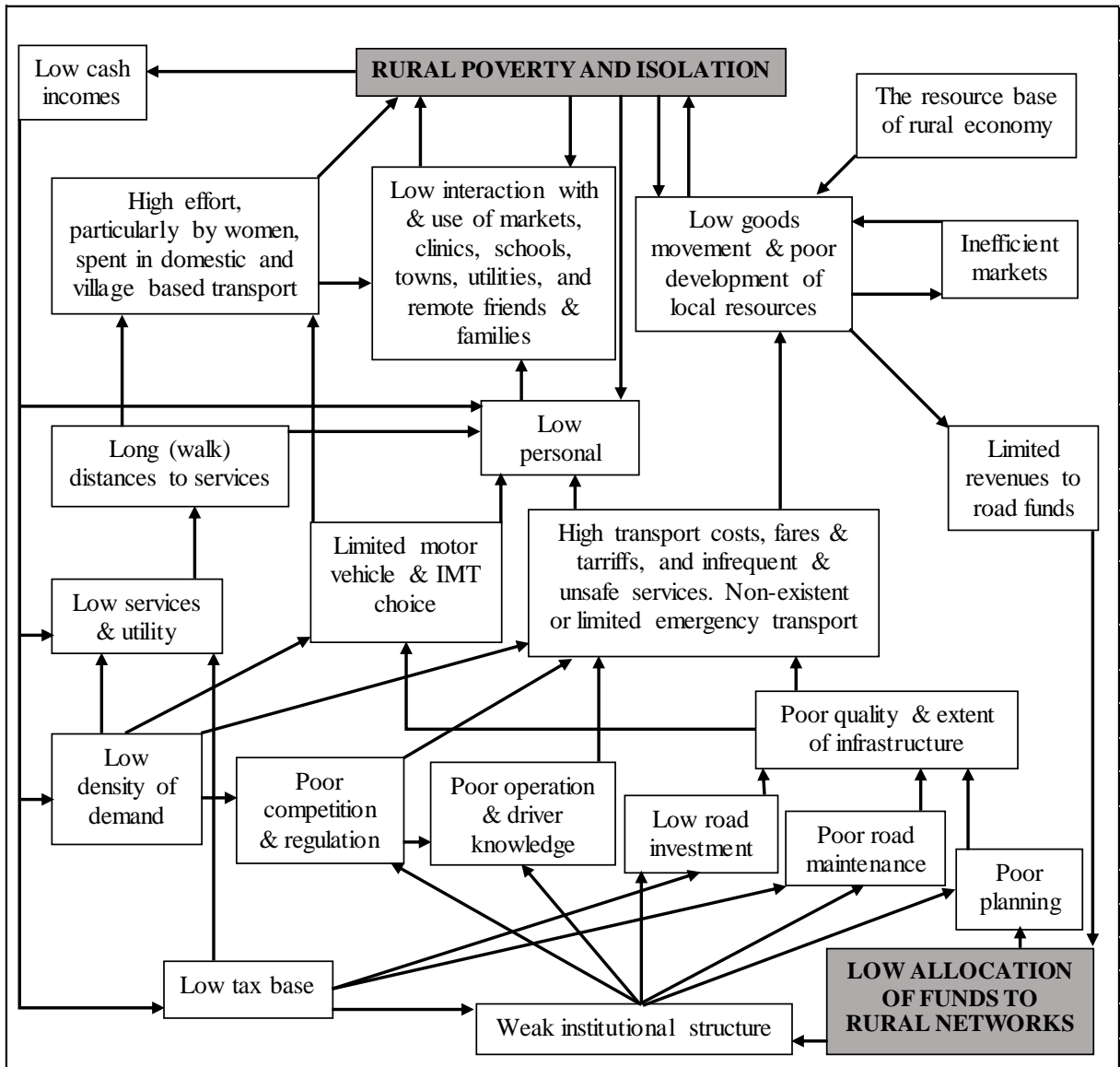


Figure 1. 1. Rural transport systems and poverty connections (Adopted from Hine, 2014)

From a case study in Vietnam, Petts et al. (2006) showed that poverty decreases with increased accessibility to an all-weather road. Cook et al. (2005, 2017) said that the sustainable development goals (SDGs) may not be achieved in developing countries if the mobility and accessibility of rural areas are not seriously considered.

Rural transport plays an indispensable role in achieving more than half of the seventeen SDGs and fulfilling the promise of the 2030 United Nations' Agenda for Sustainable Development to

‘leave no one behind’ (Cook et al., 2017). Although there is no dedicated SDG target on rural access, there are numerous linkages between rural access and the SDGs. Successful scaled up implementation of rural transport can contribute to realizing: SDG 1 to alleviate poverty; SDG 2 to achieve zero hunger and ensure food security; SDG 3 to ensure health and wellbeing; SDG 4 to provide access to education; SDG 5 to empower women in rural areas; SDG 6 to facilitate access to clean water and sanitation; SDG 8 to promote inclusive growth and economic opportunities; SDG 9 to contribute to infrastructure; and SDG 11 to contribute to sustainable cities and communities; and SDG 13 to increase climate resilience and adaptation in rural areas. In addition to indirect linkages to SDGs and associated targets, there is a direct linkage to rural access in SDG indicator 9.1.1 developed by the Interagency Expert Group on SDGs. This indicator reiterates that the proportion of the rural population who live within 2 kilometres of an all-weather road should be increased significantly.

Furthermore, unpaved roads enhance accessibility to the education services. This contributes to the quality of the education leading to having skilled communities and thus, indirectly unpaved roads contribute to SDG 7 to promote affordable and clean energy; to SDG 10 to reduce inequalities; to SDG 12 to promote responsible consumption and production; to SDG 14 to protect aquatic life; to SDG 15 to sustain life on land; to SDG 16 to promote peace, justice and strong institutions; and to SDG 17 to enhance partnerships. Efficient mobility and accessibility via improved rural roads are necessary for the affordability of services and the connectivity of communities, leading to overall improvement of the socio-economic, development and well-being of the populations in rural areas. An illustration of poverty reduction due to improved accessibility to all-weather roads is shown in Figure 1.2.

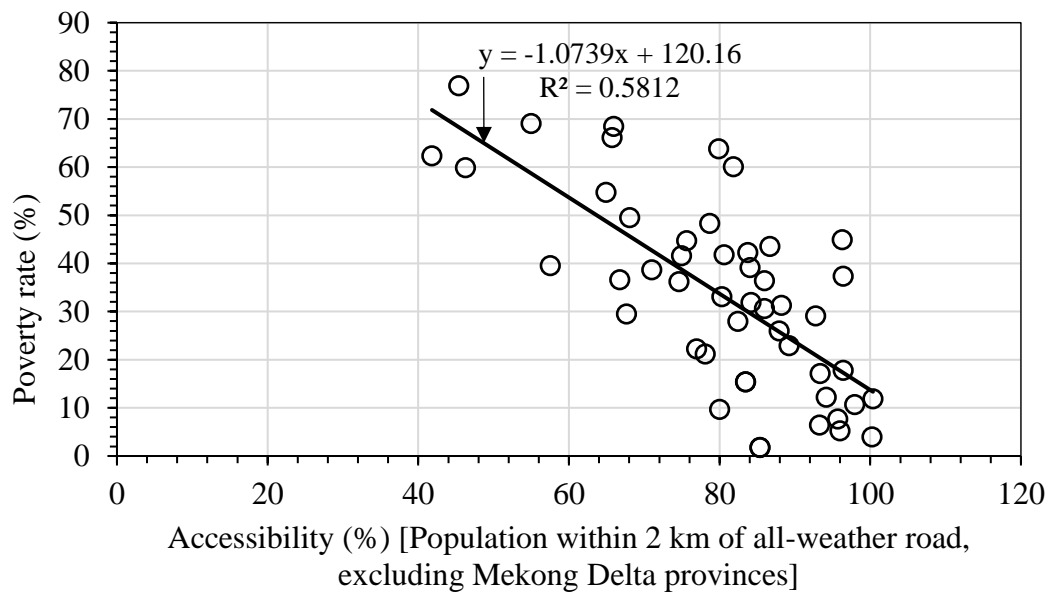


Figure 1. 2. Poverty rate and accessibility within 2 km of all-weather road (Petts et al., 2006)

Petts et al. (2006), Petts (2013) and Hine (2014) indicated that while an all-weather rural road condition is essential for poverty reduction and the well-being of rural communities, the funding for both construction and maintenance of rural roads is a heavy burden to many countries. Based on the socio-economic benefits of unpaved roads in rural areas (Riverson et al., 1991; Torero and Chowdhury, 2005; World Bank, 2008; Faiz, 2012; Burrow et al., 2014, 2016; Ngezahayo et al., 2019b, f), these roads need to be built and maintained to all-weather conditions.

Rainfall and surface water erosion are thought to be the most deteriorating agents of unpaved roads. However, little is known about the mechanisms and processes of surface water erosion of these roads. Therefore, the understanding of the erodibility of soils due to both raindrops and subsequent runoff can offer an invaluable engineering contribution, to improve the construction and reduce the maintenance cost of unpaved roads; hence, the huge importance of undertaking this study. Moreover, this study will enable the selection of appropriate soil materials with higher resistance to detachment caused by raindrops and surface water; thus, preserving the already scarce quarries of the soils used in the construction of unpaved roads.

## 1.2. Aim and Objectives of the Research

The main aim of this research was to investigate erodibility of soils in unpaved rural roads. The following objectives have been adopted to meet this aim:

1. To conduct a thorough systematic analysis of the literature to develop a knowledge base of soil erosion mechanisms in unpaved roads, and to identify the gaps in the understanding. Both were used to inform subsequent parts of the research.
2. To select appropriate soils for conducting erodibility tests.
3. To characterize and conduct erosion susceptibility tests on the selected soils.
4. To develop a rainfall simulator to help conduct erodibility tests due to both simulated rainfall intensities and subsequent surface flow.
5. Undertake laboratory tests on erosion of a range of soil types subjected to a range of simulated rainfall intensities.
6. To correlate the key factors that affect erodibility of soils which are appropriate for the construction of unpaved roads.

## 1.3. Outline Methodology

The methodology adopted for this study consists of a systematic analysis of the literature and the laboratory investigation program. As illustrated in Figure 1.3, the systematic analysis of the literature consisted of collecting published studies and systematically scrutinising these to get a basic understanding of the erodibility of soils and causal factors of erosion based on the literature. This stage provided a response to objective one of this research. The laboratory program started with the selection of suitable soils and then classification, engineering, and erosion susceptibility tests on these soils (objectives two and three). It further progressed by conducting both rainfall erosion (objectives 4 and 5) and sheet erosion tests, before analysing the data (objective 6) and completing the writing up of the PhD thesis.

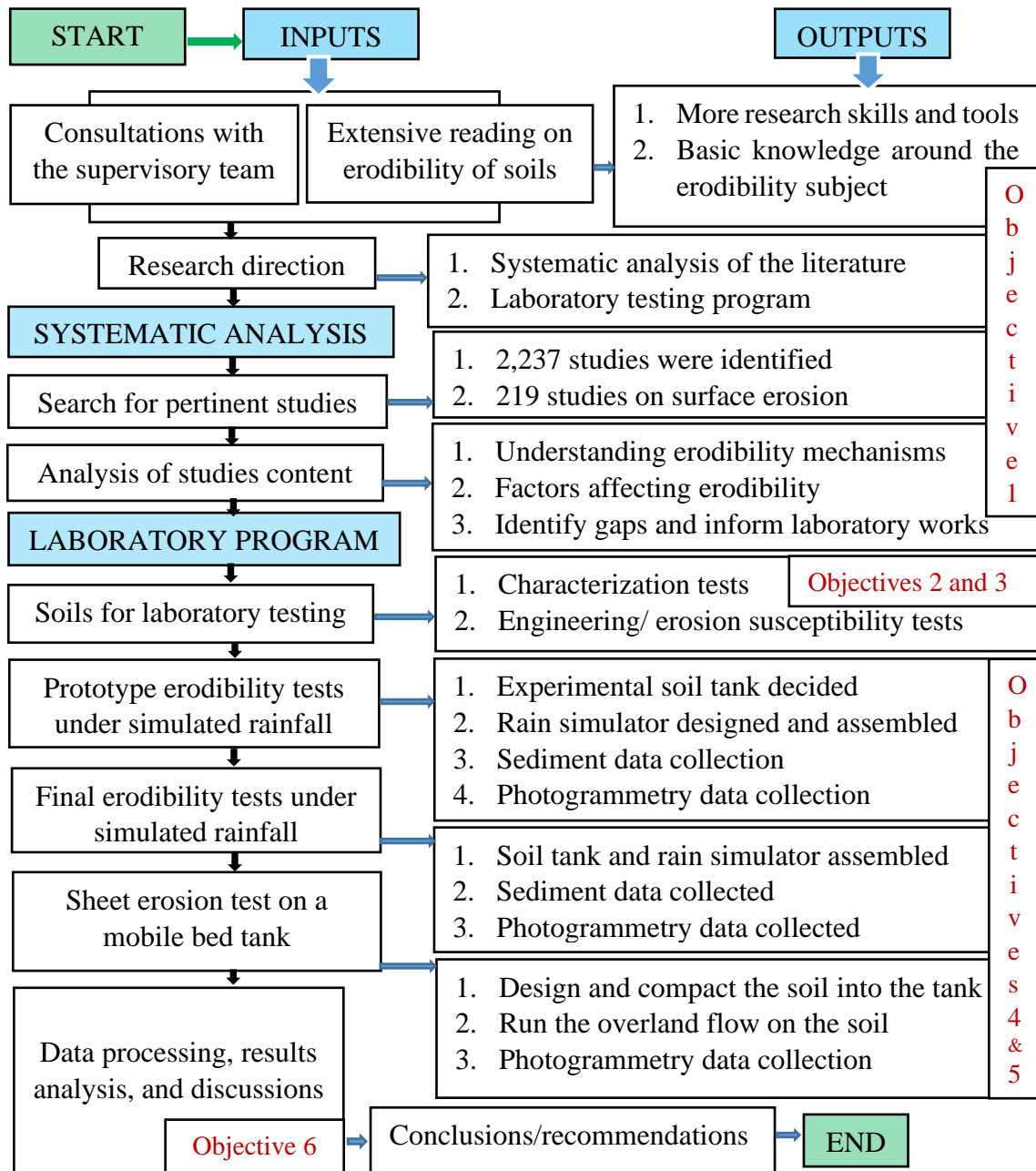


Figure 1. 3. The research flow chart

#### 1.4. Novelty and Knowledge Contribution of the Research

This research study makes the following contributions to the knowledge about the erosion of soils which are appropriate for the construction of unpaved roads:

- The study is a robust research that has systematically synthesized information on erosion processes and factors that affect erodibility of rural roads.

- This is the first study to use a laboratory rainfall simulator to investigate erodibility of soils specifically used in unpaved roads.
- This is the first study that combines the quantification and particle size distribution of the eroded soil material, and the image analysis of the changes in the numbers and sizes of soil particles at the road surface, for the whole purpose of understanding soil erodibility due to rainfall and subsequent flow.
- The study provides the development of correlations between the key factors affecting erodibility of soils used in unpaved roads.
- The results of this study enable better definitions of soil properties used to identify the suitability of soils used in unpaved roads.

In addition to the impact of this PhD research in the achievement of the SDGs, and based on its novelties and contributions to the knowledge; its academic benefits include the advancement of research in the field of erodibility of soils, and an expansion of the field's applications to the sustainability of unpaved roads.

### 1.5. Thesis Structure

This PhD thesis consists of seven chapters which are briefly described in the following order: Chapter 1 is the introduction. It gives the background and the role of rural roads, the importance of the research, the aim and objectives of the research, the methodology with the research flow chart, the novelty and knowledge contribution of the research and the thesis outline.

Chapter 2 is the literature review. It presents the systematic synthesis and analysis of published data with clarifications on: sources of data, types of published data, age and country of origin of data, and methods of assessment of the information; along with major findings based on the

main themes of erodibility of soils generally and in unpaved rural roads particularly. This chapter provides a basis for the work in Chapters 3, 4 and 5.

Chapter 3 describes the methodology. It gives the techniques to prepare the soils used for erosion tests, and the classification, engineering, and erosion susceptibility properties of those selected soils. The design and assembly of the rainfall simulator and the soil testing box as well as the schedules for both the first- and second-day erodibility tests are presented. The methods of data collection and sheet erosion test methods are all described in this chapter.

Chapter 4 provides the results. It presents the results of engineering and erosion susceptibility tests on the selected soils. Also, results from the calibration of the rainfall simulator leading to the desired rainfall intensities, drop sizes and their kinetic energy are given. The area and depth of erosion damage due to sheet flow is discussed for some soils. Typical results for eroded soils and erosion rate as well as sediment and surface particle behaviour due to simulated rainfall erosion are also presented.

Chapter 5 is the discussion chapter. It discusses the results of the laboratory testing program by quantifying sediment eroded at five-minute intervals, and the changes in the number and the size of the particles at the surface during rainfall. The sediment's particle size distribution, erosion rate and runoff coefficients with respect to soil properties, rainfall intensity, slope gradient, length, first- and second-day rainfalls, are discussed for different soils.

Chapter 6 describes the correlations of the factors affecting erodibility in unpaved roads. It presents the correlations between different factors controlled during erodibility tests that lead to measured quantities of sediment due to rainfall erosion. Those factors are clay content, plasticity index, mean particle size, maximum dry density, optimum moisture content, slope gradient, slope length, rainfall intensity, rainfall duration, and first- and second-day rainfall.

Using RapidMiner studio software, the predictive equations for erosion of soils were generated, and the relationships between measured and predicted eroded soils has been shown.

Chapter 7 presents the conclusions and recommendations. It draws together the pertinent concluding remarks of the study and makes strong recommendations for further research works.

#### 1.6. Summary

This chapter has described the problem that motivated this research study. The role of rural unpaved roads in the development and well-being of rural communities across the developing world has been briefly shown. The vital part rural roads play in the achievement of the sustainable development goals has been described briefly. However, the vulnerability and proneness of unpaved roads to rainfall erosion may make them only usable during the dry seasons and almost impassable during the rainy seasons. Rainfall erosion can lead to excessive loss of soils, formation of potholes, rills and ephemeral gullies in the road's running surface, leading to unaffordable costs and misuse of soil quarries due to recurrent maintenance needs. Since rural roads are indispensable to the socio-economic development and well-being of communities in rural areas, the poor condition of these roads due to water erosion can lead to exacerbated poverty. Therefore, it is not only important but also imperative to understand and combat erosion in unpaved roads, for those roads to effectively serve communities. Prior to this study, there has not been a single rigorous analysis that has addressed the issue of erodibility in unpaved roads, and which has provided enough data to improve both the construction and maintenance of those roads. Apart from the description of the problem, this chapter presents the aim and objectives of the study, the adopted methodology, the novelty in the methodology and the thesis outline.

## 2. LITERATURE

### 2.1. Introduction

This chapter describes the approach adopted for the review of the relevant literature on erosion of soils (with emphasis on unpaved roads) in a systematic manner followed by findings of the review. The work was a vital aspect of this study as it was used to identify both the state of knowledge and the gaps about the subject, to inform the methodology developed for this study.

### 2.2. Methodology for Systematic Analysis of Literature

This approach was first used by social scientists in 1970's before being adopted in medicine in 1980's and reshaped in its current format in 1990's (Smith et al., 2011; Bohlin et al., 2012; and Gough et al., 2017). It uses systematic methods to collect, critically evaluate, and synthesize findings both qualitatively and quantitatively from the published data. Its main steps are: (1) define the problem, (2) search for related data, (3) extraction of relevant data, (4) assess the quality of data, and (5) analyse and combine data for dissemination purpose (Usman, 2011). In this way, the resulting systematic review provides a complete and exhaustive summary of evidences which is methodical, comprehensive, clear, and reproducible. This approach was first used for a robust engineering project by Lye during his PhD which was entirely a systematic identification, analysis, evaluation, and blending of globally published data on the modulus of elasticity of concrete made with recycled materials (Lye et al., 2015).

### 2.3. Identification and Sourcing of Globally Published Data

This was carefully approached to enable strong foundation to the rest of the process. Since there are loads of publications on erodibility of soils, five questions were designed to help acquire only useful studies and avoid waste of time. These questions were:

- What is erodibility of soils?

- Can erodibility cause unpaved road's failure?
- What are the erosion types in roads?
- What are the exacerbating factors of erosion in unpaved roads?
- Where can information about erodibility of soils in roads be found?

To answer these questions, twenty key words were used in the initial search. These were applied to each of the nine search engines (Web of Science; ASCE library; ICE library; Engineering Village; FindIt@Bham; ScienceDirect; ResearchGate; Google Scholar; and Google) in turn. These search engines are known to have original scientific studies conducted with rigour and diligence and are easily accessible. Thus, the total of 2,237 mainly journal and conference papers on erodibility of soils were identified and reduced to 219 pertinent publications that were studied in detail for this study, as detailed in Table 2.1.

Table 2. 1. Studies identified for the 20 key words used in searches

Key words	Number of studies	Key words	Number of studies
Durability of road materials	51	Erodibility of soils	231
Durability of rural roads	66	Erodibility and erosion	187
Dynamic erosion	17	Erosion of earth materials	182
Design of earth and gravel roads	113	Erosion of soils	317
Failure of earth and gravel roads	118	Erosion of unpaved roads	38
Erosion tests	71	Measurements of erosion	52
Potholes in unpaved roads	58	Potholes in rural roads	43
Rural roads' failures	86	Rural roads' technology	84
Soil erosion of gravel roads	59	Soil particle detachment	152
Soil particle transport	149	Failure of unpaved roads	163
Total studies: 2, 237			

#### 2.4. Screening of Studies

The 2,237 studies were identified based on the titles and abstracts. It was then necessary to filter the studies that did not contain adequate information. The filtering of publications is described in the sections 2.4.1 and 2.4.2 on exclusion/inclusion criteria and weight of evidence.

#### 2.4.1. Inclusion and Exclusion Criteria

The initial criterion was to narrow the field to papers that included the words “water erosion” and “wind erosion”, which are the two main causes of soil erosion. This filter resulted in exclusion of 1023 studies. The second criterion was to only include publications that described factors that affect erodibility of soil and either included methods of estimating erosion or quantifying it through either theoretical, experimental or both types of studies. This resulted in exclusion of further 205 studies. The third criterion was to include only studies which used laboratory and/or field testing, modelling works, and GIS and Remote Sensing technology. This resulted in exclusion of 312 studies. At the end of all the filtering process, 697 studies remained. These were then checked for robustness in terms of weight of evidence, as described below.

#### 2.4.2. Weight of Evidence

The weight of evidence approach was used to identify those studies with clearer methods and results, more soundness, appropriateness, and relevance. According to Burrow et al. (2014, 2016), the soundness of a study is high if explicit and detailed methods, data collection and analysis of results, and interpretation are firmly based on the findings and critical comparison with other works. The soundness is medium if there are satisfactory methods and results, and the interpretation is partially warranted by the findings. Finally, the study’s soundness is low if methods and results are unsatisfactory without interpretation of findings or with the interpretation not warranted by the findings. On the other hand, appropriateness refers to the clearness and detail of the study’s road map from equipment through methods to the results, while the study’s relevance is based on its meaningful contribution to the existing knowledge.

With respect to the weight of evidence approach described above, the number of studies was reduced from 697 to 219 studies. Only about 12% (26 studies) were deemed to be good. This represents about 1% of the initial 2,237 studies identified at the start of the review process. The

small number of the studies that investigated erodibility in rural roads is a further evidence of the importance of this study. Schematization of the search process can be seen in Figure 2.1.

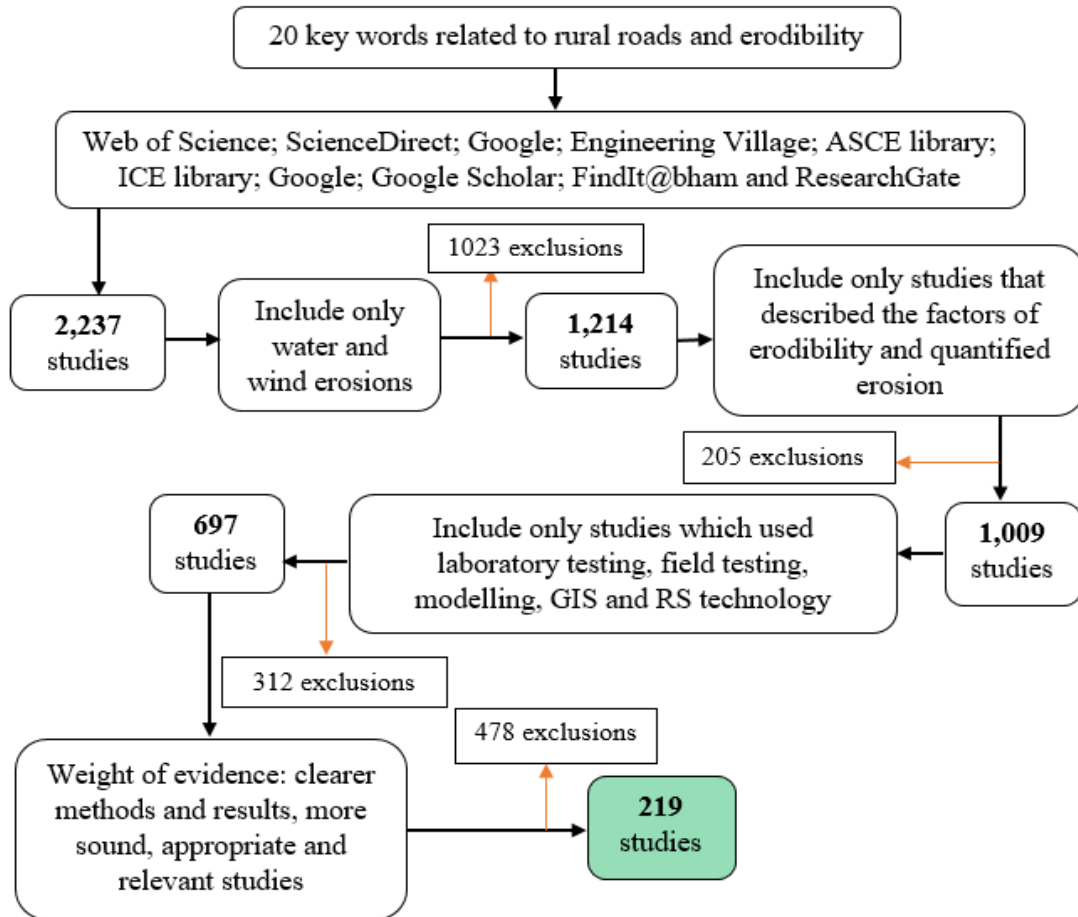


Figure 2. 1. Flow chart showing how the publications were searched and filtered to identify most suitable ones for detailed study

## 2.5. Globalization of Studies

The final 219 studies were published from 36 countries, with about 50% of these arising from the USA, China, UK, and Belgium, as shown in Figure 2.2. The top fifteen countries that contributed about 88% of studies are listed in Table 2.2. Moreover, Europe and America contributed 35.6% and 33.8% of the studies, followed by Asia with 20.5% of the studies, while Australia and Zealandia, and Africa have 5.0% of the studies each, as shown in Figure 2.3.

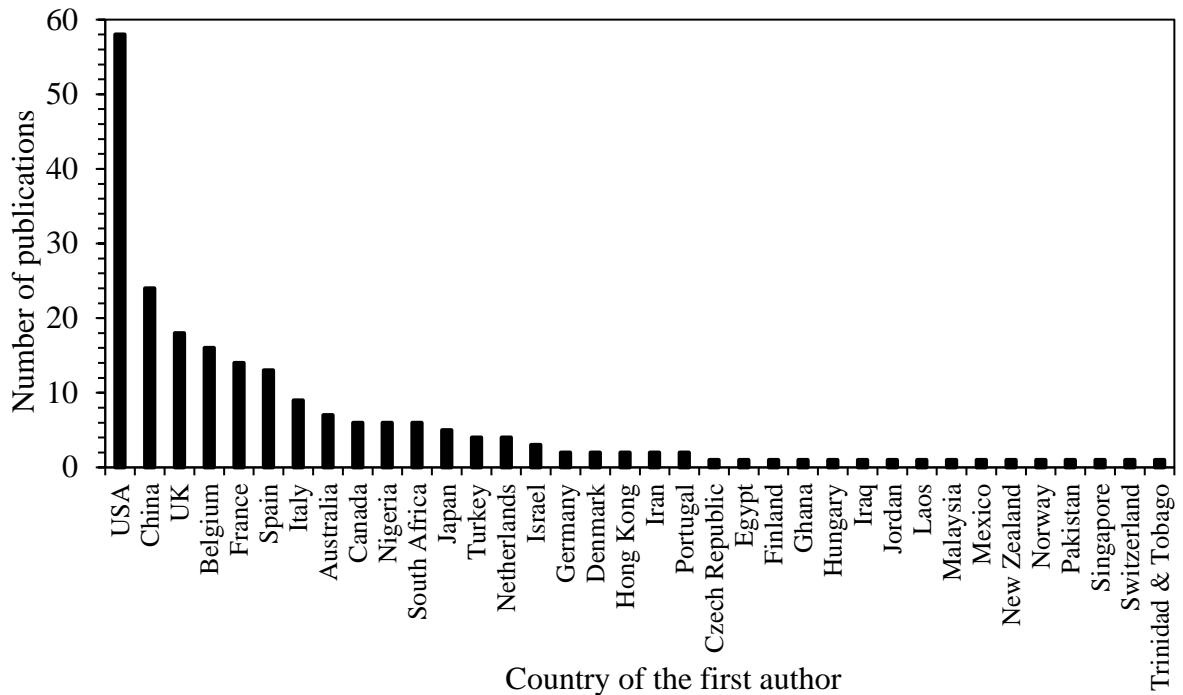


Figure 2. 2. Number and origin of the studies of the systematic analysis

Table 2. 2. Top 15 countries that contributed about 88% of studies

Key words	Number of studies	Key words	Number of studies
USA	58	Canada	6
China	24	Nigeria	6
UK	18	South Africa	6
Belgium	16	Japan	5
France	14	Turkey	4
Spain	13	Netherlands	4
Italy	9	Israel	3
Australia	7	-	-
Total studies: 193			

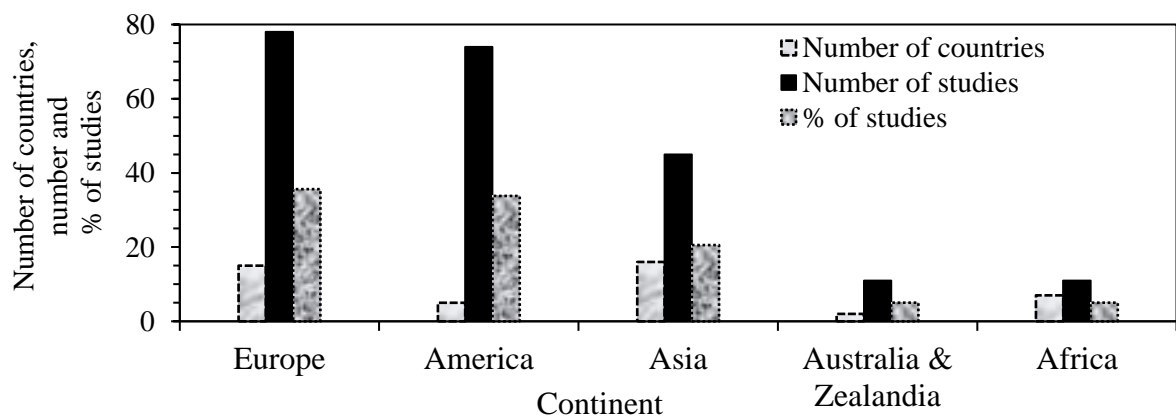


Figure 2. 3. Distribution of studies in the continents

An attempt was made to investigate the relationship between the number of publications and the percentage of unpaved roads for countries of first authors. The overall observation was that countries with higher percentage of unpaved roads, thus with more need for research on rural road contributed less publications than countries with lower percentage of unpaved roads. Some of the publications originated from countries without unpaved roads, as shown in Figure 2.4. The percentages of unpaved roads were obtained from the World Factbook (2017).

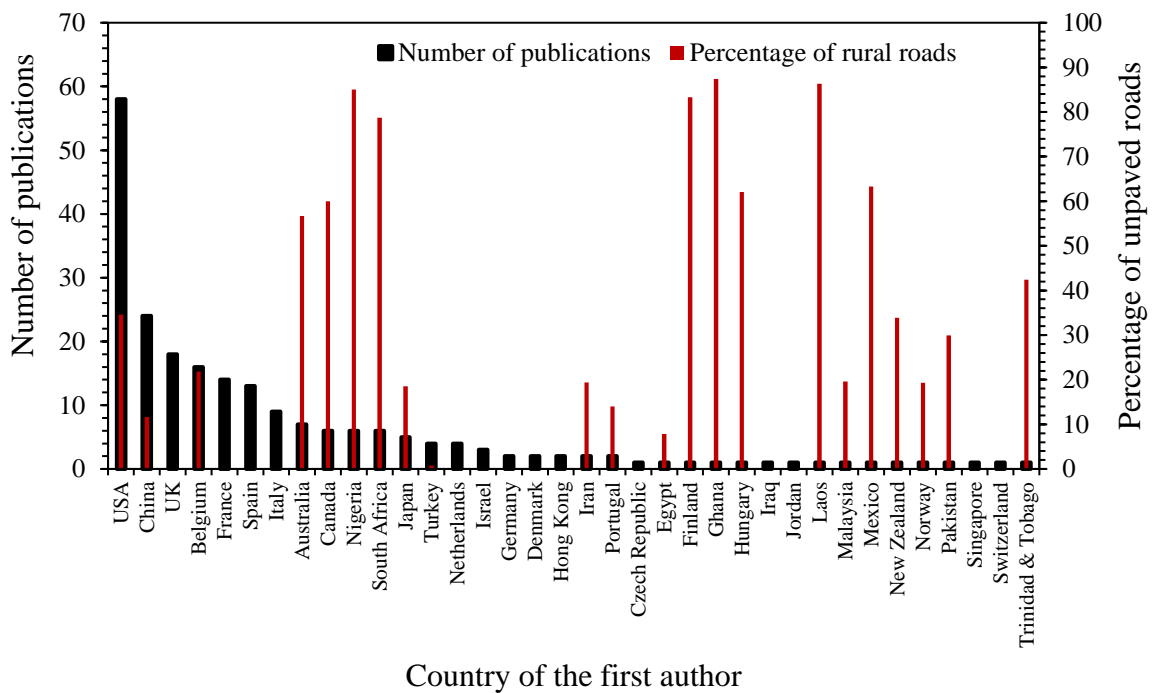


Figure 2. 4. Relationship between number of publication and percentage of unpaved roads

## 2.6. Timeline of the Studies

The earliest study located dated back to 1960. Little seems to have been published up to 1975. Thereafter, there was a steady increase in publications up to about 2010, as shown in Figure 2.5. The reason for reduction in publication on the subject is not entirely clear as the erosion of soils is important and will be of increasing importance due to the impact of climate change.

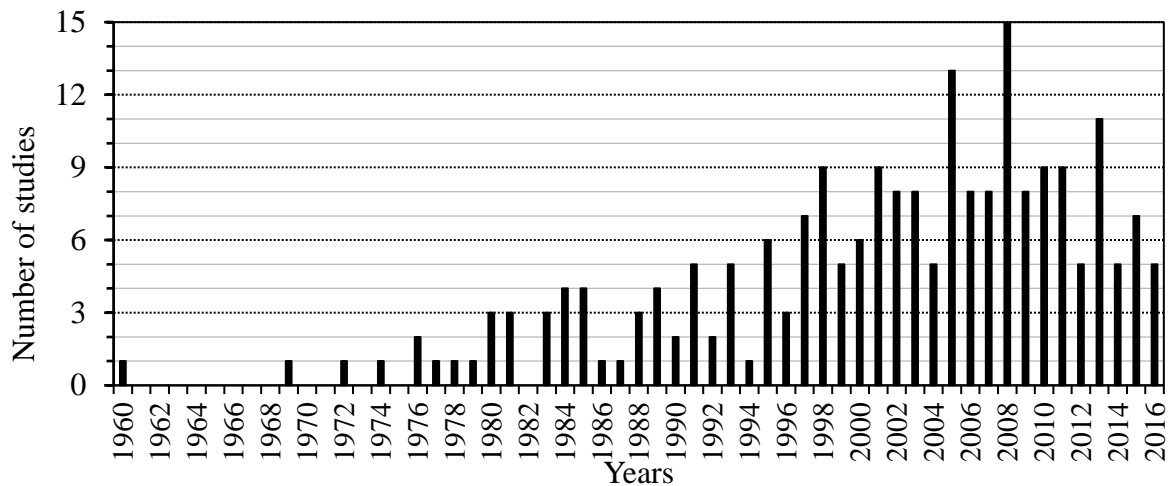


Figure 2. 5. Distribution of studies with time

### 2.7. Distribution of the Studies in terms of Themes

The 219 studies were grouped into themes that need to be studied. These were review papers, laboratory studies, *in situ* studies, and GIS and modelling studies, as shown in Figure 2.6.

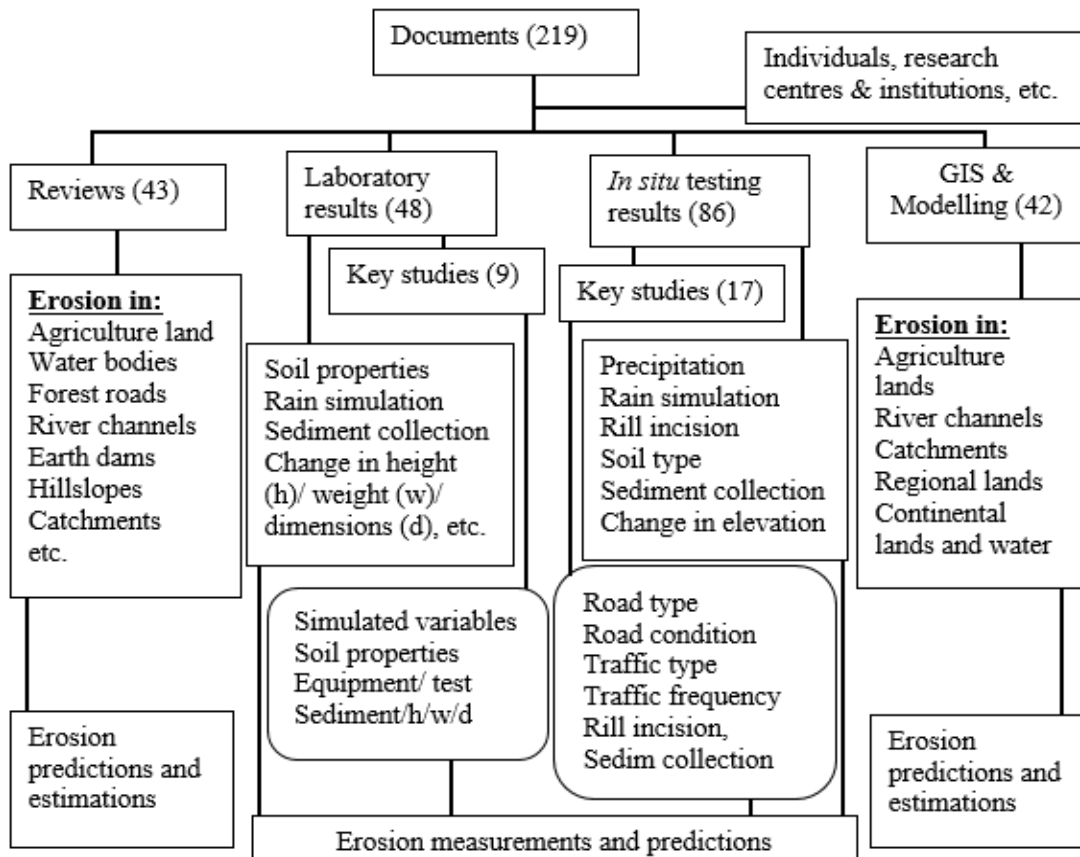


Figure 2. 6. Schematic showing number of studies under the various themes

## 2.8. The 26 Key Studies

Among the 219 final studies, 26 key studies relating to erodibility of soils in unpaved roads and compacted soils have been identified. These are 9 laboratory works and 17 field works that provided clarity to the kind of experimental works that can lead to measurement and prediction of erodibility. Table 2.3 lists these studies, study types (F: field study and L: laboratory study) and the important erodibility factors investigated by each study.

Table 2. 3. The 26 key studies

Study	Type	Studied factors affecting road's erodibility
Anderson & MacDonald, 1998	F	Gradient, drainage area, rainfall, hillslope
Briaud, 2008	L	Hydraulic shear stresses and flow velocity
Bryan, 2000	L	Erosion types, slope, and soil properties
Bryan et al., 1989	F	Soil properties, rainfall, and land use
Cao et al., 2006	F	Grasses on unpaved roads' surfaces
Cao et al., 2009	L	Detachment of road soils by flowing water
Cao et al., 2013	F	Runoff, soil type and properties
Croke et al., 2005	F	Road's length, drainage, runoff,
Dubé et al., 2004	L	Rainfall, road geometry and geology
Foltz & Burroughs, 1990	F	Wheel ruts, traffic type, runoff
Foltz et al., 2008	F	Rills, runoff, drainage, and traffic
Foltz et al., 2009	F	Runoff, compaction, wheel tracks
Haghighi et al., 2013	L	Soil texture, properties, shear stress, HET
Iverson, 1980	F	Rainfall, wheel track, surface properties
Knapen et al., 2007	L	Soil properties, concentrated flow stresses
MacDonald et al., 2001	F	Road's active area and surface properties
Paige-Green, 2006	L	Road material, cohesion, strength, PSD
Paige-Green et al., 2015	L	Soil properties, re-gravelling
Ramos-Scharrón & McDonald, 2005	F	Regrading, slope, rainfall, and drainage
Salles et al., 2000	L	Kinetic energy, PSD, splash capacity
Sheridan et al., 2008	F	Rainfall, infiltration, gradient and length
Sugden and Scott, 2007	F	Slope, maintenance, rainfall, geology
Swift Jr (1984)	F	Surface properties and traffic type
Ziegler et al., 2000	F	Compaction, splash, hydraulic detachment
Ziegler et al., 2001	F	Soil properties, erosion prediction
Ziegler et al., 2004	F	Runoff, traffic, and maintenance

## 2.9. Distribution of Studies by Types

About 90% of the studies were journal papers. Conference papers and technical reports amounted to about 5% and 3% respectively. The remainder were books, manuals, and circulars, which together contributed about 2% of all the studies. The fifteen journals contained 118 studies representing 54% of all the studies: *Catena* (32), *Earth Surface Processes and Landforms* (20), *Geomorphology* (9), *Soil Tillage and Research* (9), *American Soil Science Society* (8), *Hydrological Processes* (7), *Water Resources Research* (6), *American Society of Agricultural Engineers* (5), *American Society of Agricultural and Biological Engineers* (4), *Geotechnical and Geo-environmental Engineering* (3), *Geotechnical Testing* (3), *Engineering Geology* (3), *Transport Research Board* (3), *Agriculture, Ecosystems and Environment* (3), and *Soil Testing* (3). The other studies were obtained from seventy-two different sources.

## 2.10. Sorting, Mining and Parking of Data

The purpose of this process was to organise the studies to clearly show their content. A matrix comprising the list of all papers (219) on the vertical axis and key parameters on horizontal axis was created. The horizontal axis themes include soil and geology (e.g. soil type, PSD, plasticity and strength), environment and climate (e.g. precipitations, erosion types, weathering, dry-wet cycles and topography), road condition (e.g. geometry, drainage, maintenance and road use), and applications in which erosion and erodibility are a major factor (e.g. roads, agriculture, dams, bare and vegetated slopes). An extract of the spreadsheet matrix is shown in Figure 2.7. Data for each parameter was then extracted from papers in a separate spreadsheet for analysis and synthesis. Forty-seven (47) parameters were studied in this way. Statistical and correlation analyses were conducted to identify trends. As most of the data was presented graphically, Web-Plot Digitizer was used to scan, digitize, and create x-y data that can be treated in excel. Data for each parameter was collated, synthesized, and analysed to identify correlation and trends.



### 2.11. Analysing the Studies by the Fields of Application

The studies were analysed based on types of erosion, fields of application, and methodological approaches used during erodibility investigations. The application fields were watersheds and hillslopes, agriculture, unpaved roads, dams and embankments, and rivers and channels. Some studies were crosscutting between different fields. Dams and embankments can have similar surface erodibility as unpaved roads due to compaction of soils. Watersheds and hillslopes can also have similarities with unpaved roads when erosion is mainly coming from compacted trails due to trampling by people and/or animals. In agriculture, soils may be ploughed and loosened to allow easy penetration of plant roots, causing their high permeability and infiltration rate. Those differences can help understand why unpaved roads and agriculture soils erode differently. Rivers and channels are subject to concentrated runoff shear stresses and could help understand what happens in unpaved roads once rills and ephemeral gullies have been created by surface flow. Figure 2.8 shows the studies with respect to the field of application.

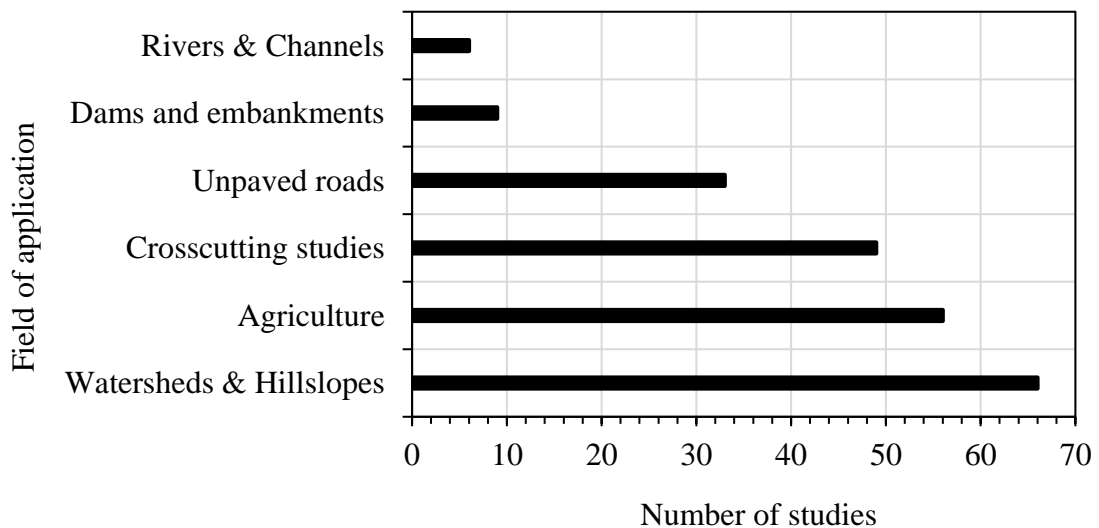


Figure 2. 8. Distribution of studies in areas of application

## 2.12. Analysing the Studies by the Types of Erosion

The studies were further analysed based on water and wind erosion types, and their main causes, as shown in Table 2.4. Nine water erosion and three wind erosion types were identified. For water erosion types, splash erosion due to raindrops kinetic energy (Salles et al., 2000; Kinnell, 2005), sheet erosion due to non-concentrated flow shear stresses (Zhang et al., 2016), rill erosion due to concentrated flow shear stresses (Allen et al., 1997) and ephemeral gully erosion due to prolonged concentrated flow shear stresses (Alfsen et al., 1996; Katz et al., 2013) are frequent in unpaved roads. Piping and internal erosion can occur in less compacted unpaved roads over subgrades rich in clay soils as infiltrated water may find exit downslope in the road's surface (Masannat, 1980; Wan and Fell, 2004). Near surface groundwater levels can cause quick saturation of unpaved road soils during rainy seasons, reduce the strength, and increase the vulnerability of those roads to erosion (Masannat, 1980). As said earlier, rills and ephemeral gullies can behave as water channels with erosion affected by concentrated shear stresses. Headcut and overtopping can result from poor drainage (Powledge et al., 1989; Temple and Hanson, 1994), with water from the cut side of the road joining the road surface flow to cause flooding and overtopping to the road's embankment fill side.

The wind erosion depends on both the natural and mechanical (due to vehicular speeds) wind's energy and the particle size of soils at the road surface (Erpul et al., 1998; Choi, 2002). Due to the amount of wind energy, small particles can be lifted and suspended into dust (suspension). Medium size particles can be lifted to short distances (saltation) while coarser particles can be rolled over the road surface (creep). From Figure 2.9, about 90% of studies focused on splash, inter-rill (sheet), and rill and gully water erosion types. This makes sense since those are the most frequently types of water erosion that occur in unpaved roads.

Table 2. 4. Erosion types that affect unpaved roads

Type	Sub-type	Key feature and reference
Water Erosion	Splash/Rainfall erosion	Raindrop kinetic detachment energy (Kinnell, 2005)
	Inter-rill/Sheet erosion	Rain kinetic energy; flow stresses (Zhang et al., 2016)
	Rill erosion	Concentrated flow shear stresses (Allen et al., 1997)
	Gully/Linear erosion	Concentrated flow shear stresses (Alfson et al., 1996)
	Piping and Internal erosion	Seepage velocity greater than critical velocity for soil transport (Masannat, 1980; Burns et al., 2006)
	Groundwater erosion	Soil saturation, pore water pressure (Masannat, 1980)
	Channel erosion	Stream and unit stream powers (Knapen et al., 2007)
	Headcut erosion	Cover failure, concentrated flow stresses and upstream erosion progress (Temple and Hanson, 1994)
	Overtopping erosion	Flooding overflow stresses (Powledge et al., 1989)
Wind erosion	Suspension, saltation, creep	Driving forces (aerodynamic drag and lift) > retarding forces (cohesion and gravity) (Choi, 2002).

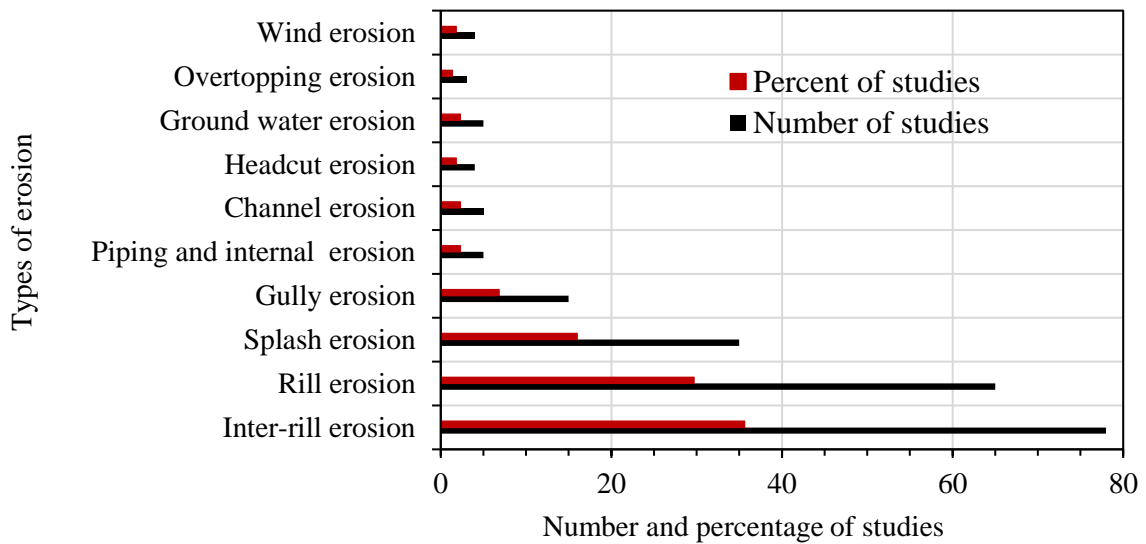


Figure 2. 9. Investigations shown in number and percentage for each type of erosion

### 2.13. Analysing the Studies by the Soils Used for Investigation

Many of the identified studies were related to the agricultural soils and published in the USA. Thus, the soil textural classification based on the USDA' sand-silt-clay triangle was used by many studies to classify the investigated soils. It was necessary to elucidate the composition of those soils to understand the type of soils used by studies. This was achieved by following the USDA' soil triangle as subdivided by Fernandez-Illescas et al. (2001), as shown in Figure 2.10

and the results of this subdivision in terms of percentages of clay, silt and sand reported by Karamage et al. (2017), as shown in Table 2.5.

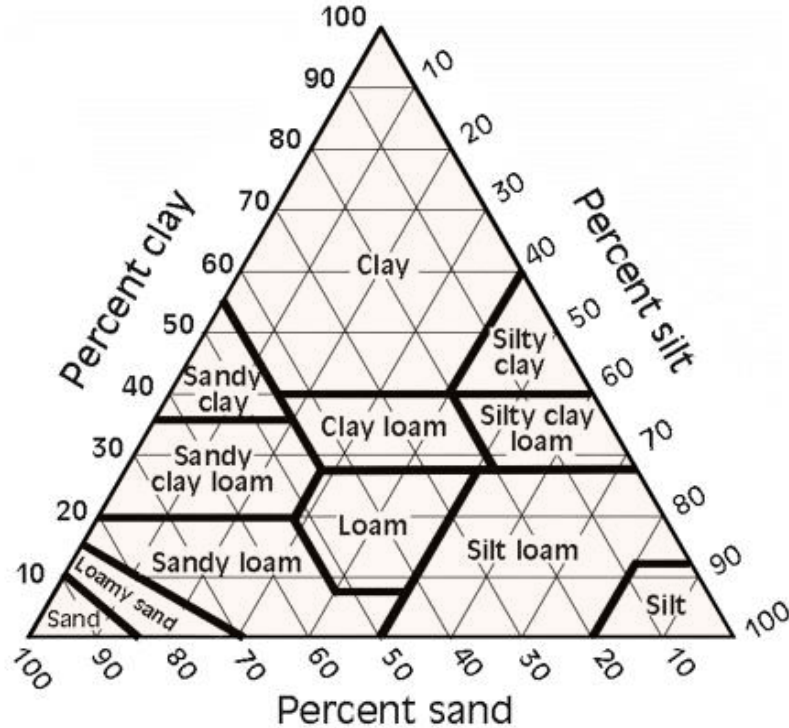


Figure 2. 10. USDA’ soil textural triangle (Fernandez-Illescas et al., 2001)

Table 2. 5. USDA’ soil classification by percent of clay, silt and sand (Karamage et al., 2017)

Soil texture name	Sand	Silt	Clay
Sandy soil	85-100	0-15	0-10
Loamy sand	70-90	0-30	0-15
Sandy loam	43-80	0-50	0-20
Loam	23-52	28-50	7-27
Silt loam	0-50	50-88	0-27
Silt	0-20	88-100	0-12
Sandy clay loam	45-80	0-28	20-35
Clay loam	20-45	15-53	27-40
Silty clay loam	0-20	40-73	27-40
Sandy clay	45-65	0-20	35-45
Silty clay	0-20	40-60	40-60
Clay	0-45	0-40	40-100

After understanding the composition of the soils, the selected studies showed that 19 soil types were used in various erosion studies, as shown in Figure 2.11. This information was very useful

since it helped to identify the soils with less or enough available information about erodibility. Highly investigated soils include soils investigated by more than fifty studies such as sand, clay, silt, and silty loam [1-37]. Medium level investigated soils included soils which were investigated by twenty-five to fifty studies such as gravel, loam (a mix of approximately equal fractions of clay, silt, and sand soils), clay loam and sandy loam [38 - 56]. Low level investigated soils were found in ten to twenty-five studies such as loamy sand, silty clay, loess, silty clay loam, sandy clay loam, and sandy clay [57 – 86]. Very low level investigated soils included all soils that were found in less than ten studies such as gravel loam, silty sand, clayey sand, gravelly sandy loam, and sandy gravel [87 - 102].

---

References: [1] Morgan, 1978; [2] Luk, 1979; [3] Arulanandan and Perry, 1983; [4] Noble and Morgan, 1983; [5] Powledge et al., 1989; [6] Torri and Poesen, 1992; [7] Archwicheai et al., 1993; [8] Torfs et al., 1996; [9] De Figueredo and Poesen, 1998; [10] Erpul et al., 1998; [11] Fullen, 1998; [12] Loch et al., 1998; [13] Robinson and Hanson, 2001; [14] Asselman et al., 2003; [15] Fell et al., 2003; [16] Dubé et al., 2004; [17] Leguédois and Le Bissonnais, 2004; [18] Wan and Fell, 2004; [19] Erpul et al., 2005; [20] Issa et al., 2006; [21] Sheppard et al., 2006; [22] Dotterweich, 2008; [23] Erpul et al., 2008; [24] Ismail et al., 2008; [25] Lachouette et al., 2008; [26] Sheridan et al., 2008; [27] Zuazo and Pleguezuelo, 2008; [28] Wuddivira et al., 2009; [29] Arthur et al., 2011; [30] Cantón et al., 2011; [31] Cao et al., 2011; [32] Flores-Berrones et al., 2011; [33] Soroush et al., 2011; [34] Al-Riffai and Nistor (2013); [35] Haghighi et al., 2013; [36] Li et al., 2015; [37] Nagy and Nagy, 2015; [38] Wischmeier and Mannering, 1969; [39] Morin and Benyamin, 1977; [40] Swift Jr, 1984; [41] Swift Jr, 1985; [42] Rauws and Govers, 1988; [43] Nearing et al., 1989; [44] Laflen et al., 1991; [43] Ekwue and Stone, 1995; [44] Cochrane and Flanagan, 1996; [45] Reichert et al., 2001; [46] Stroosnijder, 2005; [46] Knapen et al., 2007; [47] Henning et al., 2008; [48] Cantón et al., 2009; [49] Rienzi et al., 2013; [50] Shearer et al., 2013; [51] Wang et al., 2013; [52] Wang et al., 2014; [53] Yu et al., 2014; [54] Nwankwor et al., 2015; [55] Comino et al., 2016; [56] Lu et al., 2016; [57] Yariv, 1976; [58] Quansah, 1981; [59] Moore and Burch, 1986; [60] Brunori et al., 1989; [61] Ekwue, 1990; [62] Tengbeh, 1993; [63] Arnáez and Larrea, 1995; [64] Siegrist et al., 1998; [65] Sutherland and Ziegler, 1998; [66] Barthès and Roose, 2002; [67] Cerdan et al., 2002; [68] MLRRB, 2003; [69] Poesen et al., 2003; [70] Istanbuluoglu et al., 2005; [71] Zhang and Nearing, 2005; [72] Bonelli et al., 2006; [73] Knapen et al., 2007; [74] Zhang et al., 2008; [75] Cao et al., 2009; [76] Svoray and Markovitch, 2009; [77] Chang and Zhang, 2010; [78] Evans, 2010; [79] Fujisawa et al., 2010; [80] Liu and Zheng, 2010; [81] Liu et al., 2010; [82] Mizugaki et al., 2010; [83] Benahmed and Bonelli, 2012; [84] Zhu, 2012; [85] Cao et al., 2013; [86] Comino et al., 2016; [87] Finnie, 1960; [88] Savat and Poesen, 1981; [89] Poesen and Savat, 1981; [90] Meyer and Harmon, 1984; [91] Ekwue et al. 1993; [92] Parker et al., 1995; [93] Fitzjohn et al., 1998; [94] Cerdà, 2001; [95] MacDonald et al., 2001; [96] Ramos-Scharrón and MacDonald, 2005; [97] Sugden and Scott, 2007; [98] Griesmer et al., 2008; [99] Nanko et al., 2008; [100] Cerdan et al., 2010; [101] Chang and Zhang, 2011; [102] Fukubayashi and Kimura, 2014.

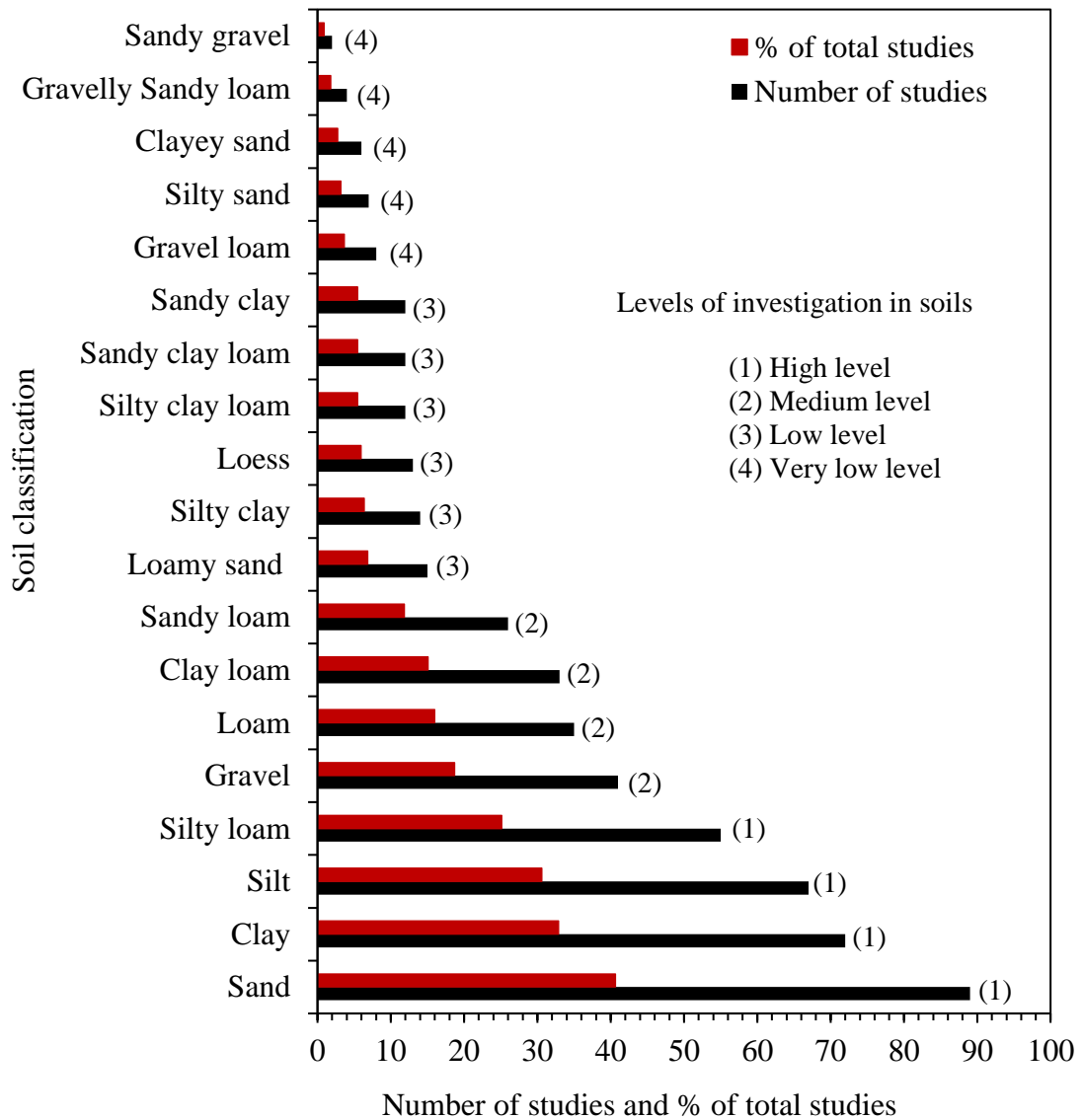


Figure 2. 11. Level of investigation in various soils by studies

#### 2.14. Use of the English China Clay (Kaolin) in Construction

The English china clay (Kaolin) is used in construction for different purposes. The English china clay (ECC) contains kaolinite which is useful in the ceramics, roads, and buildings industries (British Geological Survey, 2009). Furthermore, the metakaolin which a derivative of the heated kaolin can be used in the construction, paint, and rubber applications. Several studies used metakaolin as additive in Portland cement applications (Sabir et al., 2001; Rashad,

2015), as a precursor in geopolymers (Rashad, 2013) and in alkali activated cement materials based on slag/metakaolin ratios (Bernal et al., 2012).

In road construction, the ECC was used successfully as a binding material between granular soils (Abdullah et al., 2017) and a cement substitution in concrete pavements (Lotfy et al., 2015; Bediako et al., 2016). Moreover, granular ECC quarries by-products have been used as base and subbase road materials (Aggregates Advisory Services, 1999). The use of ECC as binder in road construction is primarily due to its ability to react with water and serve as lubricant and filler between the granular particles during compaction; hence leading to an increased density and bearing capacity of the road. Another reason for the use of the ECC in road construction is that both the ECC and its derivatives can increase the strength of geomaterials. For instance, replacement of Portland cement with up to 15% metakaolin derived from kaolin sand (heated at 650°C for one hour) increases the compressive strength by 25% and 45%, respectively for 28 and 90 days compared to the samples without cement substitutions (Kuliffayová et al., 2012; Lotfy et al., 2015). Gomes et al. (2012) activated kaolin waste using calcium hydroxide and sodium silicate. The strength developed only after calcining at 750°C for two hours. At seven days, it was about 10 MPa using calcium hydroxide and 40 MPa when sodium silicate was used.

In addition to the increase of strength, kaolinite has the smaller surface specific area of all clay minerals with about 100 m<sup>2</sup>/g, which indicates that it cannot absorb much water and keep it for long time. Montmorillonite has the largest surface specific area with about 800 m<sup>2</sup>/g. Illite has between 100 – 200 m<sup>2</sup>/g whilst smectite has about 350 m<sup>2</sup>/g (Wilson, 1999). Due to smaller surface area, kaolinite attracts less water and cannot be subject to swelling and shrinking phenomena; thus, cannot change the road's profile due to seasoning. The fixation of water by kaolinite is facilitated by its composition. Its chemical structure [Al<sub>4</sub>Si<sub>4</sub>O<sub>10</sub>(OH)<sub>8</sub>] is a 1:1 dioctahedral phyllosilicate mineral (Sperinck et al., 2011), as shown in Figure 2.12. In the

chemical structure: Al – aluminium, Si – silicon, O – oxygen, and H – hydrogen atoms. The structure has tetrahedra of SiO<sub>4</sub> forming sheets by sharing three of the four oxygen atoms whilst the fourth oxygen atoms are shared with aluminium with 6-coordination (octahedral). The aluminate and silicate are firmly tied by ion-covalent bonds.

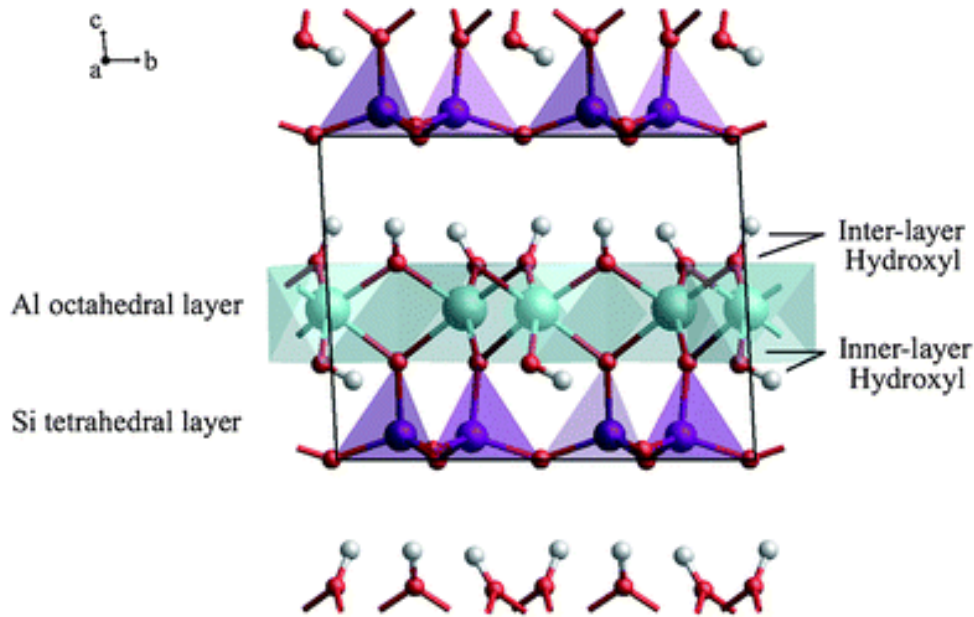


Figure 2. 12. Ideal layered structure of kaolinite (Sperinck et al., 2011)

### 2.15. Factors Affecting Erodibility of Unpaved Roads

The analysis of the published data has led to the identification of 47 factors that affect erosion of rural roads. Those factors have been grouped into geology and geotechnical factors, environment and climate factors, and road and traffic factors, as shown in Figure 2.13 and discussed in Tables 2.6, 2.7 and 2.8. The group of geology and geotechnical factors which refer to both the soils' properties and their characteristics is affected by the other two groups. For example, based on the literature, unpaved road soil behaviour changes with dry and rainy seasons (Ziegler et al., 2000). Also, traffic passes may increase the density or cause loosening of soils at the surface in the wheel paths depending on prevailing moisture content at the surface of unpaved road (Iverson, 1980; Ziegler et al., 2000; Cao et al., 2013).

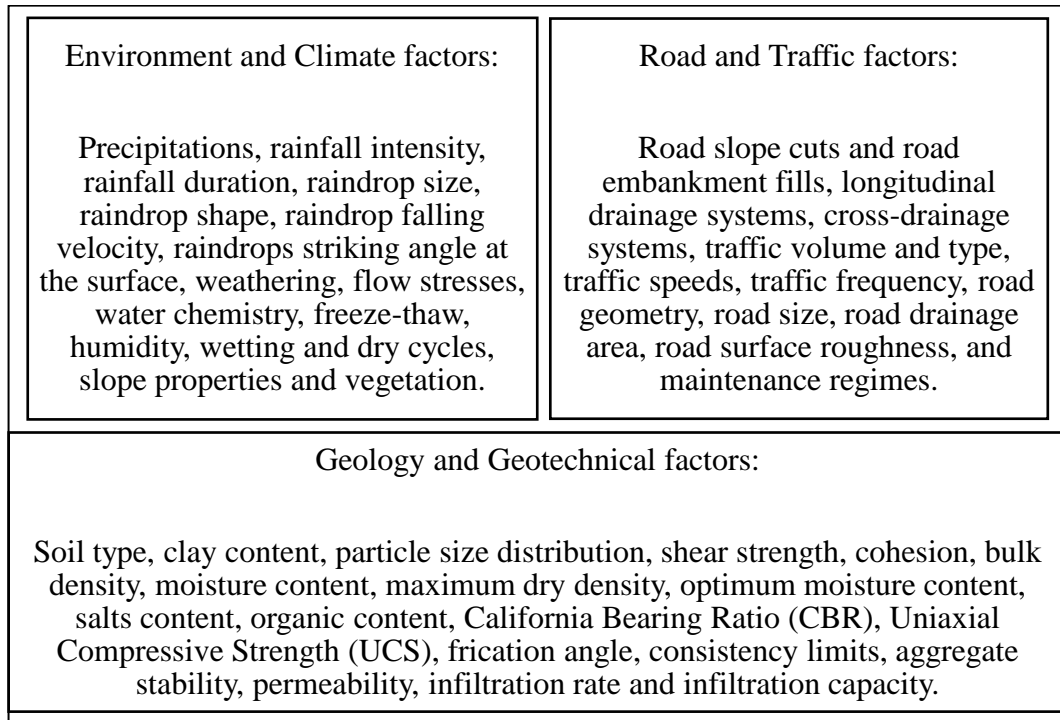


Figure 2. 13. Classification of factors that affect erosion

Furthermore, Figure 2.14 shows the number of the studies that investigated each factor. This information was useful to identify the factors that attracted more attention of the researchers than the others because of the higher effect of these factors on the erodibility of soils or because of the simplicity to study these factors. It also helped to know the factors that were less studied and that could probably be of greater emphasis if they are deemed to have significant effect in the understanding of the erodibility of unpaved roads. The uncertainties caused by using different definitions were avoided by focussing on the composition of the soils used. For example, the terms of unpaved, unsealed, unsurfaced, (engineered or native) earth, gravel, and dirty roads were used interchangeably by different studies with the same surface soils composition. Also, only the studies that used same testing methods were analysed together.

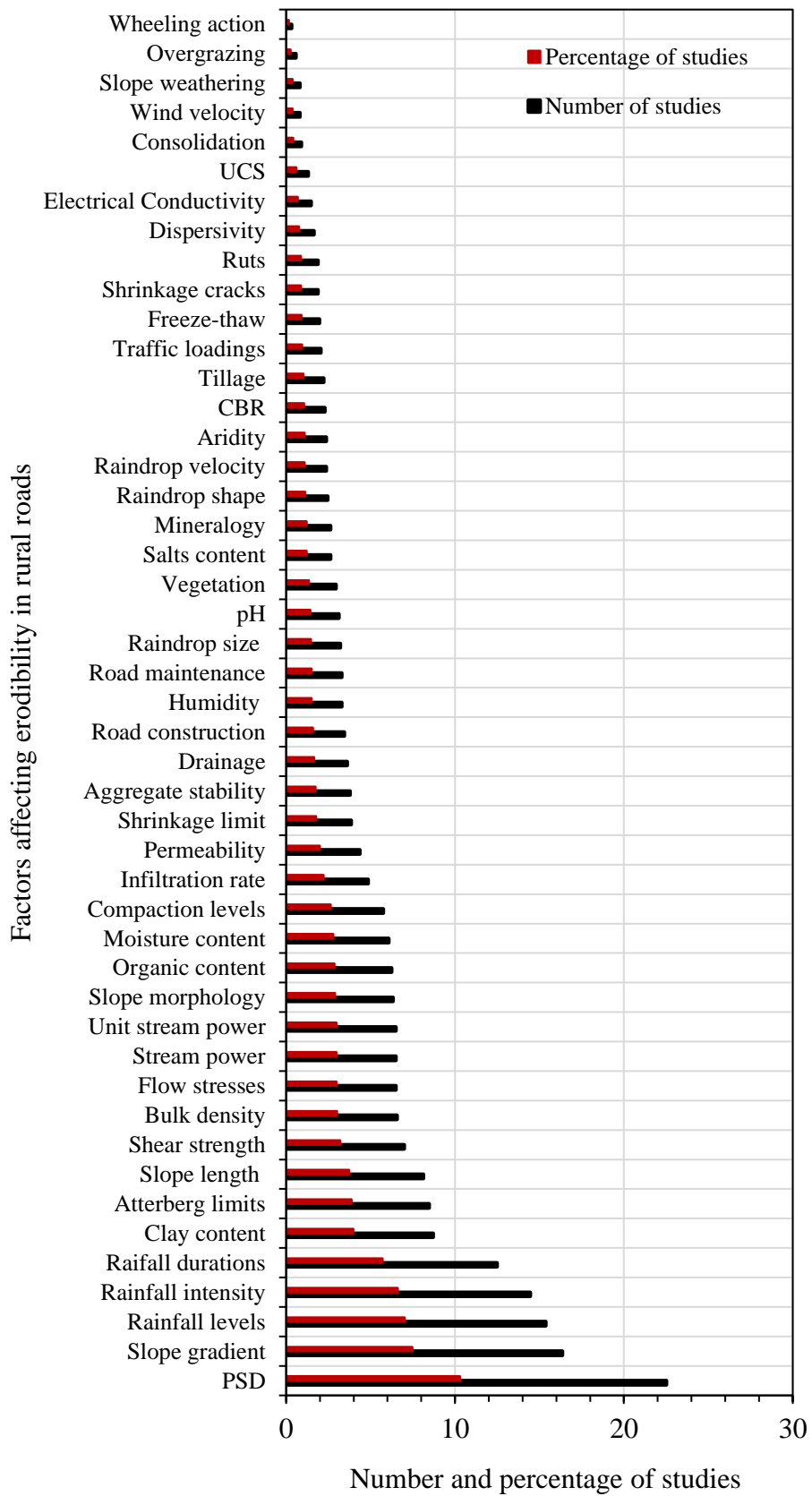


Figure 2. 14. Investigation of different factors that affect erodibility by studies

Table 2. 6. Geological and geotechnical factors of erodibility

Factors	Mechanisms	Observation
Soil type	Fines resist erosion due to cohesion, granular resist erosion due to gravity and size.	Ranges of rainfall energy for soil detachment are 80-360 micro-joules; 0.1-300 micro-joules and 40-950 micro-joules respectively for clay, silt and fine sand, and coarse sand and gravel soils [1-3].
Clay percentage	Cohesion increases with clay percentage.	Erodibility coefficients decline with increase of cohesion [4-8]
Consolidation	Consolidated clays erode at higher runoff velocities.	Unconsolidated clays detach at flow velocities of about 0.2 cm/s while consolidated clays may need up to 200 cm/s critical flow velocities [6-9].
PSD	Silt and fine sand soils erode more readily than clay and gravel soils.	Erodibility coefficient in rill erosion ( $K_r$ ) increases with silt percent increase: $K_r = (Silt \%)^{20.55}$ [5], [10-11].
Bulk density	Dry bulk density reduces detachment exponentially.	Detachment capacity ( $D_c$ ) and dry bulk density ( $dbd$ ) may be related exponentially by the relation $D_c = 6 * 10^6 e^{-0.01dbd}$ [4], [12].
Moisture content	Reduces the shear strength of soils.	Roads compacted with optimum moisture content are highly erosion resistant [13-14].
pH	High pH clays are dispersive.	If pH > 7.8 and exchangeable Na > 15%, clays are dispersive [15-16].
Salts content	Sodium (Na) and magnesium (Mg) define dispersive clays which are easily erodible.	If pH > 7.8 and exchangeable (Na + Mg) is 5 to 15%, clays are intermediately dispersive. If Na < 40%, clays are non-dispersive. If Na > 60%, pH > 7.8 and exchangeable (Na + Mg) > 15% clays are dispersive [15], [17-19].
Organic content	Soil loss reduces with increase in OC.	Detachment is in the range of 1.15 to 0.51 kg/m <sup>2</sup> /s for 1.23 to 5.64% organic content (OC) [2], [20-22].
Shear strength	More soil strength requires more eroding flow stresses.	Water stresses must rich critical stresses to defeat soil strength for erosion to occur [23-24].
CBR values	CBR values increase with increase of soil' strength.	High CBR values reflect high density and bearing capacity of roads [25-26].
Friction angle	Higher friction angles relate to lesser detachment.	Detachment increased with friction angles of 55° < 45° < 35° < 25° for same slope tangent [4], [27-28].
Plasticity	High Ip clays erode less.	High plastic silts may erode more than low plastic clays [5-6], [17].
Aggregate stability	The ability of soils to resist erosive stresses reduces detachment.	For example, detachment reduces from 1.8 to 0.7 kg/m <sup>2</sup> /s for soils with 7.09 to 24.32% water stable aggregate of 0.25 mm diameter [20], [29].
Permeability and Infiltration	Greater infiltration tends to lessen erosion.	Infiltration decreases with more particles smaller than 0.125 mm [30-32].

Citations listed in Table 2.6: [1] Kukal et al., 1991; [2] Knapen et al., 2007; [3] Foltz et al., 2008; [4] Bryan, 2000; [5] Wang et al., 2014; [6] Li et al., 2015; [7] Carey and Simon, 1984; [8] Reichert et al., 2001; [9] Salles et al., 2000; [10] Edwards et al., 2000; [11] Crim et al., 2003; [12] Yu et al., 2014; [13] Hanson and Hunt, 2007; [14] Choudhary et al., 1997; [15] Paige-Green, 2008; [16] Gidigas, 1972; [17] Briaud, 2008; [18] Paige-Green et al., 2015; [19] Boardman, 1983; [20] Ekwue, 1991; [21] Chowdary et al., 2012; [22] Nearing and Bradford, 1985; [23] Paige-Green, 2003; [24] Yarbař et al., 2007; [25] Behak, 2011; [26] Hossain, 2011; [27] Torri and Poesen, 1992; [28] Moore, 2001; [29] Jordán et al., 2010; [30] Morin and Benyamin, 1977; [31] Elliot, 1988; [32] Greene and Hairsine, 2004.

Table 2. 7. Environmental and climatic factors of erodibility

Factors	Mechanisms	Observation
Climate	Higher rainfall tends to increase erosion rates.	Wet and humid areas are more erodible than dry areas, though the latter may suffer from wind erosion [1-4].
Rainfall amount, rainfall intensity and rainfall duration	High rainfall tends to result in high total erosion.	Detachment, runoff, and erosion increase with total rainfall, its intensity and duration. Detachment increased from 0.5 to 1.8 kg/m <sup>2</sup> /s between the 4 <sup>th</sup> - and 18 <sup>th</sup> -minute of rainfall on a sand silty soil [5-9].
Raindrop properties	Drop size, shape, falling height and falling angle determine rainfall energy.	Bigger, round, and high falling raindrops have more kinetic energy and detachment [10-11].
Weathering	It softens soils.	Desiccation weakens soils [12-15].
Flow shear stresses	More stresses cause more erosion.	Sheet, rill, and gully erosions depend on overland flow stresses [16-18].
Water chemistry	pH and salts affect erosion.	Dispersive clay deflocculates with water; saline water dissolves calcium (C <sub>a</sub> ) to reduce cohesion [14], [19-20].
Wind properties	Wind direction and intensity accelerate erosion of slopes.	Wind rises erosion 3-12 times. Detachment rises to 2.7 times if wind rises from 0-25 mph [21-24].
Topography	Erosion increases with the slope length.	A 15-years survey showed more sediment from a 125 m slope than from a 70 m slope [25-26].
Slope gradient	Increases erosion, reduces infiltration.	Flow velocity and stresses increase with gradient [4-6], [27].
Freeze and thaw	Dry-wet cycles boost detachment and erosion.	Dry-wet cycles lead to about 15% aggregates loss in asphalt roads and more than 50% excessive erosion thaw-weakened soils [28-29].
Land use	Roads accelerate erosion more than other land uses.	Roads increase erosion 3-8 times. About 0.5% unpaved road and about 12% agriculture land uses in an area generate equal sediment [30-31].
Stream power	This is all about energy dissipation on both beds and banks of ruts and rills.	In forest roads for example, erosion rates increase with stream power due to big ruts and rills created by forest harvesting traffic wheels [32-35].
Flow depth	Detachment and rill erosion may reduce with surface flow depth increase.	From about 0.1 to 0.005 kg/m <sup>2</sup> /s when the flow depth increased from 2 to 16 mm. Rain energy is partially dispersed by water layer [32], [36-37].

Citations listed in Table 2.7: [1] Favis-Mortlock and Boardman, 1995; [2] Issa et al., 2006; [3] Luo et al., 2013; [4]Cao et al., 2013; [5] De Figueredo and Poesen, 1998; [6] Arnaez et al., 2007; [7] Sheridan et al., 2008; [8] Liu et al., 2010; [9] Arthur et al., 2011; [10] Obi and Salako, 1995; [11] Agassi and Bradford, 1999; [12] Paige-Green, 1999; [13] Paige-Green, 2003; [14] Paige-Green, 2008; [15] Paige-Green et al., 2015; [16] Knapen et al., 2007; [17] Briaud, 2008; [18] Cao et al., 2011; [19] García-Ruiz et al., 1997; [20] Nagy and Nagy, 2015; [21] Lyles et al., 1974; [22] Shao and Lu, 2000; [23] Choi, 2002; [24] Aksoy and Kavvas, 2005; [25] El-Swaify, 1997; [26] Walling and Probst, 1997; [27] Fox et al., 1997; [28] Akbulut and Güreç, 2007; [29] Van Klaveren and McCool, 2010; [30] Dickey et al., 1984; [31] Anderson and MacDonald, 1998; [32] Nearing et al., 1991; [33] Zhang et al., 2001; [34] Cao et al., 2009; [35] Zhang et al., 2015; [36] Torri et al., 1987; [37] Foltz et al., 2008.

Table 2. 8. Road factors of erodibility

Factors	Mechanisms	Observation
Management of the watershed in which the road is located	Bare soils erode more than vegetated soils.	Activities such as construction, agriculture, and overgrazing increase erosion [1-4].
Cutting and filling during construction	Modify topography and hydrology processes. The geomorphology is affected. Usually, more erosion happens in convexo-concave and concave slopes.	Road may generate 85 to 90% catchment sediment; 5% unpaved roads in a catchment dominate all other sediment producers. Recommended cut slope heights are about 0.6 m, 1.5 m, 3 m, and 7.5 m respectively for hillslopes gradients smaller than 15%, ranging from 15% - 30%, ranging from 30% - 60% and greater than 60% [5-12].
Drainages and slopes	Improved drainages, appropriate transverse and longitudinal slopes reduce erosion.	Longitudinal and cross drainages are essential in reducing erosion from roads. Longitudinal slopes of about 6% and cambers of about 4% are appropriate for less surface material loss due to water erosion in unpaved roads [13-18].
Maintenance	Poor maintenance may bring new and loose erodible soil materials to the surface.	Loose soils put on road surface can be carried away by surface flows easily, leading to quick formation of rills in the road' surface [9-11], [19-22].
Traffic	Hasten soil detachment and formation of ruts leading to rills and gullies.	Loosening of particles, widening, and deepening of rills by wheels' activity lead to increased soil detachment and sediment transport in unpaved roads [19-21], [23-27].
Surface cover and roughness	Vegetation covered and rough surfaces resist water velocity and stress. Gravel covered surfaces resist rainfall energy but promote infiltration which may lead to weakening of deeper road layers.	Vegetation reduces rain energy, improves infiltration by roots' penetration, and reduces flow velocities and stresses. However, vegetation with deep roots should be quickly removed from the road surface since it can lead to greater penetration of water, and deeper softening and loss of strength to greater depths. Roughness due to surface particles may reduce surface flow velocities and erosion [28-32].

Citations listed in Table 2.8: [1] Bryan et al., 1989; [2] Lane and Sheridan, 2002; [3] Liu et al., 2010; [4] Liu et al., 2016; [5] Kukal et al., 1991; [6] Dubé et al., 2004; [7] Brooks et al., 2006; [8] Rijdsdijk et al., 2007; [9] Cao et al., 2009; [10] Foltz et al., 2009; [11] Cao et al., 2013; [12] Katz et al., 2013; [13] Jungerius et al., 2002; [14] Keller and Sherar, [2003]; [15] Ramos-Scharrón and McDonald, 2005; [16] Petts et al., 2006; [17] Katz et al., 2011; [18] Petts, 2013; [19] Ziegler et al., 2000; [20] Ziegler et al., 2001; [21] Ziegler et al., 2004; [22] Petts, 2013; [23] Iverson, 1980; [24] Nearing et al., 1991; [25] Zhang et al., 2001; [26] Cao et al., 2009; [27] Zhang et al., 2015; [28] Elwell and Stocking, 1976; [29] Boardman, 1983; [30] Giménez and Govers, 2002; [31] Le Bissonnais et al., 2005; [32] Gabet and Sterberg, 2008.

## 2.16. Analysis of the Major Factors Affecting Erodibility of Unpaved Roads

Major factors analysed include clay content, plasticity index, particle size distribution, mean grain size, rainfall, rainfall intensity, rainfall duration, and road and traffic factors.

### 2.16.1. Erodibility and Clay Content

Clay content significantly influences erodibility of soils (Bryan et al., 1989; Bryan, 2000; Haghghi et al., 2013). The increase in clay content increases both the plasticity of the soil matrix and the cohesion between soil particles, which resist the detachment due to both the raindrops' kinetic energy and the surface flow shear stresses. For a given moisture content, high plasticity clays exhibit lower erosion compared to lower plasticity soils. Moreover, soils with higher clay contents usually require more kinetic energy and higher critical shear stresses for the detachment and henceforth erosion to be initiated. A detailed analysis using eleven soils investigated by Knapen et al. (2007) and Haghghi et al. (2013) has led to the understanding of erosion rate versus shear stresses; erosion rate versus plasticity index; and plasticity index versus critical shear stresses, as shown in Figures 2.15, 2.16, 2.17 and 2.18.

Based on the data extracted from the literature, Figure 2.15 shows the results of erosion rate versus shear stress from laboratory erosion tests. The details of the tested soils in terms of composition, plasticity, number of samples, and correlations between erosion rate and shear stress are shown in Table 2.9. The data shows that clay soils do not erode readily as higher critical shear stresses are required due to much cohesion compared to loamy sand and silty loam, which not only erode at lower critical shear stresses but also have more erosion rates. At critical shear stresses smaller than  $5 \text{ N/m}^2$ , loamy sand (a) and silty loam (a) reached erosion rate greater than  $0.1 \text{ kg/m}^2/\text{s}$  while clay (cc) did not reach erosion rate of  $0.05 \text{ kg/m}^2/\text{s}$  at shear stresses greater than  $150 \text{ N/m}^2$ . The increased clay content effect in reducing erodibility of soils

was previously said in studies by Carey and Simon, 1984; Reichert et al., 2001; Briaud, 2008; Wang et al., 2014; Yu et al., 2014; and Li et al., 2015.

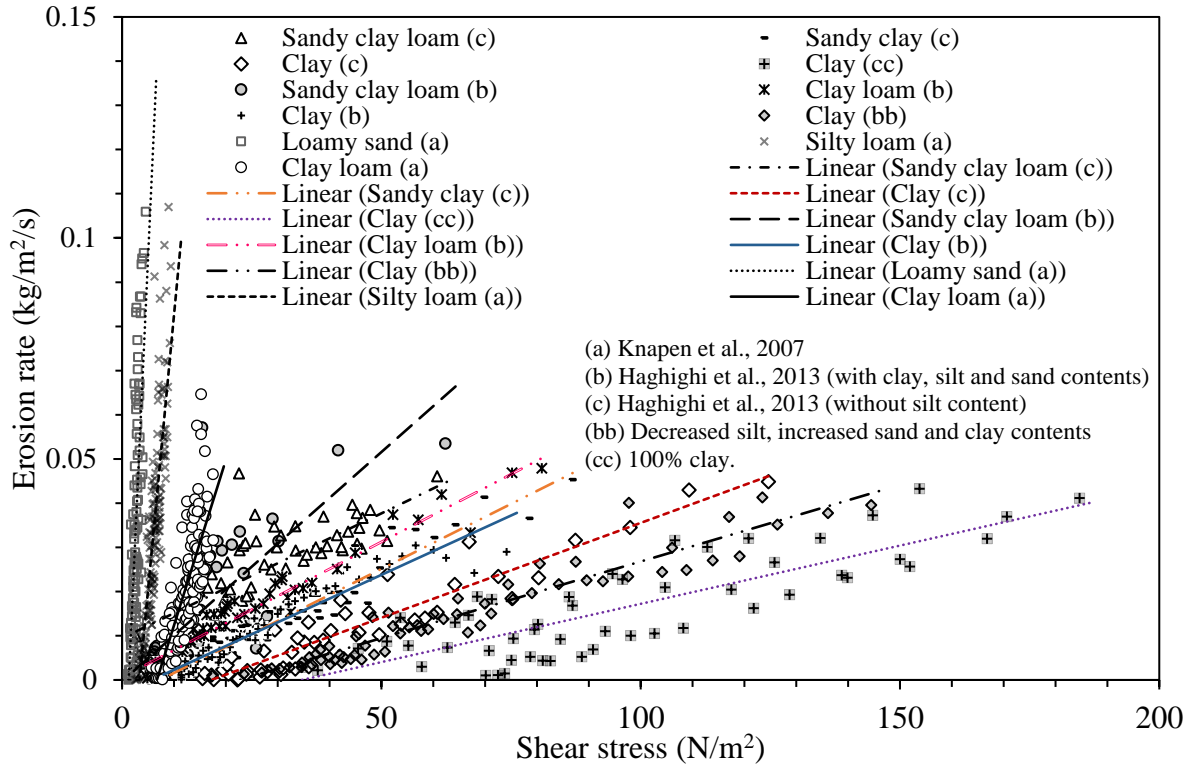


Figure 2. 15. Erosion rate as a function of shear stresses and clay content

Table 2. 9. Composition of the soils in Figure 2.15 and the regression lines' equations

Soil type	C	M	S	W <sub>L</sub>	W <sub>P</sub>	I <sub>P</sub>	N	Relationships $E_r$ and $\tau$
Loamy sand <sup>a</sup>	-	-	-	-	-	0.2*	94	$E_r = 0.0257\tau - 0.0333$ ; $R^2 = 0.477$
Silty loam <sup>a</sup>	-	-	-	-	-	0.3*	140	$E_r = 0.0124\tau - 0.0419$ ; $R^2 = 0.707$
Clay loam <sup>a</sup>	-	-	-	-	-	3.2*	118	$E_r = 0.0037\tau - 0.0251$ ; $R^2 = 0.593$
Sandy clay loam <sup>b</sup>	25	5	70	13.5	-	4.5*	42	$E_r = 0.001\tau - 0.0003$ ; $R^2 = 0.6185$
Sandy clay loam <sup>c</sup>	30	0	70	16.9	11.5	5.3	64	$E_r = 0.0006\tau - 0.0095$ ; $R^2 = 0.572$
Clay loam <sup>b</sup>	35	25	40	19.6	13.9	5.7	60	$E_r = 0.0006\tau - 0.0006$ ; $R^2 = 0.949$
Clay <sup>b</sup>	45	40	15	26.9	20.4	6.5	51	$E_r = 0.0006\tau - 0.0006$ ; $R^2 = 0.949$
Sandy clay <sup>c</sup>	50	0	50	23.8	16.7	7.1	52	$E_r = 0.0006\tau - 0.0043$ ; $R^2 = 0.916$
Clay <sup>c</sup>	70	0	30	31.2	21.3	9.9	49	$E_r = 0.0004\tau - 0.0074$ ; $R^2 = 0.901$
Clay <sup>bb</sup>	65	5	30	26.1	21.7	4.4	63	$E_r = 0.0003\tau - 0.0079$ ; $R^2 = 0.915$
Clay <sup>cc</sup>	100	0	0	41.3	30.2	11.1	52	$E_r = 0.0003\tau - 0.0091$ ; $R^2 = 0.688$

<sup>a</sup>, <sup>b</sup>, <sup>bb</sup>, <sup>c</sup> and <sup>cc</sup> as explained in Figure 2.15; C: clay (kaolin, %), M: silt (%), S: sand (%), W<sub>L</sub>: liquid limit (%), W<sub>P</sub>: plastic limit (%), I<sub>P</sub>: plasticity index (%); x\*: predicted I<sub>P</sub>, n = number of samples

From Table 2.9, the plasticity index of loamy sand, silty loam, clay loam and sandy clay loam was predicted as it was not given by the studies. This is explained in the next section 2.15.2. Generally, plasticity index increases with the increase of clay content. However, the silt content can also influence the plasticity. The example is for clay <sup>bb</sup> and sandy clay <sup>c</sup>. The former has 65% clay content, 5% silt content and a plasticity of 4.4%, while the latter has 50% clay content and 0% silt content but a greater plasticity of 7.1%. The correlations between erosion rate and shear stress are generally meaningful ( $R^2 > 0.5$ , except for loamy sand) and show that erosion can only occur if a given critical shear stress is attained. This is shown by negative values of erosion rate if the shear stress equates zero in the relationship between erosion rate and shear stress, as shown in Table 2.9. Also, the correlation equations show that erosion rate increases with the increasing shear stress.

Figures 2.16 relates the mean erosion rate to the plasticity index. The mean erosion rate and the mean critical shear stress were calculated for each soil reported in Figure 2.15 (Knapen et al., 2007; Haghghi et al., 2013). Generally, a high plasticity index corresponds to a low erosion rate and a need for higher critical stress. The correlation equation in Figure 2.16 is meaningful ( $R^2 = 0.7454$ ) but should only be applied to soils of plasticity indices ranging from about 0.2% to about 11.1% considered by the studies presented in Figure 2.15.

In Figure 2.17, the gradient is the ratio of the erosion rate to shear stress and decreases with an increase of the plasticity index ( $R^2 = 0.9276$ ) to indicate the decrease in erodibility with an increase in clay content. Examples are clay <sup>bb</sup> and clay <sup>c</sup> which differ in their erosion, with the former's plasticity index being less than half of the latter's only because 5% of the clay in the latter was replaced by 5% of the silt in the former (Table 2.9).

Figure 2.18 shows that gradient decreases with an increase in critical shear stress, which means that there is need for higher critical stress and lower erosion for highly cohesive soils. The stronger correlation between the gradient and the plasticity index ( $R^2 = 0.9276$ , Figure 2.17) than between the gradient and critical shear stress ( $R^2 = 0.7341$ , Figure 2.18) shows that although good correlations were drawn between the erosion rate and critical shear stress, plasticity offers an alternative option for erodibility analysis. Using plasticity index for erodibility analysis can be an advantage since it is easy to determine this property in the laboratory than it is for critical shear stress.

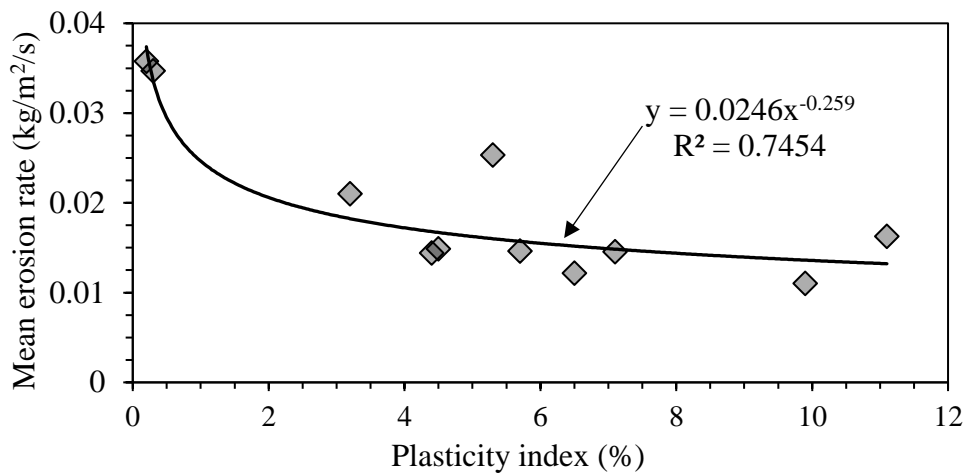


Figure 2. 16. Erosion rate as a function of the plasticity of soils

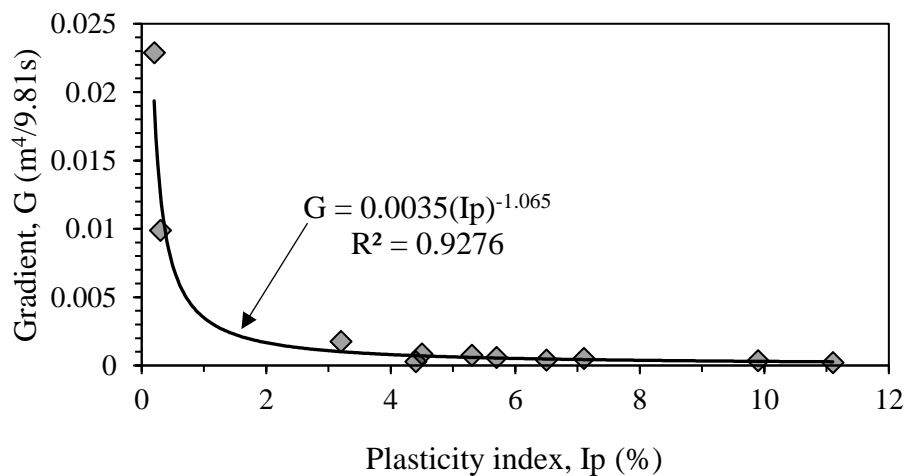


Figure 2. 17. Gradient and plasticity index

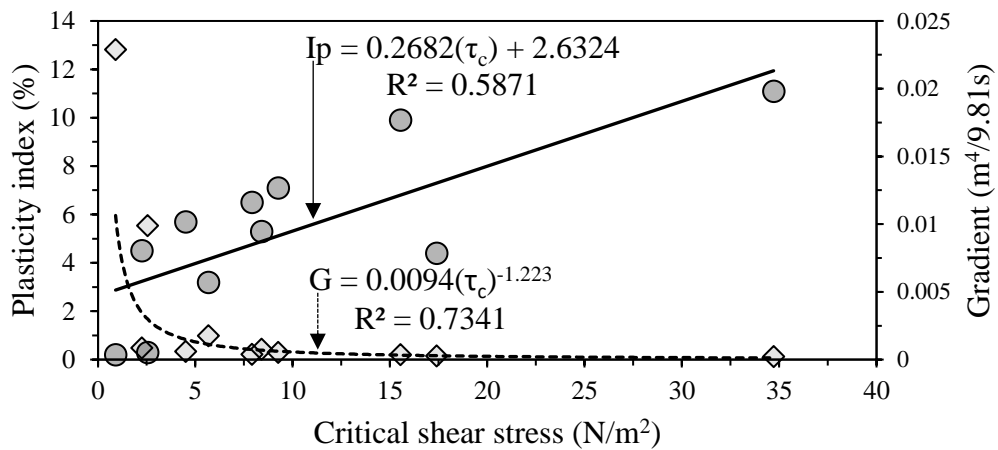


Figure 2. 18. Plasticity and gradient of erodibility as functions of critical shear stress

Figure 2.19 shows the mean erosion rates plotted against the mean shear stresses. A logarithmic correlation ( $R^2 = 0.622$ ) was found between the two parameters and it shows that mean erosion rate decreases from the soils of smaller mean critical shear stress to the soils of higher critical shear stress. The mean critical shear stress for loamy sand <sup>a</sup> is about 2.7 N/m<sup>2</sup> and caused a mean erosion rate of about 0.036 kg/m<sup>2</sup>/s compared to about 96.4 N/m<sup>2</sup> and about 0.016 kg/m<sup>2</sup>/s for clay <sup>cc</sup>. However, the correlation line shows higher decreases of mean erosion rate for soils that require less than about 25 N/m<sup>2</sup> mean critical shear stress or soils with less clay content and lower plasticity (loamy sand <sup>a</sup>, silty loam <sup>a</sup>, clay loam <sup>a</sup>, sandy clay loam <sup>b</sup>, clay loam <sup>b</sup> and sandy clay loam <sup>c</sup>). This is highlighted by the envelope (A) which shows a steady decrease of the mean erosion rate as the mean critical shear stress increases. The mean erosion rate decrease decreases for soils that need mean critical shear stress greater than about 25 N/m<sup>2</sup> (clay <sup>b</sup>, sandy clay <sup>c</sup>, clay <sup>c</sup>, clay <sup>bb</sup> and clay <sup>cc</sup>) with likelihood of the correlation line to almost flatten for soils that need more than 100 N/m<sup>2</sup> critical shear stress (high and extremely plastic clays) due to their high resistance to erosion stresses. This is indicated by the envelope (B) which shows a gentle decrease of the mean erosion rate as the mean critical shear stress increases.

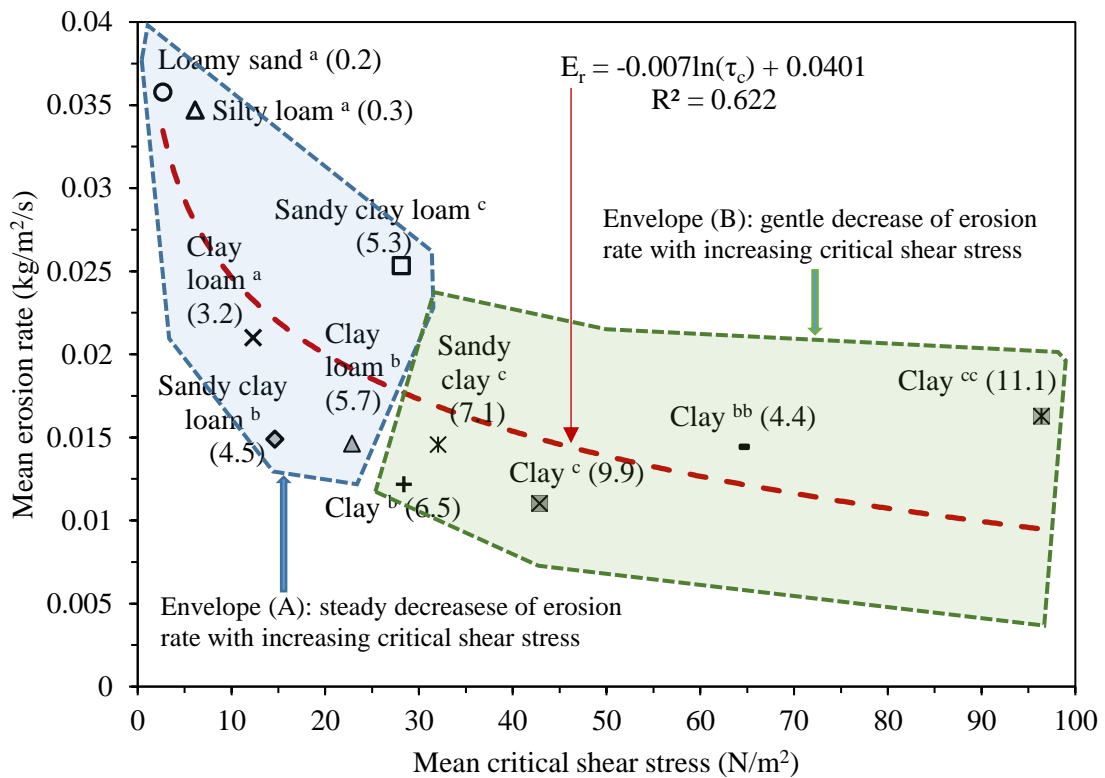


Figure 2. 19. Mean erosion rate and critical shear stress. Plasticity index is in parentheses

### 2.16.2. Erodibility and Plasticity Index

Knapen et al. (2007), Haghghi et al. (2013) and Crim et al. (2003) confirmed a general increase in critical shear stress with an increase in the plasticity index for low plastic soils ( $1 \leq I_p < 7$ ), medium plastic soils ( $7 \leq I_p < 17$ ), high plastic soils ( $17 \leq I_p \leq 35$ ), and extremely plastic soils ( $I_p > 35$ ), as shown in Figures 2.19, 2.20 and 2.21. However, some soils showed that although they have a high plasticity index, these soils erode at very small critical shear stresses. This could be due to high silt content since silt particles are easily detachable (Salles et al., 2000; Briaud, 2008), high moisture content and high organic content which lower the soil' strength (Crim et al., 2003; Knapen et al., 2007). Examples of those soils include silts of high plasticity, soft clays, clayey silty and sandy soils, organic clays and organic silts, and some of those were described in the field as brown, dark brown, grey clay and silt soils (Crim et al., 2003).

Figure 2.20 relates the critical shear stress and plasticity index for soils with clay, silt and sand contents (Crim et al., 2003; Knapen et al., 2007; Haghghi et al., 2013); clay and sandy soils (Haghghi et al., 2013); and soils at different compaction levels as shown by N-values where N is the number of blows to penetrate 300 mm from the standard penetration test (Chen and Cotton, 1988), namely loose soils (N ranges from 4 to 10), medium compact soils (N ranges from 10 to 30) and compact soils (N ranges from 30 to 50). Moreover, Figure 2.20 agrees with the work of Crim et al. (2003) that critical shear stress ( $\tau_c$ ) increases with plasticity index. It was noted that critical shear stress increases as the gradient (G) decreases, while the plasticity index increases as the gradient decreases. Therefore, it can be deduced that cohesive soils need high critical shear stress, though these soils usually have low erosion rates.

Granular soils show high erosion rates at small critical shear stress, which decreases as soil particle size increases (Carey and Simon, 1984). Some of the soils considered in Figure 2.15 did not have plasticity index values (Knapen et al., 2007; Haghghi et al., 2013). These were predicted based on soil descriptions and on the plasticity index of sandy clay loam <sup>c</sup> and clay <sup>cc</sup> which were 5.3% and 11.1% respectively. Using the plasticity index values of these two soils and the erosion rates registered for these soils and based on the erosion rates obtained for the soils with unknown plasticity index; excel software was used to predict the plasticity index for the latter soils. Henceforth, the plasticity index values have been obtained for loamy sand <sup>a</sup>, silty loam <sup>a</sup>, clay loam <sup>a</sup> and sandy clay loam <sup>b</sup>, as shown in Table 2.9.

Upon having the plasticity index values for all the soils in Table 2.11, their mean critical shear stresses and their mean erosion rates, as shown in Figure 2.19, Equation 2.1 to predict erosion rate ( $E_r$ ) in terms of shear stress ( $\tau$ ) and plasticity index ( $I_p$ ) was then developed:

$$E_r = \frac{7.1 + 0.0573\tau - I_p}{121.01} \quad (\text{Eq. 2.1})$$

Equation 2.1 was used to develop a prediction chart of erosion rates when the plasticity index and shear stress are known, as in Figure 2.21. The chart gives critical shear stress that initiates erosion when the predicted erosion rate equates to zero. Overall, the prediction chart shows that non-plastic and low plastic soils erode at critical shear stresses as small as 0.0001 N/m<sup>2</sup>; while extremely plastic soils need critical shear stresses that are greater than 485 N/m<sup>2</sup>. The area comprising soils that require critical shear stress smaller than 100 N/m<sup>2</sup> is of interest to unpaved roads due to recommended plasticity indexes for the surface layer of those roads. Keller and Sherar (2003) and Paige-Green et al. (2015) recommend a plasticity index smaller than 10% for unpaved roads while ASANRA (2013) and Shearer et al. (2013) recommend up to about 12% for gravel roads. Ideal plasticity index of 6% for unpaved road surface soils was recommended by the studies by Keller and Sherar (2003), Shearer et al. (2013) and Paige-Green et al. (2015).

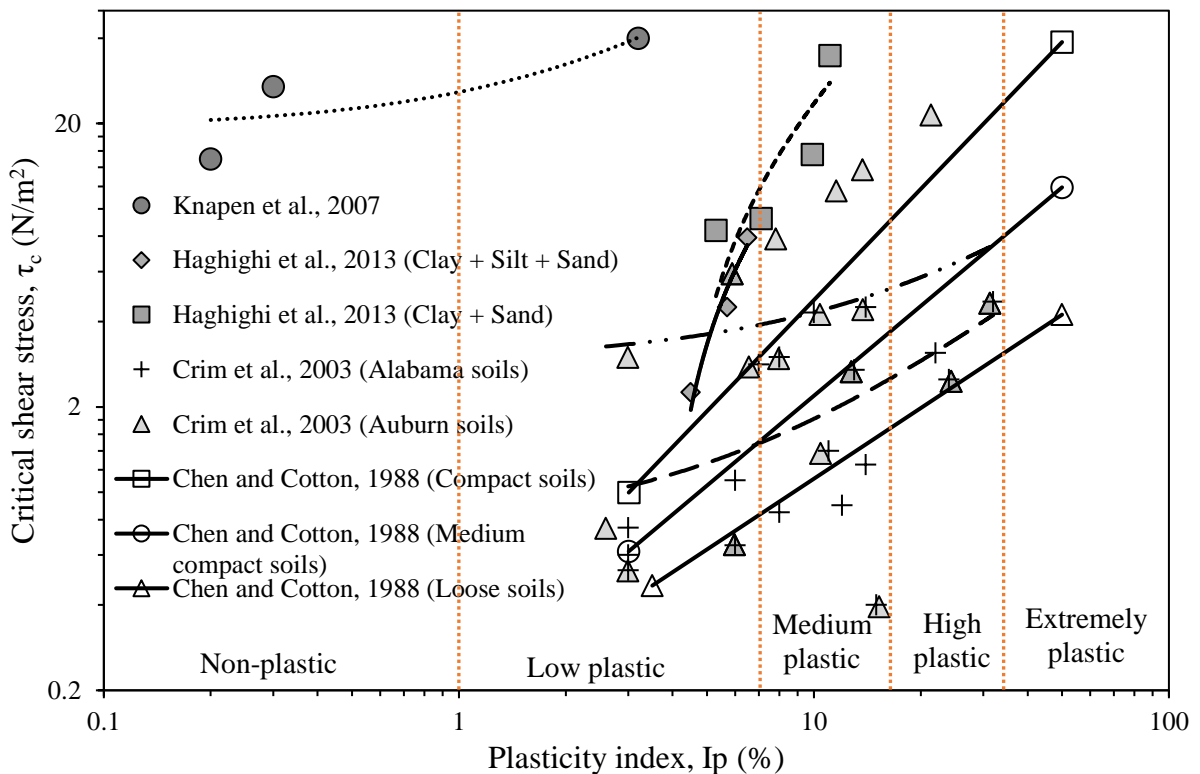


Figure 2. 20. Critical shear stress as a function of the plasticity of soils

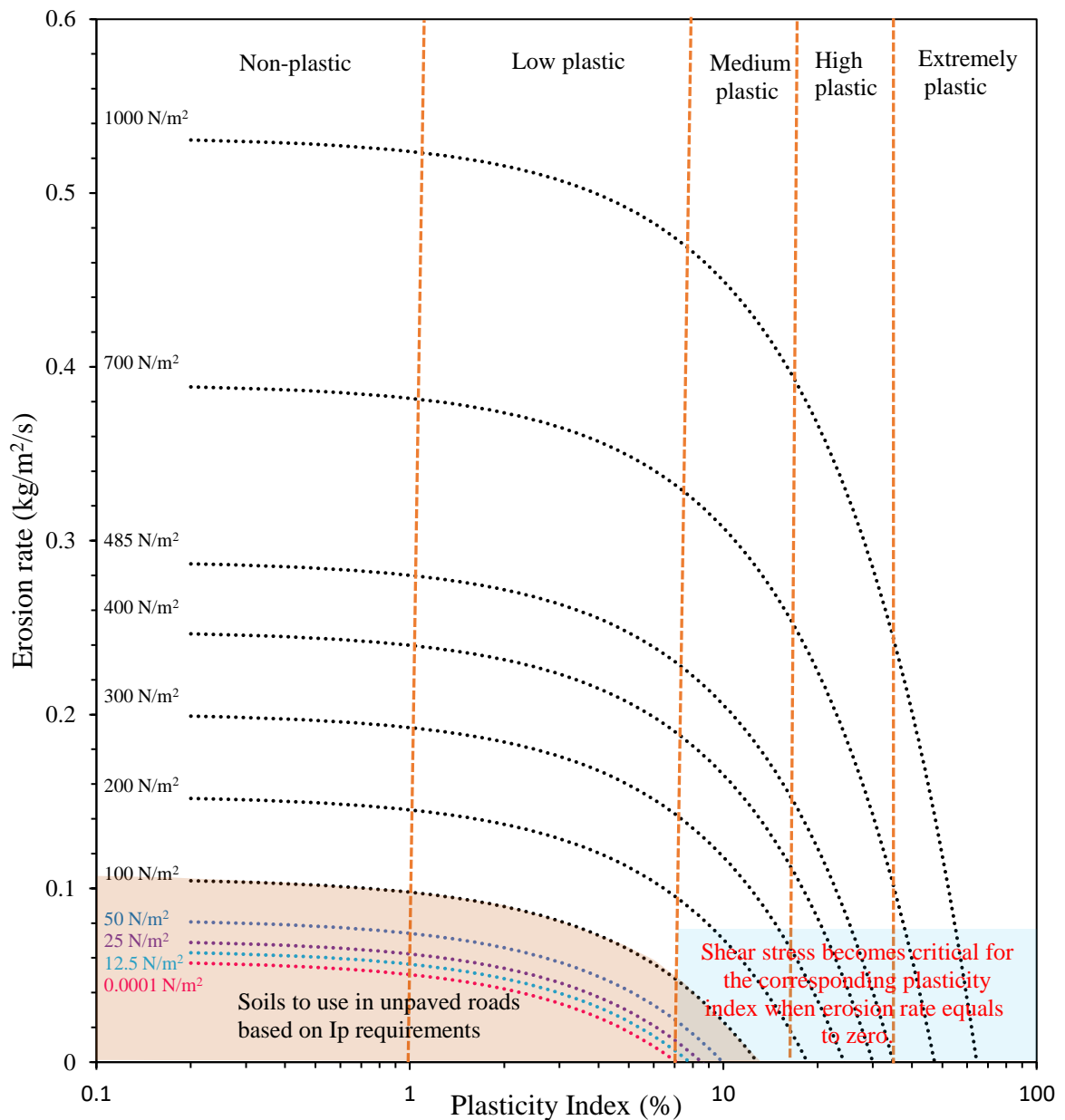


Figure 2. 21. Erosion rate, plasticity index and critical shear stress

### 2.16.3. Erodibility and Particle Size Distribution

Particle size distribution is the key property to assess the suitability of soils for use in the construction of unpaved roads. It affects the degree of compaction of a soil and hence both shear strength (hence bearing capacity) and erodibility to control the performance of the road. Salles et al. (2000) proposed an envelope for the thresholds of the raindrops' energy required to detach the soils in relation to the soil's mean particle size. Salles et al. (2000) considered both the

results from the laboratory experiments and the results by different researchers (Ekern and Muckenhim, 1947; McCarthy, 1980; Kerényi, 1981; Sharma and Gupta, 1989; Sharma et al., 1991), as shown in Figure 2.22. The envelope shows that soils of about  $0.02 \text{ mm} \leq D_{50} \leq 0.7 \text{ mm}$  (silt and fine sand) can be detached by raindrops' kinetic energy smaller than about  $280 \mu\text{J}$ . The energy then increases to about  $200 \mu\text{J} - 330 \mu\text{J}$  for soils of about  $D_{50} < 0.001 \text{ mm}$  and a range of about  $50 \mu\text{J} - 850 \mu\text{J}$  for the soils of about  $0.08 \text{ mm} \leq D_{50} \leq 7 \text{ mm}$ . Since granular soils are predominantly used for road construction, soils of about  $0.08 \text{ mm} \leq D_{50} \leq 7 \text{ mm}$  can be of a better resistance to detachment due to raindrops' kinetic energy. Carey and Simon (1984) had developed an envelope for critical flow velocities for erosion with respect to the particle size of soils, as shown in Figure 2.22. The envelope shows that silt and fine sand can erode at smaller velocities ranging from about  $0.15 \text{ cm/s}$  to  $2 \text{ cm/s}$ . Critical flow velocities can range from about  $0.16 \text{ cm/s}$  to  $110 \text{ cm/s}$  for clay soils and from about  $2 \text{ cm/s}$  to  $110 \text{ cm/s}$  for gravel soils. Both the envelopes show that gravel soils can better resist erosion due to rainfall and surface flow.

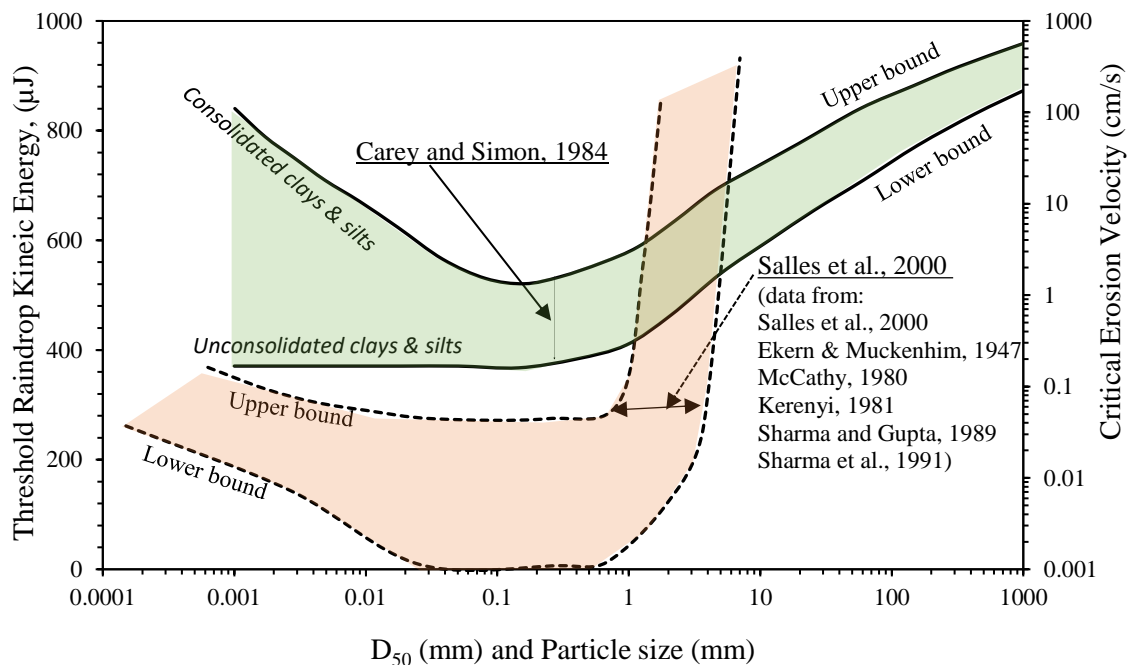


Figure 2. 22. Threshold raindrop kinetic energy and critical erosion velocity versus mean particle size of the soil

Critical shear stress and the mean particle size relationships for clay, silt, sand, and gravel soils were developed as can be seen in Figure 2.23. Based on the results from the studies by Briaud (2006, 2008) and Briaud et al. (2001); Briaud (2008) reported that fine sand soils are the most erodible soils. Briaud (2008) further showed that critical shear stresses for fine soils are generally bound by two lines that form a V-shape and decrease from clay soils to fine sand soils. The lower line has critical shear stress of about  $2 \text{ N/m}^2$  at  $D_{50} = 0.0001 \text{ mm}$ , which reduces to about  $1 \text{ N/m}^2$  at  $D_{50} = 0.1 \text{ mm}$ . This line can be defined by  $\tau_c = 0.05(D_{50})^{-0.4}$ . The upper line for those soils has a critical shear stress of about  $1000 \text{ N/m}^2$  at  $D_{50} = 0.001 \text{ mm}$ , which reduces to about  $0.3 \text{ N/m}^2$  at  $D_{50} = 0.15 \text{ mm}$ . This line can be defined by  $\tau_c = 0.006(D_{50})^{-0.2}$ . For sand and gravel soils, Briaud (2008) found that critical shear stress and mean particle size are roughly equal, though of different units. Furthermore, the two properties were related by a line defined by  $\tau_c = D_{50}$ . This line shows increasing critical shear stress from about  $0.15 \text{ N/m}^2$  at  $D_{50} = 0.15 \text{ mm}$  to about  $10 \text{ N/m}^2$  at  $D_{50} = 10 \text{ mm}$ . A curve by Shields in 1936 was also given by Briaud (2008) and shows minimum critical shear stress of about  $0.1 \text{ N/m}^2$  at  $D_{50} = 0.1 \text{ mm}$  increasing to about  $10 \text{ N/m}^2$  at  $D_{50} = 10 \text{ mm}$ .

During this study, the data from Sheppard et al. (2006) and Crim et al. (2003) was added to the Briaud (2008)' diagram. This data confirmed that fine sand soils are the most erodible soils. A logarithmic relationship between silt and fine sand soils was developed and shows that critical shear stress of about  $1.2 \text{ N/m}^2$  at  $D_{50} = 0.025 \text{ mm}$  reduces to about  $0.5 \text{ N/m}^2$  at  $D_{50} = 0.3 \text{ mm}$ . The logarithmic relationship for this change of critical shear stress from silt to sand can be given by  $\text{Log}(\tau_c) = 0.41 - 2.69D_{50}$ . Moreover, based on the minimum and maximum  $D_{50}$ , a location for rural road surface material suggested in Figure 2.32 was proposed.

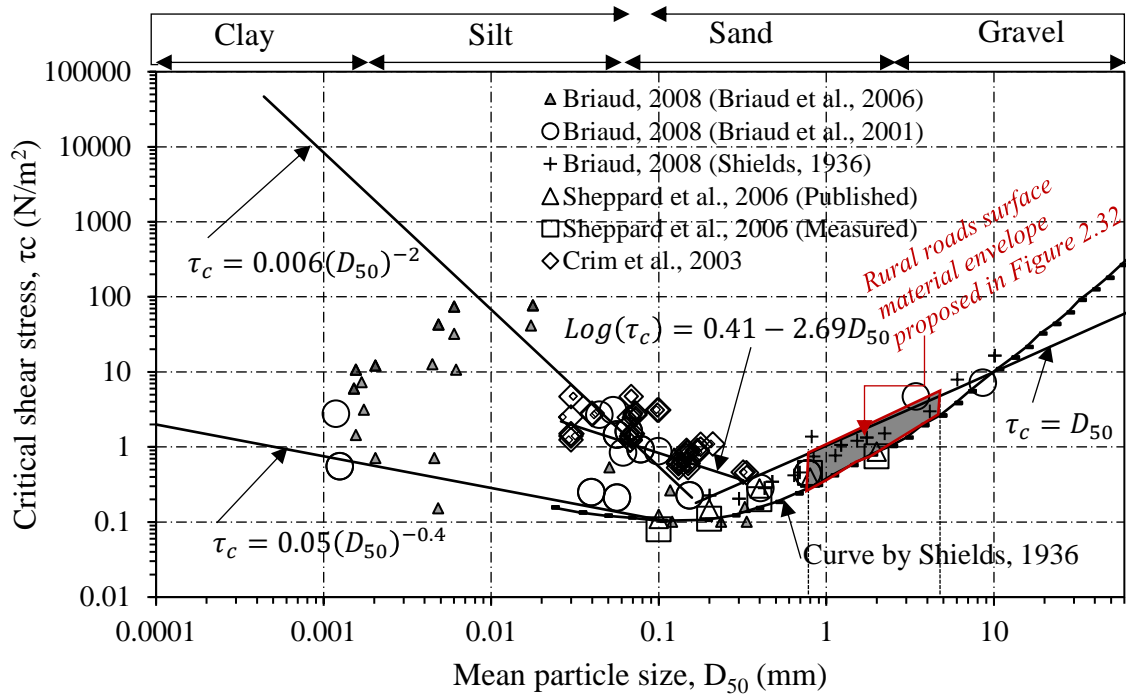


Figure 2.23. Critical shear stress versus mean particle size of soils

The soil texture is mainly associated with the soil's particle size distribution. The coefficient of erodibility (K-value) which is the measure of the effects of soil properties and the surrounding environment on the soil loss was measured for different soil textures. Although it is difficult to measure K-values in the laboratory; these mainly depend on eroded soils, rain erosivity, surface cover, slope gradient and length (Van der Knijff et al., 1999). Wischmeier and Smith (1978) elaborated a soil-erodibility nomograph (Appendix 1, Figure 1) which can help approximate K-values based on the content of silt and very fine sand, sand, organic matter, soil structure and permeability. The nomograph may be less helpful in unpaved roads since it does not consider the key factors in road construction such as particle size distribution, mean particle size, clay content, density and strength of soils, and slopes. K-values are better for measure of average long-term erodibility of agricultural soils due to sheet and rill erosions (Bryan et al., 1989). Thus, it seems that only extensive laboratory and field erodibility tests can help understand erodibility of soils in roads. K-values only give an indication of erodibility, but the problem in

unpaved road is to quantify soil loss so that maintenance can be planned accordingly. Therefore, erosion rate is more helpful than K-values in unpaved roads. Table 2.10 gives examples of K-values for different soils and soils of similar coefficients are shown in remarks.

Table 2. 10. Typical coefficients of erodibility for different soil textures

Textural class	C	M	S	K – Values	Remarks
Loamy sand (C < 18%, S > 65%)	9 13 <sup>c</sup>	8 1 <sup>c</sup>	83 85 <sup>c</sup>	0.0115 <sup>a</sup> ; 0.0259 <sup>b</sup> ; 0.022 <sup>c</sup> ; (0.031 <sup>c</sup> ; 0.051 <sup>c</sup> ; 0.023 <sup>c</sup> ; 0.012 <sup>c</sup> )	K-RUSLE; SL, LS, S
Sandy clay loam (18% < C < 35% & S > 15% or C < 18% & 15% < S < 65%)	27 15 <sup>c</sup> 23 <sup>c</sup> 23 <sup>c</sup>	15 13 <sup>c</sup> 22 <sup>c</sup> 20 <sup>c</sup>	58 72 <sup>c</sup> 55 <sup>c</sup> 57 <sup>c</sup>	0.0311 <sup>a</sup> ; 0.0453 <sup>b</sup> ; 0.023 <sup>c</sup> ; 0.047 <sup>c</sup> ; 0.046 <sup>c</sup> ; (0.064 <sup>c</sup> ; 0.015 <sup>c</sup> ; 0.068 <sup>c</sup> ; 0.106 <sup>c</sup> ; 0.017 <sup>c</sup> ; 0.073 <sup>c</sup> )	K-RUSLE; SiCL, SL, L, SCL, SiL, CL
Silty loam (C < 35% & S < 15%)	18	74	8	0.0438 <sup>a</sup> ; 0.0353 <sup>b</sup>	K-RUSLE; M & SiCL
Silty clay (35% < C < 60%)	48	48	4	0.0339 <sup>a</sup> ; 0.0184 <sup>b</sup>	K-RUSLE; SC, CL, SiC, SiCL
Clay (C > 60%)	80	20	0	0.017 <sup>a</sup> ; 0.0072 <sup>b</sup>	K-RUSLE
Expansive clay	-	-	-	0.26 <sup>d</sup>	t/ha; R = E <sub>60</sub> x I <sub>30</sub>
Loess (silty loam)	-	-	-	0.02 <sup>d</sup>	t/hm <sup>2</sup> h hm <sup>-2</sup> MJ <sup>-1</sup>
Sandy loess	-	-	-	0.015 <sup>d</sup>	Sandy silt loam
Loess (silty loam)	-	-	-	0.0713 - 0.4467 <sup>d</sup> ; 0.007 - 0.302 <sup>d</sup>	kg/m <sup>2</sup> /mm; soil loss/runoff depth
Loess (silty loam)	-	-	-	0.01 - 0.544 <sup>d</sup>	ls/g; scour (Qt/W)
Loess brown soil	-	-	-	0.36 - 0.38 <sup>d</sup>	Nomogram
Clay	62 <sup>c</sup> 53 <sup>c</sup> 58 <sup>c</sup>	13 <sup>c</sup> 17 <sup>c</sup> 21 <sup>c</sup>	25 <sup>c</sup> 30 <sup>c</sup> 21 <sup>c</sup>	0.21 <sup>d</sup> ; 0.012 <sup>c</sup> ; 0.014 <sup>c</sup> ; 0.01 <sup>c</sup> ; (0.029 <sup>c</sup> ; 0.045 <sup>c</sup> ; 0.024 <sup>c</sup> ; 0.049 <sup>c</sup> ; 0.037 <sup>c</sup> ; 0.039 <sup>c</sup> ; 0.044 <sup>c</sup> ; 0.051 <sup>c</sup> ; 0.06 <sup>c</sup> ; 0.047 <sup>c</sup> ; 0.055 <sup>c</sup> )	RUSLE; CL; SC
Clay loam	32 <sup>c</sup>	24 <sup>c</sup>	44 <sup>c</sup>	0.28 <sup>d</sup> ; 0.007 <sup>c</sup>	RUSLE
Loam	-	-	-	0.38 <sup>d</sup>	RUSLE
Sandy loam	11 <sup>c</sup> 12 <sup>c</sup>	11 <sup>c</sup> 21 <sup>c</sup>	78 <sup>c</sup> 67 <sup>c</sup>	0.27 <sup>d</sup> ; 0.016 <sup>c</sup> ; 0.025 <sup>c</sup> ; (0.03 <sup>c</sup> ; 0.071 <sup>c</sup> ; 0.056 <sup>c</sup> ; 0.022 <sup>c</sup> )	
Sand	9 <sup>c</sup>	5 <sup>c</sup>	86 <sup>c</sup>	0.05 <sup>d</sup> ; 0.008 <sup>c</sup>	
Sandy clay	38 <sup>c</sup>	11 <sup>c</sup>	51 <sup>c</sup>	0.035 <sup>c</sup>	kg/m <sup>2</sup> /mm
Silt	-	-	-	0.4612 <sup>d</sup>	
Lateritic soils	-	-	-	0.226 <sup>d</sup>	
Silty clay loam	39 <sup>c</sup>	41 <sup>c</sup>	20 <sup>c</sup>	0.01 <sup>c</sup>	C; CL

C, M and S: clay, silt and sand percentages given by references <sup>a</sup> and <sup>b</sup> except if indicated; K-values are also possible for types of soils indicated in the remarks; RUSLE: Revised Universal Soil Loss Equation. <sup>(a)</sup> Grimm et al., 2003; <sup>(b)</sup> Van der Knijff et al., 1999; <sup>(c)</sup> Loch et al., 1998; <sup>(d)</sup> Wang et al., 2013. SL: sandy loam, LS: loamy sand, SCL: sandy clay loam, L: loam, SiCL: silty clay loam, CL: clay loam, SC: sandy clay, SiC: silty clay; (x): K-values whose soil compositions are not given in this table for the reference <sup>(c)</sup>. Qt/W: Quantity/weight; E<sub>60</sub>: is the 60-minutes rainfall kinetic energy; I<sub>30</sub>: is the 30mm/hr rainfall intensity.

#### 2.16.4. Erodibility and Rainfall

Rainfall amount is regarded as a major factor that affects soil loss. Researchers used both erosion models (Boardman and Favis-Mortlock, 1993; Dubé et al., 2004), and experimental works (Foltz and Burroughs, 1990; Durnford and King, 1993; De Figueredo and Poesen, 1998; Issa et al., 2006; Arnaez et al., 2007; Foltz et al., 2008; Liu et al., 2010; Arthur et al., 2011; Cao et al., 2013) to argue that generally soil loss increases with the increase in rainfall amount.

During the calibration of the Washington Road Surface Erosion Model, Dubé et al. (2004) used average annual rainfall from 74 locations, unpaved road surface of about 61 m length, 4.6 m width and 4% slope gradient. Unpaved roads were native surfaces on silt loam, sandy loam, loam, and clay loam soils and the same soils had been used to calibrate the Water Erosion Prediction Project -WEPP (Nearing et al., 1989; Laflen et al., 1991). The data from all the 74 test sites showed a power function with combined exponent of 1.5. Exponents for individual soils were about 1.3 for loam and clay loam, 1.4 for silt loam and 1.9 for sandy loam as can be seen in Figure 2.24. Exponentially increasing erosion due to increased average annual rainfall (AAR) had also been reported in previous studies (Swift Jr, 1984, 1985 and Luce and Black, 1999). From their study, Dubé et al., 2004 decided that a rainfall factor  $F_r = (AAR)^{1.5}$  can be used for the Washington Road Surface Erosion Model alongside other factors such as geologic erosion factor, tread surfacing factor, road width and traffic factors, road slope factor, cut-slope height factor, cut-slope cover factor, delivery factor, and road age factor. For the reasons not discussed by Dubé et al. (2004) some data showed a lot of scatter between 60 in and 80 in average annual rainfall, as shown in Figure 2.24. Although this should not affect the model as it happened to all the soils but was due to differences in detachability of soils and erosivity of the rainfall intensities. As shown in Figure 2.25, Leguédois and Le Bissonnais (2004) reported

high splash erosion of total soil loss for silt loam than for clay loam, as cumulative rainfall increases. This agrees with Figure 2.24 as silt loam data scattered more than clay loam data.

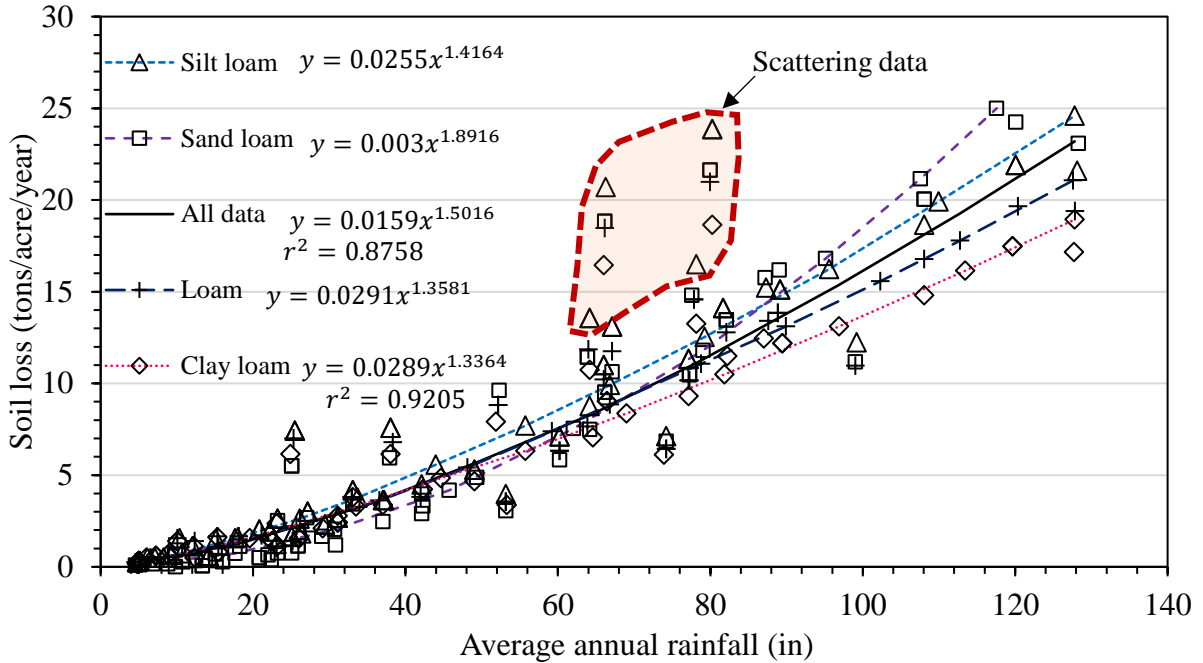


Figure 2. 24. Predicted soil loss versus average annual rainfall (Dubé et al., 2004)

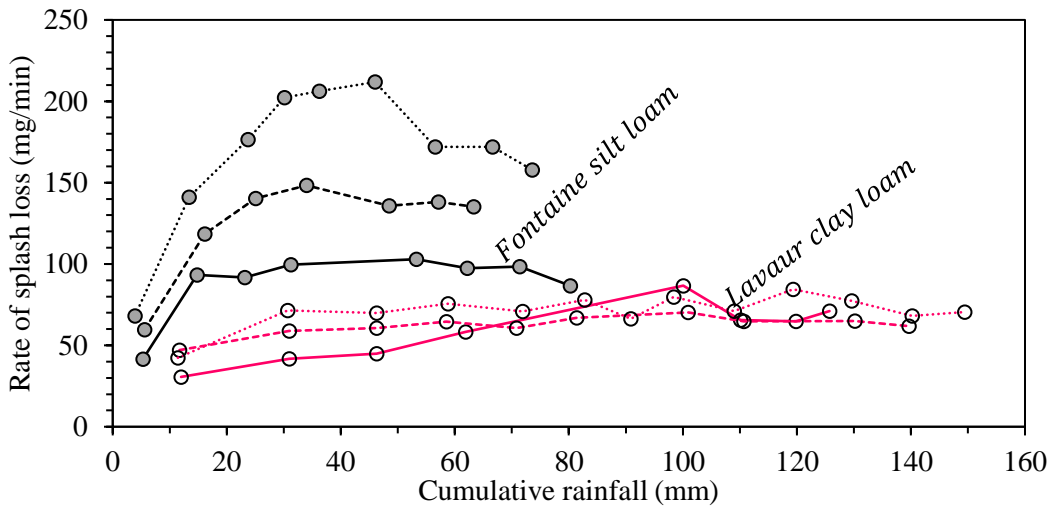


Figure 2. 25. Splash evolutions for three replicated simulations on silt loam and clay loam soils (Leguédais and Le Bissonnais, 2004)

### 2.16.5. Erodibility, Rainfall Duration and Vegetative Cover

Researchers have shown that while the cumulative soil loss increases with the duration of the rainfall, the peak sediment delivery from unpaved roads and bare slopes is usually between 5

and 20 minutes from the start of the rainfall (Foltz et al., 2008; Liu et al., 2010; Liu and Zheng, 2010; Luo et al., 2013). After this time, sediment delivery reduces until it attains an almost constant delivery state. In Figure 2.26, Liu et al. (2010) showed sediment deliveries from 2 m long, 0.55 m wide, 0.35 m deep and 15% slope sections of roads planted with different degrees of grass cover ranging from 0% to 70%. Results show that increase in vegetative cover significantly reduced soil loss due to rainfall. However, vegetative cover differences showed little effect on the time of the peak sediment delivery which was achieved at about 10 min to 15 min from the start of the rainfall for all the soils. Sediment delivery seemed stable after about 25 min of the rainfall except for the road without grass cover, which expectedly showed highest erosion. Sediment delivery rate peak reduced from about 106 mg/m<sup>2</sup>/min to about 34 mg/m<sup>2</sup>/min when the grass cover increased from 0% to 70%.

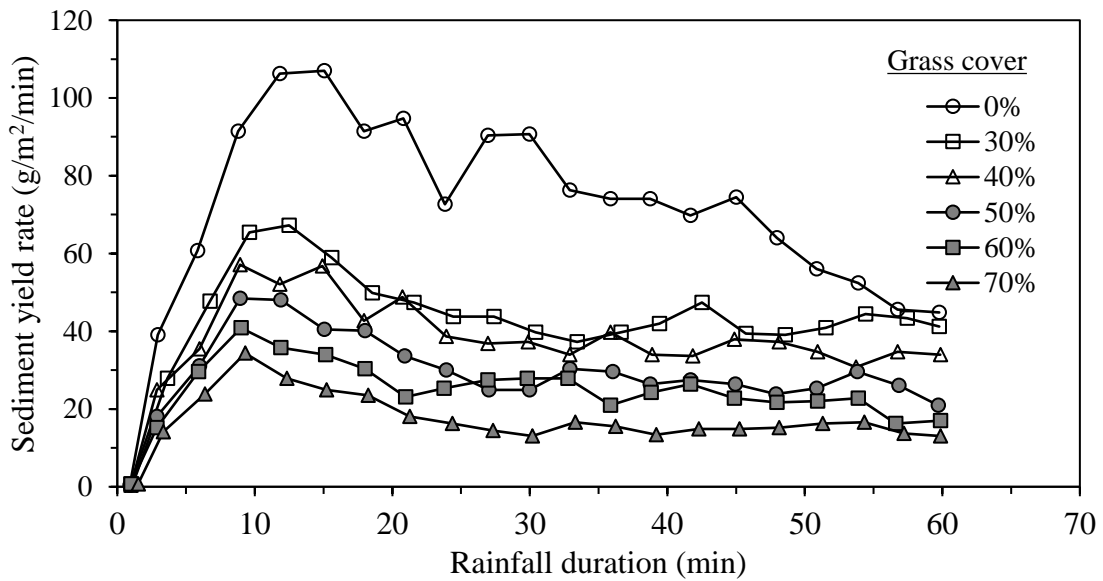


Figure 2. 26. Sediment yield rate versus rainfall duration for road sections with different grass cover percentages (Liu et al., 2010)

#### 2.16.6. Erodibility and Rainfall Intensity

Several studies (De Figueredo and Poesen, 1998; Arnaez et al., 2007; Foltz et al., 2008; Liu et al., 2010; Arthur et al., 2011; Cao et al., 2013; Luo et al., 2013) said that the rain intensity is an

important factor in erosion studies, with an undeniable consensus that for the same slopes, erosion rate reduces with the reduction in rain intensity. Cao et al. (2013) conducted erosion tests on unpaved loess road using rainfall intensities ranging from 43.8 mm/hr to 142.2 mm/hr, and 10.5%, 17.6% and 26.8% slopes. The results have been that both small rainfall intensities and small slopes give smaller soil losses. Figure 2.27 shows the results for the 26.8% slope.

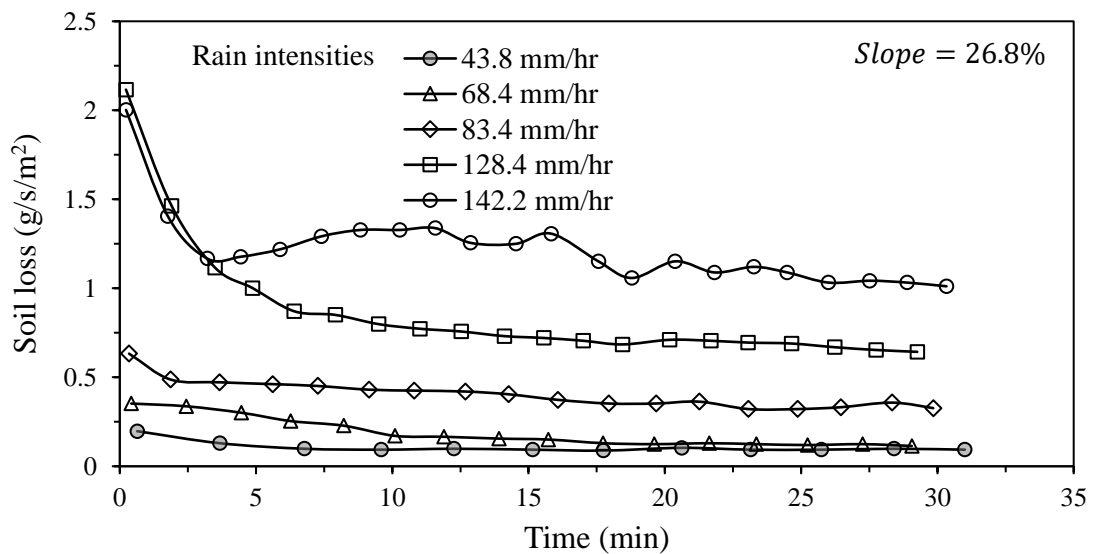


Figure 2. 27. Soil loss as a function of rain intensity and duration (Cao et al., 2013)

#### 2.16.7. Erodibility, Runoff Discharge and Slope Gradient

Slope gradient and runoff discharge are the other environmental factors that influence erodibility and sediment delivery from unpaved roads (Boardman, 1983; El-Swaify, 1997; Bryan, 2000; Croke and Mockler, 2001; Croke et al., 2005; Arnaez et al., 2007; Katz et al., 2011, 2013; Ali and Sterk, 2015).

Figures 2.28 and 2.29 show that in addition to the road category, the influence of gradient and flow discharge on the exacerbation of erosion of those roads are a concern. According to Cao et al. (2009), a main road (MR) is an unpaved road of about 3 m wide that is eligible for large vehicles. A secondary road (SR) is an unpaved road of about 2 m wide and mostly used by

small vehicles. Trails (TR) refer to paths, less than 0.5 m wide, made by farmers and livestock on slopes. As stated in Table 2.10, due to erodible cuts and fills introduced during construction, unpaved roads modify topography and hydrology, and increase erosion rate within catchments. For example, when those roads constitute about 5% of the total area, their sediment contribution can be as high as 85 to 90% of the total sediment (Nearing et al., 1991; Torri and Poesen, 1992; Arnáez and Larrea, 1995; Rijdsdijk et al., 2007). Increased slope gradients lead to increased flow velocity and discharge with increased power of sheet, rill and gully erosions, which can lead to the total destruction of unpaved roads (Iverson, 1980; Swift, 1984; Govers, 1985; Croke and Mockler, 2001; Giménez and Govers, 2002 and Katz et al., 2013).

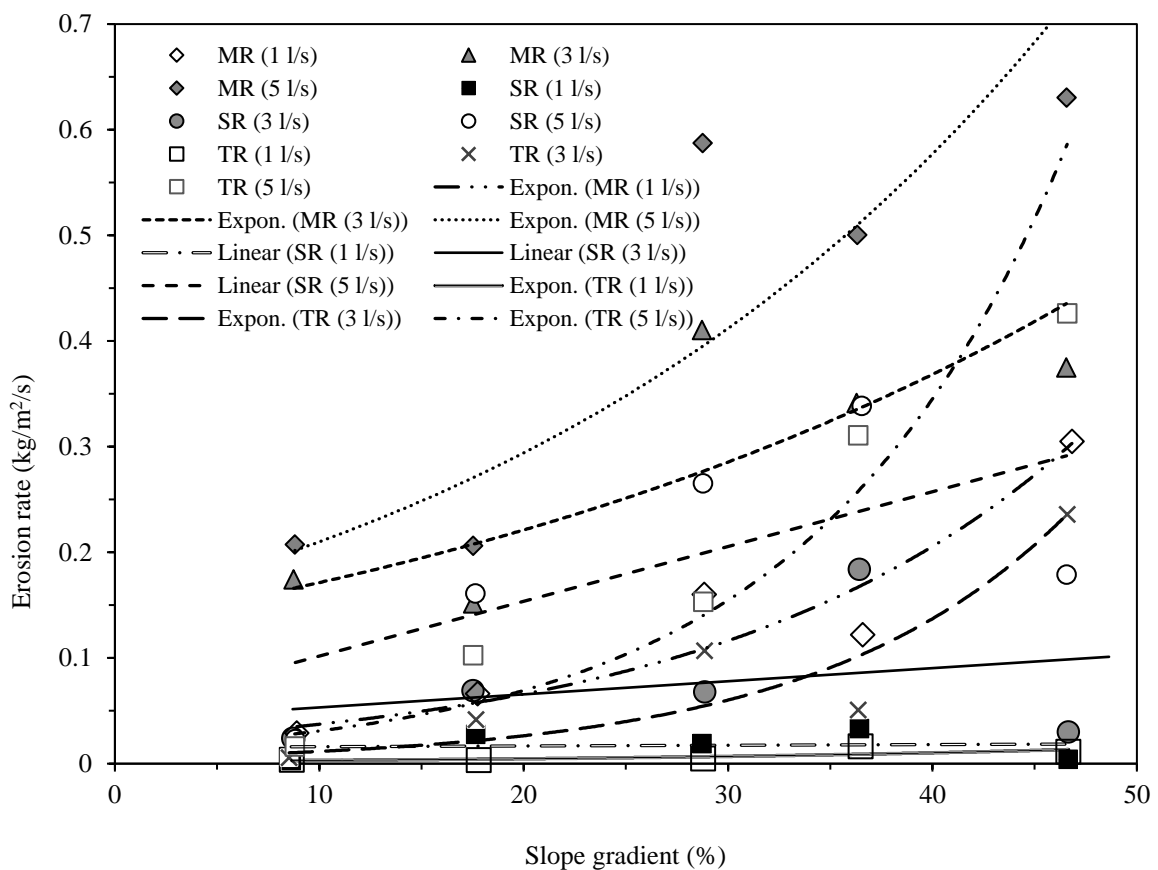


Figure 2. 28. Erosion rate as a function of the road gradient, road type and surface flow discharge (Cao et al., 2009)

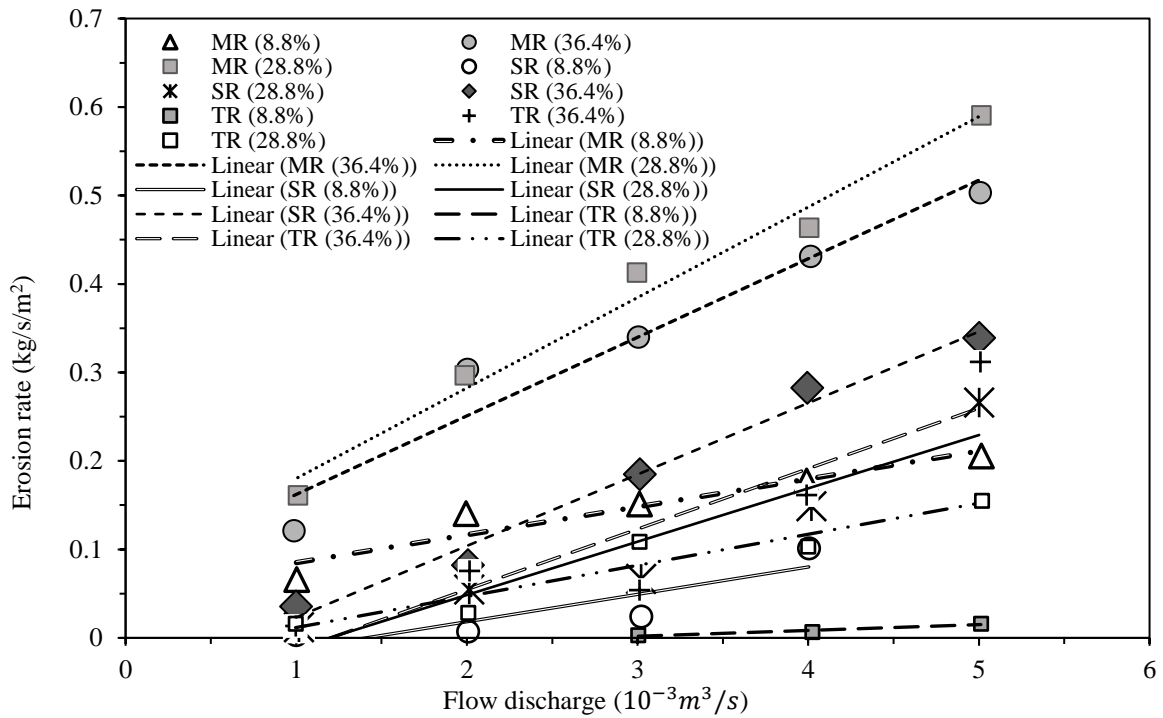


Figure 2. 29. Erosion rate as a function of surface flow discharge, road type and gradient (Cao et al., 2009)

The other rainfall related factors which affect erosion of rural roads include the size of the raindrops. Usually the bigger the size of the raindrop, the higher its kinetic energy and henceforth more ability to detach soil particles (Nearing and Bradford, 1985; Obi and Salako, 1995; Agassi and Bradford, 1999; Salles et al., 2000; Salles and Poesen, 2000). In the regions of heavy rainfall intensity, increased flow depths may be noticed on the road surface and lead to increased stream powers for more concentrated erosion in rills and gullies (Nearing et al., 1991, 1999; Zhang et al., 2001; Cao et al., 2009; Zhang et al., 2009; Li et al., 2015; Zhang et al., 2015).

On the other hand, increased wind velocity and intensity, which could be due to the morphology of the area, increase surface soil detachment in dry seasons (Lyles et al., 1974; Pedersen and Hasholt, 1995; Choi, 2002; Erpul et al., 2002). Moreover, the land use such as agriculture, overgrazing and deforestation activities on the upper hillslope may lead to increased supply of

sediment onto the road surface and contribute to the total sediment from the road (Boardman, 1983; Arnaez et al., 2007). Extremes of climate in terms of temperature affect the overall humidity of the road surface and its dry–wet cycles. Excessive humidity can cause loss of soils' strengths and thus, increase the vulnerability of the soils to water eroding stresses. Also, excessive dryness can lead to both crumbling of surface particles by traffic wheels, hence their availability to future runoff transport and to wind erosion (Noble and Morgan, 1983; Riezebos and Epima, 1985; Morgan et al., 1998; Aksoy and Kavvas, 2005; Akbulut and Gürer, 2007; Van Klaveren and McCool, 2010).

#### 2.16.8. Erodibility, Road and Vehicular Traffic

The geometry of the road in terms of longitudinal and transverse slopes is one of the factors of soil erosion in unpaved roads (Foltz and Burroughs, 1990; Cao et al., 2006, 2009, 2011, 2013; Foltz et al., 2009). Similarly, the size of the road surface area frequently used by traffic is likely to influence surface erodibility, due to both loosening and grinding of surface particles by traffic wheels (MacDonald et al., 1997; Anderson and MacDonald, 1998).

Traffic type which may consist of heavy trucks and/or small vehicles, the traffic volume, and timing of the traffic with respect to the rainfall affect erodibility of unpaved roads (Iverson, 1980; Ziegler et al., 2001). Essentially, wheels action on an unpaved road cause two types of erosion. Firstly, the pre-storm erosion which removes loose soils, broken by wheels, from the surface. The interaction between the surface soils and wheels in the dry season is active in loosening and dislodging those fine soils, which are later removed in dust emissions by both naturally and traffic-speed generated (mechanical) wind (Iverson, 1980; Ziegler et al., 2001, 2004). Secondly, the during-storm erosion which happens when driving during rainfall is characterised by increased sediment production due to dislodgement and redistribution of soils

by wheel passes and runoff flow. During this erosion, there is accelerated formation of rills and hence accelerated sediment transport (Iverson, 1980; Ziegler et al., 2001, 2004).

Moreover, the poor construction and maintenance of unpaved roads may result in presence of poorly compacted soil at the surface of rural roads and is likely to contribute more sediment from those roads (Ziegler et al., 2000, 2001, 2004; Cook et al., 2013). Also, the poor drainage systems, which cannot effectively and efficiently convey the runoff from the road surface, can lead to softening of the road due to increased moisture and hence the increase of the road's erodibility (Katz et al., 2013; Henning et al., 2014; Keller and Sherar, 2003). The roughness of the road surface can reduce surface flow velocities and encourage infiltration, hence leading to weakening of the road; whereas proper compaction discourages infiltration and encourage flow speeds leading to quick removal of runoff from the road' surface hence reduced erosion (Iverson, 1980; Giménez and Govers, 2002; Ramos-Scharrón and McDonald, 2005).

Iverson (1980) used off-road vehicles (ORVs) on a granular, non-cohesive terrain used for recreational purpose. Overall, it was a gravelly sand terrain. Results from 20 min intense 50 rainfall simulation tests, with an average rainfall intensity of 66 mm/hr, over the plots used and non-used by ORVs showed an average of 20 times more sediment in plots used by ORVs as shown in Figure 2.30. This was due to ORVs breaking down the particles in the wheel paths for the runoff to carry them as sediment easily. Similar trend of results was found in both active and abandoned roads (Foltz et al., 2009; Cao et al., 2011).

Erosion studies of unpaved roads derived relationships between soil detachment and flow rates, flow shear stress, stream power and unit stream power (Cao et al., 2009, 2011). Other studies related erosion and traffic action (Foltz and Burroughs, 1990; Ziegler et al., 2000), erosion and road maintenance activities (Ziegler et al., 2004; Cao et al., 2006), and erosion and road

geometry (Sugden and Scott, 2007; Cao et al., 2013). Erosion from unpaved roads has been positively related to the runoff shear stresses (Cao et al., 2011). However, Cao et al. (2009) said that due to difficulties in simulating all road factors affecting erodibility, assumptions and extrapolations not carefully thought of may lead to overestimating erosion from unpaved road during laboratory experiments.

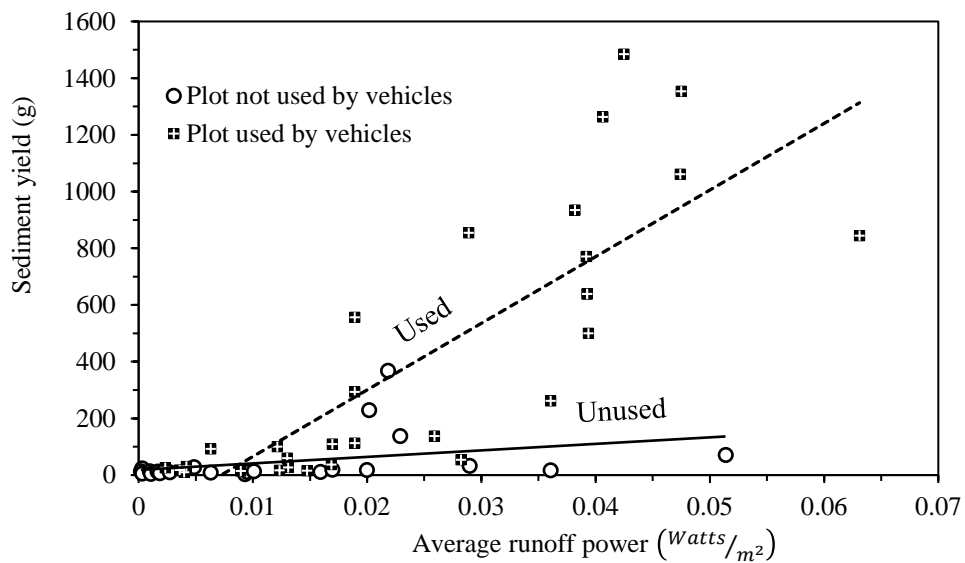


Figure 2. 30. Sediment production as affected by traffic passes (Iverson, 1980)

Foltz et al. (2008) conducted a study to investigate the effect of cumulative surface flow on rill erodibility and critical shear stress on unpaved roads. One of the findings was that with increasing surface flow depth, rill erodibility decreased exponentially. Critical shear stress was unaffected by surface flow depth. As shown in Figure 2.31, road erodibility changed over time with consecutive surface flow events and although those changes were little noticed for inter-rill erosion, they were of greater importance once rills formed. Those changes should be considered during road erosion model calibrations to avoid over-estimates. For example, combined inter-rill and rill erosions showed a peak sediment delivery of about 2 g/m<sup>2</sup>/s, 1 g/m<sup>2</sup>/s and 0.75 g/m<sup>2</sup>/s, respectively for the first, second and third 30 min surface flow events. Inter-

rill erosion was about 0.25 g/m<sup>2</sup>/s for all the three surface flow events. Similar results were reported by Foltz and Burroughs, 1990).

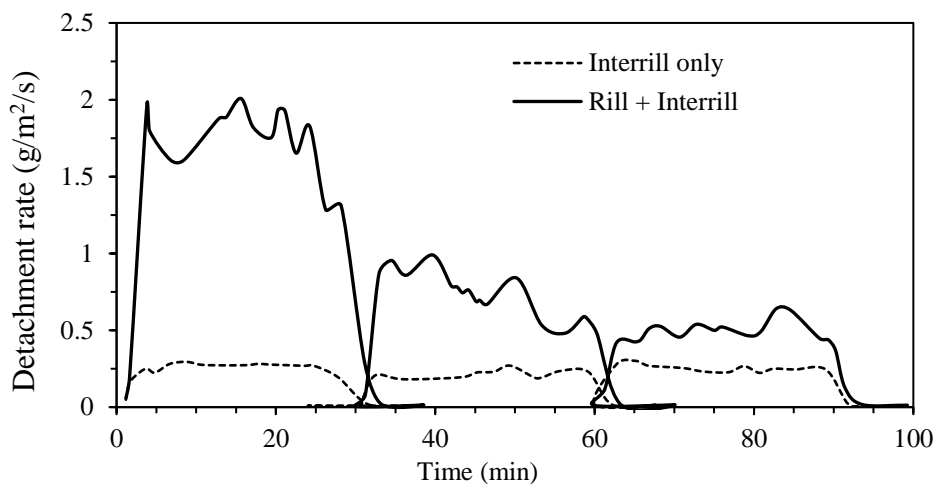


Figure 2. 31. Detachment rate with time as of presence of rills (ruts) (Foltz et al., 2008)

All those factors which exacerbate erosion of rural unpaved roads have led to researchers concluding that those roads are not only more erodible when compared to other land uses, but also contribute more sediment into the surrounding environment. For example, Erosion increases by 3 to 8 times in areas of high unpaved roads density (3 to 4 km/km<sup>2</sup>) and 1.3 to 2 times in areas of low road density (< 2 km/km<sup>2</sup>) (Anderson and MacDonald, 1998). It was found that when 0.5% of a catchment area is made up of unpaved roads and 12% of the same catchment area is made up of agricultural land, those two land uses generate about equal erosion sediment (Ziegler et al., 2004). Moreover, unpaved roads contribute rapid flow and sediment to streams, with 38% to 45% of the sediment caused by rain detachment due to the exposed surface of those roads (Ziegler et al., 2000).

#### 2.17. Erosion Resistant Unpaved Roads

Rural roads should be designed and constructed to become serviceable on a year-round basis. All-weather rural roads are only achievable if constructed using suitable soil materials

supported by the provision of efficient and effective drainage, maintenance programme and regulated traffic use.

To contribute to the achievement of all-weather rural roads, an envelope for good soil materials that can be used in their construction and effectively combat their erodibility was designed. The envelope was based on global studies by Gidigasu (1972), Aziz and Ramaswamy (1992), Alzubaidi (1999), Keller and Sherar (2003), Yarbast et al., (2007), Edvardsson (2009), and Behiry (2013). Since most of these studies designed their envelopes based on the compaction ability and the grading curve of the soil materials only, the newly designed envelope (Figure 2.32) considers not only those properties but also the self-packing quality to maximize compaction levels and their resistance to water erosion. The self-packing was guaranteed using Andreasen and Andersen's modified model as provided in the Equation 2.2 (Brouwers and Radix, 2005):

$$P(D) = \left( \frac{D^q - D_{\min}^q}{D_{\max}^q - D_{\min}^q} \right) \quad (\text{Eq. 2.2})$$

where  $P(D)$  = cumulative % finer than the particle size  $D$ ;  $D_{\min}$  and  $D_{\max}$  are the fixed minimum and maximum particle sizes of the material mix; and  $q$  is a parameter such that  $0 < q < 1$  though the model's better parking is for  $q \leq 0.5$ .

On the other hand, the resistance to erosion was assured by comparing the envelope from Figure 2.32 to the South African (SA) diagram for the performance of soil materials in unsealed roads (Paige-Green, 2006). In the SA diagram, the designed envelope is referred to as "based on the literature" as shown in Figure 2.33. Another advantage of this envelope is that it has combined the selection of the soils from studies based on materials around the world, which could make it applicable globally. The envelopes by individual studies that were combined to give the "based on the literature" envelope, are also plotted in the SA diagram. These are envelopes A,

B, C, D, E and F, respectively for the studies by Edvardsson (2009), Aziz and Ramaswami (1992), Alzubaidi (1999), Yarbařt et al. (2007), Keller and Sherar (2003) and Gidigasu (1972).

The “based on the literature” envelope sits in the middle of the good zone of the SA diagram. However, about 5% lies in the slippery zone and this could be due to a high value (8%) of the linear shrinkage considered during this study, as suggested by Gidigasu (1972) and Paige-Green et al. (2015). Nonetheless, this should not question the quality of the designed envelope since the plasticity of the soil on the surface of the road is likely to reduce with time, due to both surface water and wind progressively removing fine soil particles.

The SA diagram is subdivided into five zones: namely, the slippery zone, the erodible zone, the corrugations and ravels zone, the ravels zone, and the good zone. The latter is described by  $16 \leq G_c \leq 34$  and  $100 \leq S_p \leq 365$  where  $G_c$  is the grading coefficient and  $S_p$  is the shrinkage product. The  $G_c$  and  $S_p$  parameters are given by the following equations (Paige-Green, 2006):

$$S_p = L_s * P_{0.475} \quad (\text{Eq. 2.3})$$

$$G_c = (P_{26.5} - P_{2.0}) * P_{4.75} / 100 \quad (\text{Eq. 2.4})$$

where  $P_i$  is the percentage of the material finer than “i” in the sieve analysis test; and  $L_s$  is the linear shrinkage of the soil.

The designed “based on the literature” envelope has the mean particle size  $D_{50}$  which ranges from 0.8 mm to 4.8 mm. According Shields’ curve and Briaud (2008), and as indicated in Figure 2.23, the soils in the envelope need the critical shear stresses ranging from about  $0.5 \text{ N/m}^2$  to  $5 \text{ N/m}^2$ . These soils classify as medium plastic according to Figure 2.20; with a plasticity smaller than 12% (ideally 6%) as suggested for good unpaved road surface soils (Paige-Green, 1999, 2006; Keller and Sherar, 2003; ASANRA, 2013; Paige-Green et al., 2015).

The envelopes that were used during this study, partly or fully, fall out of the good zone of the SA diagram. However, these envelopes respect the requirements for either the shrinkage product or for the grading coefficient and seem to be useful in some environments, while they may be questionable in others. The envelopes (A) by Edvardsson (2009), (B) by Aziz and Ramaswami (1992), and (C) by Alzubaidi (1999) all fall into the erodible zone of the SA diagram, though they meet the shrinkage product requirements. The envelope (D) by Yarbaşt et al. (2007) has its important part in the good zone but also parts of it fall in the erodible and corrugations and ravel zones. The envelope (E) by Keller and Sherar (2003), which was designed on the base of the performance of materials in semi-tropical, tropical, and arid environments falls completely in the good zone. However, the latter envelope covers a small range of material due to small ranges of the shrinkage product and grading coefficient. Finally, only about 45% of the envelope (F) suggested by Gidigas (1972) located in the good zone and about 55% is in the “ravels” zone. This can be due to the envelope’s high grading coefficient values which also suggest that the envelope covers more coarse gravel soils.

The limitations of those envelopes for the selection of soil materials for the construction of unpaved roads as discussed in the previous paragraph can be associated to the availability of soils and the environment of the countries in which those envelopes were designed. For example, Alzubaidi’s (1999) and Edvardsson’s (2009) envelopes were designed in Sweden, and Azizi and Ramaswami’s (1992) envelope was designed in Singapore. These three envelopes significantly considered temperate climates’ effects on unpaved roads’ deterioration. Hence, they may not perform effectively in tropical climate like the Gidigas (1972)’s envelope designed in Ghana.

The consideration of the envelopes which were designed in different environments proves to be vital in the design of the “based on the literature” envelope for the selection of soils to use in the construction of rural roads with potential to resist erosion processes. The “based on the literature” envelope not only provides a balance between climate change effects on unpaved roads’ deterioration, but also meets, at 95%, the requirements for erodibility resistance in terms of the shrinkage product and the coefficient of grading, as shown in Figure 2.33.

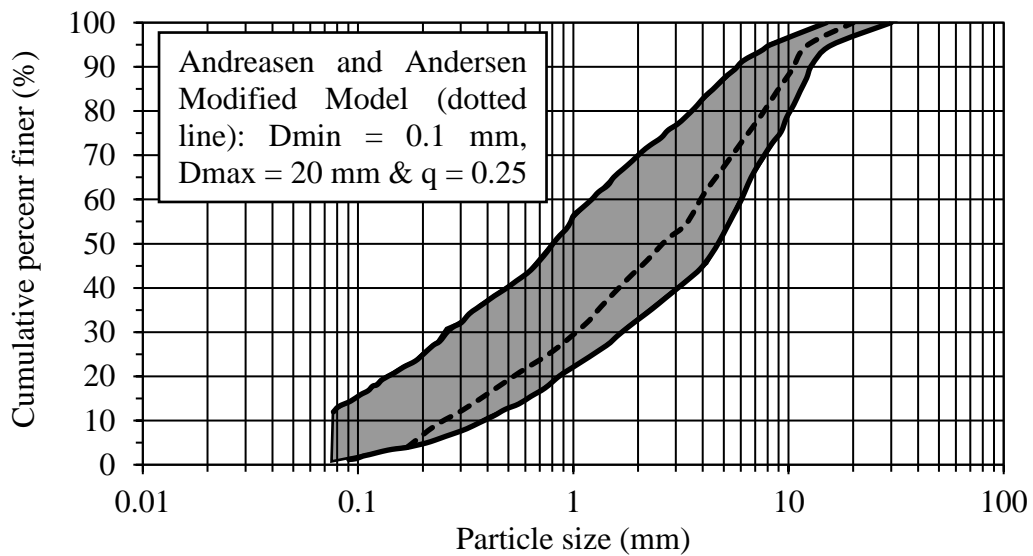


Figure 2. 32. Proposed envelope for soils that resist erosion in unpaved roads

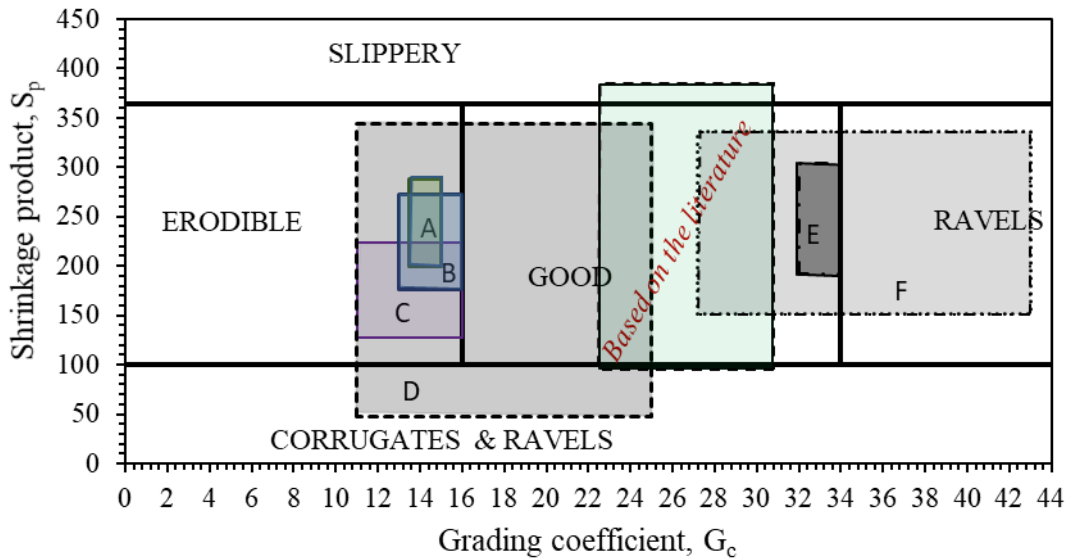


Figure 2. 33. Allocation of the envelope into the South African diagram

## 2.18. Summary

The systematic analysis approach was used in this chapter to investigate the existing knowledge and the gaps in knowledge on the erodibility of soils in rural roads. The focus was put on 219 selected global studies, published since 1960 from 36 countries. Those studies resulted from the screening, by inclusion/exclusion criteria, and the weight of evidence process applied to a total of 2,237 studies obtained from nine search engines using twenty key words. The 19 soil types used in erosion studies have been grouped into four groups according to the level of investigation. Moreover, the 47 factors which affect erosion of rural roads have been identified and discussed in detail. These are mainly under three groups: soil and geotechnical factors, climate and environmental factors, and road and traffic factors.

Based on the systematically analysed literature, it was found that:

- The soil properties are important in the determination of erosion rates from rural roads. Clay soils exhibit more resistance to the detachment from both raindrops and runoff flows. Silt and fine sand soils are more vulnerable to erosive forces. Erodibility of soils decreases with increase in particle size from fine sand to gravel soils and with increase in cohesion from fine sand to clay soils.
- The soil properties including particle size distribution, mean particle size, moisture content, bulk density and maximum dry density have been investigated significantly during erodibility studies.
- The sand, clay and silt soil types have been the most investigated soils by about 41%, 33% and 31% of the consulted studies, respectively. In contrast, sandy gravel, gravelly sandy loam, and gravel loam have been the least investigated soils by about 1%, 2% and 3% of consulted studies, respectively. Overall, gravelly soils were among the least investigated, which could justify less information on erodibility of unpaved roads.

- The total rainfall, rainfall intensity, and rainfall duration, the geometry of the road (longitudinal and transversal gradients) and the position of the road within the hillslope are the environmental factors that greatly influence the erodibility of rural roads.
- The primary action of traffic wheels is to loosen surface soils. In dry seasons, those soils can be windblown by both the natural wind and the mechanical wind generated by traffic speeds. In rainy seasons, traffic wheels create and widen rills to accelerate the transport of sediment down slopes by surface water runoff.

Using the data from the literature, an envelope for good soil materials to use at the surface of unpaved rural roads was designed. The “based on the literature” designed envelope was compared to the South African diagram for the performance against defects for soils used on the surface of unsealed roads. The envelope sits in the good zone (of the South African diagram) of the soils which are not erodible, and which cannot lead to excessive slippery, corrugations and raveling in the surface of the unpaved roads.

## 3. METHODOLOGY

### 3.1. Introduction

The literature focussed on the review of previous experimental investigations on erodibility of soils which included apparatus used, soil types, how test beds were constructed, findings and interpretation of results. The aim was to inform the rest of the PhD thesis, including the methodology. Most importantly, the selection of the soils for use in this study based on their suitability for both the construction of unpaved roads and erosion investigations. The emphasis was put on the particle size distribution and plasticity index due to their vital influence on the erosion mechanisms in unpaved roads, as discussed in the sections 2.16.1 to 2.16.8 and section 2.17 of the literature. All this information was used to inform the apparatus and test methodologies used for this study to address the gaps identified during the literature review. The apparatus and methodologies of the test methods are described in this Chapter.

### 3.2. Methodology Flow Chart

The answers to three objectives including the selection of soils suitable for both erodibility tests and construction of unpaved roads; characterization, engineering, and erosion susceptibility tests on the selected soils; and the design and construction of both the rainfall simulator and the soil testing box to conduct erodibility tests were provided. Furthermore, a methodology for undertaking sheet erosion tests is briefly described. An estimation of the quantities of the different soils used is also shown. The methods for data collection and tools for data analysis are briefly described. A flow chart describing the methodology is shown in Figure 3.1.

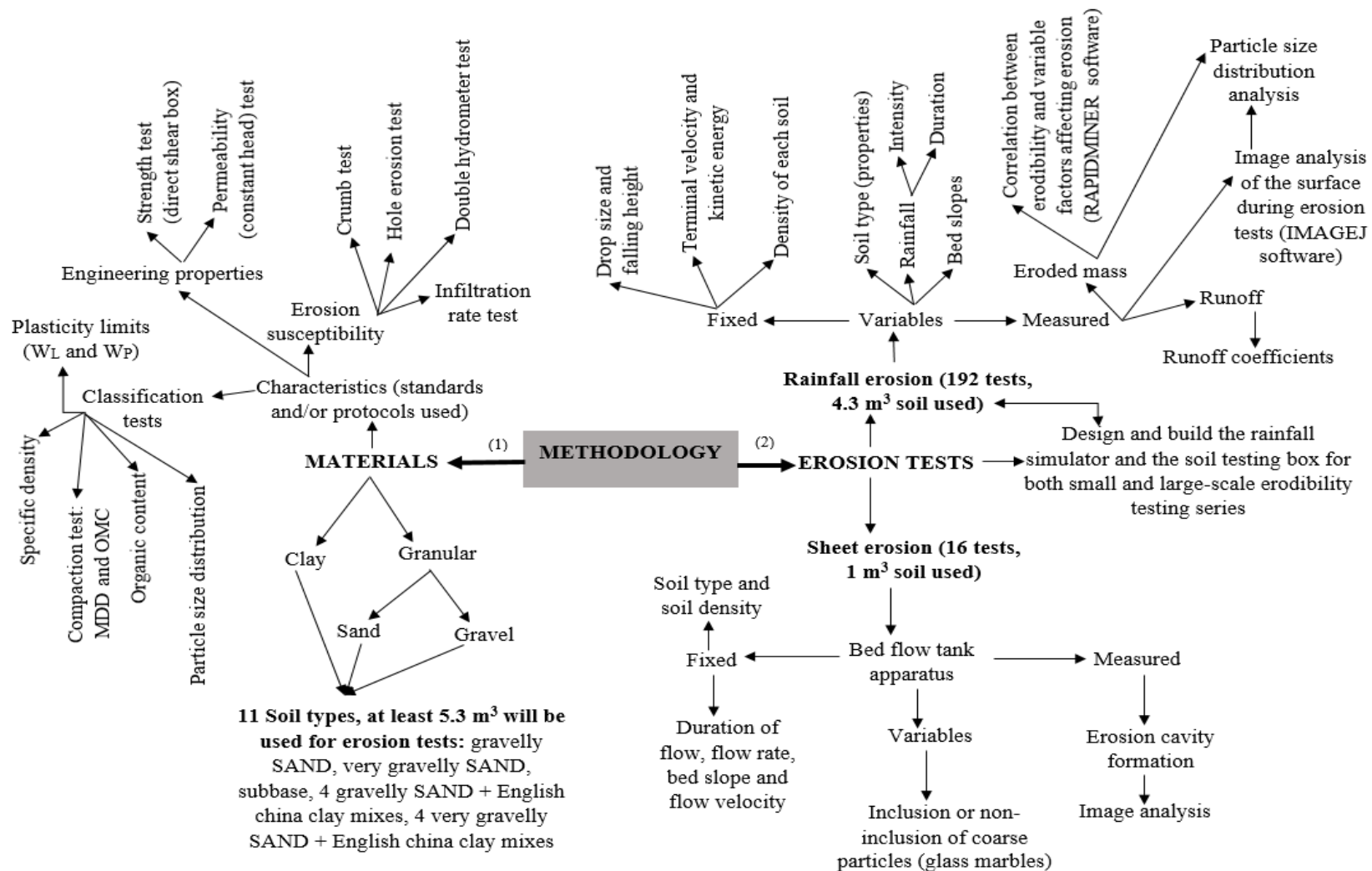


Figure 3. 1. Summary map of the key steps of the methodology

### 3.3. Selection of Soils for Erosion Tests

The selection of the soils used in this study based on the need to make unpaved road so that the need for new borrow pits is reduced, as these are increasingly becoming scarce (Paige–Green et al., 2015), and on the suitability of the soils for erosion testing (ASTM, 2015). Three soils (clay, sand, loam) are suggested for erosion tests based on the grain size and plasticity (ASTM, 2015; Ngezahayo et al., 2019a, e), as shown in Table 3.1. Well-graded soils are required for the construction of unpaved road as these can achieve high compaction levels. In addition to the grain distribution, the plasticity index which ensures bonding between soil grains is another important property in unpaved roads. Ideally, the plasticity index of unpaved road surface soils should be about 6% though a range from 0% to 12% is acceptable (Keller and Sherar, 2003, ASANRA, 2013, Shearer et al., 2013 and Paige-Green et al., 2015).

Table 3. 1. Suitability of soils for erosion tests (ASTM, 2015; Ngezahayo et al., 2019a, e)

Particle (mm)	Clay	Loam	Sand
D <sub>15</sub>	> 0.0015	> 0.05	> 0.001
D <sub>50</sub>	0.001–0.1	0.01–1.0	0.8–2.0
D <sub>85</sub>	0.01–1.0	0.5–5.0	1.0–10
D <sub>100</sub>	< 10	< 25	< 40
Plasticity index (%)	> 14	1.0–8.0	-

It would have been ideal to get the soils for use in the laboratory from countries where majority road network comprises unpaved roads and erosion is a serious problem such as in the Sub-Saharan Africa. However, this was not possible due to technical and financial issues such as sampling and the cost of transporting samples to the UK. Soils were prepared by mixing clay, sand, and gravel soils in the Civil Engineering Laboratory at the University of Birmingham.

Accordingly, a gravelly SAND (GS) soil was mixed with 0%, 5%, 10%, 15%, and 20% English china clay (ECC). Similarly, a very gravelly SAND (VGS) soil was mixed with 0%, 5%, 10%,

15% and 20% ECC. A road subbase soil was used without ECC content. The main soils (gravely SAND, very Gravelly SAND and Subbase) offered the opportunity to study the effect of particle size while the ECC percentages allowed to study the effect of both clay content and plasticity index, to the erodibility of unpaved roads. The different clay contents helped to have some of the mixes into the good zone of unsurfaced road soils (Paige-Green, 2006) and into the envelope of unpaved road soils “based on the literature” (Ngezahayo et al., 2019c), as discussed in Chapter 2. All the 11 soils were classified according to BS 5930 (2015), as shown in Table 3.2.

### 3.4. Characterization of the Selected Soil Materials

Particle size distribution, Atterberg limits, Proctor compaction, direct shear box, California Bearing Ratio, organic content, and constant head permeability tests were undertaken to characterise the selected soils. Summary results and testing standards are given in Table 3.3.

#### 3.4.1. Particle Size Distribution

The particle size distribution of the soils was obtained using sieve analysis and hydrometer tests as detailed by BS 1377: 2 (1990). The PSD curves are given in Figures 3.2 and 3.3.

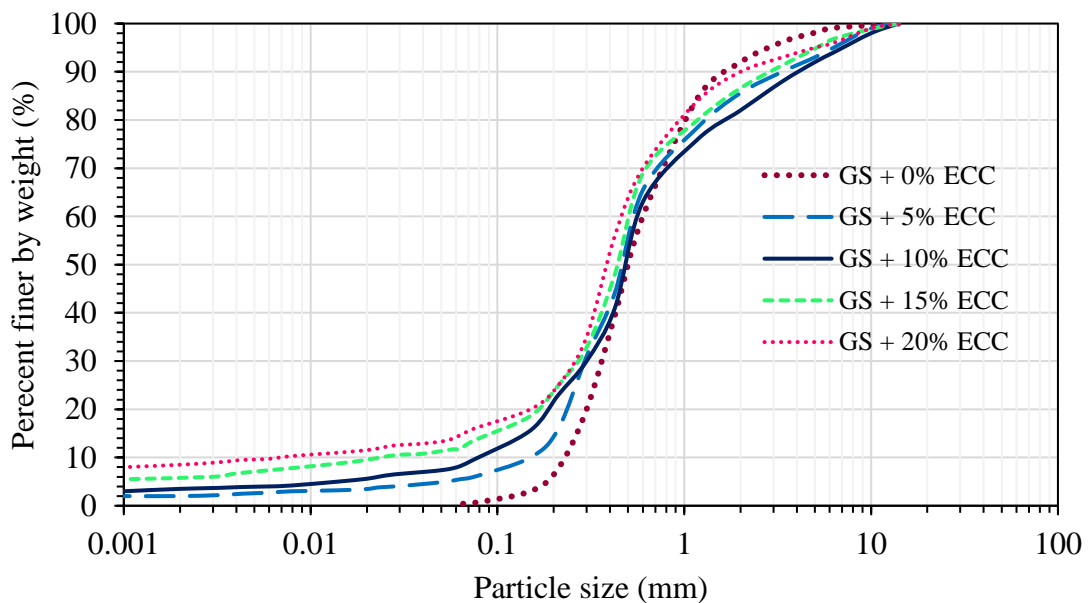


Figure 3. 2. PSD of gravelly SAND soil mixed with English china clay

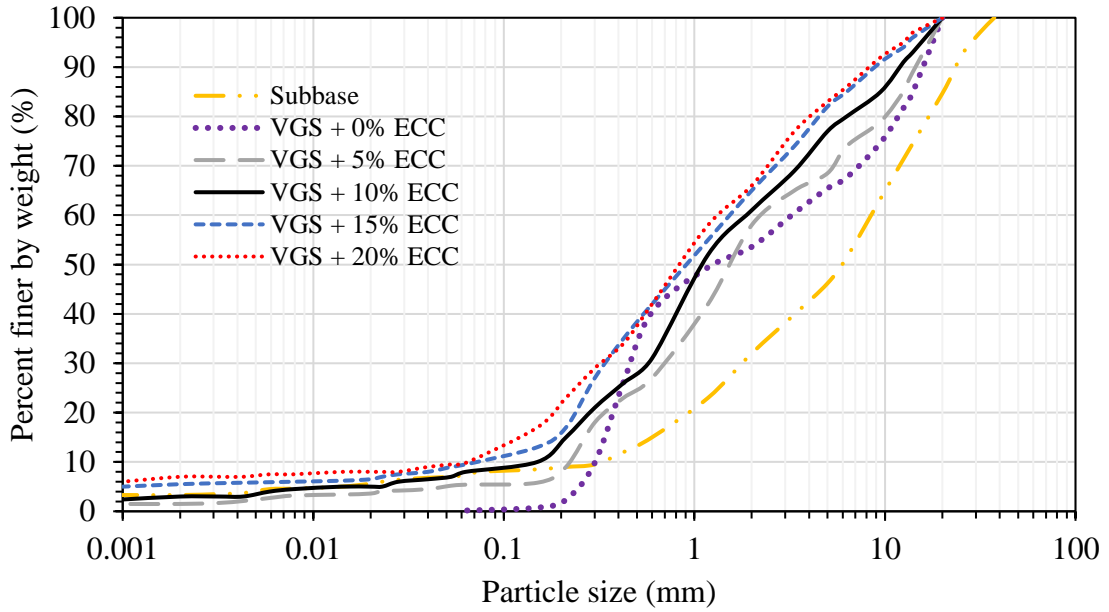


Figure 3.3. PSD of subbase and very gravelly SAND mixed with English china clay

Table 3.2. Classification of soils used in this study (BS 5930: 2015)

Main soil type	Added English china clay-ECC (%)	Classification of the mix
Gravel SAND (GS)	0	Gravel SAND
	5	Clayey gravelly SAND
	10	Clayey gravelly SAND
	15	Clayey gravelly SAND
	20	Clayey gravelly SAND
Very gravelly SAND (VGS)	0	Very Gravelly SAND
	5	Clayey very gravelly SAND
	10	Clayey very gravelly SAND
	15	Clayey very gravelly SAND
	20	Clayey very gravelly SAND
Subbase	-	Gravel

### 3.4.2. Classification and Engineering Properties of Selected Mixes

As stated earlier, several routine standard tests were performed on all the selected soils for classification purposes and to ascertain their engineering properties. These results were used in interpreting the results of the erodibility tests conducted on these materials. Table 3.3 summarises the tests, results and standards used.

Table 3. 3. Summary table of the standards tests

Soil property	Soil description											Standard used
	GS	GS + 5% ECC	GS + 10% ECC	GS + 15% ECC	GS + 20% ECC	VGS	VGS + 5% ECC	VGS + 10% ECC	VGS + 15% ECC	VGS +20% ECC	Subbase	
Mean grain size ( $D_{50}$ , mm)	0.52	0.50	0.46	0.44	0.40	1.2	1.6	1.1	0.9	0.8	6.0	BS 1377-2:1990
Coefficient of uniformity ( $C_u$ )	1.8	5.0	4.6	9.1	12.5	11	10	10.5	22.8	20	28	
Coefficient of gradation ( $C_c$ )	1.1	1.6	2.7	3.9	2.8	0.3	1.1	1.0	1.1	1.3	3.9	
Liquid limit ( $W_L$ , %)	-	19	28	31.6	35	-	17	21	26	31	27	BS 1377-2:1990
Plastic limit ( $W_P$ , %)	-	13.8	20.1	21.8	22.8	-	12.7	15.3	18.4	21.9	21.5	
Plasticity index ( $I_P$ , %)	-	5.2	7.9	9.8	12.2	-	4.3	5.7	7.6	9.1	5.5	
Linear shrinkage ( $L_s$ , %)	-	2.4	3.7	4.6	5.7	-	2	2.7	3.6	4.3	2.6	
Particle density ( $G_s$ , $Mg/m^3$ )	2.53	2.55	2.56	2.57	2.59	2.58	2.61	2.6	2.62	2.62	2.59	BS 1377-2:1990
Maximum dry density (MDD, $Mg/m^3$ )	1.82	1.94	1.96	2.04	2.10	1.89	2.05	2.21	2.24	2.25	2.19	BS 1377-4:1990
Optimum moisture content ( $W_{opt}$ , %)	9	10.3	9.1	8.5	9.5	9.2	8.6	8.4	8.5	8.6	8.8	
Friction angle ( $\phi^\circ$ )	37	32	28	23	21	35	34	31	30	30	39	BS 1377-7:1990 (direct shear box)
Cohesion ( $c$ , $N/m^2$ )	0.3	4.3	11.2	16	24.2	0	2.2	4	11	15	5.7	
Organic content - by loss on ignition (%)	0.4	0.9	1.3	1.6	2.3	0.3	0.7	0.9	1.3	1.3	4.8	BS 1377-3:1990
Unsoaked CBR after compaction (%)	0.47	3.1	4.3	6.1	6.5	4.5	8.6	11.7	14.1	17.1	28.5	BS 1377-4:1990
Unsoaked CBR after 1 day (%)	0.55	4.2	5.2	7.4	7.6	5.1	9.2	13.1	16.7	19.8	36.5	
Unsoaked CBR after 5 days (%)	0.7	7.1	13	15.3	16.3	9.3	15.2	22	28.1	30.6	62.3	
Unsoaked CBR after 10 days (%)	1.1	9.7	17.1	19.1	21.4	11.1	21.4	30.3	35.1	37.8	76	
Unsoaked CBR after 15 days (%)	1.1	9.8	17.6	19.8	22.5	11.5	21.6	32.2	36.4	39.5	77	
Permeability – constant head ( $k$ , $cm/s$ )	$2.6 \times 10^{-2}$	$2.1 \times 10^{-3}$	$3.0 \times 10^{-4}$	$2.2 \times 10^{-4}$	$1.5 \times 10^{-4}$	$2.8 \times 10^{-2}$	$2.5 \times 10^{-3}$	$3.2 \times 10^{-4}$	$2.7 \times 10^{-4}$	$1.9 \times 10^{-4}$	$7.6 \times 10^{-2}$	BS 1377-5:1990

### 3.5. Engineering Behaviour of Selected Soil Mixes

In addition to characterisation tests, the infiltration rate and erosion susceptibility tests were undertaken to assess the engineering behaviour of selected soils with respect to water as a key agent of erodibility.

#### 3.5.1. Infiltration Rate

The rate at which water permeates through the soil was studied using the standard constant head permeability test. Since the downward entry of water into the soil (infiltration) is important, the infiltration rate was also measured. The infiltration test method adopted was developed by Johnson (1963). The test procedure consists of pouring a known amount of water on the surface of the soil and recording the time needed for water to infiltrate in full or partially. Both the soil and water on the top of it must be contained in a cylindrical mould of impermeable internal walls to ensure that there is only vertical infiltration of water. Therefore, each soil sample was compacted to the maximum dry density in the California Bearing Ratio mould. After compaction, 500 ml of water was poured on the top of the soil and the depth of infiltrated water was measured with time to ascertain the infiltration rate. The volume of infiltrated water at different time intervals could be determined. The mould was sealed to both the base and the collar by the black tape to avoid possible leakages, as shown in Figure 3.4.

The method used in this study was preferred to other methods of infiltration rate measurement due to its simplicity and less cost. Other methods were discussed by Lili et al. (2008) and include the double-ring infiltrometer, modified double-ring, rainfall simulation, modified rainfall simulation, run off-on-ponding, run off-on-out, disc permeameter and linear source methods. Most of these are favourable for field measurements and require expensive equipment.

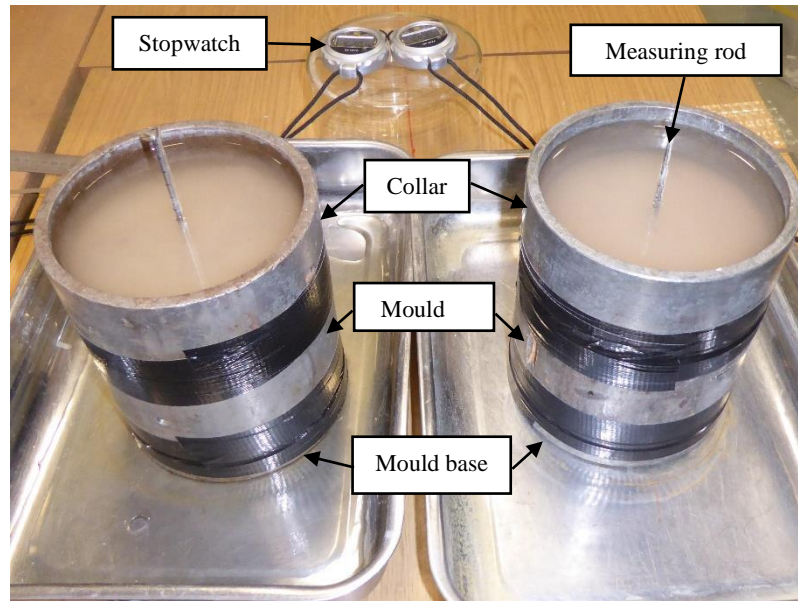


Figure 3. 4. Infiltration rate test setting

### 3.5.2. Erosion Susceptibility Tests

It was necessary to assess the susceptibility to erosion of the selected soils before undertaking an intensive erosion testing program. The crumb, the double hydrometer, and the hole erosion tests were conducted.

#### 3.5.2.1. Crumb Test

Dispersive soils are the soils which deflocculate when immersed in water. Such soils are cause for many engineering and structural failures (Paige-Green, 2008; Nagy and Nagy, 2015). The fastest and least complicated test to investigate dispersive soils is the crumb test. It consists of immersing crumbs of samples in either distilled water or a dilute solution of sodium hydroxide and observing the reaction of the colloids in the suspension (BS 1377-5:1990; Maharaj, 2011).

Crumb samples of 4 cm-diameter and 6 cm-height were extracted from compacted soils by means of coring and oven-dried for 24 hours. The weights of dry crumbs were about 100 g; thus, each was immersed in about 500 g of water according to Maharaj (2011). Usually, crumb samples can be air dried, remoulded or oven dried (Maharaj, 2011) and the latter was adopted

due to its ability to provide more stability and therefore easy handling of samples before being tested. Samples of GS and VGS soils mixed with ECC proportions were prepared and tested as in Figure 3.5 and examined according to Table 3.4. Two tests were conducted per each sample.

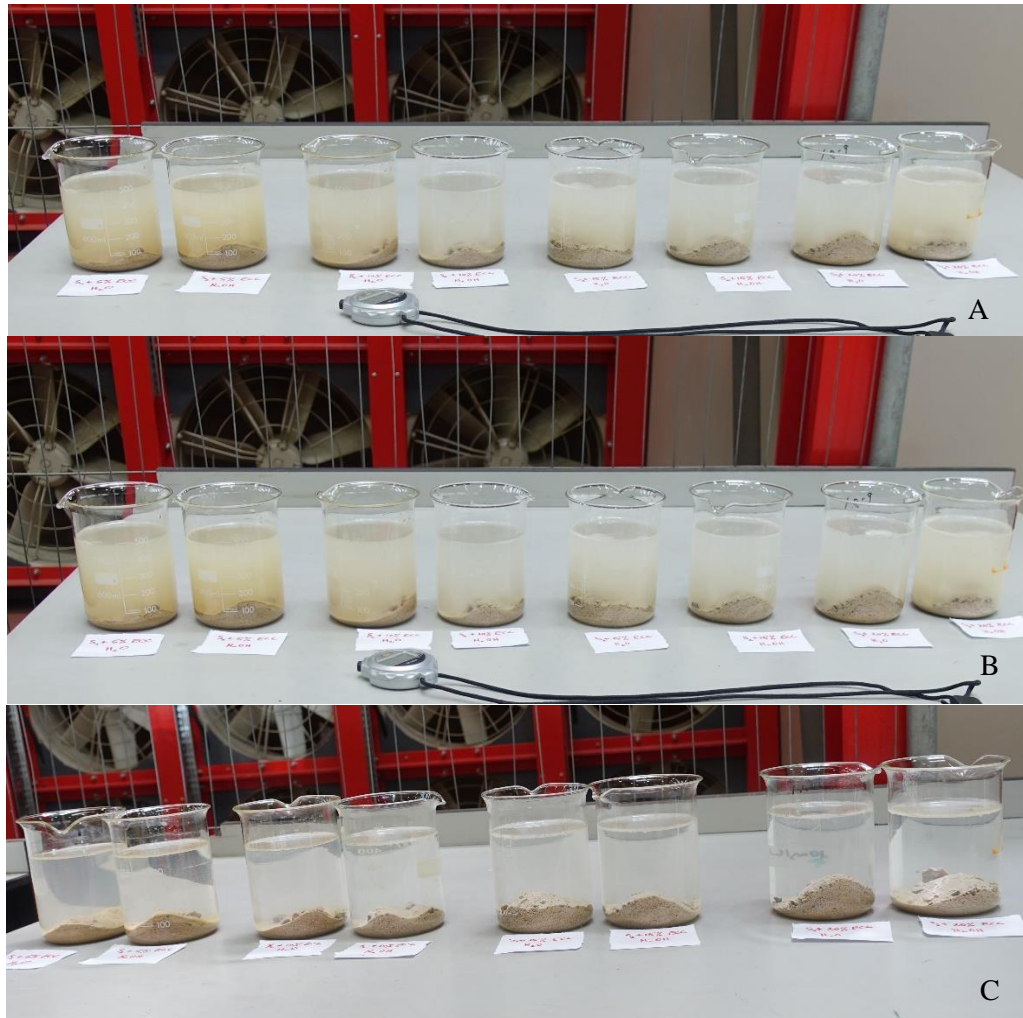


Figure 3. 5. Colloidal reaction of samples after 10 min (A); 1 hour (B); and 2 hours (C)

Table 3. 4. Description of crumb test grades of reaction (Maharaj, 2011)

Grade	Reaction	Description
1	No reaction	Crumbs may slake without cloudiness by colloids' suspension
2	Slight reaction	Bare hint of cloudiness in water at surface of crumb
3	Moderate reaction	Easily recognisable cloud of colloids in suspension, usually spreading out in thin streaks on bottom of beaker
4	Strong reaction	Colloids' cloud covers nearly the whole bottom of the beaker, usually as a thick skin

### 3.5.2.2. Double Hydrometer Test

The SCS double hydrometer test was conducted according to BS 1377-2 (1990). A standard hydrometer test and a parallel test for which a solution of hexametaphosphate was added were performed. The quantity (%) of particles finer than 0.005 mm was obtained for both tests. The dispersion ratio is an expression of the quantity of those particles in the parallel test as a percentage of the same particles in the standard test. Based on the dispersion ratio, the soil samples containing ECC were classified according to Table 3.5.

Table 3. 5. Double hydrometer test interpretation (Maharaj and Paige-Green, 2013)

Dispersion ratio (%)	Description
> 50	Highly dispersive
30–50	Moderately dispersive
15–30	Slightly dispersive
< 15	Non-dispersive

### 3.5.2.3. Hole Erosion Test (HET)

The HET test is usually suitable for clay soils. It was conducted for the purpose of comparing the erosion rate for the mixes of GS and ECC in a range of proportions. The samples of 12.5 cm length and 5.1 cm diameter were compacted to the maximum dry density into the transparent Plexiglas moulds. A 3 mm diameter hole was pre-drilled hole in the centre of the samples before being tested. Thin plastic washers with centred holes bigger than the pre-drilled hole were placed at both ends of the sample, which was then placed into the test set up. The duration of the test was set to 3 minutes. However, both the pressure and flow rate were found to be excessive for granular soils and only GS containing 15% ECC and 20% ECC were tested successfully. GS containing 10% ECC was tested for 1 minute, while GS + 5% ECC and GS + 0% ECC soils could not be tested as these were quickly washed away from the moulds. At the end of the tests, melted wax was casted into the erosion holes. Details are shown in Figure 3.6.

The melted wax cooled into the erosion hole and was used to estimate the size of the hole formed during erosion. The perimeter of the dry wax stick was taken at three positions to have upstream (Up), middle (Mp) and downstream (Dp) perimeters, respectively. The average of the three perimeters was considered as the perimeter of the erosion hole. Three tests were conducted for each sample for repeatability purpose, as shown in Figure 3.6(E).

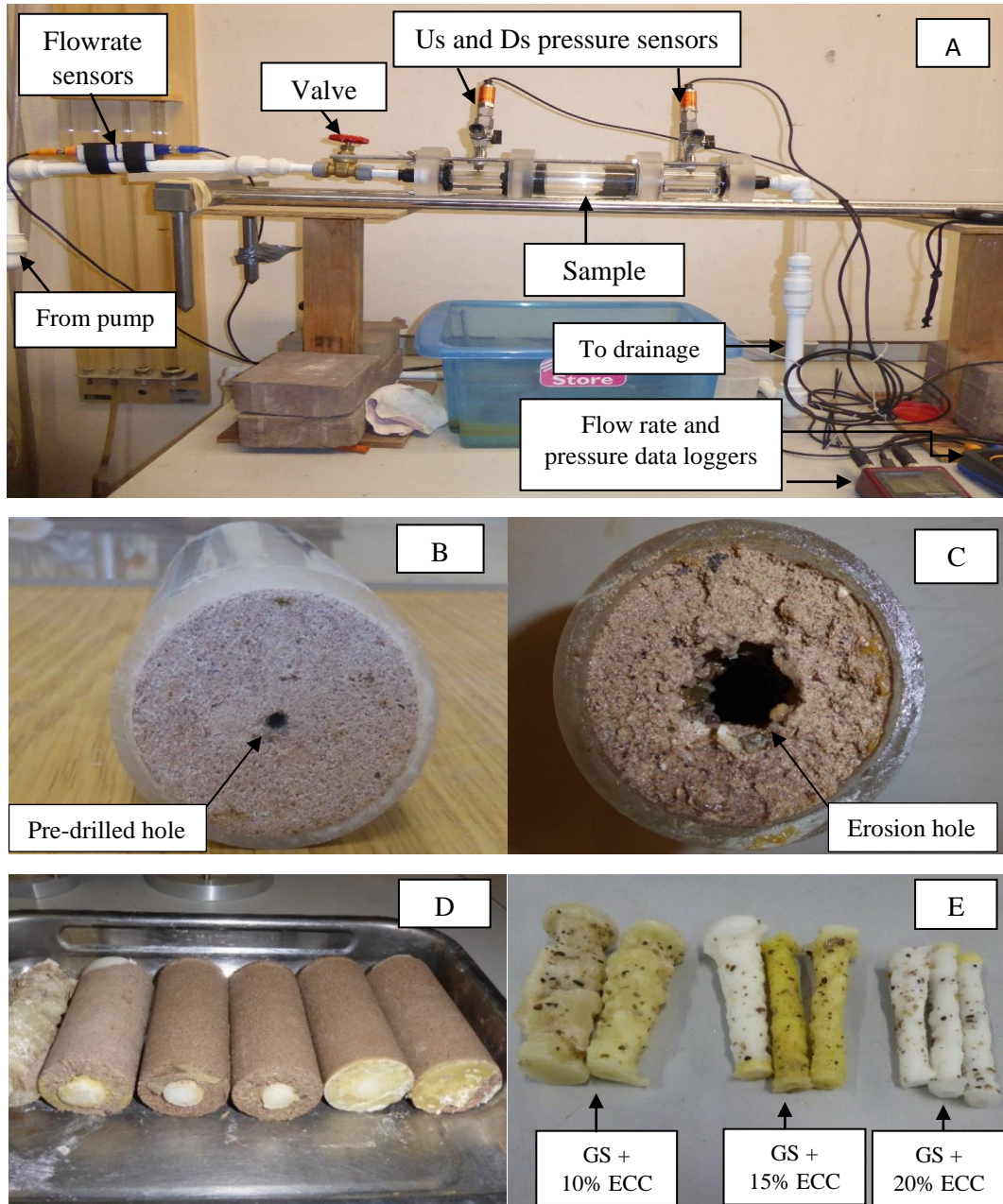


Figure 3. 6. Hole erosion test set up (A); pre-drilled sample before test (B); tested sample with erosion hole (C); casting of wax into the erosion hole (D); and wax casts of erosion holes (E)

From the perimeter, an average diameter ( $D_2$ ) of the hole made by erosion was calculated as follows:

$$D_2 = \frac{p}{\pi} \quad (\text{Eq. 3.1})$$

where  $p$  is the average perimeter of the erosion hole (cm) and  $\pi = 3.14$ .

After obtaining the diameters, the volume ( $V$ ) of eroded soil was computed as follows:

$$V = \frac{\pi}{4} (D_2^2 - D_1^2) * h \quad (\text{Eq. 3.2})$$

where  $D_1$  is the pre-drilled hole diameter (cm) and  $h$  is the length of the sample (cm).

### 3.6. Rainfall Simulator for Erodibility Tests

The main objective of this study was to assess erodibility of unpaved roads due to rainfall erosion. The apparatus to help conduct erodibility tests was a rainfall simulator. Stages of designing and constructing an effective rainfall simulator are explained in the next sections.

#### 3.6.1. Overview on Rainfall Simulators

Simulated rainfall has been used successfully to investigate the susceptibility to erosion mainly for agriculture soils (Moore et al., 1983; Aksoy et al., 2012; Horne, 2017). There are two types of rainfall simulators: drop-forming and pressurized simulators, and each of these has merits and demerits, as shown in Table 3.6. The simulated rainfall can mimic natural rainfall's effect on the detachment of unpaved roads' surface soils. This is vital since erosion on the surface of those roads is due to soil detachment caused by both rainfall energy and the flow shear stress.

For this study, the pressurized rainfall simulator was preferred as it met both the requirements to effectively conduct erosion tests and overcome the limitations imposed by the laboratory sites such as the source of water and the height from which the raindrops fall. A comparison between the drop forming- and pressurised-nozzle simulators can be seen in Table 3.6.

Table 3. 6. A comparison between drop-forming and pressurized rainfall simulators

	Drop-forming simulators	Pressurised simulators
Advantages	They are suitable for small plots (less than 10 m <sup>2</sup> ) and hence suitable for laboratory works due to limited spaces. High spatial uniformity of raindrops (> 90%) and easy control on drop size are attainable. The raindrops of natural rains are reproducible (1 - 6 mm). The raindrops fall by gravity force (Aksoy et al., 2012; Aksoy et al., 2017; Horne, 2017).	They are suitable for laboratory and field tests and can perform for wider plots (10 – 500 m <sup>2</sup> ). Variable rainfall intensities and random raindrop sizes are obtained, with spatial uniformity of raindrops greater than 80%. Reproduced natural raindrops sizes. Maximum drop size and kinetic energy are achievable for the heights less than 4 m. They are portable and have high resistance to wind effect (Aksoy et al., 2012; Aksoy et al., 2017; Ngezahayo et al., 2019a, e).
Disadvantages	Low rainfall intensities. Drops form from lower heights with difficulty to achieve terminal velocities and kinetic energy of raindrops. About 9 m needed to achieve maximum drop sizes and kinetic energy (Moore et al., 1983; Aksoy et al., 2017).	High rainfall intensities (greater than 200 mm/hr) than naturally occurring rainfall can be achieved. Drop velocities can be exaggerated due to water pressure. There is less control on drop size (Tossel et al., 1987; Sheridan et al., 2008; Aksoy et al., 2012; Aksoy et al., 2017).
Operational limits	They are mostly stationary and have poor performance to wind. Impractical for field use due to high heights needed (Aksoy et al., 2012; Horne, 2017).	May need to be powered by pumps and generators to help raindrops fall at desired velocities (Tossel et al., 1987; Sheridan et al, 2008; Aksoy et al., 2012; Aksoy et al., 2017).

### 3.6.2. Design of the Rainfall Simulator

Designing and constructing a suitable rainfall simulator was an important objective of this study. Horne (2017) said that the accuracy of a pressurized rainfall simulator depends on its ability to reproduce the ranges of natural rain drop sizes, the raindrops' terminal velocity, the rainfall intensity, and the uniform drop distribution over the tested area.

The rainfall nozzles and the pipes to feed water to the nozzles were selected. The pipes were perforated to make 6 mm diameter holes in which the downward nozzles were inserted. Since the nozzles weight would increase once filled with water, smaller nozzles were preferred to avoid the likelihood of them coming off due to weight. Henceforth, the 250 ml nozzles and 15 mm x 1.5 mm BARRIER PE-X pipes (BS 7291-3: 2010) were chosen for the construction of the rainfall simulator. Water was supplied from the water tap to the rainfall simulator. Due to the non-cylindrical shape of the nozzles' bottoms, which would prevent them to be fitted into the pipe holes securely, the original bottoms were cut off and the nozzles inserted into a new 6 mm x 4 mm (external x internal diameter) nylon pipe bottom. The spacing between nozzles on the same pipe was 2.3 cm centre to centre, while the spacing between two successive pipes was 5 cm. Since the T-joints between horizontal pipes allowed 10 cm spacing, two layers of pipes were superimposed and connected using a crossing hose pipe at one end to ensure an even supply of water in both layers.

The details of the steps discussed above are shown in Figures 3.7 and 3.8. The height of 2 m above the surface of the soil samples was deemed enough to produce the necessary drop size and kinetic energy to help conduct erodibility tests (Aksoy et al., 2012; ASTM, 2015).

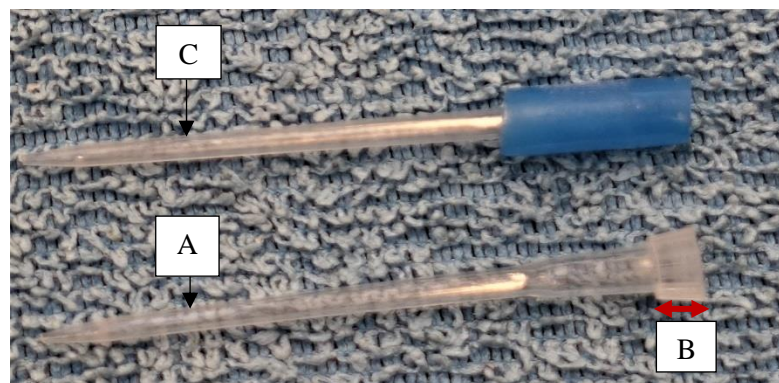


Figure 3. 7. Supplied nozzle (A), original nozzle bottom to be cut off (B) and modified nozzle inserted into new nylon pipe (bleu) bottom (C)

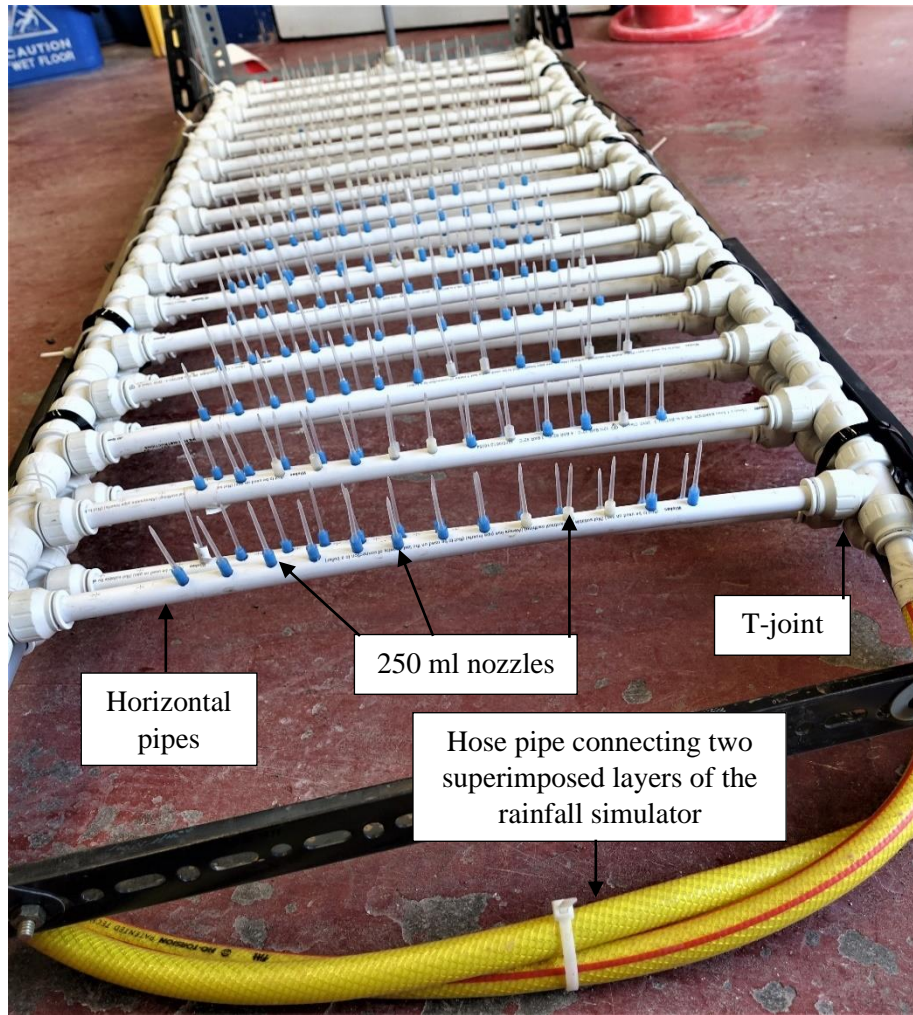


Figure 3. 8. A top view of the overturned rainfall simulator

### 3.6.3. Design of the Simulated Rainfall Intensity

Since this study was about erodibility of soils in unpaved roads, it was sensible to use rainfall intensities more representative of the regions with high percentages of those roads. Thus, rainfall intensities from Sub-Saharan Africa (Rwanda and Democratic Republic of Congo) which can also occur in many countries worldwide were selected. According to Mohymont et al. (2004), Demarrée and Van de Vyver (2013), and Wagesho and Claire (2016), 30 mm/hr, 51 mm/hr and 68 mm/hr rainfall intensities which generally occur for about 60 min, 35 min and 21 min respectively every 2 years in those countries were selected. The IDF curves from KARAMA hydrology station in Rwanda is shown in Figure 3.9.

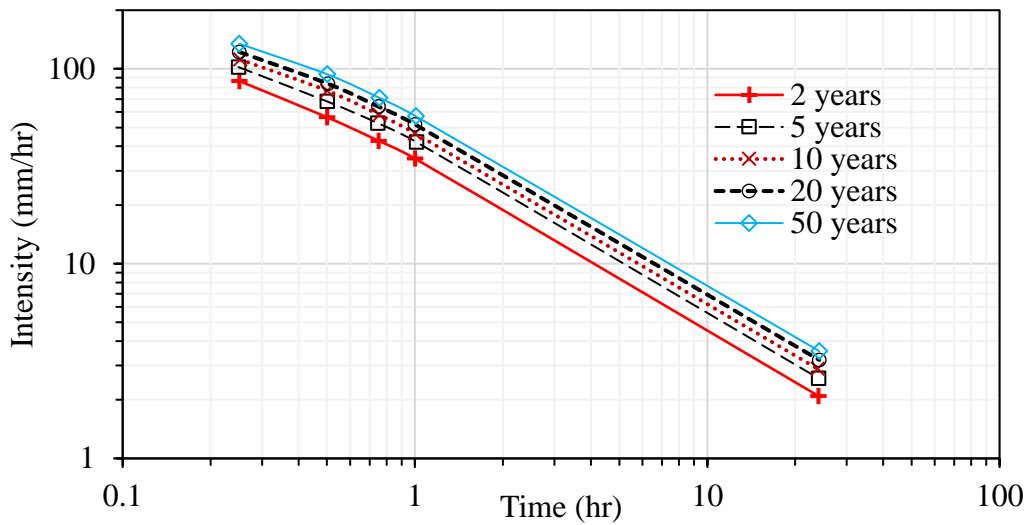


Figure 3. 9. IDF curves from KARAMA, Rwanda (Demarreé and Van de Vyver, 2013)

#### 3.6.4. Determination of the Raindrops' Size

The size of raindrops can be determined using various methods: stain method, momentum method, immersion method, oil method, photographic method, and flour method (Horne, 2017). The stain method relates the stain due to raindrops on absorbent surfaces such as filter and blueprint papers to the diameter of the raindrops (Eigel and Moore, 1983; Aksoy et al., 2012; Horne, 2017; Ricks et al., 2019). In contrast, the momentum method uses both pressure transducers and piezoelectric sensors to determine the raindrops' sizes (Kathiravelu et al., 2016; Horne, 2017; Ricks et al., 2019). During the immersion method, raindrops are collected into an oil and surrounded due to the low density of the oil, and drop diameters are obtained using a microscope (Eigel and Moore, 1983; Horne, 2017). The oil method differs from the immersion method by the fact that the former uses a specific type of low-density oil and a high level of viscosity which help when taking photographs of the raindrops enveloped by the oil. Raindrop diameters are then determined from these photographs (Aksoy et al., 2012; Horne, 2017).

The photographic method accurately gives quick estimation of the size and shape of raindrops. However, this method not only requires expensive equipment but also fails to produce a good

raindrop distribution due to count errors related to superimposition of multiple drops or to a windy testing site which can cause drop drift and inaccurate measurement (Kathiravelu et al., 2016; Horne, 2017). On the other hand, the flour method consists of collecting raindrops in pans that contain plain flour and the drops' diameters are determined from the pellets formed by water and flour. This method was preferred for this study due to its simplicity and less cost (Eigel and Moore, 1983; Horne, 2017). It is discussed in detail in the following section.

### 3.6.5. Flour Method for Raindrop Size Determination

The flour method was developed by Bentley in 1904 (Laws and Parsons, 1943; Eigel and Moore, 1983). Although this method is not standardised, ASTM was in the process to make it a standard test (Horne, 2017). This method represents the shape of natural raindrops ranging from 1 - 6.1 mm (Horne, 2017; Ricks et al., 2019). The method consisted of collecting raindrops in the pans of about 21 cm diameter, filled with a 2.5 cm thick layer of plain flour from Tesco' supermarket. Three evenly spaced pans were placed at 30 cm from the ground below the rainfall simulator for each of the three target rainfall intensities for 3 seconds. The pans reflected the position of the soils to be tested. Two tests were conducted per each rainfall intensity and an average number of the raindrops considered (Eigel and Moore, 1983; Horne, 2017).

As the rainfall hit the flour in the pans, wet pellets formed and placed in the open air for at least 12 hours for the pellets to dry out. Using a spoon, air-dried pellets were separated from the rest of the flour, then manually sieved on the 0.213 mm sieve to remove excess flour. Double pellets formed due to close raindrops were removed and disregarded. The pellets were then oven-dried at 43 °C for 6 hours before being sieved for 2 minutes, on the sieves of 4.75 mm, 2.36 mm, 2.00 mm, 1.18 mm, 0.85 mm, 0.60 mm, and the pan. After sieving, the pellets retained on each sieve were weighed and counted. The mean diameter of the raindrops was estimated using Eq. 3.3.

$$D_r = \sqrt[3]{\left(\frac{6}{\pi}\right) W m_R} \quad (\text{Eq. 3.3})$$

where  $D_r$  is the mean raindrops' diameter (mm) and  $W$  is the mean weight of the raindrops (mg) and  $m_R$  is the ratio of the mass of the raindrop to the mass of the pellet which is obtained using the flour-calibration line (Appendix 1, Figure 2) suggested by Laws and Parsons (1943). Figure 3.10 shows the raindrops collection into the flour and the dried pellets after sieving.



Figure 3. 10. Raindrops collection into the flour (A), separating air-dried pellets from the flour (B) and sieved oven-dried pellets (C)

### 3.7. Design of the Soil Test Container

Knapen et al. (2007) reported different dimensions for soil testing boxes that were used during 27 studies on 113 soil types from Australia, Belgium, Brazil, Canada, Italy, Iran, Israel, Mexico, South Africa, and USA. The soils were either undisturbed or sieved in sizes ranging from 2 mm to 50 mm; the bed slopes ranged from 0% to 40%; while the source of eroding water was either surface runoff or simulated rainfall intensities ranging from 20 mm/hr to 127 mm/hr. More information can be seen in appendix 3. The observation on the soil testing boxes used in previous studies showed that the key dimension was the length (L) of the box which was about 2 to 65 times the width (W). There was no direct relationship between width and depth (H) of the box; each of these dimensions could be smaller or greater than the other. Overall, the boxes dimensions ranged from 0.5 m x 0.05 m x 0.13 m to 22 m x 0.4 m x 0.76 m, for length x width x depth of the box. Based on the discussions above, the soil boxes of 0.6 m x 0.3 m x 0.17 m for the small-scale testing and 1.2 m x 0.3 m x 0.17 m for the large-scale testing of erodibility were used. Small- and large-scale tests will be described in the next sections. The side and base joints of the boxes were sealed to avoid leakages, whilst the inner surfaces were waterproofed.

### 3.8. Small-scale Testing of Erodibility

It was impossible to scale the length of the road surface subjected to erosion, which may be many tens of meters, in a laboratory study. Thus, attention is required in monitoring erosion. Since the length of the road is important in erosion acceleration (Ziegler et al., 2000, 2004; Cao et al., 2009, 2011, 2013), erodibility tests were undertaken on two slope lengths; the longer being twice the shorter. Results from the two slope lengths enabled to depict the effect of the length of the road on erodibility of unpaved roads. The tests on the shorter slope were referred to as small-scale erodibility tests, whilst the tests on the longer slope were referred to as large-scale erodibility tests.

The soil type, slope lengths, slope gradient and rainfall intensities were the important factors in deciding the number of tests to be carried out. Moreover, it was decided to always carry out two tests on each soil sample with 24 hours (1 day) between the two. This time gap between the two tests allowed the sample to lose some surface wetness and reflect what happens in unpaved roads when it rains for two successive days. The test duration was fixed to 30 minutes, which was considered adequate in terms of measuring erosion (Knapen et al., 2007).

For small-scale tests, flowmeter readings were 0.4 l/min, 0.6 l/min and 0.8 l/min respectively for 30 mm/hr, 51 mm/hr and 68 mm/hr. Ninety-two small-scale erodibility tests were conducted, as shown in Table 3.7, where √ indicates performed test and — indicates no test. Figure 3.11 shows a small-scale rainfall simulator with a soil sample placement after being compacted. A side view of the system during the test is shown with the rainfall simulator and the soil testing box held on supports (S). Dimensions of the box sides and back walls were 0.23 m above the soil surface to prevent splashed particles to escape from the box. Detached and eroded sediment was conveyed by the gutter (B) into the collection receptacle (T).

Table 3. 7. Schedule of small-scale erodibility tests

Soil type	Rainfall intensity (mm/hr)			Slope gradient (%)		Number of tests
	30	51	68	0	6	
GS	√	√	√	√	√	6
GS + 5% ECC	√	√	√	√	√	6
GS + 10% ECC	√	√	√	√	√	6
GS + 15% ECC	√	√	√	√	√	6
GS + 20% ECC	√	√	√	√	√	6
VGS + ECC	—	—	√	√	√	2
VGS + 5% ECC	—	—	√	√	√	2
VGS + 10% ECC	—	—	√	√	√	2
GS + 15% ECC	—	—	√	√	√	2
GS + 20% ECC	—	—	√	√	√	2
Subbase	√	√	√	√	√	6
Number of first day tests						46
Number of second day tests						46
Total number of small-scale erodibility tests						92

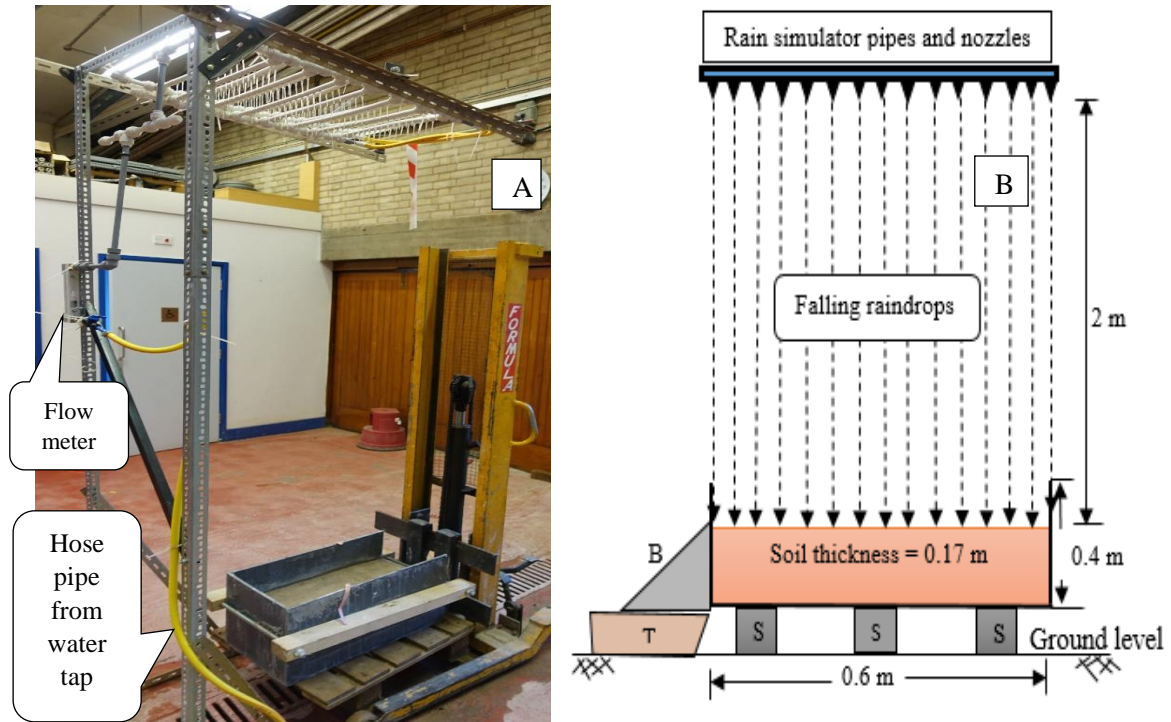


Figure 3. 11. Small-scale testing: sample placement after being compacted (A) and side view during testing (B)

### 3.8.1. Moisture and Density Variations during Erodibility Tests

Moisture variations during erodibility tests under simulated rainfall was essential to check since it was going to support findings from infiltration rate tests, as discussed in section 3.5.1, and indicate the degradation of soils' shear strength due to rainfall. During the tests, part of rainfall water migrated downwards (infiltration) and increased the moisture content of soil samples with subsequent reduced shear strength and therefore more vulnerability of soils to erosion. Another part of rainfall formed the runoff that transported detached soil particles (sediment).

To check the moisture changes during erosion test duration, six core tubes were inserted into the soil after 5 min intervals for 30 min rainfalls. The tubes were covered at the top to prevent further raindrops on the cored samples. It was done for all the three rainfall intensities on the soils which contain English china clay to provide additional information on how water permeates through soils. Moisture contents were measured following BS 1377-2: 1990, on

extruded samples and cut at 0–3 cm, 8–10 cm and 14–17 cm from the top surface of the soil downwards. Since the soils were compacted at maximum dry density, cutting the extruded sample, and checking moisture content at different positions helped to observe changes in moisture with time due to rainfall. The sampling process is shown in Figure 3.12.

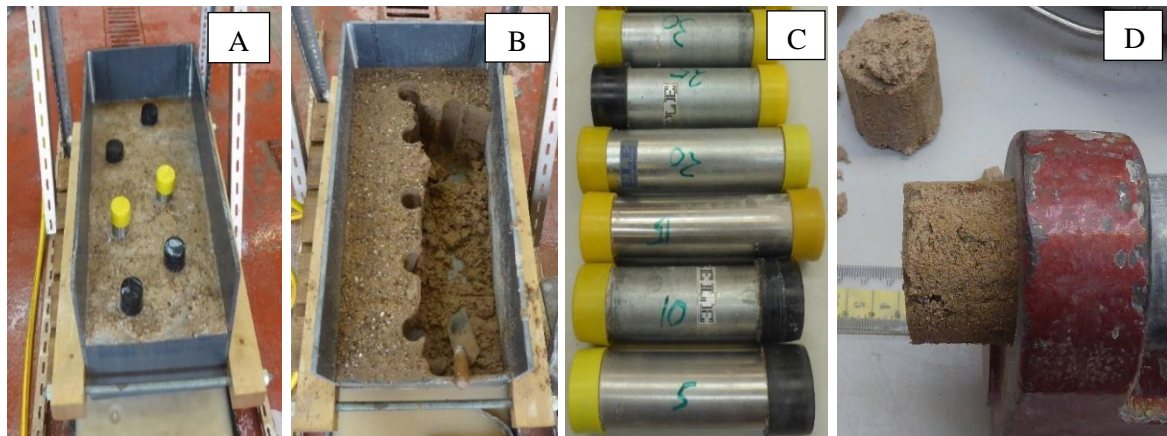


Figure 3. 12. Core cutters inserted into soil every 5 min (A), core cutters removed (B), samples into core cutters (C), and samples' extrusion from core cutters (D)

### 3.8.2. Data Collected During the Small-scale Erodibility Tests

Two types of data were collected during the erodibility tests. Firstly, the sediment eroded due to both detachment by raindrops' kinetic energy and subsequent runoff water was collected every 5 min for 30 min. The collected runoff was weighed before oven-drying to ascertain the dry weight of the sediment. The dried sediment was then sieved for PSD analysis.

Secondly, photographs were taken every 5 min at the surface of the tested soil samples using a Sony camera and were analysed using ImageJ software (Ferreira and Rasband, 2012) to obtain the particle size of soils at the surface of the tested soils at different time intervals. By considering the particle size distribution from both the sediment and from the surface photographs it was possible to experimentally see which soil particles were eroded first and faster than the others.

### 3.9. Large-scale Testing of Erodibility

The large-scale erodibility tests were conducted on soil samples compacted into the 1.2 m x 0.3 m x 0.17 m (L x W x H) soil box, as discussed in section 3.7. Unlike the small-scale tests, a new slope of 12% was added to the schedule for soils mixed with 20% English china clay. As the box was very heavy when filled with soils and the compaction had to be done with the box being at zero slope (flat), a hydraulic jack system was used to lift and support to the desirable slopes during erodibility tests. The walls and base of the box were made in solid metal panels to avoid any deflections that may happen due to compacting large amount of soils into the box. Other design and construction criteria for both the soil testing box and the rainfall simulator were the same as for the small-scale tests, as discussed in section 3.7. For the larger test, air was introduced into the rainwater system to speed up the flow through the pipes to produce the target simulated rainfall intensities. This is discussed in detail in the section 3.9.1. The schedule of the tests conducted is shown in Table 3.8, with  $\checkmark$  for the test performed and — for no test.

Table 3. 8. Schedule of large-scale erodibility tests

Soil type	Rainfall intensity (mm/hr)			Slope gradient (%)			Number of tests
	30	51	68	0	6	12	
GS	$\checkmark$	$\checkmark$	$\checkmark$	$\checkmark$	$\checkmark$	—	6
GS + 5% ECC	$\checkmark$	$\checkmark$	$\checkmark$	$\checkmark$	$\checkmark$	—	6
GS + 10% ECC	$\checkmark$	$\checkmark$	$\checkmark$	$\checkmark$	$\checkmark$	—	6
GS + 15% ECC	$\checkmark$	$\checkmark$	$\checkmark$	$\checkmark$	$\checkmark$	—	6
GS + 20% ECC	$\checkmark$	$\checkmark$	$\checkmark$	$\checkmark$	$\checkmark$	$\checkmark$	9
VGS + ECC	—	—	$\checkmark$	$\checkmark$	$\checkmark$	—	2
VGS + 5% ECC	—	—	$\checkmark$	$\checkmark$	$\checkmark$	—	2
VGS + 10% ECC	—	—	$\checkmark$	$\checkmark$	$\checkmark$	—	2
GS + 15% ECC	—	—	$\checkmark$	$\checkmark$	$\checkmark$	—	2
GS + 20% ECC	—	—	$\checkmark$	$\checkmark$	$\checkmark$	$\checkmark$	3
Subbase	$\checkmark$	$\checkmark$	$\checkmark$	$\checkmark$	$\checkmark$	—	6
Number of first-day tests							50
Number of second-day tests							50
Total number of large-scale erodibility tests							100

### 3.9.1. Enlargement of the Rainfall Simulator

The larger size of the soil box meant that rainfall simulator had to be enlarged accordingly. Except the slope length that was doubled (from 0.6 m to 1.2 m), the other detail of the box was like the small-scale testing box. Figure 3.13 shows a photograph of the enlarged soil testing box and rainfall simulator. Unlike the small-scale rainfall simulator, it was not possible to achieve the target intensities for the large-scale rainfall simulator directly from the water tap. The water tap was not enough to move through the pipes and form adequate raindrops sizes.

Since the water tap was the only possible source of water, it was necessary to find ways of increasing the flow rate that should reach the rainfall simulator. Hence, a flow control zone (CZ) was designed by provision of two flowmeters namely, the GARDENA® flowmeter (1) to indicate the flowrate directly from the water tap and the COLE-PALMER® flowmeter (4) with a valve (5). The valve, by open-close movements, helped to introduce air into the flow and increase flowrates that satisfied the size of the rainfall simulator for all the target intensities. However, the introduction of air caused lots of oscillations of the flow meter's bob leading to difficulties in the precise reading of the flow rate for a given rainfall intensity. For this reason, a pressure gauge (3) was added between the two flow meters and the calibration of rainfall intensities based on the three devices. The main valve (2) served to close the flow temporarily between the supply water tap and the rainfall simulator while the pipe (6) conveyed water to the rainfall simulator. Details of the flow control zone are shown in Figure 3.14. Using the tap flow rate from GARDENA® flowmeter, aird flow rate from COLE-PALMER® flowmeter and the pressure gauge, calibration for target rainfall intensities was achieved. Readings were checked for the three devices before starting each erodibility test, as shown in Figure 3.15.

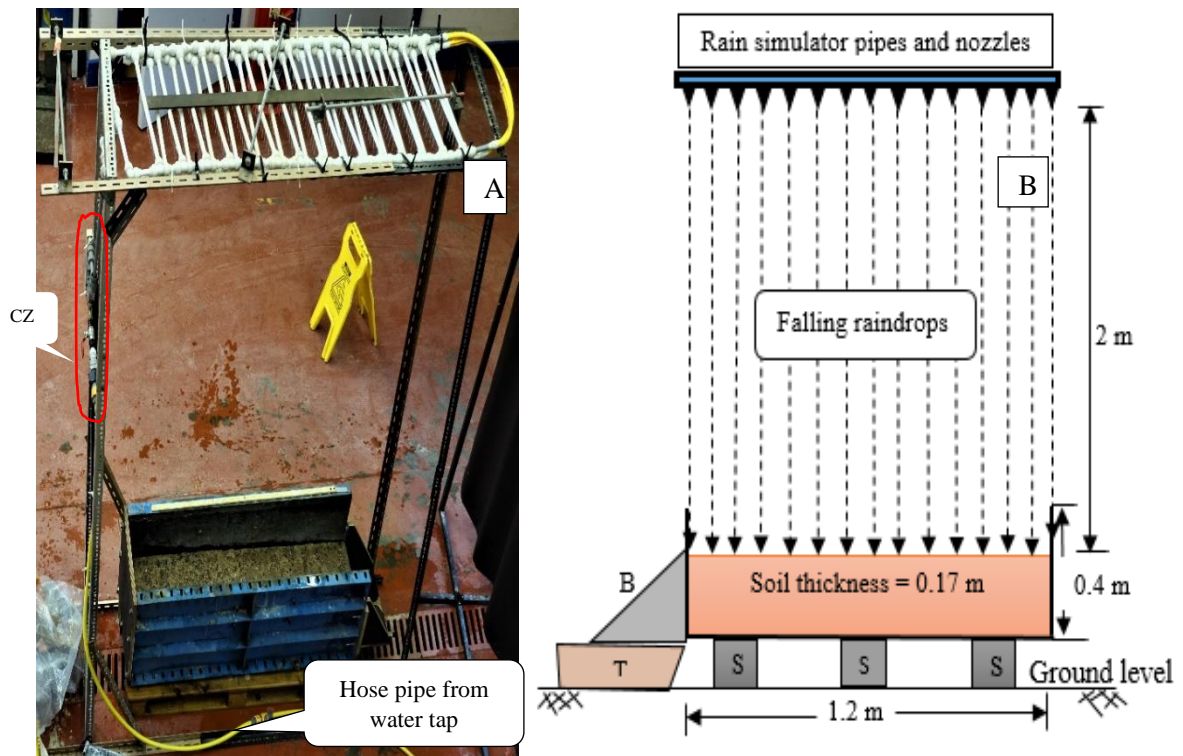


Figure 3. 13. Large-scale testing: rainfall simulator with flow control zone (CZ) and soil sample (A) and side view of the rain simulator during the test (B)

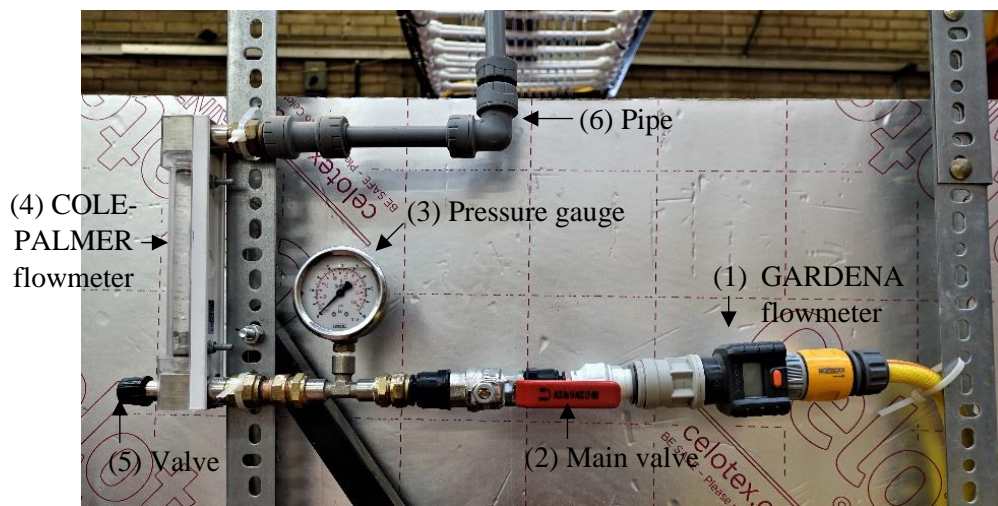


Figure 3. 14. Detail of the flow control zone (CZ)

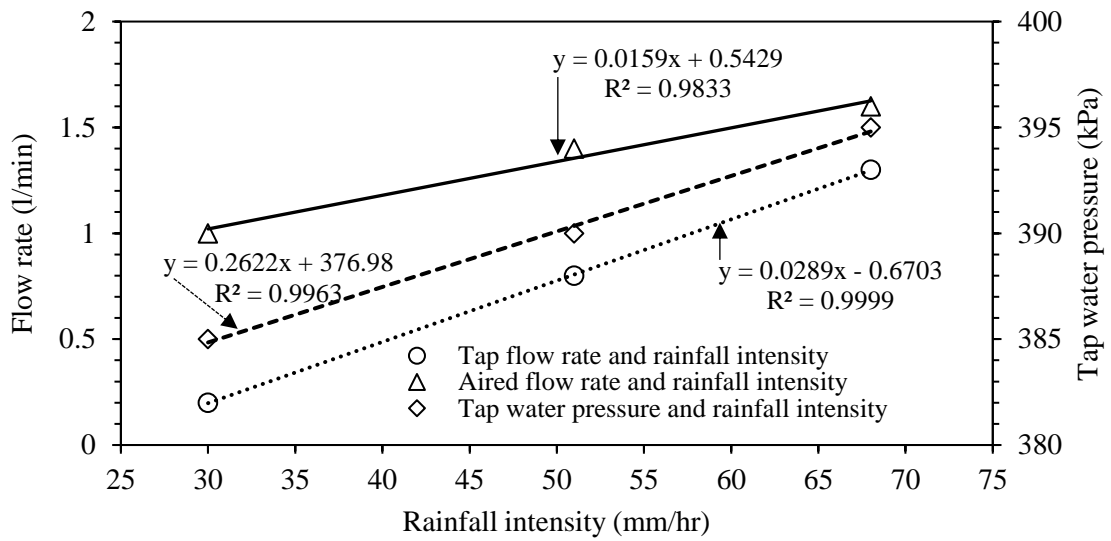


Figure 3. 15. Calibration of rainfall intensities for large-scale rainfall simulator

### 3.9.2. Homogeneity of Compacted Samples

The soils were compacted before being tested. Maintaining the same compaction levels for the whole sample and for all the samples (comprising the same soil materials) was important. The homogeneity of the samples was controlled by maintaining the same dry mass of soil samples to be compacted at the same optimum moisture content (shown in Table 3.3), maintaining the same mixing protocol, and compacting the soils in the same manner in three layers of equal thickness using a vibratory hammer. Furthermore, a 33-mm hand vane shear (HVS) test was carried out on six soils only for only comparison purposes between the compaction test results in the Proctor mould and in the soil testing box. The average of readings from three different locations in the box was considered. The hand vane shear test, which is usually performed on cohesive soils (BS 1377-7:1990), was modified to push only 7 cm of the rod into the soil while usually at least 20 cm should be pushed into the ground. The average of three tests was taken for the HVS in the Proctor compaction mould while an average of three locations was considered for the HVS in the testing box. Table 3.9 shows that results of both tests were to confirm homogeneity in compaction levels achieved in both compaction mould and testing box.

Table 3. 9. Average hand vane shear test results in compaction moulds and soil testing box

Soil type	HVS in compaction mould (kPa)	HVS in soil testing box (kPa)
GS + 10% ECC	53	50.2
GS + 15% ECC	55	53.8
GS + 20% ECC	57.5	56.2
VGS + 10% ECC	49.4	48.3
VGS + 15% ECC	50.5	51.8
VGS + 20% ECC	56.1	54.8

### 3.9.3. Data Collected During the Large-scale Erodibility Tests

Data for erodibility analysis was collected in the same way as for the small-scale testing, as explained in section 3.8.2. Figure 3.16 shows the process from the mixing of the soils; compaction of samples; sediment collection, drying in the oven and readying for sieve test.



Figure 3. 16. Mixing samples in electric mixer (A); compaction by electric hammer (B); collected runoff and sediment (C); oven-drying sediment (D); and sediment for sieving (E)

The dry sediment was prepared by careful brushing to remove it from tray walls before being grinded and poured into sieves for particle size distribution analysis according to BS 1377-2 (1990). The sieves used were 10.0 mm, 6.3 mm, 5.0 mm, 3.35 mm, 2.0 mm, 1.18 mm, 0.63 mm, 0.425 mm, 0.3 mm, 0.212 mm, 0.150 mm, 0.063 mm, and the pan.

### 3.10. Calibration of ImageJ Software

ImageJ was used to analyse the surface particle size changes during erodibility tests. This software was preferred over others such as Matlab because of its simplicity and free of charge availability for academic researchers. Moreover, ImageJ had been used accurately to study the behaviour of particles both in static and moving conditions (Ferreira and Rasband, 2012). To check the efficiency of the ImageJ software, a photograph was taken after 5 min of a 30 mm/hr rainfall intensity on a GS + 5% ECC soil, and a 20 cm x 20 cm portion of the photograph was analysed using the software. At the same time, the sediment eroded during these 5 min was collected and oven dried. The idea was that the particle size distribution of the control soil, GS + 5% ECC, should be the same or nearly the same as the sum of particle size distributions of both the collected sediment and the remaining surface particles.

The idea of analysis of the soil particle changes due to erosion on a constant surface was used by Ngezahayo et al. (2019a, e) based on the following hypotheses:

- If the number of surface particles reduces with increasing rainfall duration, the mean particle size increases to show that the smaller particles eroded before larger particles.
- If the number of surface particles increases with increasing rainfall duration, the mean particle size decreases to show that the larger particles eroded before smaller particles.
- If the number of surface particles remains the same regardless of an increasing rainfall duration, the mean particle size remains the same to show that both smaller and larger particles eroded at the same rate.

### 3.11. Sheet Erosion Tests

The sheet erosion tests were undertaken on GS + 20% ECC and VGS + 20% ECC soils. The tests aimed at visually assessing the influence of coarse particles on erosion simulating presence of gravel at the road surface. Some amendments were made on those soils as follows:

1. The soils were compacted at the maximum dry density, into the bed flow tank.
2. As in (1) but with glass marbles buried about 1 mm from the surface.
3. As in (1) but with buried glass marbles so that about 25% of the size is exposed.

The soil samples were compacted so that the surface slope was 2%, within a bed flow tank of 2.1 m x 0.2 m x 0.17 m (length x width x depth). The glass marbles of 14-mm diameter were used during the sheet erosion tests. These were carefully pushed into the soil after compaction. Forty-two glass marbles were in three lines parallel to the side of the bed flow tank and in 14 lines across the width of the bed flow tank. They were at a spacing of 15 cm and 9 cm along the length and the width respectively, as shown in Figures 3.17 and 3.18. The same sample was tested for the first time, second time after 24 hours, third time after ten days from the second test and fourth time after 24 hours of the third test. These tests were mentioned as first- and second-day, and tenth- and eleventh-day tests, as shown in Table 3.10.

Table 3. 10. Schedule of sheet erosion tests

Soil type	1 <sup>st</sup> and 2 <sup>nd</sup> day tests	10 <sup>th</sup> and 11 <sup>th</sup> day tests	Number of tests
GS + 20% ECC	√	√	4
GS + 20% ECC + buried glass marbles	√	—	2
GS + 20% ECC + exposed glass marbles	√	—	2
VGS + 20% ECC	√	√	4
VGS + 20% ECC + buried glass marbles	√	—	2
VGS + 20% ECC + exposed glass marbles	√	—	2
Total number of tests			16

Each sheet erosion test consisted of passing, for two hours, a runoff flow of 15 l/min flow rate. For every test, five photographs were taken: before, every 30 min and after the test to analyse the growth of erosion features due to runoff flow. Thus, about 80 photographs were taken for sheet erosion tests analysis. The flow velocities for each soil sample are shown in Table 3.11.

Table 3. 11. Flow velocities during sheet erosion tests

Soil type	Flow velocity (m/s)
GS + 20% ECC	0.315
GS + 20% ECC + buried glass marbles	0.315
GS + 20% ECC + exposed glass marbles	0.285
VGS + 20% ECC	0.302
VGS + 20% ECC + buried glass marbles	0.302
VGS + 20% ECC + exposed glass marbles	0.273

Considering the velocities in Table 3.11, and the mean particle size of the tested soils (ignoring glass marbles), the velocities were greater than critical flow velocities. Thus, they were enough to cause sheet erosion on the soils. Figure 3.19 shows the location of the soils into the envelopes of critical velocity and particle size suggested by Carey and Simon (1984) and Pham (2008).

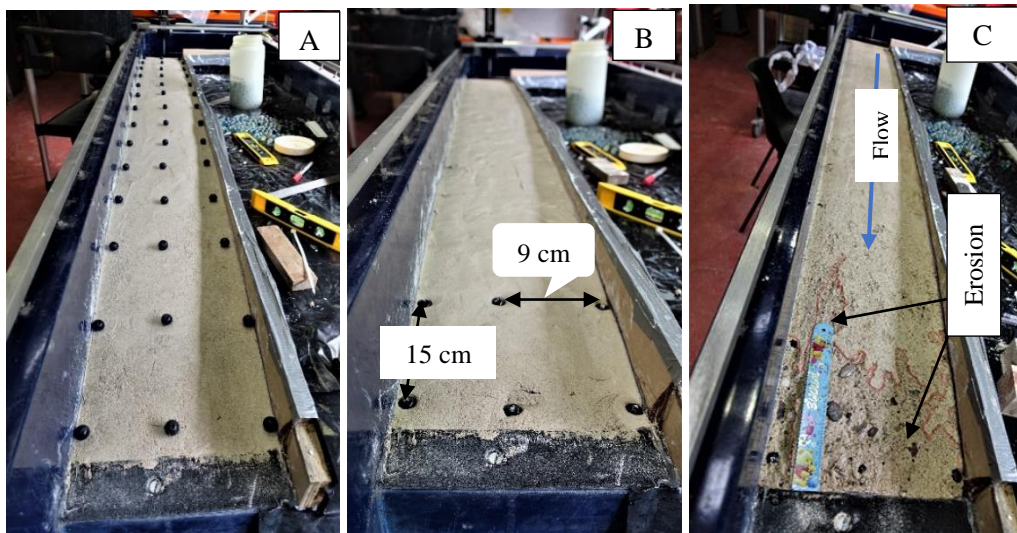


Figure 3. 17. The VGS + 20% ECC sample with glass marbles before being embedded (A); glass marbles being embedded into the soil (B); and after sheet erosion test (C)

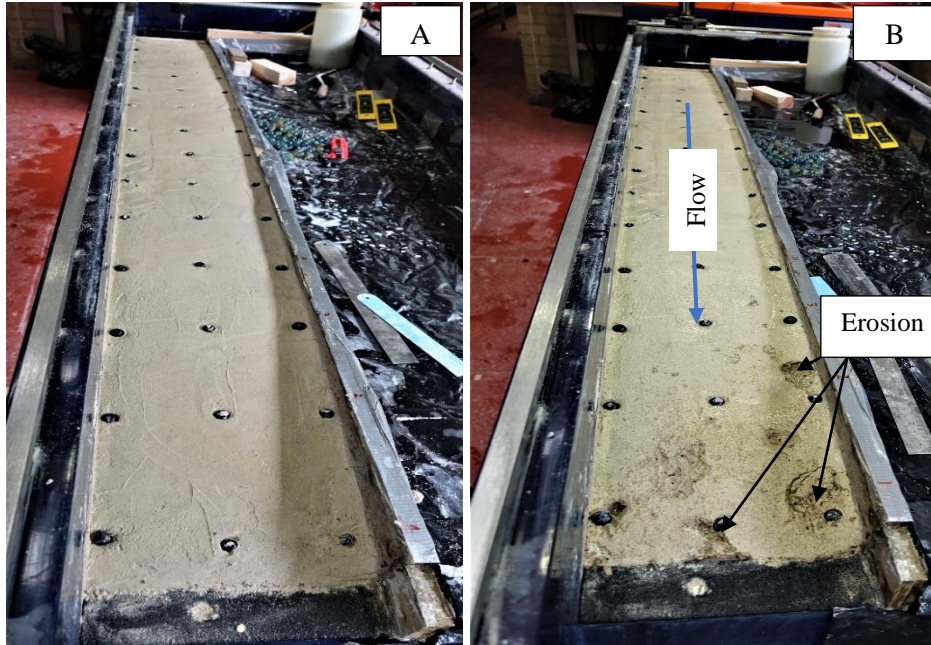


Figure 3. 18. The GS + 20% ECC sample with glass marbles exposed to the surface before the sheet erosion test (A); and after the sheet erosion test (B)

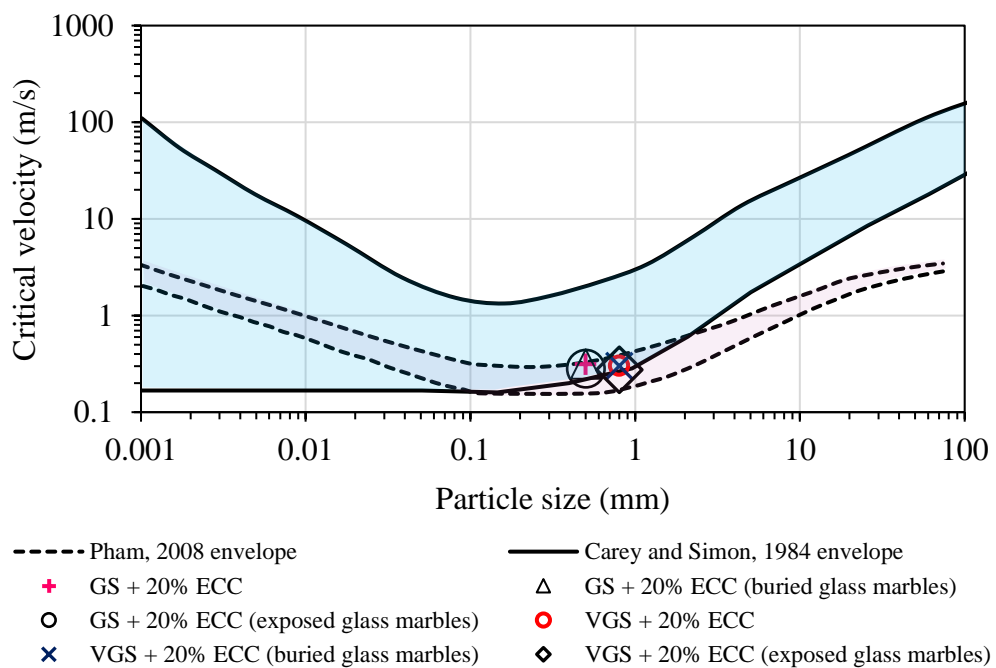


Figure 3. 19. Locating the soils used for sheet erosion tests into envelopes by Carey and Simon, 1984 and Pham, 2008

The following Table 3.12 summarises the number of erosion susceptibility and erodibility tests, with the number of repetitions and justifications for non-repeated tests.

Table 3. 12. Summary of erosion susceptibility and erodibility tests: repetitions and justifications

Test	Total number of tests	Repetitions	Justification
Infiltration rate	11	-	The results agreed with the results from the constant permeability test.
Crumb test	32	1	Eight tests for each of the samples were prepared with H <sub>2</sub> O and 0.001N solution of NaOH. The single repetition performed showed identical results.
Double hydrometer test	16	-	Eight tests for each of the samples prepared with distilled water and parallel tests prepared with hexametaphosphate were undertaken. The results for dispersivity agreed with the results from the crumb test.
Hole erosion test	9	3	Three repetitions for the tests on three soils. Average results recorded.
Moisture variation	8	-	The results agreed with the results from the permeability tests.
Hand vane shear test (modified to test homogeneity of samples)	16	2	Each test was performed in the Proctor mould and at three locations in the soil testing box for the same sample. The agreement of the records from both the Proctor mould and the average of the records from the soil testing box suggested that there was little need for test repetitions.
Flour method test	6	1	For each test, 3 plates were used to collect raindrops into the flour. This was a repetition since the droplets can be collected using one plate. Thus, 18 collections were made. The mean drop sizes were obtained from formed pellets.
Small-scale erosion tests	92	-	Each test was performed for 30 min for two successive days on each sample. Although with some changes at the surface, the second-day test could be a repetition since the trend of results agreed with the first-day test results. Furthermore, the same samples were tested in the same conditions in the large-scale tests and the trend of results agreed with the small-scale tests' results.
Large-scale erosion tests	100	-	Each test was performed for 30 min for two successive days on each sample. Although with some changes at the surface, the second-day test could be a repetition since the trend of results agreed with the first-day test results. Also, the same samples were tested in the same conditions as in the small-scale tests and the trend of results agreed with the large-scale tests' results.
Sheet erosion tests	16	-	The tests were designed to set up the challenge for future work on the effect of surface particles to the formation of erosion features such as potholes and rills.

### 3.12. Correlating the Factors Affecting Erodibility

RapidMiner Studio was used to correlate the key factors affecting erodibility and develop the predictive equations for erosion in unpaved roads. All the laboratory rainfall erosion test data was added to an Excel file and imported into RapidMiner studio software. RapidMiner accepts a spreadsheet of up to 500 rows and unlimited number of columns. The columns are identified as regular attributes except one which must be identified as a label (target) attribute. The software predicts the values for the label attribute based on the regular attributes. In this study, clay content, plasticity index, mean particle size, maximum dry density, optimum moisture content, slope length and gradient, and rainfall intensity and duration are regular attributes; while the measured eroded mass is the label attribute, as shown in Table 3.13.

The model process was designed as shown in Figure 3.20. It has seven operators which are: (1) the data input operator which reads the excel spreadsheet; (2) the select attributes operator in which the attribute types are confirmed; (3) the set role operator which distinguishes between regular and label attributes; (4) the split data operator which splits data into the model training and testing data; with 70% training data to improve the the model and 30% testing data to check the correctness of the model. The other operators are: (5) the linear regression operator which informs the software of the type of regression needed; (6) the apply model operator which executes the information provided by previous operators; and (7) the performance operator which connects to the results' pot and gives the model's performance in terms of parameters such as squared correlation ( $R^2$ ) and root mean square (RMS).

Table 3. 13. Typical spreadsheet of data preparation

Data number	Regular attributes									Label
	Clay content (%)	Plasticity index (%)	Mean particle size D <sub>50</sub> (mm)	Maximum dry density (Mg/m <sup>3</sup> )	Optimum moisture content (%)	Slope length (m)	Slope gradient (%)	Rain intensity (mm/hr)	Rain duration (min)	Measured eroded mass 1st tests (g)
1	0	0	0.41	1.82	9	6.0	0.00	30	5	51.94
12	0	0	0.41	1.82	9	6.0	0.00	51	30	154
25	0	0	0.41	1.82	9	6.0	6.00	51	5	65.1
36	0	0	0.41	1.82	9	1.2	6.00	68	30	234.16
37	0	0	1.2	1.89	9.2	6.0	0.00	68	5	81.06
46	5	0	1.2	1.89	9.2	6.0	6.00	68	20	120.96
98	10	7.9	0.46	1.96	9.1	1.2	0.00	30	5	37.94
99	10	7.9	0.46	1.96	9.1	1.2	0.00	30	10	67.76
100	10	7.9	0.46	1.96	9.1	1.2	0.00	30	15	53.9
134	10	5.7	1.1	2.21	8.4	1.2	0.00	68	5	77
145	10	5.7	1.1	2.21	8.4	1.2	6.00	68	30	128
146	15	9.8	0.48	2.04	8.5	1.2	0.00	30	5	24.5
147	15	9.8	0.48	2.04	8.5	1.2	0.00	30	10	43.76
194	20	12.2	0.5	2.1	9.5	1.2	0.00	30	5	30.8
222	20	12.2	0.5	2.1	9.5	1.2	6.00	51	25	80.92
223	20	12.2	0.5	2.1	9.5	1.2	6.00	51	30	82.46
238	20	9.1	0.8	2.25	8.6	1.2	0.00	68	15	67.06
272	3	5.5	6	2.19	8.8	1.2	0.00	51	20	94.528
295	3	5.5	6	2.19	8.8	1.2	6.00	68	30	190.4



Figure 3. 20. Design of the model process

### 3.13. Summary

Eleven soils: gravelly SAND and very gravelly SAND soils mixed with up to 20% ECC and a subbase soil were used in this study. Classification and engineering tests' results were shown in Table 3.3. Infiltration, HET, crumb and double hydrometer tests were conducted to assess the soils' behaviour with water. The soils were compared with the ASTM (2015) suitable soils for erosion tests shown in Table 3.1. Soils containing ECC classified as loam, those without ECC classified as sand; while the subbase material was not suitable for erosion tests. A rainfall simulator was designed and built as detailed in sections 3.6.1 to 3.6.5. It was used for small-scale tests, as described in section 3.8, and enlarged for large-scale tests, as described in section 3.9. Soil testing boxes were constructed accordingly. In total, 192 erosion tests were undertaken including 92 small-scale and 100 large-scale tests, as shown in Tables 3.7 and 3.8. Laboratory tests took about 20 months (Feb. 2018 – Sept. 2019). About 4.3 m<sup>3</sup> of soils were used with 2.26 m<sup>3</sup> of gravelly SAND, 1.17 m<sup>3</sup> of very gravelly SAND, 0.55 m<sup>3</sup> of subbase and 0.32 m<sup>3</sup> of ECC. Water flowrates were 0.4 l/min, 0.6 l/min and 0.8 l/min for small-scale tests and 0.2 l/min, 0.8 l/min and 1.2 l/min for large-scale tests respectively for 30 mm/hr, 51 mm/hr and 68 mm/hr rainfall intensities. Each test was carried out for 30 minutes, about 4400 litres of water were used, 1800 litres for small-scale tests and 2600 litres for large-scale tests. Eroded soil was collected at 5 min intervals (i.e. 6 collections per test), about 1152 sieve analysis tests were conducted on oven-dried sediment while about 1344 photographs were taken to study surface particle behaviour during rainfall erosion using ImageJ software. About 1 m<sup>3</sup> of soil was used for sixteen sheet erosion tests. ECC was about 0.2 m<sup>3</sup> and each of gravelly SAND and very gravelly SAND was about 0.4 m<sup>3</sup>. Working at a flow rate of 15 l/min for 2 hrs, sheet erosion tests used at least 25.2 m<sup>3</sup> of tap water. Finally, the data was prepared, and a process designed for the RapidMiner studio to generate erosion predictive equations in unpaved roads.

## 4. RESULTS

### 4.1. Introduction

The Chapter 4 contains the results from engineering and erosion susceptibility tests conducted on the selected soils. The results from the design and calibration of the rainfall simulator are also presented to prove that it is the right equipment to conduct erodibility tests using simulated rainfall. Typical results of the rainfall erodibility tests are shown, and all the data related to both the amount of eroded sediment, erosion rate, behaviour of the particles at the surface and runoff coefficients during erodibility tests is graphically presented. Sheet erosion results are also briefly described herein.

### 4.2. Infiltration Rate Test Results

The infiltration test was conducted as described in section 3.5.1. The results showed that the infiltration reduced with increases in clay content in the soil samples. The same trend was found for the permeability tests, where increases in clay content corresponded to reduction of the permeability coefficients. The initial infiltration rates were about 3.4 mm/s, 3.0 mm/s and 2.9 mm/s for subbase, VGS and GS soils, respectively. These reduced gradually to about 0.3 mm/s for subbase and VGS, and about 0.4 m/s for GS in about 180 seconds when the 500 ml of water poured at the surface had almost totally infiltrated, as shown in Figure 4.1 (A).

Initial infiltration rates were about 0.23 mm/s, 0.15 mm/s, 0.05 mm/s and 0.03 mm/s for GS + 5% ECC, GS + 10% ECC, GS + 15% ECC and GS + 20% ECC, respectively. These values reduced to 0.02 mm/s and 0.01 mm/s before the total infiltration of all water in about 1200 seconds and 2580 seconds respectively for GS + 5% ECC and GS + 10% ECC. Infiltration reduced to about 0.001 mm/s for both GS + 15% ECC and GS + 20% ECC, as can be seen in

Figure 4.1 (B). The 500 ml of water could take more than 24 hours to infiltrate into GS + 15% ECC and GS + 20% ECC, due to smaller infiltration rate for those soils.

Initial infiltration rates of about 0.35 mm/s, 0.21 mm/s, 0.07 mm/s and 0.03 mm/s were observed for VGS + 5% ECC, VGS + 10% ECC, VGS + 15% ECC and VGS + 20% ECC, respectively. Infiltration reduced to about 0.03 mm/s and 0.015 mm/s in about 1200 seconds and 2700 seconds respectively for VGS + 5% ECC and VGS + 10% ECC and to about 0.005 mm/s for both VGS + 15% ECC and VGS + 20% ECC, as can be seen in Figure 4.1 (C). Like GS + ECC mixes, 500 ml of water could take more than 24 hours to infiltrate completely into VGS + 15% ECC and VGS + 20% ECC.

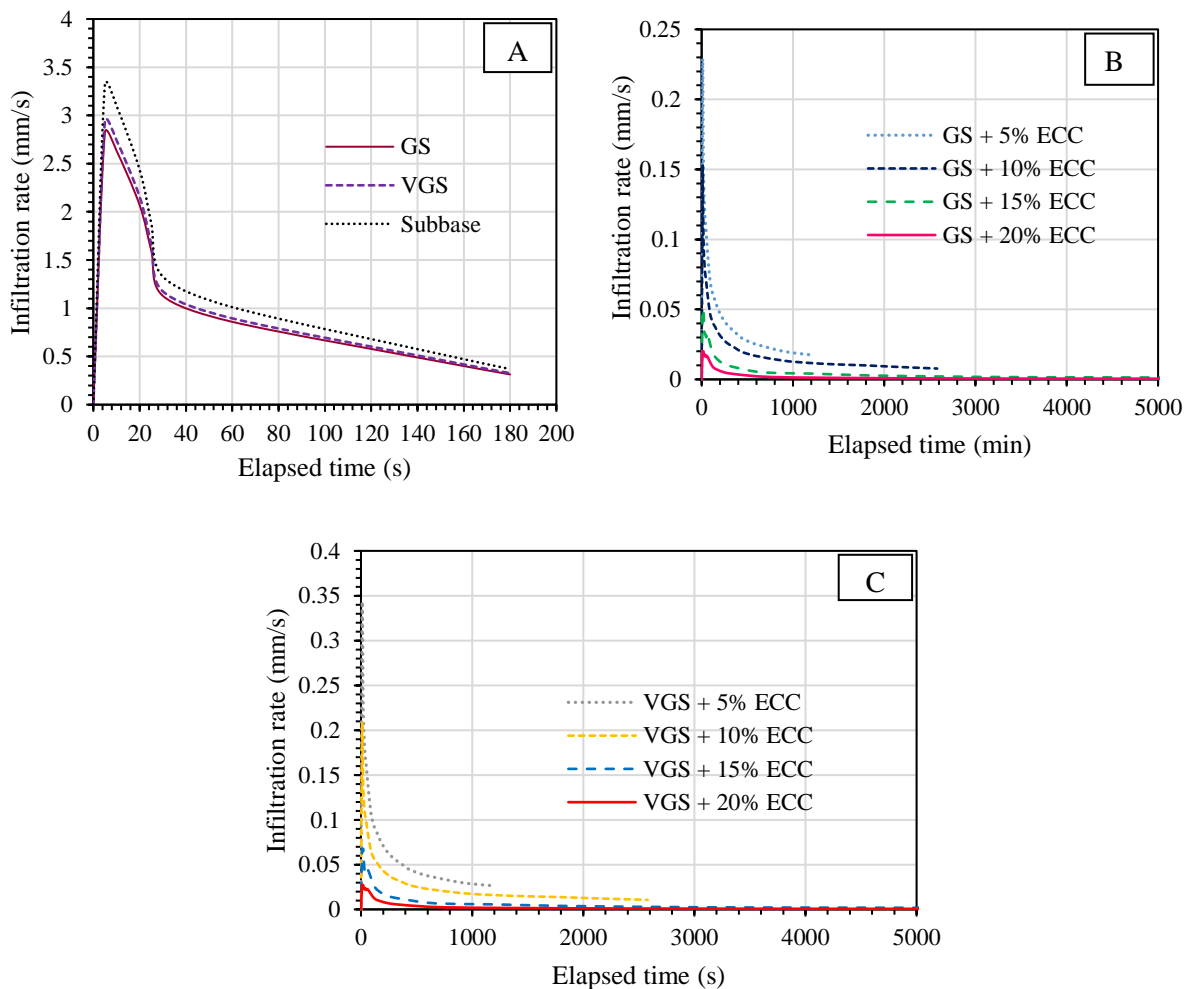


Figure 4. 1. Infiltration rate versus elapsed time for selected soils

### 4.3. Erosion Susceptibility Tests

Both the crumb and double hydrometer tests were undertaken to assess the susceptibility to erosion of the selected soils, as described in sections 3.5.2.1 and 3.5.2.2. Furthermore, the hole erosion test was conducted to compare erosion rate for a range of selected soils, as described in section 3.5.2.3.

#### 4.3.1. Crumb Test Results

The crumb test results should be interpreted after about 10 min of crumb immersion, although dispersive soils may need about 2 hours for colloids to settle down (Maharaj, 2011; Maharaj and Paige-Green, 2013). At 10 minutes, all the samples classified as moderately dispersive, while colloids settled completely in about 2 hours. However, there was little distinction between soils tested in distilled water and those tested in dilute NaOH solution, which is usual for soils without strong reaction (Maharaj and Paige-Green, 2013). The results for the two tests have been identical that there was no need to record the averages. Results are shown in Table 4.1.

Table 4. 1. Results of the crumb test

Solution	Time (min)	Samples' grade of reaction							
		GS + 5% ECC	GS + 10% ECC	GS + 15% ECC	GS + 20% ECC	VGS + 5% ECC	VGS + 10% ECC	VGS + 15% ECC	VGS + 20% ECC
Distilled H <sub>2</sub> O	10	3	3	3	3	3	3	3	3
	60	2	2	3	3	2	2	2	3
	120	1	1	1	2	1	1	1	1
	180	1	1	1	1	1	1	1	1
0.001N NaOH	10	3	3	3	3	3	3	3	3
	60	2	2	3	3	3	3	3	3
	120	1	2	2	2	1	1	1	2
	180	1	1	1	1	1	1	1	1

#### 4.3.2. Double Hydrometer Test Results

The results from double hydrometer test are presented in the Table 4.2. These show that the selected soils ranged from non-dispersive to slightly dispersive.

Table 4. 2. Results of the double hydrometer test

Soil sample	< 0.005 mm, standard test (%)	< 0.005 mm, parallel test (%)	Dispersion Ratio	Description
GS + 5% ECC	3	0.4	13	Non-dispersive
GS + 10% ECC	4	0.7	17.5	Slightly dispersive
GS + 15% ECC	7.1	1.5	21.1	Slightly dispersive
GS + 20% ECC	10.2	2.8	27.5	Slightly dispersive
VGS + 5% ECC	3	0.3	10	Non-dispersive
VGS + 10% ECC	5.9	0.7	11.9	Non-dispersive
VGS + 15% ECC	6.5	1.3	20	Slightly dispersive
VGS + 20% ECC	7.6	2	26.3	Slightly dispersive

#### 4.3.3. Hole Erosion Test Results

The mass  $M$  (g) of the eroded soil was obtained by multiplying the volume of the soil by the density at which the latter was compacted to; while the erosion rate  $E$  (g/s) was the fraction of the mass to the test duration,  $T$  (s), as shown in Table 4.3.

Table 4. 3. Hole Erosion Test results

Sample	Up (cm)	Mp (cm)	Dp (cm)	Avp (cm)	D <sub>2</sub> (cm)	V (cm <sup>3</sup> )	M (g)	T (s)	E (g/s)
GS + 20% ECC									
1	6.5	6.5	7.1	6.7	2.1	42.2	91.9	180	0.511
2	6.7	6.4	7.3	6.8	2.2	43.6	94.8	180	0.527
3	6	6	6.2	6.1	1.9	34.2	74.4	180	0.413
Average				6.5	2.1	39.9	87.1	180	0.484
GS + 15% ECC									
1	7.2	7.5	7.3	7.3	2.3	51.1	117.5	180	0.653
2	7.8	8.3	9.6	8.6	2.7	70.6	162.3	180	0.902
3	6.8	7	7.6	7.1	2.3	48.2	110.8	180	0.616
Average				7.7	2.4	56.2	129.3	180	0.718
GS + 10% ECC									
1	9.8	10.7	11.5	10.7	3.4	110.8	243.7	60	4.1
2	10.6	14.5	12.8	12.6	4	156.4	334	60	5.734
3	10.2	12.5	11.4	11.4	3.6	126.1	277.5	60	4.625
Average				11.6	3.7	130.4	288.4		4.867

Expectedly, the erosion rate was higher for soils with lower clay content. The average diameter of the hole after the erosion test was 2.1 cm, 2.4 cm, and 3.7 cm respectively for GS + 20% ECC,

GS + 15% ECC, and GS + 10% ECC. In the same order, the erosion rate was 0.484 g/s, 0.718 g/s and 4.867 g/s. This, regardless the fact that GS + 10% ECC was tested for 1 minute only while GS + 15% ECC and GS + 20% ECC were tested for 3 minutes. Three samples were conducted for each sample and the mean result considered.

The results from a data logger showed that the flow rate from the pumping system changed from 30.75 l/min to 26.22 l/min for GS + 10% ECC; 30.89 l/min to 28.54 l/min for GS + 15% ECC; and 29.15 l/min to 27.89 l/min for GS + 20% ECC. Differences in initial and final flow rate reflect the degree of increase of the erosion hole. The bigger the difference, the bigger the hole erosion and the more erodible was the soil sample. Those differences were 4.23 l/min; 2.35 l/min and 1.28 l/min respectively for GS + 10% ECC; GS + 15% ECC and GS + 20% ECC.

Figure 4.2 illustrates the pressure changes for the erosion test on GS + 20% ECC. The data logger showed that initially, both the upstream (entrance) pressure  $p_1$  and the difference of pressure  $dp_1$  were high due to lack of the downstream (exit) pressure  $p_2$ . By opening the valve to allow the jet of water to erode the sample,  $p_1$  attained the peak of about  $3.9 \text{ N/m}^2$  in about 12 seconds. During this time,  $p_2$  was about negative  $0.6 \text{ N/m}^2$ , probably due to particles eroded from upstream blocking the pre-drilled hole and reducing the pressure at which water reached the exit point. The pressure  $p_2$  attained the peak of about  $1.5 \text{ N/m}^2$  at about 25 minutes. When  $p_2$  attained its peak, both  $p_1$  and  $dp_1$  had started to reduce gradually due to widening of the erosion hole that had already occurred upstream. At about 150 seconds, both  $p_1$  and  $p_2$  looked stable. Erosion hole was big enough and there was little resistance to the water jet from the soil sample. Overall,  $p_1$  attained the peak of about  $3.9 \text{ N/m}^2$  and reduced to about  $1 \text{ N/m}^2$ ,  $p_2$  attained the peak of about  $1.5 \text{ N/m}^2$  and reduced to about  $1.2 \text{ N/m}^2$  while  $dp_1$  attained the peak of about  $3.7 \text{ N/m}^2$  and reduced to about  $-0.2 \text{ N/m}^2$ .

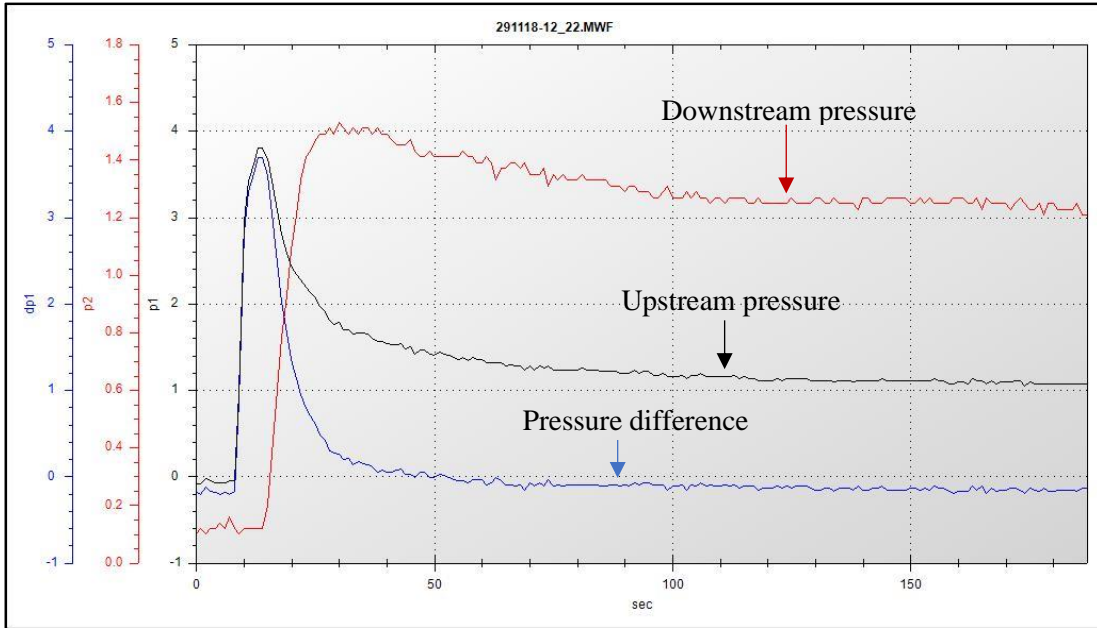


Figure 4. 2. Pressure changes for erosion test on GS + 20% ECC

#### 4.4. Flour Method Test Results

The average numbers of the raindrops from two tests for the three rainfall intensities of 30 mm/hr, 51 mm/hr and 68 mm/hr respectively were 113, 163 and 187 raindrops. There is a linear relationship between rainfall intensity and number of drops as shown in Figure 4.3.

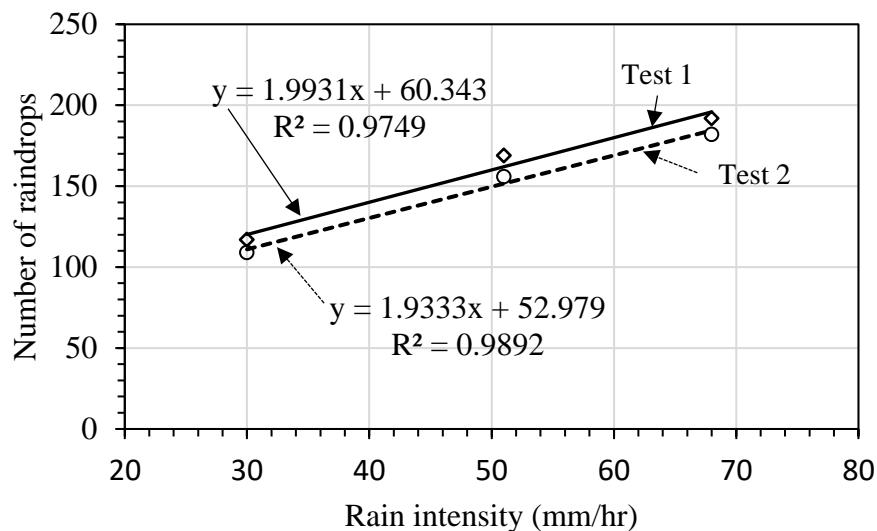


Figure 4. 3. Number of drops falling on 21 cm diameter pan in 3 seconds for different rain intensities

The weights of dry pellets obtained during the sieve analysis test were 1.72 g, 2.87 g and 3.66 g respectively for rainfall intensities of 30 mm/hr, 51 mm/hr and 68 mm/hr. By dividing the weights by the number of pellets, the average weights of the pellets were found to be 15.2 mg, 17.6 mg, and 19.6 mg, respectively. According to Laws and Parsons (1943), the ration of the mass of the raindrop to the mass of the pellets ( $m_R$ ) are about 1.1, 1.11 and 1.12. Applying the above values into Equation 3.3, the mean raindrop size ( $D_r$ ) was found to be 3.0 mm, 3.2 mm, and 3.5 mm respectively for the 30 mm/hr, 51 mm/hr and 68 mm/hr rainfall intensities. Both the number of raindrops and the average drop size increased with the increase in the rainfall intensity. Due to a small number of rainfall intensities, a small concavity appears on the curve connecting the drop sizes. The raindrop sizes from different studies are shown in Figure 4.4.

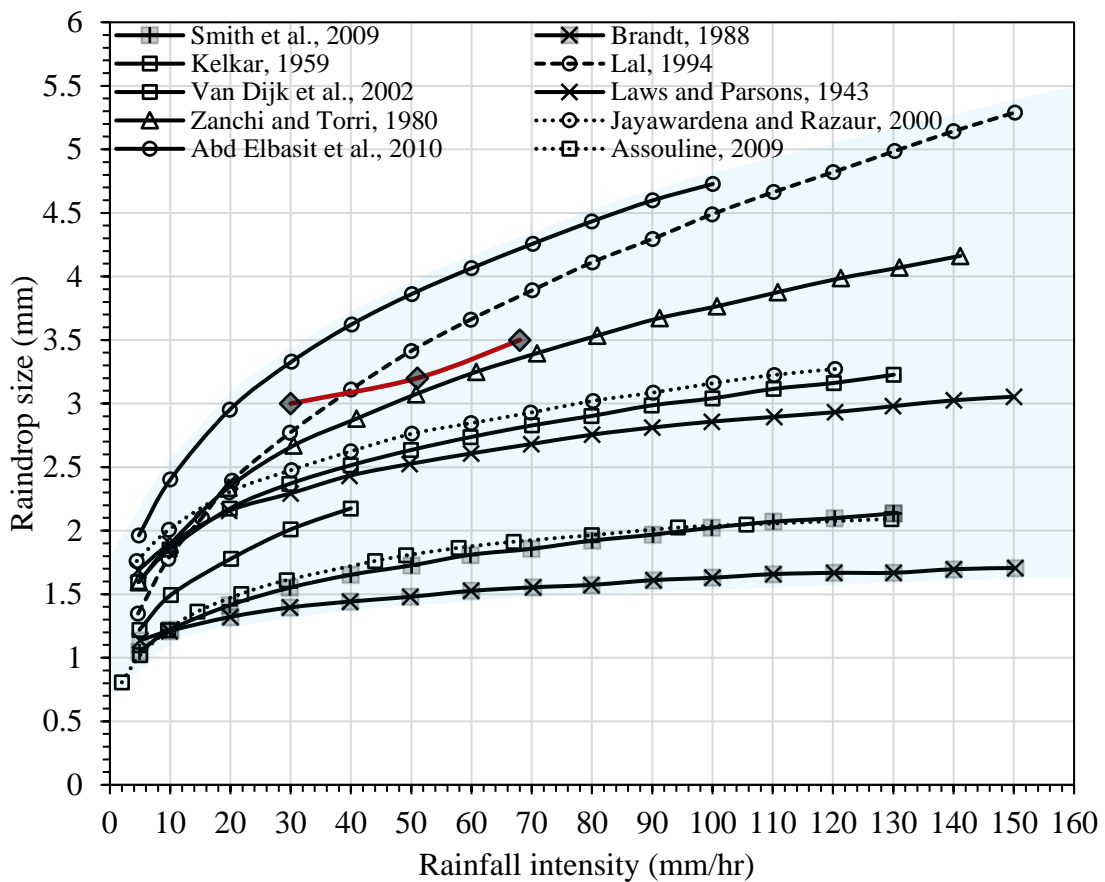


Figure 4. 4. Comparison of the simulated raindrops' sizes and the raindrops' sizes reported by other researchers

#### 4.5. Determination of the Kinetic Energy from the Simulated Rainfall

The purpose of determining the raindrops' sizes was to determine the kinetic energy embodied in the raindrops which is responsible for soil detachment and therefore soil erosion. The relationship used to obtain the rainfall's kinetic energy is given in equation 4.1.

$$KE = \frac{1}{2}mv^2 \quad (\text{Eq. 4.1})$$

where KE is the kinetic energy (J); m is the mass of the raindrop (kg); and v is the terminal velocity (m/s) at which the drop hits the soil surface.

The mass of the raindrops was calculated from the bulk density relationship which is given by the ratio of mass to the volume. Therefore, the mass of the raindrop was calculated as follows:

$$m = \rho V \quad (\text{Eq. 4.2})$$

where  $\rho$  is the density of water ( $\text{mg}/\text{mm}^3$ ); and V the volume of the raindrop ( $\text{mg}/\text{mm}^3$ ).

Assuming the spherical shape of the raindrops, the volume of individual raindrops was calculated as the volume of the sphere with the same diameter as in the next relation:

$$V = \frac{4}{3}\pi\left(\frac{D_r}{2}\right)^3 \quad (\text{Eq. 4.3})$$

where V is the volume of the raindrop ( $\text{mm}^3$ ); and  $D_r$  the raindrop diameter (mm).

Using Equations 3.5 and 3.6 and keeping in mind that the density of water is equal to  $1\text{mg}/\text{mm}^3$ , the mass of an individual raindrop was found to be 14.13 mg, 17.15 mg and 22.1 mg respectively for the 30 mm/hr, 51 mm/hr and 68 mm/hr simulated rainfall intensities.

After determining the mass for individual raindrops, the next step was to obtain the terminal velocity to be able to apply Equation 4.1. This was achieved by using the ASTM (2015) chart that correlates the fall velocity, fall height and raindrop diameter as shown in Figure 4.5. In this study, a fall height of 2 m was used in the experimental set up. At this height, the estimated fall

velocities were 5.2 m/s, 5.21 m/s and 5.22 m/s respectively for the raindrops of the 30 mm/hr, 51 mm/hr and 68 mm/hr simulated rainfall intensities. Consequently, and by application of Equation 4.1, the kinetic energy from individual raindrops was calculated as  $1.935 \times 10^{-4}$  Joules,  $2.44 \times 10^{-4}$  Joules and  $3.011 \times 10^{-4}$  Joules respectively for the 30 mm/hr, 51 mm/hr and 68 mm/hr simulated rainfall intensities, as shown in Table 4.4.

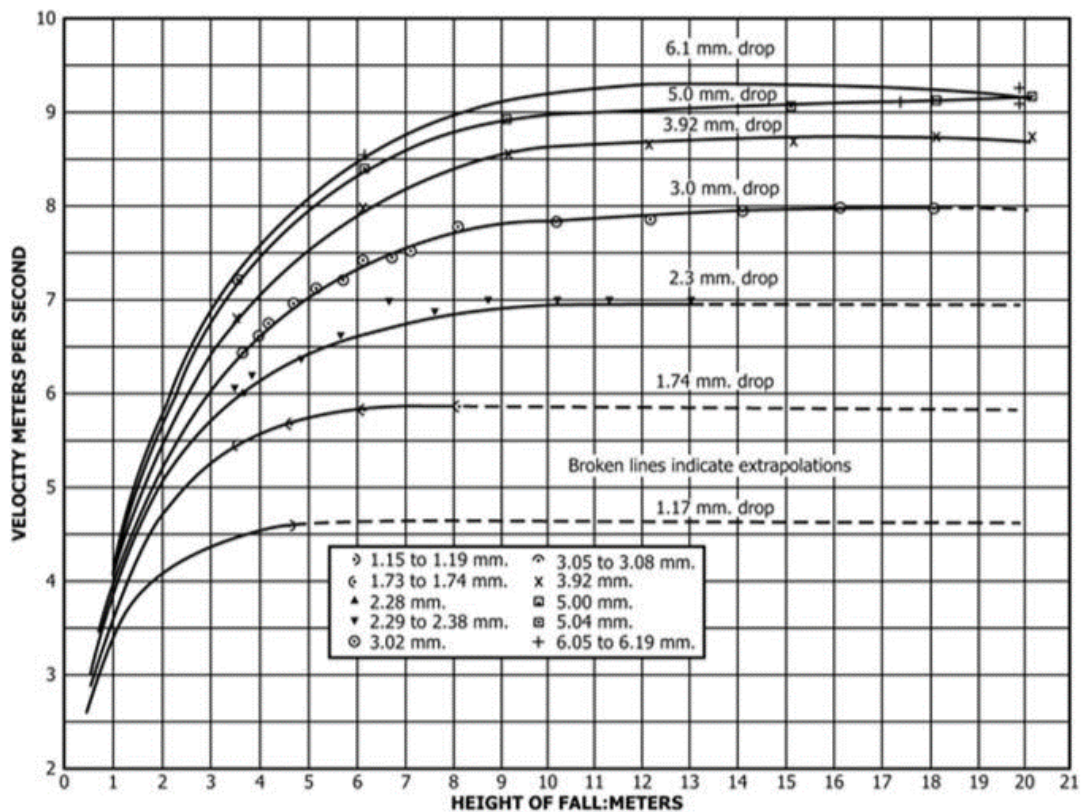


Figure 4. 5. Fall velocity due to the size and fall height of the raindrops (ASTM, 2015)

Table 4. 4. Kinetic Energy (KE) embedded in raindrops

Rainfall intensity, I (mm/hr)	Mean size (diameter), Dr (mm)	Volume of raindrop, V (mm <sup>3</sup> )	Mass of raindrop, m (mg)	Fall velocity, v (m/s)	Kinetic Energy, KE (μJ)
30	3	14.13	14.13	5.2	193.5
51	3.2	17.15	17.15	5.21	244
68	3.5	22.1	22.1	5.22	301.1

#### 4.6. Performance of the Rainfall Simulator

Moore et al. (1983), Horne (2017), Ngezahayo et al. (2019a, e) and Ricks et al. (2019) reported the coefficient of uniformity (CU) - measure of consistency of raindrops spatial distribution which must range from 80% to 100% for acceptable performance of a rainfall simulator. CU is called the coefficient of Christiansen who introduced it in 1942 (Horne, 2017). It was calculated by collecting rainwater in 6 same-size graduated cylinders for 10 min and using equation 4.4.

$$CU = 100 \left[ 1 - \left( \frac{\sum (|D_i - D_m|)}{n * D_m} \right) \right] \quad (\text{Eq. 4.4})$$

Where CU is the coefficient of uniformity (%);  $D_i$  is the depth of water in the graduated cylinder (cm);  $D_m$  is the mean depth of water in graduated cylinders (cm); and  $n$  is the number of graduated cylinders. In this study, the rain simulator was performing evenly over the tested area with a CU of 100%.

#### 4.7. Key Outcomes from Material Selection and Rainfall Simulator Calibration

Many important outcomes from material selection, and rainfall simulator design and calibration were found. These included the awareness of the quality of selected soils for unpaved road surface, the suitability of selected soils for erodibility investigation, the kinetic energy from the raindrops of the target rainfall intensities and the ability of the raindrops to detach the selected soils, the moisture variations during erodibility tests and the strength gains of the soil mixes due to additions of the English china clay. These are discussed in the next sections.

##### 4.7.1. Quality of Selected Materials for Unpaved Roads' Surface Soils

Using Eq. 2.3 and Eq. 2.4 and the results of the classification tests as presented in Figures 3.2 and 3.3, and in Table 3.3, the shrinkage product and the grading coefficient of the soils were calculated. These parameters then helped to locate the soils in the South African diagram

(Paige-Green, 2006) for unsealed roads' soils performance, as in Figure 4.6. Five soils (GS + 10% ECC, GS + 15% ECC, GS + 20% ECC, VGS + 15% ECC and VGS + 20% ECC) located into the good zone, one soil (GS + 5% ECC) located in the erodible zone and five soils (GS + 0% ECC, VGS + 0% ECC, VGS + 5% ECC, VGS + 10% ECC and Subbase) located into the zone of corrugates and raveling of the diagram. This study will show differences in erodibility of all those soils including the soils located in the good zone.

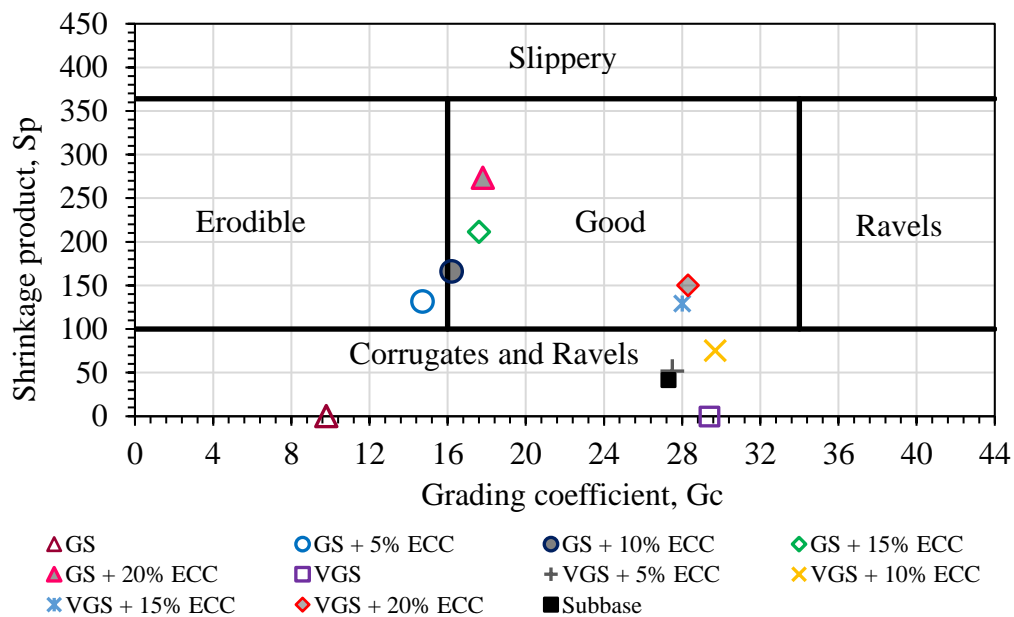


Figure 4. 6. Location of the soils used in the unpaved road soils' performance diagram (Paige-Green, 2006)

#### 4.7.2. Quality of Selected Soils for Erodibility Tests

Using Figure 3.2 and Figure 3.3 to obtain  $D_{15}$ ,  $D_{50}$ ,  $D_{85}$  and  $D_{100}$  of the selected soils, and referring to Table 3.1 for soils which are suitable for erodibility tests (ASTM, 2015, Ngezahayo et al., 2019a, e), it was found that GS and VGS classified as sand, while the mixes of those soils with ECC classified as loam. All those soils were acceptable for erodibility tests. Only the subbase soil was not suitable for erosion tests due to its  $D_{50} = 6$  mm and  $D_{85} = 20$  mm which were out of the sizes recommended by ASTM (2015), as indicated in Table 3.1.

### 4.7.3. Detachment of Selected Soils due to Raindrops' Kinetic Energy

The effect of the three target rainfall intensities to the selected soils was compared to the work by Salles et al. (2000) who drew an envelope of the thresholds raindrops' kinetic energy to initiate detachment of soils in relation to the mean particle size of soils. All the selected soils, except the subbase, fitted in the envelope, which was a proof of their suitability for erodibility tests. The subbase soil plotted outside the envelope due to its coarser particles, which firmly resist detachment. An envelope by Carey and Simon (1984) for soil detachment due to critical flow velocity and the soil's particle size was also given. The envelopes are shown in Figure 4.7.

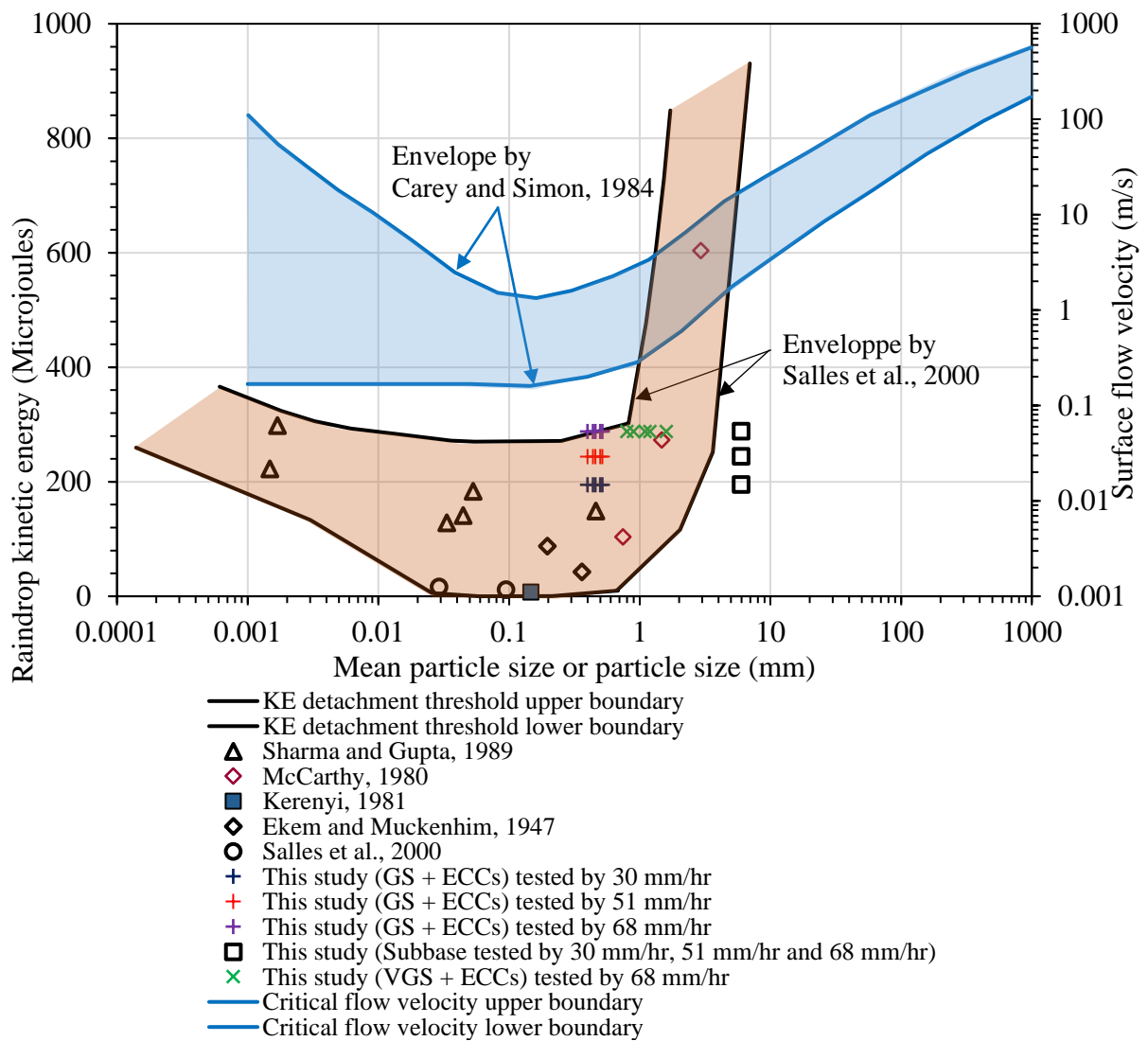


Figure 4. 7. Detachment of selected soils due to raindrops' kinetic energy

#### 4.7.4. Moisture Content Variation during Rainfalls

Although all the soils were tested for moisture variation during rainfall events, only results from one soil tested with three rainfall intensities and results from three soils tested with one rainfall intensity were presented to maintain the clarity of information. The aim was to assess the differences in the effect of rainfall intensities to changes in moisture content (soil strength) during rainfall erosion. Also, to assess how different soils resist the infiltration of rainfall. This data augmented to what was observed during constant head permeability and infiltration tests. Henceforth, GS + 20% ECC soil was tested with 30 mm/hr, 51 mm/hr and 68 mm/hr to investigate moisture changes due to rainfall intensity and duration. Moisture content increased with both rainfall duration and intensity. As shown in Figure 4.8, top 3 cm were the most affected by rainfall as indicated by moisture changes. These increased from 9.8% to 10.4%, 10.1% to 10.3% and 9.6% to 10.3% between the 5<sup>th</sup> and 30<sup>th</sup> minute of the rainfall respectively for 30 mm/hr, 51 mm/hr and 68 mm/hr rainfall intensities. Similarly, moisture changes in the middle part (8–10 cm) of the sample were 9.2% to 9.8%, 9.2% to 10% and 9.3% to 9.9%. Little moisture changes occurred in the bottom zone (14–17 cm) of the sample, less than 2%, for all the rainfall intensities which confirm little infiltration rate of the material.

Moreover, using the 51 mm/hr rainfall intensity to the tested soils showed that moisture contents were higher in the lower layers of samples as ECC percentage reduced due to high infiltration rate as shown in Figure 4.9. In the top 3 cm, moisture contents increased from 11.1% to 14%, 10.3% to 10.6% and 10.1% to 10.3% between the 5<sup>th</sup> and 30<sup>th</sup> minute of the rainfall respectively for GS + 10% ECC, GS + 15% ECC and GS + 20% ECC. Similarly, in the middle part of the sample (8–10 cm), these were 9.5% to 12%, 9.5% to 10.1% and 9.2% to 10% respectively. In the bottom part of the sample (14–17 cm) moistures were 9% to 10.2%, 9% to 9.4% and 9.1% to 9.2%.

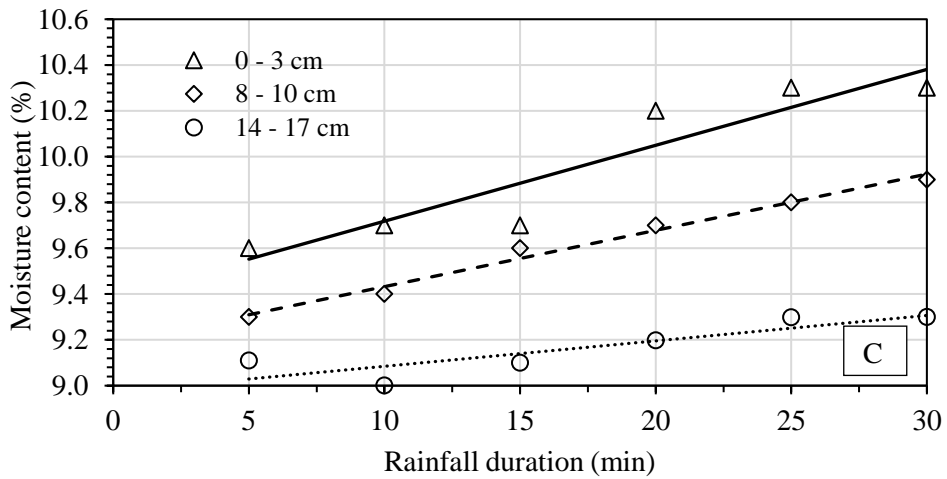
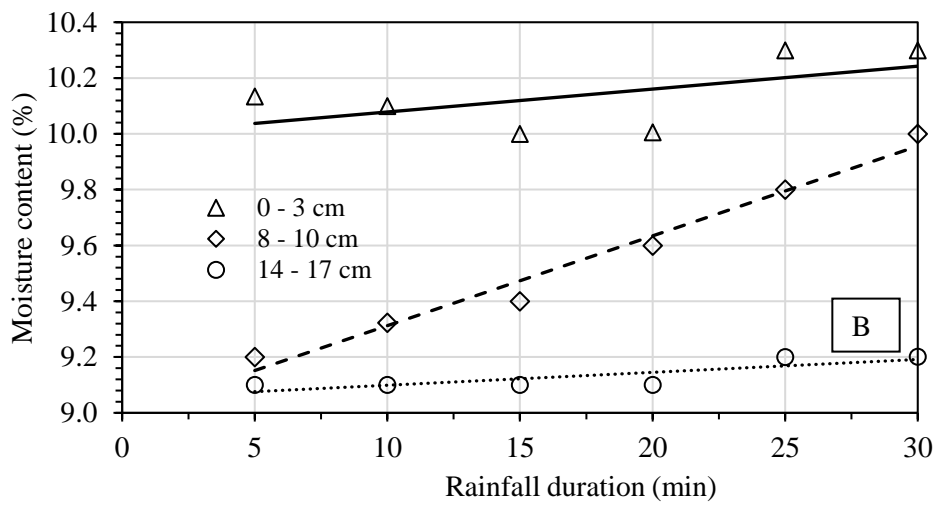
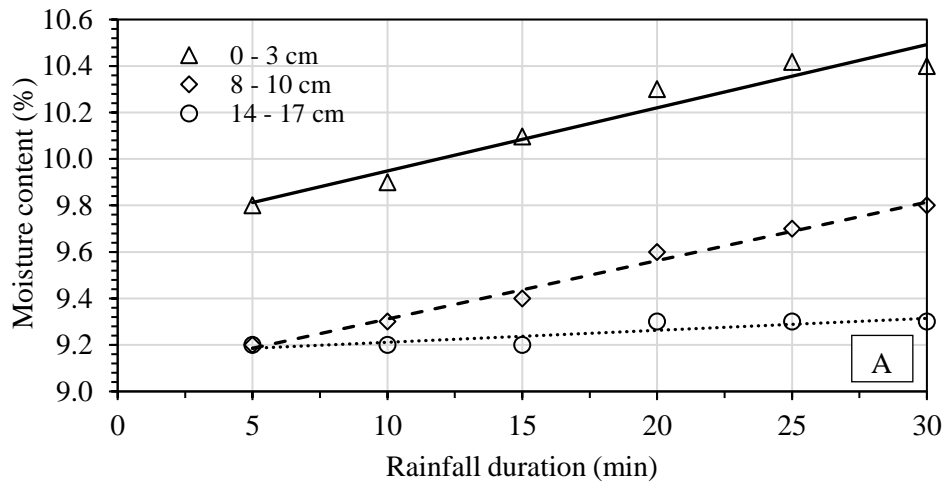


Figure 4. 8. Measured moisture content variations with depth for GS + 20% ECC soil tested using 30 mm/hr (A), 51 mm/hr (B), and 68 mm/hr (C) rainfall intensities

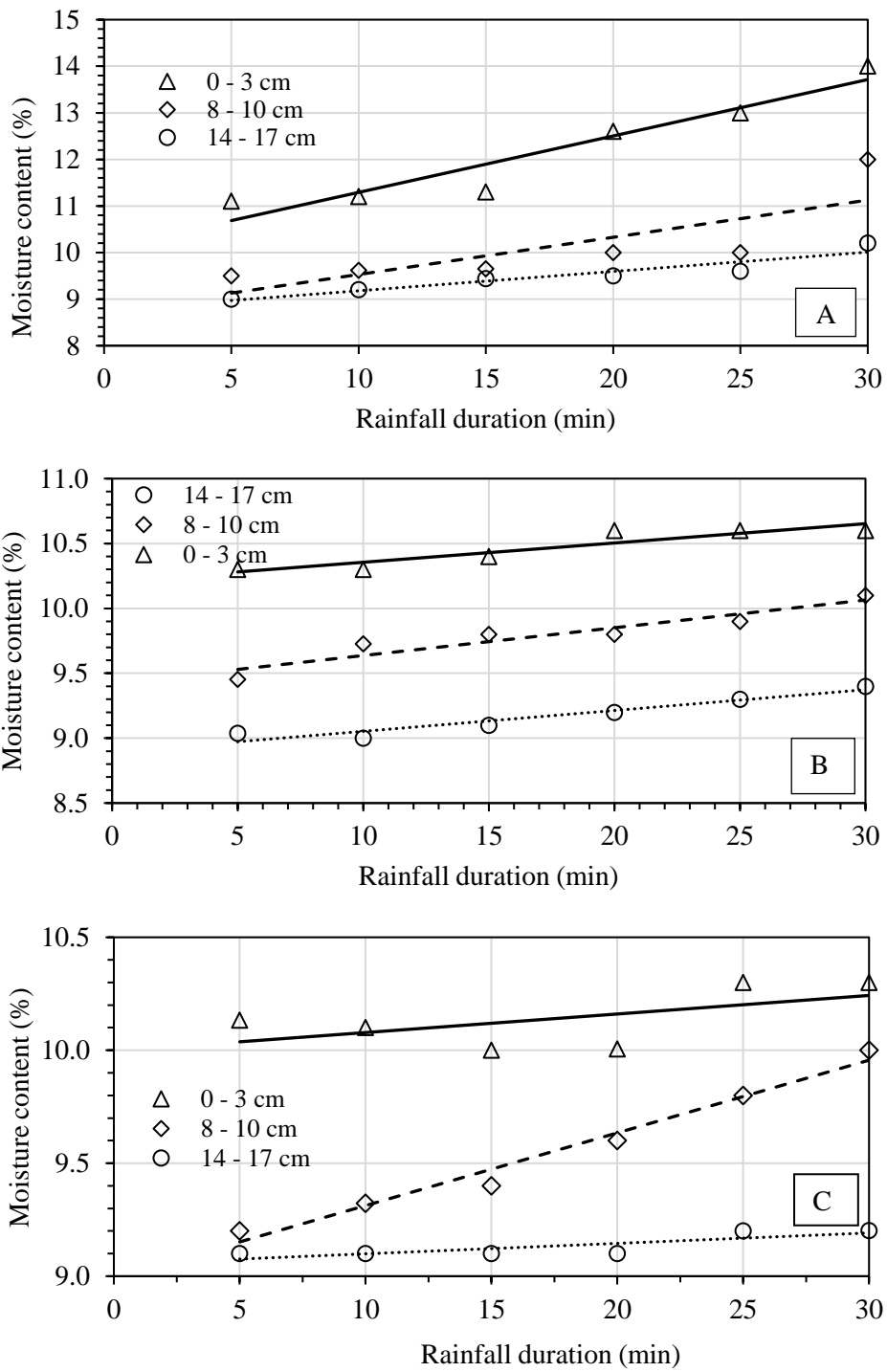


Figure 4. 9. Measured moisture content variations with depth for GS + 10% ECC (a), GS + 15% ECC (b), and GS + 20% ECC (c) soils tested using 51 mm/hr rainfall intensity

#### 4.7.5. Strength Improvement due to Increased English China Clay Content

Unsoaked CBR tests were undertaken on the selected soils and increased with increases in time after compaction, ECC content, and particle size, as shown in Figures 4.10 and 4.11. For GS + ECC soils, CBR values were very low (1% to 7%) immediately after compaction but increased significantly with time. At 15 days, CBR values were 1.1%, 9.8%, 17.6%, 19.8% and 22.5% respectively for GS + 0% ECC, GS + 5% ECC, GS + 10% ECC, GS + 15% ECC and GS + 20% ECC (Ngezahayo et al., 2019b). In Figure 4.11, CBR values were higher for VGS + ECC soils and ranged from 4.5% to 17.1% immediately after compaction. At 15 days, these increased to 11.5%, 21.6%, 32.3%, 36.4% and 39.5% respectively for VGS + 0% ECC, VGS + 5% ECC, VGS + 10% ECC, VGS + 15% ECC and VGS + 20% ECC soils. Subbase had the highest CBR values ranging from 28.5% immediately after compaction to 77% at 15 days. The increases in strength with time were due to reduced moisture and improved bonding between particles (Gomes et al., 2012; Kuliffayová et al., 2012; Lotfy et al., 2015; Paige-Green et al., 2015; Ngezahayo et al., 2019b). CBR results suggest that unpaved roads should be given about two weeks after compaction to develop the bearing capacity before being availed for the traffic use.

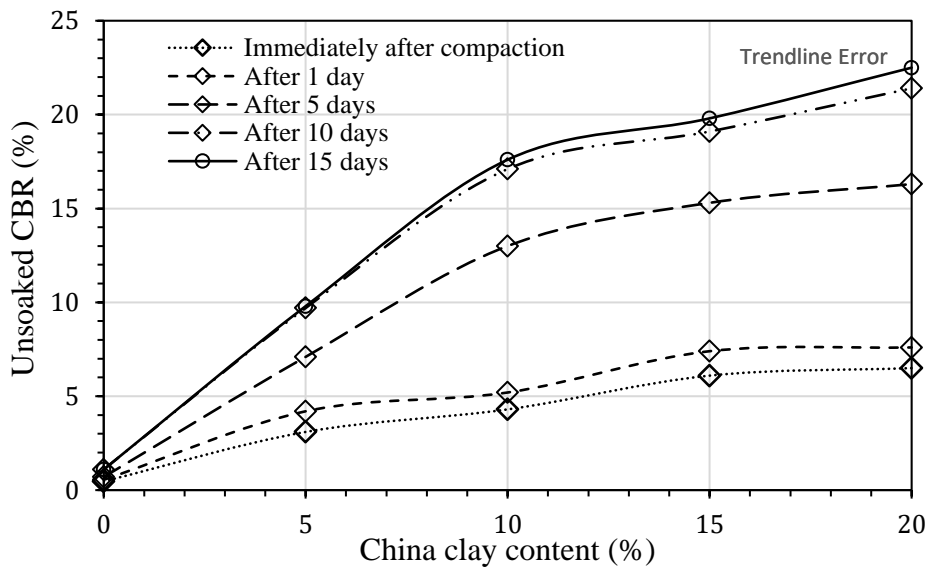


Figure 4. 10. CBR changes in GS + ECC mixes (Ngezahayo et al., 2019b)

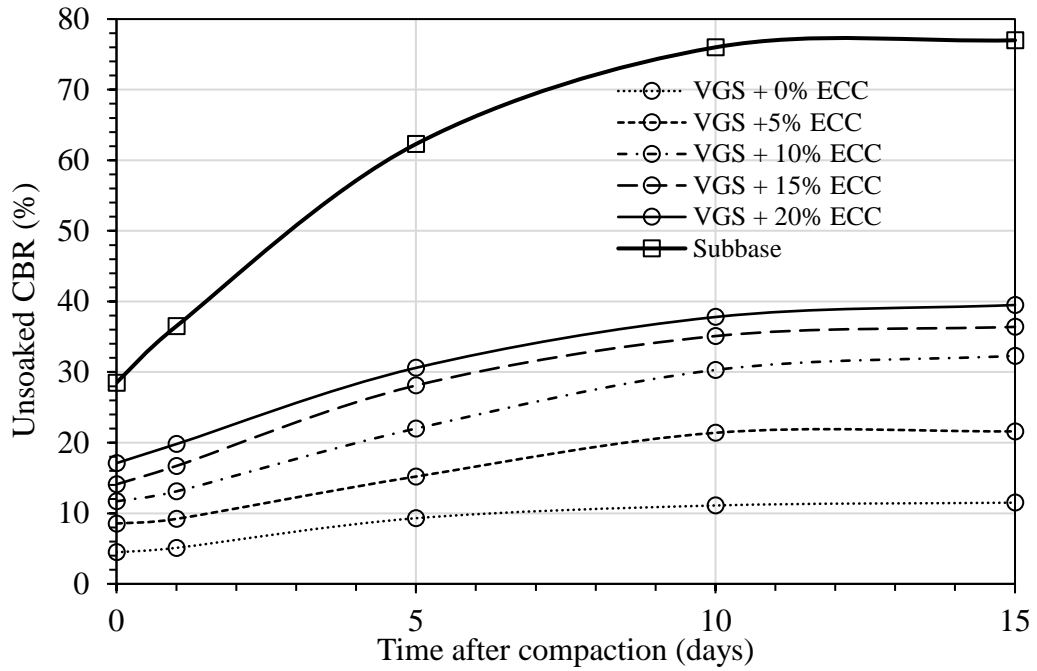


Figure 4. 11. CBR changes in VGS + ECC mixes and subbase

#### 4.8. ImageJ Software Calibration Results

ImageJ gives both the diameter and the number of particles of the same size. Thus, assuming that surface particles were spheres, the volume of individual particle ( $V_{particle}$ ) in  $mm^3$  for a soil particle of diameter (D) was calculated as follows:

$$V_{particle} = \frac{4}{3} \pi \left( \frac{D}{2} \right)^3 \quad (\text{Eq. 4.5})$$

The mass of soil particles ( $m_{particles}$ ) in kg for the same size was calculated as follows:

$$m_{particles} = \frac{V_{particles} * G_s * N}{1000} \quad (\text{Eq. 4.6})$$

where  $G_s$  is the soil's particle density and N is the number of particles.

The total mass of the particles at the surface was then calculated as follows:

$$m_{total} = \sum_{i=1}^{i=n} m_{particles} \quad (\text{Eq. 4.7})$$

where n is the number of different particle sizes appearing at the surface.

The percentage of retained particles was calculated using the following relation:

$$\% \text{ retained} = \frac{m_{\text{particles}}}{m_{\text{total}}} * 100 \quad (\text{Eq. 4.8})$$

Using equations 4.7 and 4.8, the cumulative percentages of the finer particles were calculated. The PSD curves for the control soil, eroded sediment, and surface particles were plotted. Also, a summation of the sediment and the surface particles curves was plotted. The almost superimposition between control soil and the combined sediment – surface particles curves shows that ImageJ performs satisfactorily, shown in Figure 4.12.

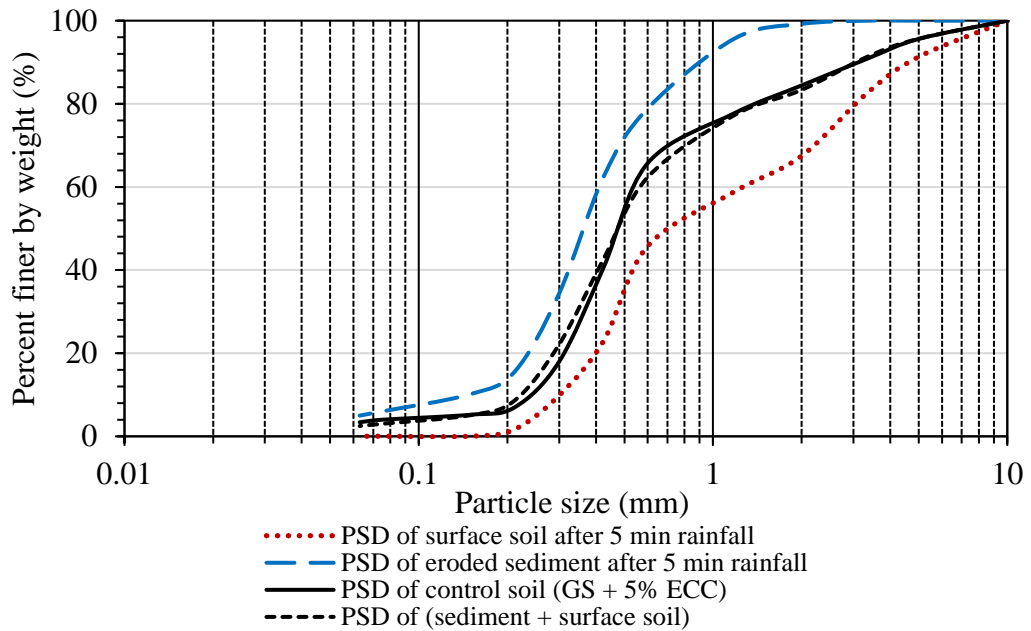


Figure 4. 12. Calibration of ImageJ software

#### 4.9. Sheet Erosion Test Results

The visual observations during and after testing using photographs, together with measurements of lengths, widths and depths of the eroded areas were used:

- (1) To quantify the area and depth of erosion damage due to the surface flow.
- (2) To observe the progression of erosion damage with time and for different types of soils.
- (3) To observe the effect of the presence of coarser soil particles in the road surface.

#### 4.9.1. Area and Depth of Erosion Damage after the first- and second-day Tests

The two main forms of surface erosion caused by the runoff flow due to a 15 l/min flow rate (equivalent to the runoff from a 68 mm/hr rainfall intensity on the tested soils) were the formation of potholes for the GS + 20% ECC, as shown in Figure 4. 13 (A to C') and the loss of a thin layer of surface soils for the VGS + 20% ECC, as shown in Figure 4.13 (D to E'). These two soils were preferred to the others as they were found to be less erodible during rainfall erosion tests; thus, the other soils that contained a lower clay content would show greater erosion due to sheet flow.

A common observation for both soils was that the two forms of erosion features concentrated between zero and thirty centimetres on the downslope, which was due to increased flow velocity of water on the 2% inclined bed slope. Not only the runoff velocities were increased on the downslope, but also abrasion by previously detached particles rolling into the flow increased the subsequent detachment of further particles. It was further noticed that erosion damage could be started by the detachment of a single small particle, followed by the particles that were in contact with the detached particle. As neighbouring particles were detached, an eroded area started to grow upstream in the direction opposing the direction of flow. The direction of erosion growth was the same for potholes. Neighbouring potholes could link up to create a rill with the tendency of the flow to follow the rill, which similarly leads to the rill's growth in the upstream direction through head-cut action. Similar observations for the growth of erosion were found by Horne (2017) when he was designing and constructing a rainfall simulator for large-scale testing of erosion control practices and products.

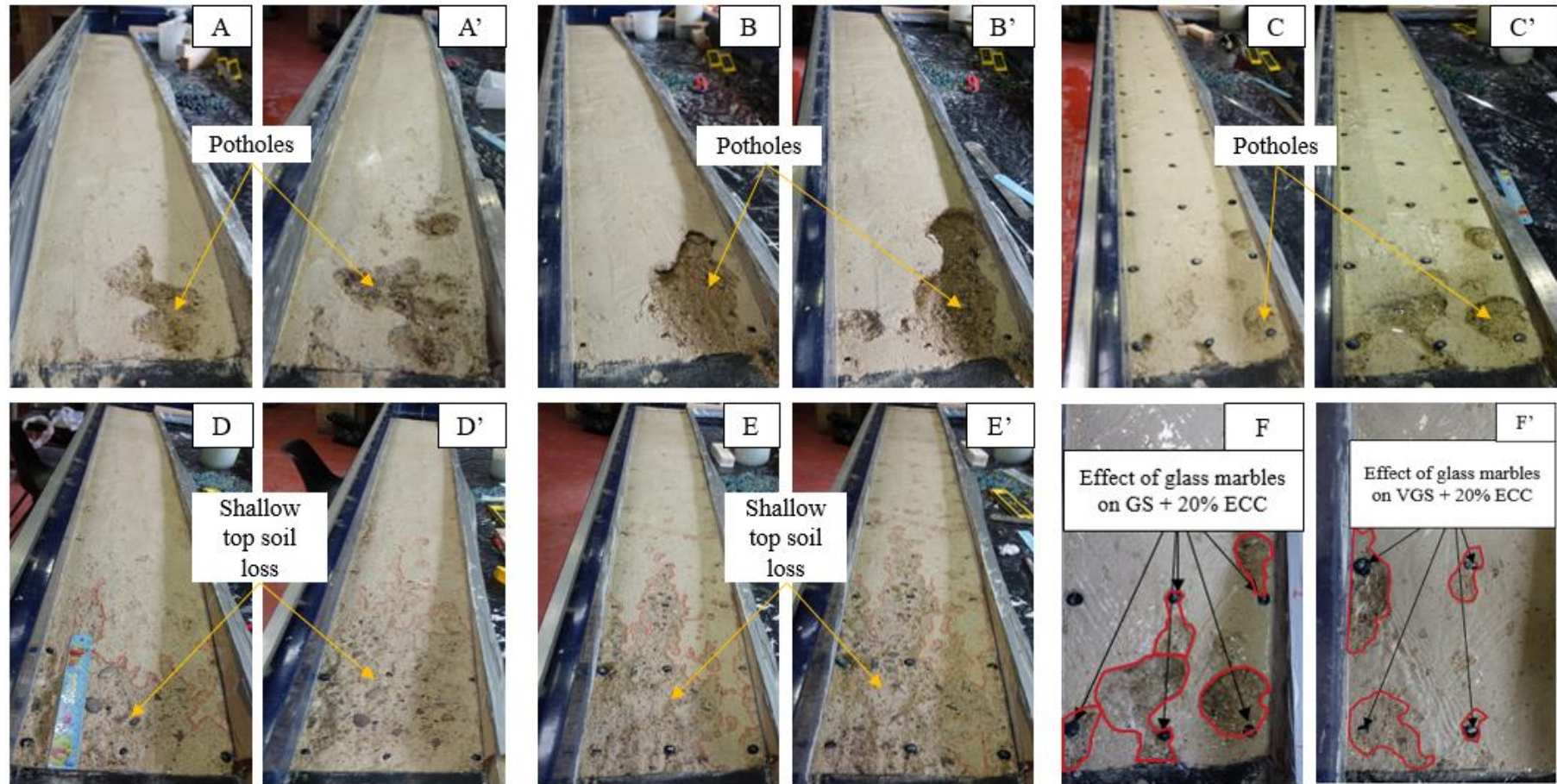


Figure 4. 13. Sheet erosion on GS + 20% ECC without glass marbles: (A) first-day test, (A') second-day test; GS + 20% ECC + buried glass marbles: (B) first-day test, (B') second-day test; GS + 20% ECC + exposed glass marbles: (C) first-day test and (C') second-day test. Sheet erosion on VGS + 20% ECC without or with buried glass marbles: (D) first-day test, (D') second-day test; VGS + GS + 20% ECC + exposed glass marbles: (E) first-day test, (E') second-day test. Effect of exposed glass marbles on GS + 20% ECC (F) and on VGS + 20% ECC (F').

The progression of erosion damage was affected by the soil's particle size and distribution (clay content was the same), the flow velocity, and whether the soil contained exposed glass marbles. Henceforth, it was found that the severity of erosion was higher for GS + 20% ECC soils than for VGS + 20% ECC soils. It is true that the later soil could have a wider area affected by erosion, as shown in Figure 4.14, but it is the depth and width of the formed potholes or rills in the former soil that is more worrying and threatening to the road users, as shown in Figure 4.15.

Removal of the upper thin layer, results in water penetrating to a greater depth leading to a more turbulent flow in these locations. This results in removal of materials, until equilibrium is reached. As the tests for both the soils were run over a two-hour period, equilibrium was not achieved as the area of erosion continued to grow. It was found that the surface flow velocities were high enough only to remove top surface soils, but not enough to displace the coarser particles and create an open pothole, as seemed to be the case for VGS + 20% ECC soil. Therefore, the eroded areas seemed to be wide and shallow in VGS + 20% ECC soils compared to the GS + 20% ECC soils. This suggests that the selection of unpaved road materials must include particle density, particle size and particle size distribution. Gravel-sized particles must be (by weight) more than sand-sized particles, as this will allow the road to resist both the raindrops' kinetic energy and the runoff flow velocities efficiently (Carey and Simon, 1984; Salles et al., 2000; Ngezahayo et al., 2019a, b, c).

In Figure 4.14, the areas damaged by the surface erosion were measured and plotted for the first- and second-day two-hour sheet erosion tests. As discussed in previous paragraphs, the area of erosion damage was slightly bigger, in decreasing order, for: VGS + 20% ECC + exposed glass marbles; VGS + 20% ECC + buried glass marbles; GS + 20% ECC + exposed glass marbles; VGS + 20% ECC; GS + 20% ECC + buried glass marbles; and GS + 20% ECC.

Respectively, the area of erosion damage was 0.066 m<sup>2</sup>, 0.062 m<sup>2</sup>, 0.056 m<sup>2</sup>, 0.054 m<sup>2</sup>, 0.05 m<sup>2</sup> and 0.042 m<sup>2</sup> after the first-day test; and 0.116 m<sup>2</sup>, 0.113 m<sup>2</sup>, 0.105 m<sup>2</sup>, 0.101 m<sup>2</sup>, 0.085 m<sup>2</sup> and 0.082 m<sup>2</sup> after the second-day test.

In contrast, in Figure 4.15, the average depths of erosion damage were measured and plotted, and there was a big difference in the depths of erosion between GS + 20% ECC and VGS + 20% ECC soils. In fact, the depth of erosion damage was higher, in decreasing order, for: GS + 20% ECC; GS + 20% ECC + buried glass marbles; GS + 20% ECC + exposed glass marbles; VGS + 20% ECC + buried glass marbles; VGS + 20% ECC; and VGS + 20% ECC + exposed glass marbles. Respectively, the depth of erosion damage for those soils was 11.1 mm, 11 mm, 10 mm, 5.4 mm, 4.6 mm and 3.8 mm after the first-day test; and 38 mm, 37.1 mm, 35.1 mm, 9.6 mm, 7.8 mm and 6.7 mm after the second-day test.

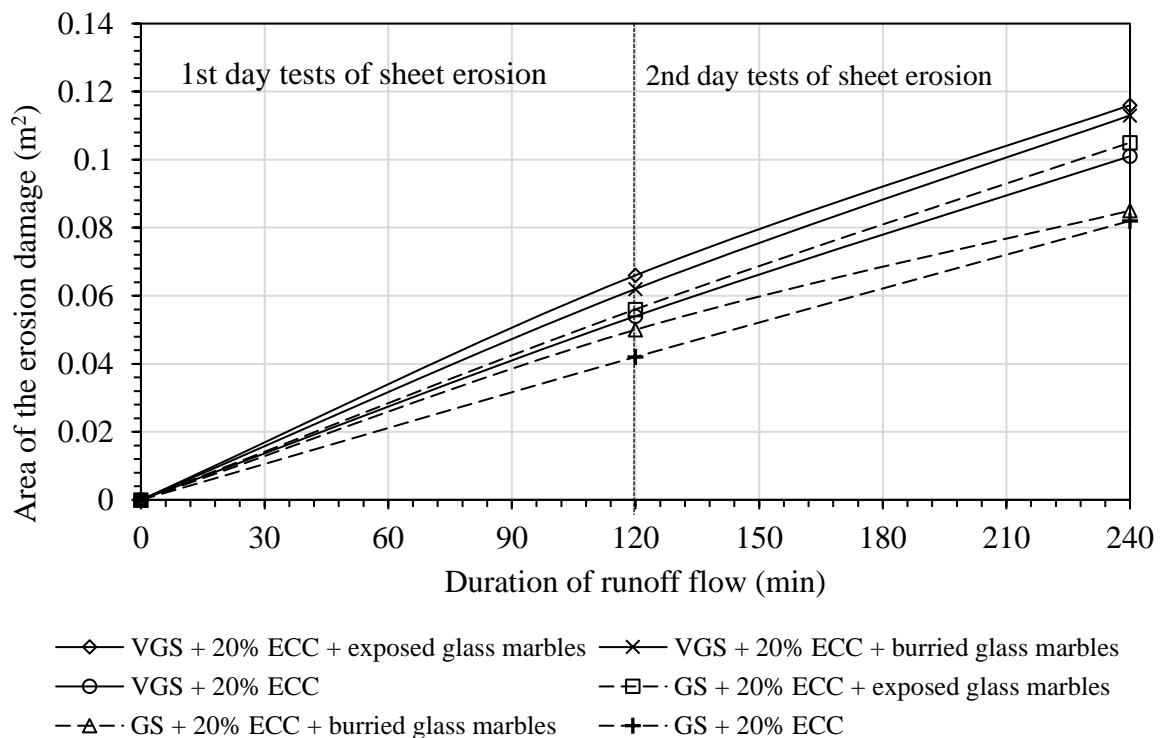


Figure 4. 14. Areas of erosion damage and runoff duration

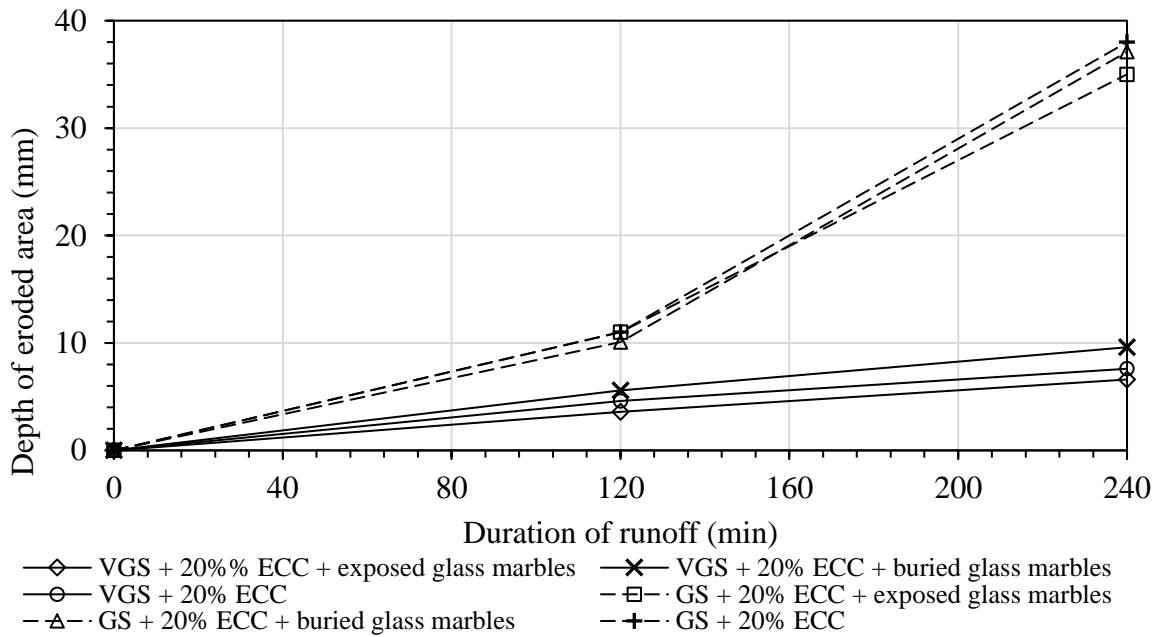


Figure 4. 15. Depths of erosion damage and runoff duration

#### 4.9.2. Area and Depth of Erosion Damage after the tenth- and eleventh-day Tests

As it is shown in Figure 4.16, for the GS + 20% ECC and VGS + 20% ECC soils without glass marbles which were further tested after the tenth and eleventh days from the second-day test, both the area and depth of erosion grew progressively. The area of damage increased to about 0.13 m<sup>2</sup> and 0.15 m<sup>2</sup> respectively at the end of the tenth- and eleventh-day tests for VGS + 20% ECC. Similarly, it increased to about 0.12 m<sup>2</sup> and 0.135 m<sup>2</sup> respectively at the end of the tenth- and eleventh- day tests for GS + 20% ECC. However, there was a reduction in the rate of the erosion growth after the tenth-day test, which was due to the long time between the second- and the tenth-day tests which allowed the soils to develop more strength because of a reduction in moisture content. Unlike the small difference in the growth of the damaged area, Figure 4.17 shows that the depth of the damaged area continued to be much bigger for GS + 20% ECC than for VGS + 20% ECC. After the tenth and the eleventh days of the second-day test, the depth of eroded area increased to about 9.8 mm and 10 mm respectively for VGS + 20% ECC. Similarly, it increased to about 60 mm and 70 mm respectively for GS + 20% ECC.

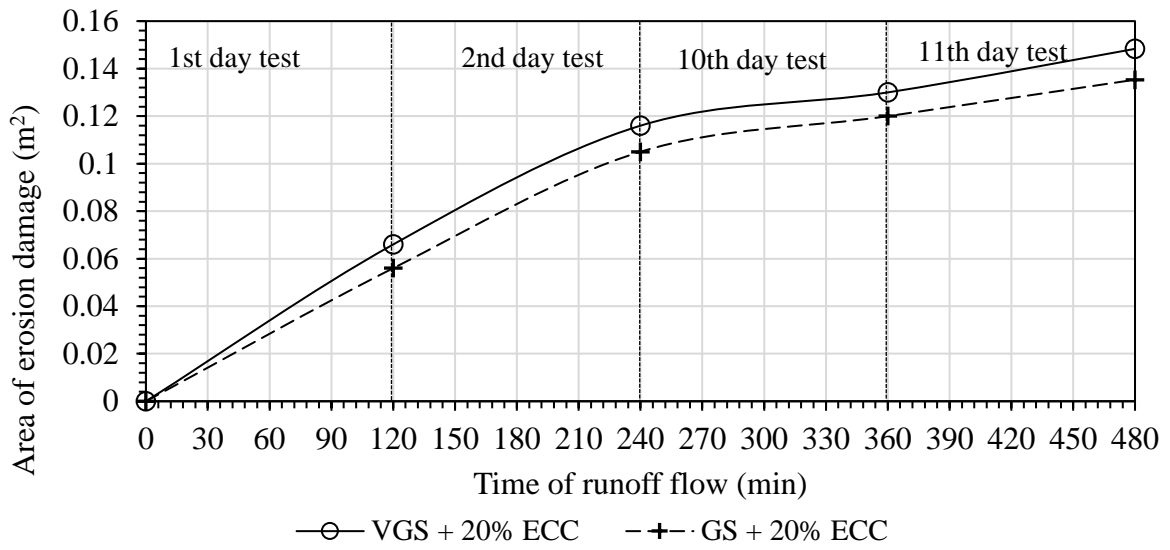


Figure 4. 16. Areas of erosion damage due to time of runoff flow

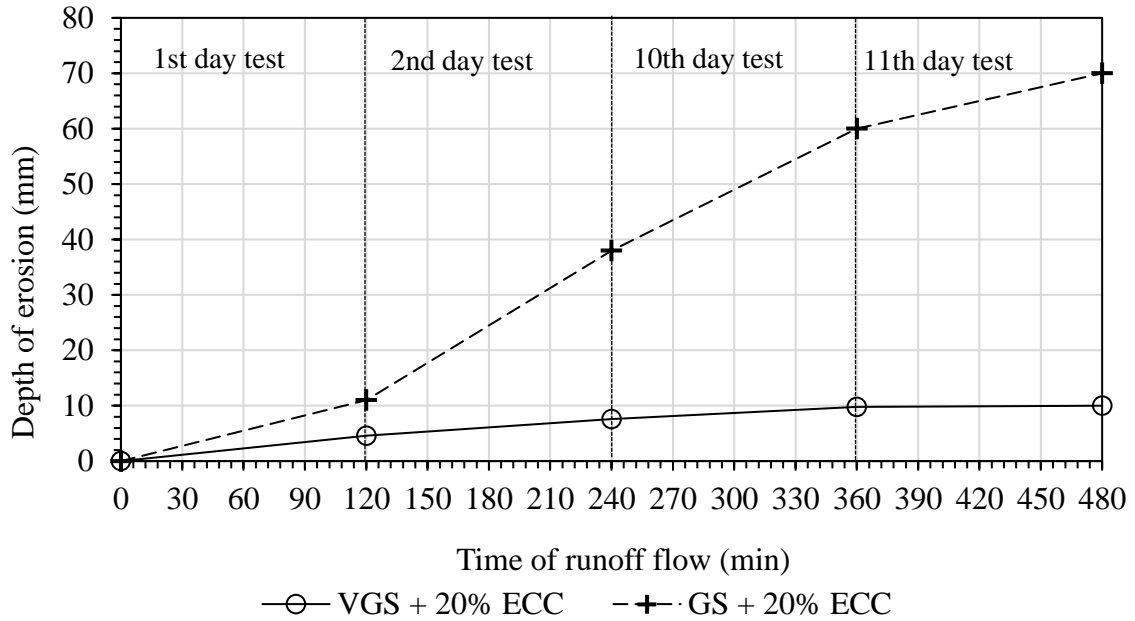


Figure 4. 17. Depths of erosion damage due to time of runoff flow

#### 4.9.3. Effect of Glass Marbles in the Formation of Potholes

The formation of potholes mainly due to surface water is one of the widely encountered forms of surface defects in unpaved roads. The sheet erosion tests on GS + 20% ECC and VGS + 20% ECC revealed that the particle size of the soils on the surface of roads significantly influences the formation and growth of potholes. Under the same testing conditions (slopes and testing

duration), it was found that the potholes formed more easily on a GS + 20% ECC soil than on a VGS + 20% ECC soil. The main difference in the two soils, which can be associated with the difference in pothole formation, was their  $D_{50}$ : 0.41 mm for the former and 1.2 mm for the latter.

Although the glass marbles reduced the flow velocities by acting as small barriers, at the same time they caused turbulence flow manifested by flow waves. Generally, the pothole started very near the glass marble or at the intersection of the waves from neighbouring glass marbles and then grew upstream, as shown in Figure 4.13 (F and F'). Thus, the presence of coarser particles extending above the general surface profile of the road can accelerate formation of potholes. In addition to this, as traffic wheels transit over the protrusion (exposed gravels), gravels may start to wobble, leading to an accumulation of water around them or dislodging them and leading to the initiation of pothole formation.

#### 4.10. Simulated Rainfall Erodibility Test Results

The main data from rainfall erodibility tests was the dry sediment which was obtained after weighing and oven drying of the collected runoff, as mentioned in sections 3.8.2. Cumulative sediment was obtained by adding up individual collections of sediment and the erosion rate was calculated in relation to the size of soil testing box. Further data such as runoff coefficients were also obtained based on the collected runoffs. Since the data was huge, only a typical data collection spreadsheet is shown for the first-day erodibility tests on GS and VGS soils mixed with 20% ECC, as shown in Tables 4.5 and 4.6. The tests with lower and higher erosion are highlighted for both the collected sediment and the calculated erosion rate. For eleven soils, first- and second-day tests, small-scale (Ss) and large-scale (Ls) tests, there are forty-three more tables of results not shown. However, all tests' results are graphically presented to support the discussion.

Table 4. 5. Eroded soil (g) during rainfall erosion tests for GS and VGS mixed with 20% ECC

Type		1st day tests																		
Scale		Large Scale (Ls): GS + 20% ECC						Small Scale (Ss): GS + 20% ECC						Ss: VGS + 20% ECC		Ls: VGS + 20% ECC				
Rain		30 mm/hr		51 mm/hr		68 mm/hr		30 mm/hr		51 mm/hr		68 mm/hr		68 mm/hr		68 mm/hr				
Time (min)		S = 0%	S = 6%	S = 0%	S = 6%	S = 0%	S = 6%	S = 12%	S = 0%	S = 6%	S = 0%	S = 6%	S = 0%	S = 6%	S = 0%	S = 6%	S = 0%	S = 6%	S = 12%	
0		0	0	0	0	0	0	0	0	0	0	0	0	0	0	0	0	0	0	0
5		27.8	70.4	54.9	146.3	40.8	221.1	345.8	10.3	13.1	20.3	39.0	19.0	29.0	25.5	29.5	68.3	121.4	229.0	
10		44.7	88.0	57.2	159.2	45.0	231.2	317.4	16.1	20.3	26.1	51.3	52.9	57.8	36.0	49.0	94.5	169.5	268.4	
15		32.9	77.0	43.7	125.0	58.6	206.9	301.5	16.7	21.0	39.7	68.8	48.6	64.4	37.9	40.9	80.9	149.4	238.7	
20		32.4	72.4	37.1	123.9	54.4	199.6	268.4	14.8	18.0	37.8	60.0	43.1	53.4	30.9	36.9	76.5	139.7	217.0	
25		30.4	65.7	32.2	116.9	52.3	196.8	244.0	14.5	14.0	34.5	57.3	41.4	44.7	31.0	33.4	70.7	134.3	210.6	
30		29.0	62.0	30.9	111.7	48.7	192.5	234.9	12.2	13.0	32.2	54.6	40.0	43.8	25.0	27.0	69.3	134.0	198.3	

Table 4. 6. Erosion rate (kg/m<sup>2</sup>/s) during rainfall erosion for GS and VGS mixed with 20% ECC

Type		1st day tests												VGS + 20% ECC						
Scale		Large Scale: GS + 20% ECC						Small Scale: GS + 20% ECC						Small scale		Large scale				
Rain		30 mm/hr		51 mm/hr		68 mm/hr		30 mm/hr		51 mm/hr		68 mm/hr		68 mm/hr		68 mm/hr				
Time (min)		Slope = 0%	Slope = 6%	Slope = 0%	Slope = 6%	Slope = 0%	Slope = 6%	Slope = 12%	Slope = 0%	Slope = 6%	Slope = 0%	Slope = 6%	Slope = 0%	Slope = 6%	Slope = 0%	Slope = 6%	Slope = 0%	Slope = 6%	Slope = 12%	
0		0	0	0	0	0	0	0	0	0	0	0	0	0	0	0	0	0	0	0
5		0.0013	0.0033	0.0025	0.0068	0.0019	0.0102	0.0160	0.0009	0.0012	0.0019	0.0036	0.0018	0.0027	0.0024	0.0027	0.0032	0.0056	0.0106	
10		0.0034	0.0073	0.0052	0.0141	0.0040	0.0209	0.0307	0.0024	0.0031	0.0043	0.0084	0.0067	0.0080	0.0057	0.0073	0.0075	0.0135	0.0230	
15		0.0049	0.0109	0.0072	0.0199	0.0067	0.0305	0.0447	0.0040	0.0050	0.0080	0.0147	0.0112	0.0140	0.0092	0.0111	0.0113	0.0204	0.0341	
20		0.0064	0.0142	0.0089	0.0257	0.0092	0.0398	0.0571	0.0054	0.0067	0.0115	0.0203	0.0151	0.0190	0.0121	0.0145	0.0148	0.0268	0.0441	
25		0.0078	0.0173	0.0104	0.0311	0.0116	0.0489	0.0684	0.0067	0.0080	0.0147	0.0256	0.0190	0.0231	0.0149	0.0176	0.0181	0.0331	0.0539	
30		0.0091	0.0202	0.0119	0.0363	0.0139	0.0578	0.0793	0.0078	0.0092	0.0176	0.0306	0.0227	0.0271	0.0173	0.0201	0.0213	0.0393	0.0631	

#### 4.10.1. Eroded Sediment from GS and VGS mixed with 20% ECC

For first-day tests, major sediment producers included large-scale experiments on GS + 20% ECC and VGS + 20% ECC tested using 68 mm/hr at a 12% slope, and GS + 20% ECC tested using 68 mm/hr at a 6% slope. For the first two soils, there was higher kinetic energy from higher rainfall intensity, more runoff formation at the surface due to the larger testing box, and a greater flow velocity because of a higher slope gradient which increased the detachment. For the third soil, there was more runoff and a smaller  $D_{50}$  of the granular tested soils. Respectively, the sediment produced by those soils at 15 and 30 min of rainfall was about 965 g and 1712 g, 736 g and 1362 g, and 659 g and 1248 g. The low sediment producers were the small-scale tests on GS + 20% ECC tested with 30 mm/hr at 0% and 6% slopes, and GS + 20% ECC tested using 51 mm/hr at a 0% slope. Respectively, the sediment produced by those soils at 15 and 30 min of rainfall was about 43 g and 84 g, 54 g and 99 g, and 86 g and 190 g. This was due to lower kinetic energy because of less rainfall intensity; lower slope gradients that reduced the flow velocity; and a smaller testing box that discouraged runoff formation. Generally, the peak sediment delivery was achieved in the first 5 min to 15 min, as shown in Figure 4.18.

For second-day tests, the major sediment producers were the large-scale experiments on GS + 20% ECC and VGS + 20% ECC tested using 68 mm/hr at a 12% slope, and GS + 20% ECC tested using 68 mm/hr at a 6% slope. The causes are as discussed for the first-day tests. Respectively, their cumulative sediment at 15 and 30 min of rainfall was about 633 g and 1230 g, 577 g and 1109 g, and 541 g and 983 g. The low sediment producers were the small-scale experiments on GS + 20% ECC tested using 30 mm/hr at 0% and 6% slopes, and VGS + 20% tested with 68 mm/hr at a 0% slope. For the first soil, the lower amount of erosion was due to less kinetic energy that reduced the detachment caused by raindrops, and a shorter testing box that minimized the surface flow formation that could detach and transport more sediment. For

the second soil, greater  $D_{50}$  helped to resist rainfall detachment while a higher infiltration and a shorter length of the testing box minimized the runoff. Respectively, sediment at 15 and 30 min of rainfall was 66 g and 112 g, 88 g and 146 g, and 88 g and 155 g, as shown in Figure 4.19.

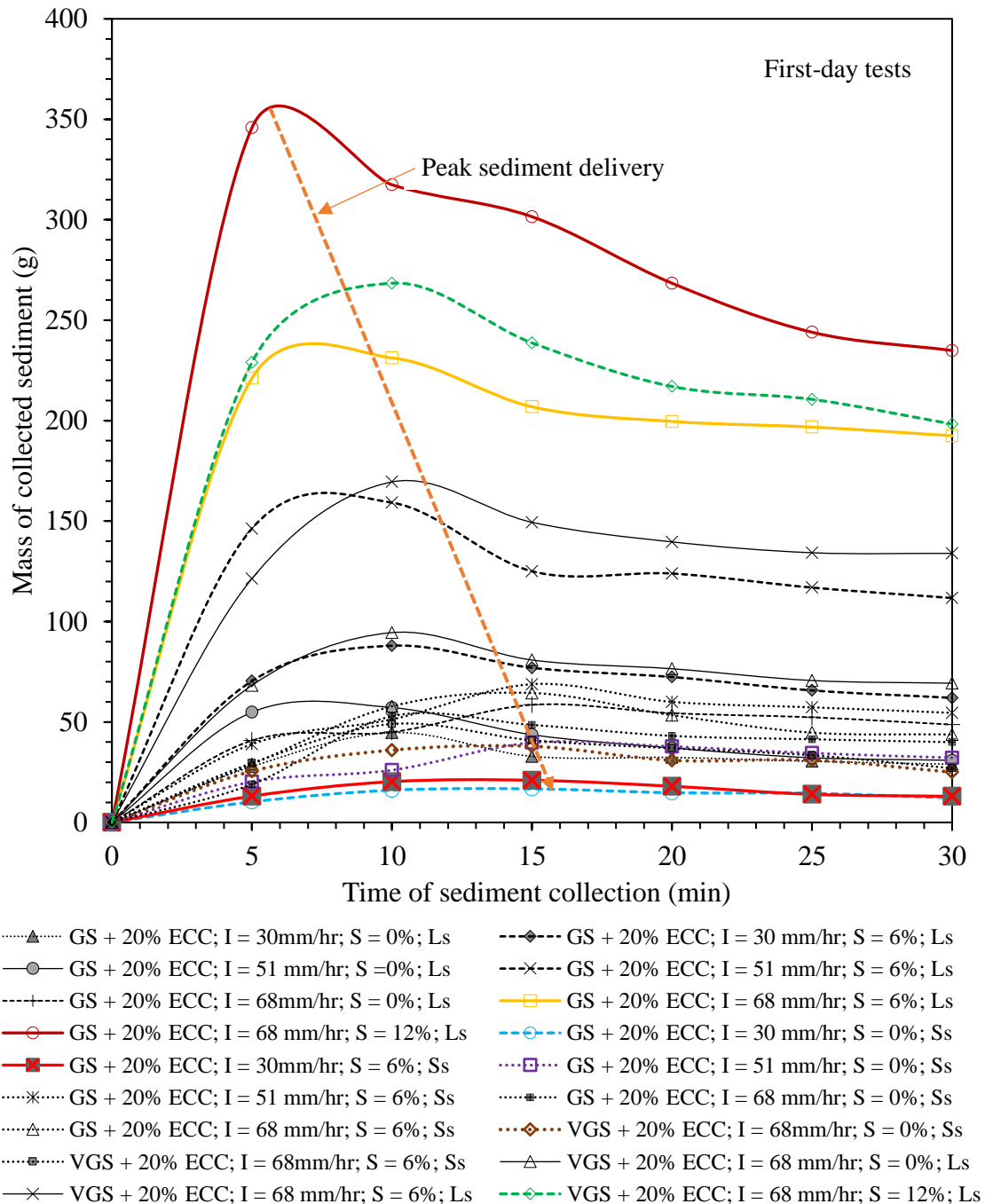


Figure 4. 18. Sediment from small- and large-scale first-day experiments for GS + 20% ECC and VGS + 20% ECC

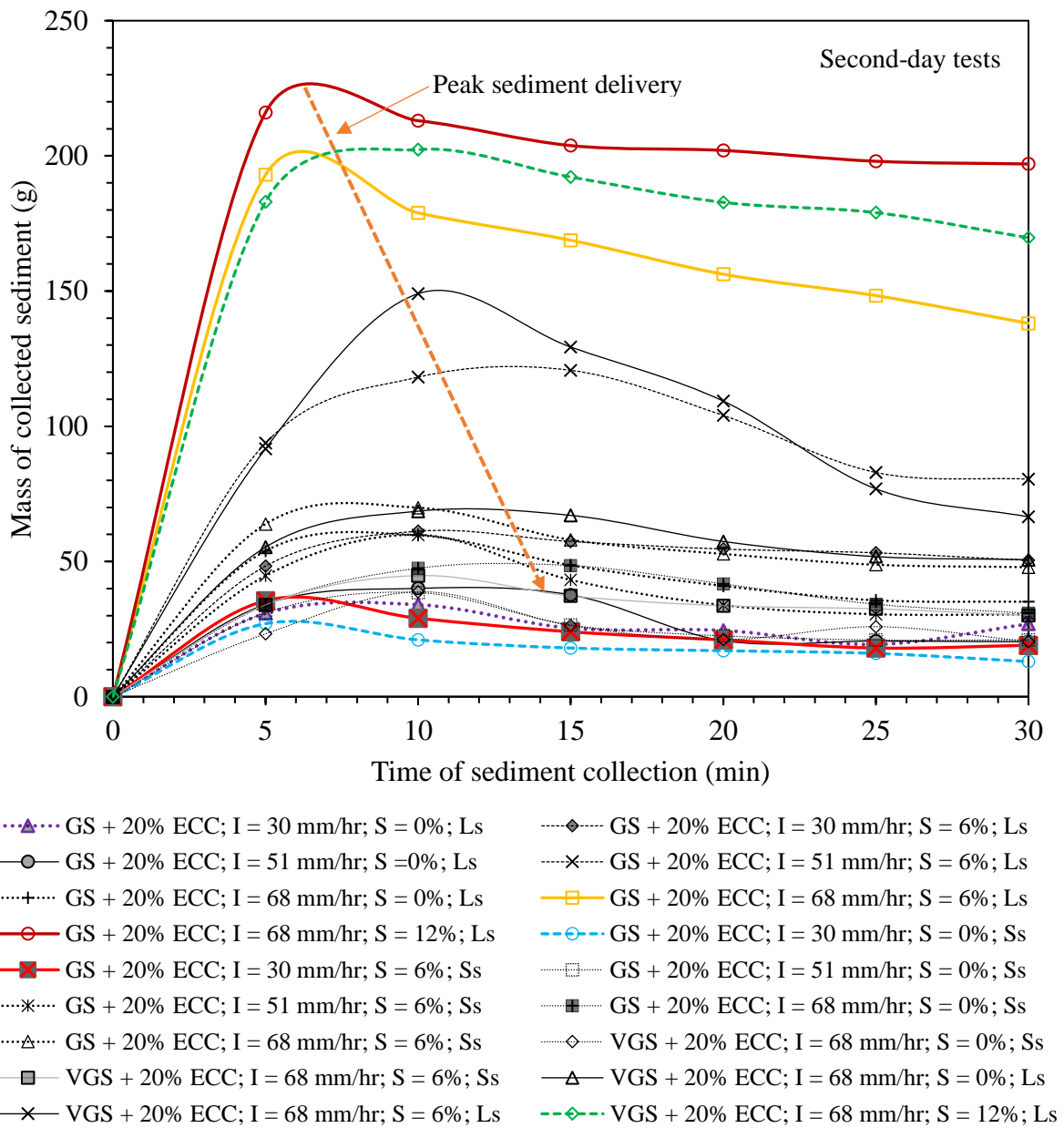


Figure 4. 19. Sediment from small- and large-scale second-day experiments for GS + 20% ECC and VGS + 20% ECC

#### 4.10.2. Eroded Sediment from GS and VGS mixed with 15% ECC

Generally, more eroded soils were collected in the first-day tests. These were from large-scale tests on: GS + 15% ECC and VGS + 15% ECC tested using 68 mm/hr at a 6% slope; GS + 15% ECC tested using 51 mm/hr at a 6% slope; and GS + 15% ECC tested using 68 mm/hr at a 0% slope. At 15 and 30 min of rainfall, the sediment eroded from these soils was about 820 g and

1440 g, 501 g and 903 g, 410 g and 833 g, and 464 g and 757 g, respectively. The higher rainfall intensity, longer slope and greater slope gradient were the main causes of more erosion. Less soil erosion was found from the small-scale tests on: VGS + 15% ECC tested with 68 mm/hr at 0% and 6% slopes; GS + 15% ECC tested using 30 mm/hr at 0% and 6% slopes, and GS + 15% tested with 51 mm/hr at a 0% slope. At 15 and 30 min of rainfall, this was about 100 g and 138 g, 126 g and 168 g, 80 g and 180 g, 141 g and 270 g and 146 g and 272 g, respectively. The less erosion was due to the shorter testing box and greater  $D_{50}$  for VGS + 15% ECC mixes; while less rainfall intensity, shorter testing box and lower slope gradient caused less erosion in GS + 15% ECC mixes. Details are shown in Appendix 2, Figure 1.

The second-day tests showed more soil loss on the large-scale tests with GS + 15% ECC tested using 68 mm/hr and 51 mm/hr at a 6% slope, and VGS + 15% ECC tested using 68 mm/hr at a 6% slope. This was mainly due to the larger soil testing box, higher rainfall intensity and greater slope gradients. Respectively, the sediment from those soils at 15 and 30 min of rainfall was about 544 g and 962 g, 396 g and 721 g, and 287 g and 548 g. Less sediment was produced by the small-scale tests on: GS + 15% ECC using 30 mm/hr at a 0% slope; VGS + 15% ECC tested using 68 mm/hr at 0% and 6% slopes; and GS + 15% tested with 30 mm/hr at a 6% slope. The cumulative sediment from those soils at 15 and 30 min of rainfall was about 83 g and 143 g, 78 g and 146 g, 110 g and 185 g, and 114 g and 204, respectively. Overall, the lower amount of erosion was due to the shorter length of the testing box, the greater  $D_{50}$  of the tested soils, lower rainfall intensities and lower slope gradients. Details are shown in Appendix 2, Figure 2.

#### 4.10.3. Eroded Sediment from GS and VGS mixed with 10% ECC

More soil loss was observed for the first-day large-scale tests on: GS + 10% ECC and VGS + 10% ECC tested using 68 mm/hr at a 6% slope, GS + 10% ECC tested using 68 mm/hr at a 0% slope and a small-scale test on GS + 10% ECC using 68 mm/hr at a 6% slope. The cumulative

soil eroded at 15 and 30 min of rainfall for those soils was about 866 g and 1513 g, 799 g and 1454 g, 521 g and 869 g, and 616 g and 993 g, respectively. The causes for more erosion were the scale of the testing box, higher rainfall intensity and greater slope gradient. Less soil loss was noted for the small-scale tests on: GS + 10% ECC tested with 30 mm/hr at a 0% slope, GS + 10% ECC using 51 mm/hr at a 0% slope, VGS + 10% tested with 68 mm/hr at a 0% slope and GS + 10% ECC tested with 30 mm/hr at a 6% slope. The eroded soils at 15 and 30 min of rainfall was about 129 g and 259 g, 188 g and 369 g, 254 g and 406 g, and 250 g and 433 g, respectively. Lower amount of erosion was due to the shorter testing box, lower rainfall intensity, lower slope gradient and greater  $D_{50}$ . Details are shown in Appendix 2, Figure 3.

The second-day tests showed more soil loss from large-scale tests on: GS + 10% ECC and VGS + 10% ECC tested using 68 mm/hr at a 6% slope; GS + 10% ECC tested using 51 mm/hr at a 6% slope and a small-scale test on GS + 10% ECC using 68 mm/hr and 51 mm/hr at a 6% slope. The cumulative sediment for these tests after 15 and 30 min of the rainfall was about 619 g and 1129 g, 562 g and 970 g, 393.4 g and 698 g, 547 g and 966 g and 343 g and 633 g, respectively. Similar to the first-day tests, the causes for more erosion were the larger testing box, higher rainfall intensity, and a greater slope gradient. Lower amount of erosion was found from the small-scale tests on GS + 10% ECC using 30 mm/hr at a 0% slope, VGS + 10% ECC using 68 mm/hr at a 0% slope, GS + 10% tested with 30 mm/hr at a 6% slope, GS + 10% ECC using 51 mm/hr at a 0% slope and large-scale test on GS + 10% ECC using 30 mm/hr at a 0% slope. Overall, less soil loss was due to the shorter testing box, greater  $D_{50}$ , lower rainfall intensity and gradient. Respectively, the cumulative eroded soil at 15 and 30 min of rainfall was about 125 g and 214 g, 165 g and 256 g, 157 g and 289 g, 178 g and 332 g, and 160 g and 318 g. A detailed graph of the results can be seen in Appendix 2, Figure 4.

#### 4.10.4. Eroded Sediment from GS and VGS mixed with 5% ECC

For the first-day tests, more sediment was found from the large-scale tests on GS + 5% ECC and VGS + 5% ECC using 68 mm/hr at a 6% slope; GS + 5% ECC using 68 mm/hr at a 0% slope; and GS + 5% ECC using 51 mm/hr at a 6% slope, and a small-scale test on GS + 5% ECC using 68 mm/hr at a 6% slope. Respectively, the cumulative eroded soil increased from 964 g to 1817 g, 931 g to 1786 g, 628 g to 1087 g, 537 g to 1063 g and 619 g to 1043 g at 15 and 30 min of rainfall. The main causes for more erosion were the larger testing box, higher rainfall intensity and greater slope gradient. On the other hand, low sediment was generally produced by the small-scale tests on GS + 5% ECC using 30 mm/hr at a 0% slope, GS + 5% ECC using 51 mm/hr at a 0% slope, VGS + 5% tested with 68 mm/hr at a 0% slope and GS + 5% ECC using 30 mm/hr at a 6% slope. The sediment increased from about 143 g to 317 g, 213 g to 409 g, 317 g to 513 g, and 289 g to 521 g, respectively between 15 and 30 min of rainfall. Less erosion was caused by the short testing box, lower slope gradient and rainfall intensity, and greater  $D_{50}$  of surface soils. However, a large-scale test on GS + 5% ECC using 30 mm/hr at 0% a slope was the second lowest sediment producer with 183 g and 369 g. Apart from the lower rainfall intensity, this was due to a higher infiltration caused by less clay content, and together discouraged formation of the runoff. Only particles near the exit of the flow were moved or splashed to the gutter and collected. Details are shown in Appendix 2, Figure 5.

Similarly for the second-day tests, more soil loss was found for the large-scale tests on GS + 5% ECC and VGS + 5% ECC using 68 mm/hr at a 6% slope; GS + 5% ECC using 51 mm/hr at a 6% slope and GS + 5% ECC using 68 mm/hr at a 0% slope, and a small-scale test on GS + 5% ECC using 68 mm/hr at a 6% slope. Respectively, the sediment from these soils between 15 and 30 min of rainfall increased from 689 g to 1260 g, 644 g to 1163 g, 597 g to 1082 g, 533 g to 982 g, and 548 g to 1032 g. Most of the causes for more erosion are the same as for the

first-day tests. However, due to improved infiltration rate after the erosion of lots of finer particles by the first-day rainfall; the slope gradient outscored the rainfall intensity in influencing erodibility. For example, GS + 5% ECC tested using 51 mm/hr at a 6% slope eroded more than when it was tested using 68 mm/hr at a 0% slope. Unexpectedly, the less soil loss was found from the large-scale tests on GS + 5% ECC using 30 mm/hr at a 0% slope with 120.9g and 214.6 g. As stated earlier, this was due to a higher infiltration rate and a lower rainfall intensity. The larger scale of the testing box had little influence to erosion acceleration due to the very thin flow formation. Thus, only the particles nearby the exit of the flow were moved or splashed to the gutter for collection. Other low sediment producers were small-scale tests on GS + 5% ECC using 30 mm/hr at a 0% slope, VGS + 5% using 68 mm/hr at a 0% slope, GS + 5% ECC using 30 mm/hr at a 6% slope and VGS + 5% ECC using 68 mm/hr at a 6% slope. It was mainly due to a lower rainfall intensity, a greater  $D_{50}$  leading to a greater infiltration, and a lower slope gradient. Respectively, the sediment between 15 and 30 min of rainfall increased from 154 g to 215 g, 184 g to 300 g, 175 g to 315 g, and 210 g to 354 g. A detailed graph of the results can be seen in Appendix 2, Figure 6.

#### 4.10.5. Eroded Sediment from GS and VGS mixed with 0% ECC

Soil loss from gravelly SAND and very gravelly SAND without ECC content was generally the highest. During the first-day tests, more sediment was produced by the large-scale tests on GS + 0% ECC using 68 mm/hr at 6% and 0% slopes; VGS + 0% ECC using 68 mm/hr at a 0% slope, GS + 0% ECC using 51 mm/hr at a 0% slope, GS + 0% ECC using 51 mm/hr at a 6% slope and a small-scale test on GS + 0% ECC using 68 mm/hr at a 6% slope. Respectively, these soils' sediment between 15 and 30 min of rainfall increased from 794 g to 1665 g, 738 g to 1436 g, 660 g to 1330 g, 645 g to 1204 g, 594 g to 1163 g, and 652 g to 1137 g. The major factor that accelerated erosion was the higher rainfall intensity that compensated for the greater

infiltration rate and allowed the formation of a slightly thicker surface flow to transport particles. Detachment was easier due to lack of cohesion. After the saturation of the soils and the formation of the flow, the particles had more degrees of freedom and easily moved with the flow, leading to more sediment collection. Furthermore, the low sediment producers were the small-scale tests on: GS + 0% ECC using 30 mm/hr at a 0% slope; GS + 0% ECC using 51 mm/hr at a 0% slope; GS + 0% tested with 30 mm/hr at a 6% slope; VGS + 0% ECC using 68 mm/hr at a 0% slope; and a large-scale experiment on GS + 0% ECC at 0% slope. Respectively, the sediment between 15 and 30 min of rainfall increased from 163 g to 364 g, 260 g to 551 g, 287 g to 573 g, 331 g to 590 g and 274 g to 602 g. Overall, the lower amount of erosion was due to the lower rainfall intensity and lower slope gradient. Greater  $D_{50}$  discouraged surface flow formation because of higher infiltration, leading to fewer particles transported for collection. Detailed results are shown in Figure 4.20.

The results from the second-day tests showed that the major sediment producers were large-scale tests on: GS + 0% ECC using 68 mm/hr at 6% and 0% slopes; GS + 0% ECC using 51 mm/hr at 6% and 0% slopes; and a small-scale test on GS + % ECC using 68 mm/hr at a 6% slope. The eroded soil at 15 and 30 min of rainfall was 673 g and 1403 g, 571 g and 1064 g, 507 g and 971 g, 486 g and 967 g, and 570 g and 1081 g, respectively. The causes of more erosion were the same as for the first-day tests. However, smaller particles had been eroded by the first-day rainfall events, leading to a reduction in erosion, since the bigger soil particles were able to resist detachment due to both the raindrops' energy and the flow velocity. Differently, less sediment was collected from the small-scale tests on: VGS + 0% ECC using 68 mm/hr at a 6% slope; GS + 0% ECC using 30 mm/hr at 6% and 0% slopes; GS + 0% using 51 mm/hr at a 0% slope; and a large-scale experiment on GS + 0% ECC using 30 mm/hr at a 0% slope. The eroded soil at 15 and 30 min of rainfall was about 155 g and 278 g, 174 g and 362 g, 162 g and

398 g, 325 g and 603 g, and 208 g and 385 g, respectively. This was also due to the causes related to lower rainfall intensities, lower slope gradients and  $D_{50}$ , as discussed in the first-day tests. Detailed results are shown in Figure 4.21.

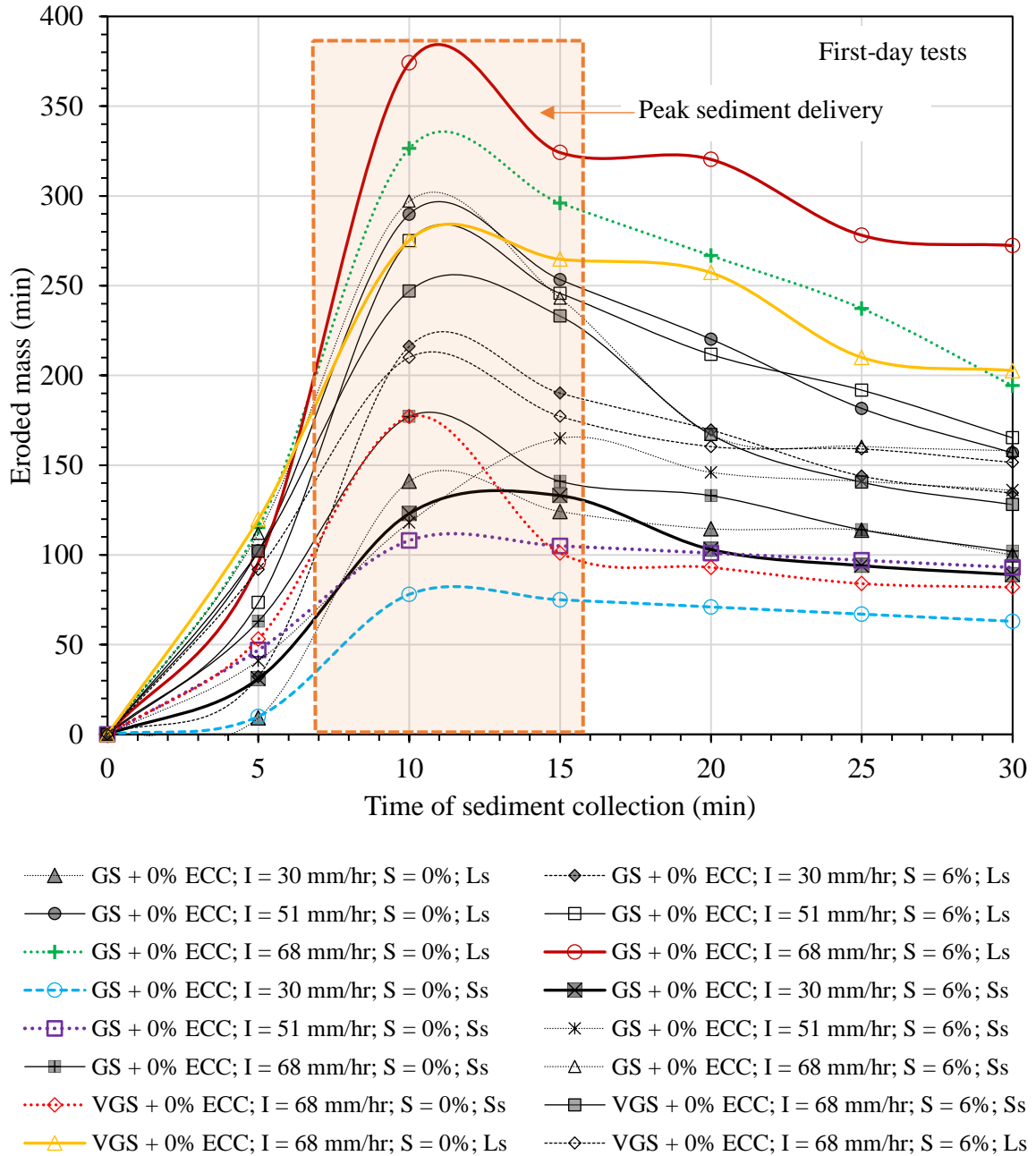


Figure 4. 20. Sediment from small- and large-scale first-day experiments for GS + 0% ECC and VGS + 0% ECC

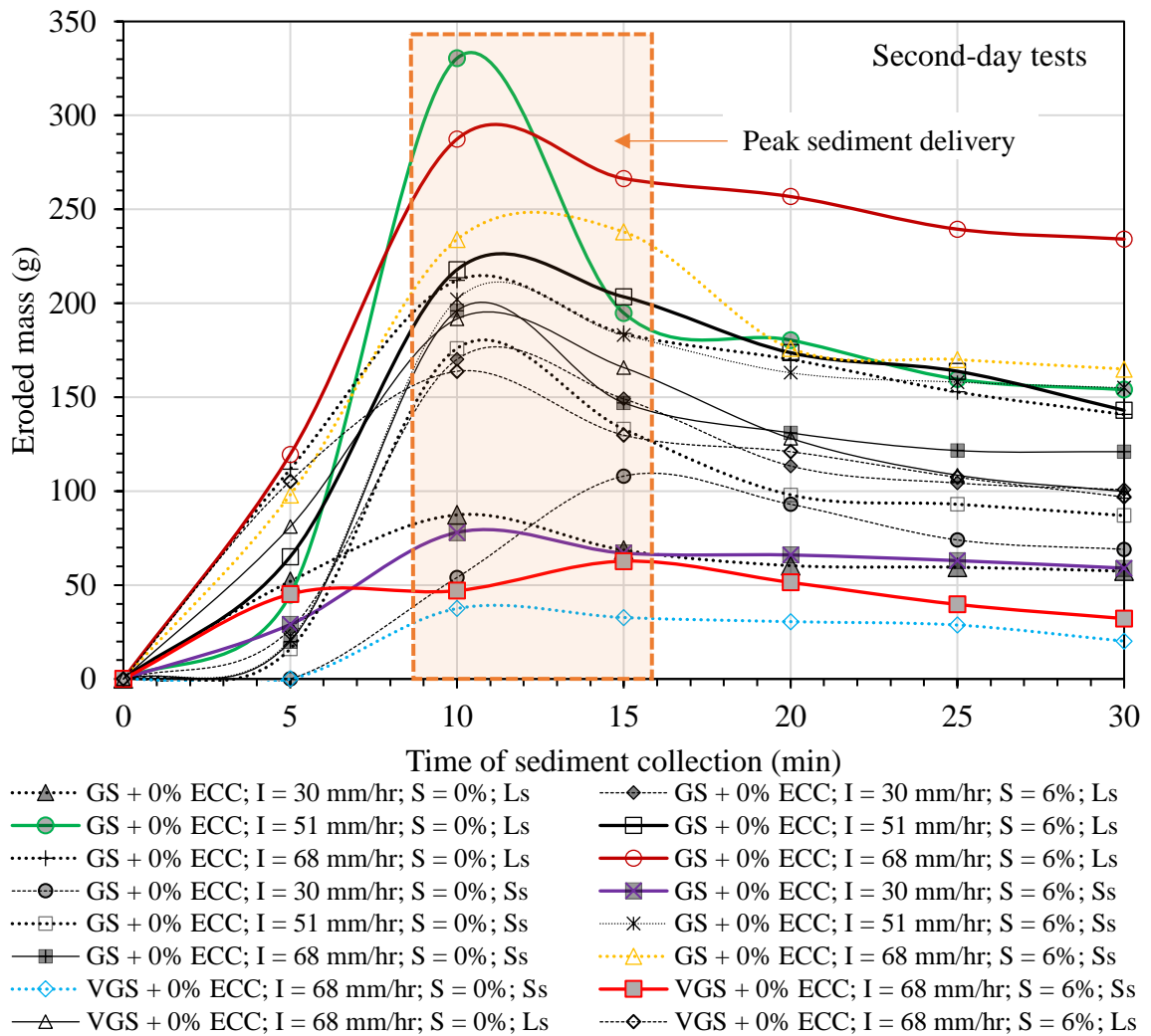


Figure 4. 21. Sediment from small- and large-scale second-day experiments for GS + 0% ECC and VGS + 0% ECC

#### 4.10.6. Eroded Sediment from Subbase

The subbase soil was generally less erodible. For the first-day tests, more erosion occurred for the large-scale tests using 68 mm/hr at a 6%; 30 mm/hr at a 6% slope; 68 mm/hr at a 0% slope; and 51 mm/hr at 6% and 0% slopes. The sediment from these tests between 15 and 30 min of rainfall increased from 129.6 g to 190 g, 100 g to 181 g, 101 g to 173 g, 93 g to 159 g, and 74 g to 124 g, respectively. Lower erosion occurred with the small-scale tests using 30 mm/hr at 6% and 0% slopes, 68 mm/hr at a 0% slope, and 51 mm/hr at 6% and 0% slopes. Respectively,

the eroded sediment between 15 and 30 min of rainfall increased from 18 g to 28 g, 25 g to 29 g, 32 g to 34 g, 26 g to 34 g and 30 g to 37 g. Details are shown in Figure 4.22.

Similarly, the second-day tests on the subbase soil showed more erosion from the large-scale tests using 68 mm/hr at 6% and 0% slopes, and 51 mm/hr at 6% and 0% slopes. The sediment increased from 110 g to 189 g, 86 g to 139 g and 73 g to 120 g between 15 and 30 min of rainfall. Less erosion occurred with the small-scale experiments using 68, 51 and 30 mm/hr at a 0% slope, with each test' sediment being about 10 g during the 30 min of rainfall. For some tests, there was no sediment content in the runoff after about 20 min. This was the case for 68 mm/hr at 0% and 6% slopes as well as for 30 mm/hr at 0% slope, as shown in Figure 4.23.

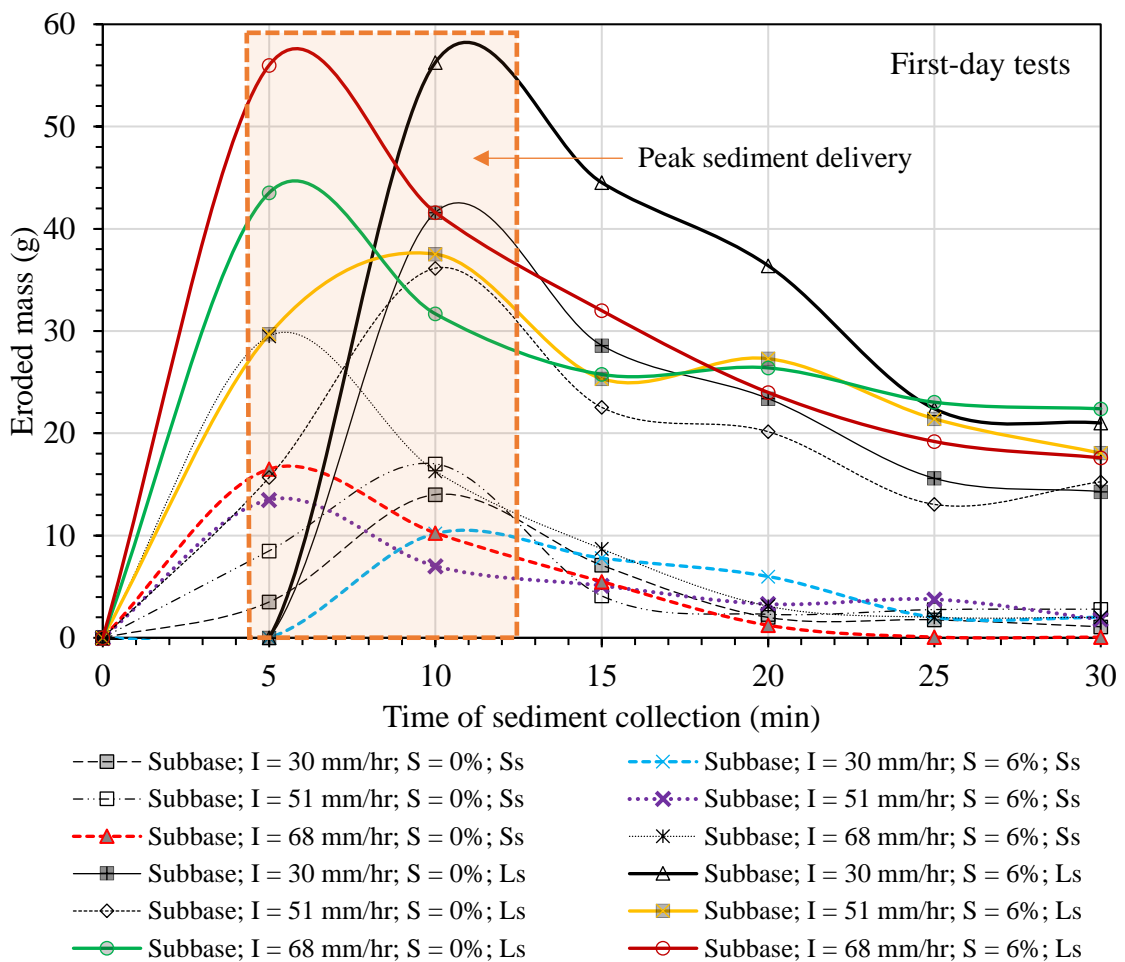


Figure 4. 22. Sediment from small- and large-scale first-day experiments subbase

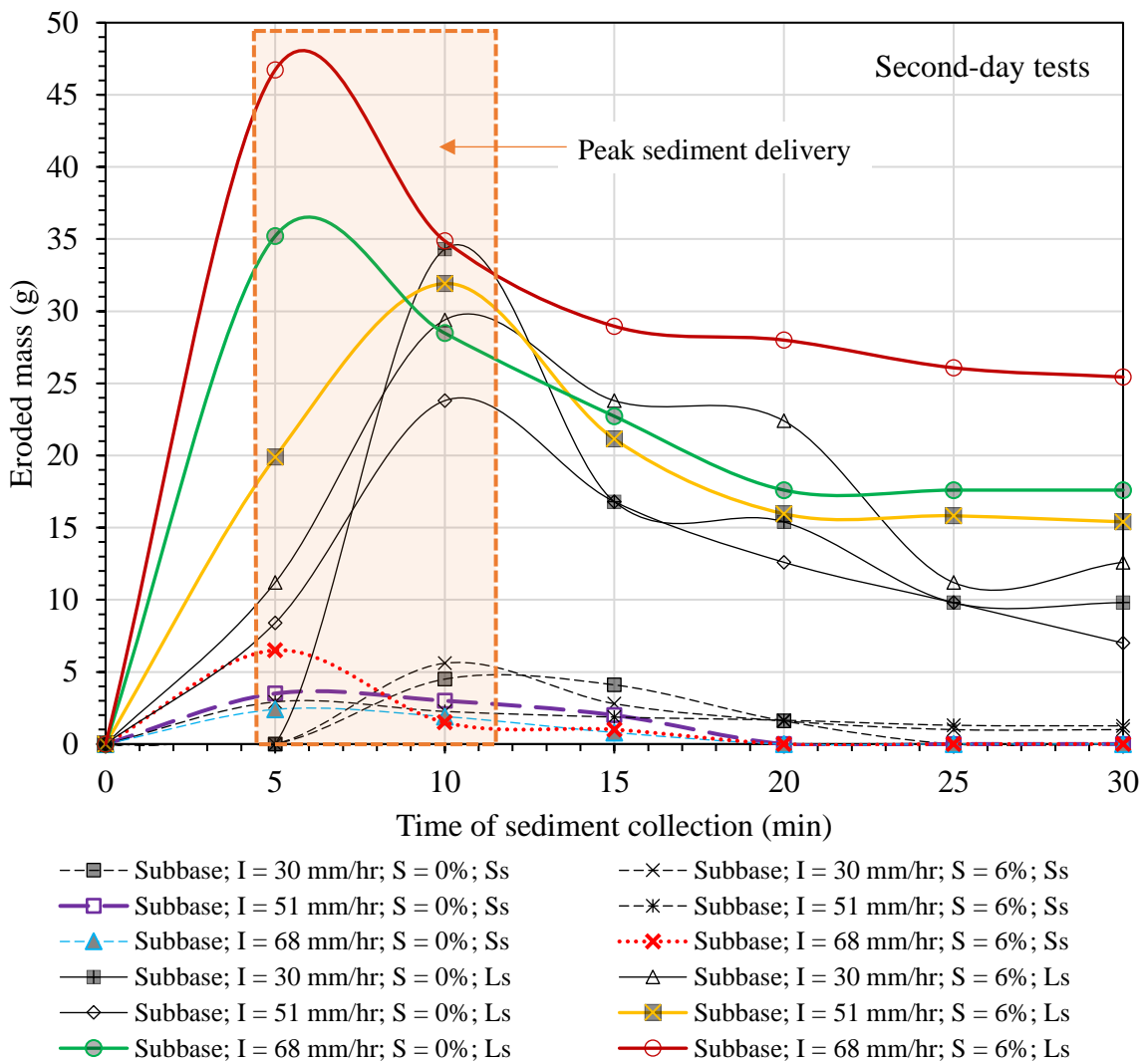


Figure 4. 23. Sediment from small- and large-scale second-day experiments subbase

#### 4.11. Erosion Rate

The erosion rate is the mass of eroded soil material per unit area per second. In this study, the erosion rate was calculated by dividing the collected sediment by the area of the samples (top view area of the soil testing box) per second. Due to this definition, some erodibility tests that had more cumulative sediment may not necessarily have a higher erosion rate. Since the area of the large-scale box was twice the small-scale box's area, it could only have a greater erosion rate if the sediment from the large-scale tests is more than double the sediment from the small-scale tests. This did not occur in most cases and thus, most higher erosion rates were found for

the small-scale tests. As for the sediment collection data, the erosion rate data after 30 min of the rainfall is also presented in ascending order from the soils containing higher clay content downwards. Most acceleration and deceleration factors of erodibility have been discussed previously in connection with the sediment collection data, and remain the same. The only factor that makes the data look differently is the area (size) of the testing box.

#### 4.11.1. Erosion Rate for GS and VGS mixed with 20% ECC

Generally, these are the mixes with the lowest erosion rate because of more clay content and thus, greater cohesion. Nevertheless, for the first-day tests, the higher erosion rates were 0.079 kg/m<sup>2</sup>/s, 0.063 kg/m<sup>2</sup>/s and 0.058 kg/m<sup>2</sup>/s respectively for the large-scale tests on GS + 20% ECC and VGS + 20% ECC, tested using 68 mm/hr at a 12% slope, and GS + 20% ECC tested using 68 mm/hr at a 6% slope. Also, the lower erosion rates were 0.007 kg/m<sup>2</sup>/s, 0.009 kg/m<sup>2</sup>/s and 0.009 kg/m<sup>2</sup>/s respectively for the small-scale tests on GS + 20% ECC, using 30 mm/hr at 0% and 6% slopes, and on GS + 20% ECC using 51 mm/hr at a 0% slope, as shown in Figure 4.24. Generally, the greater cohesion (more clay content) reduced detachment and promoted formation of runoff and sediment from the larger soil testing box due to less infiltration. Sediment from the shorter soil testing box was less than half of the sediment from the larger box due to limited flow, leading to higher erosion rates from large-scale tests.

Similarly, for the second-day tests on GS + 20% ECC and VGS + 20% ECC, the higher erosion rates were from the large-scale tests with 0.057 kg/m<sup>2</sup>/s, 0.051 kg/m<sup>2</sup>/s and 0.046 kg/m<sup>2</sup>/s respectively for GS + 20% ECC and VGS + 20% ECC tested using 68 mm/hr at a 12% slope and GS + 20% ECC tested using 68 mm/hr at a 6% slope. Furthermore, the lower erosion rates were from the small-scale tests using 68 mm/hr on VGS + 20% ECC at a 0% slope, and the large-scale tests using 30 mm/hr and 51 mm/hr at 0% slope. Those were 0.0072 kg/m<sup>2</sup>/s, 0.0072 kg/m<sup>2</sup>/s and 0.008 kg/m<sup>2</sup>/s respectively. Detailed results are shown in Figure 4.25.

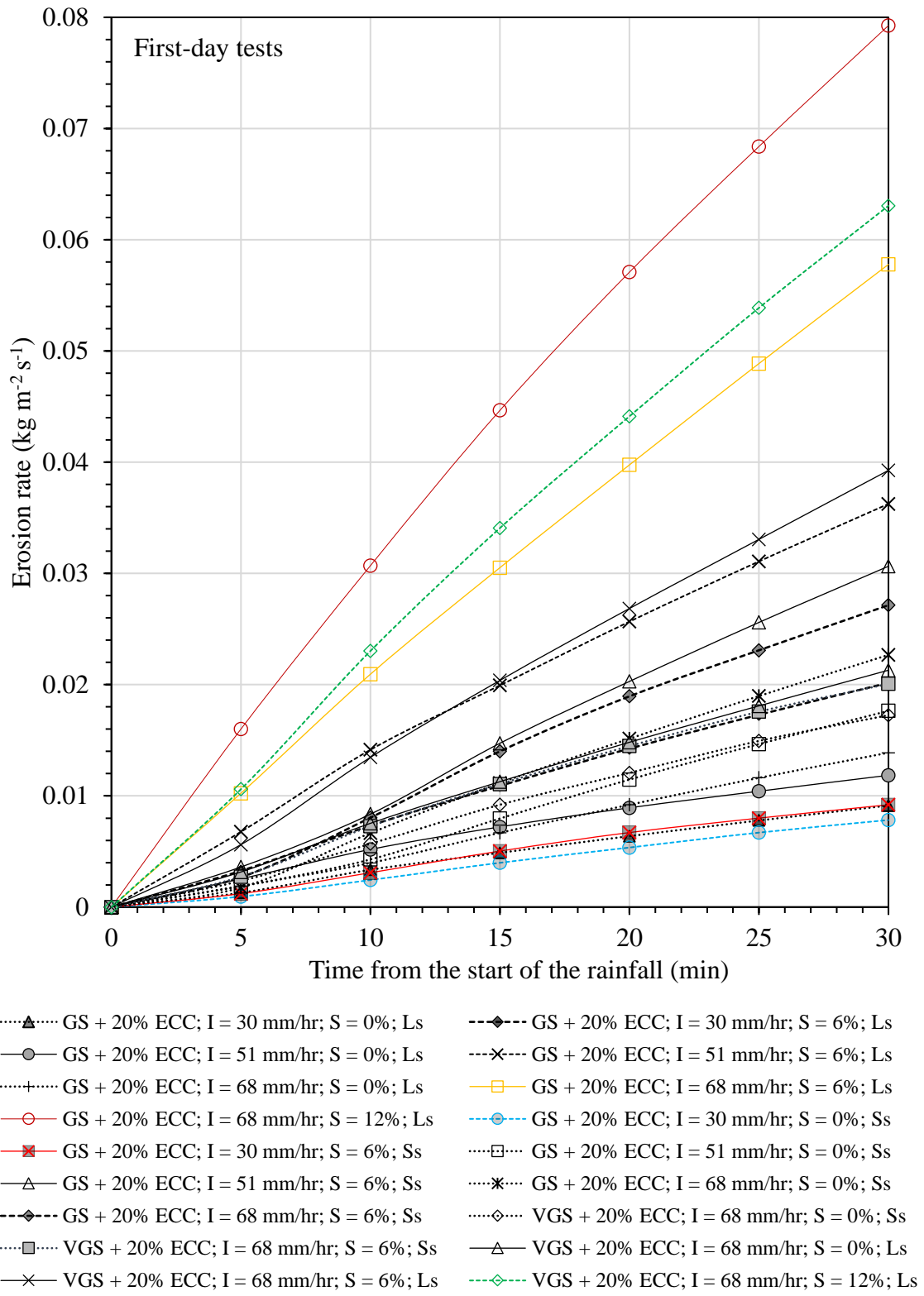


Figure 4. 24. Erosion rate from small- and large-scale first-day experiments for GS + 20% ECC and VGS + 20% ECC

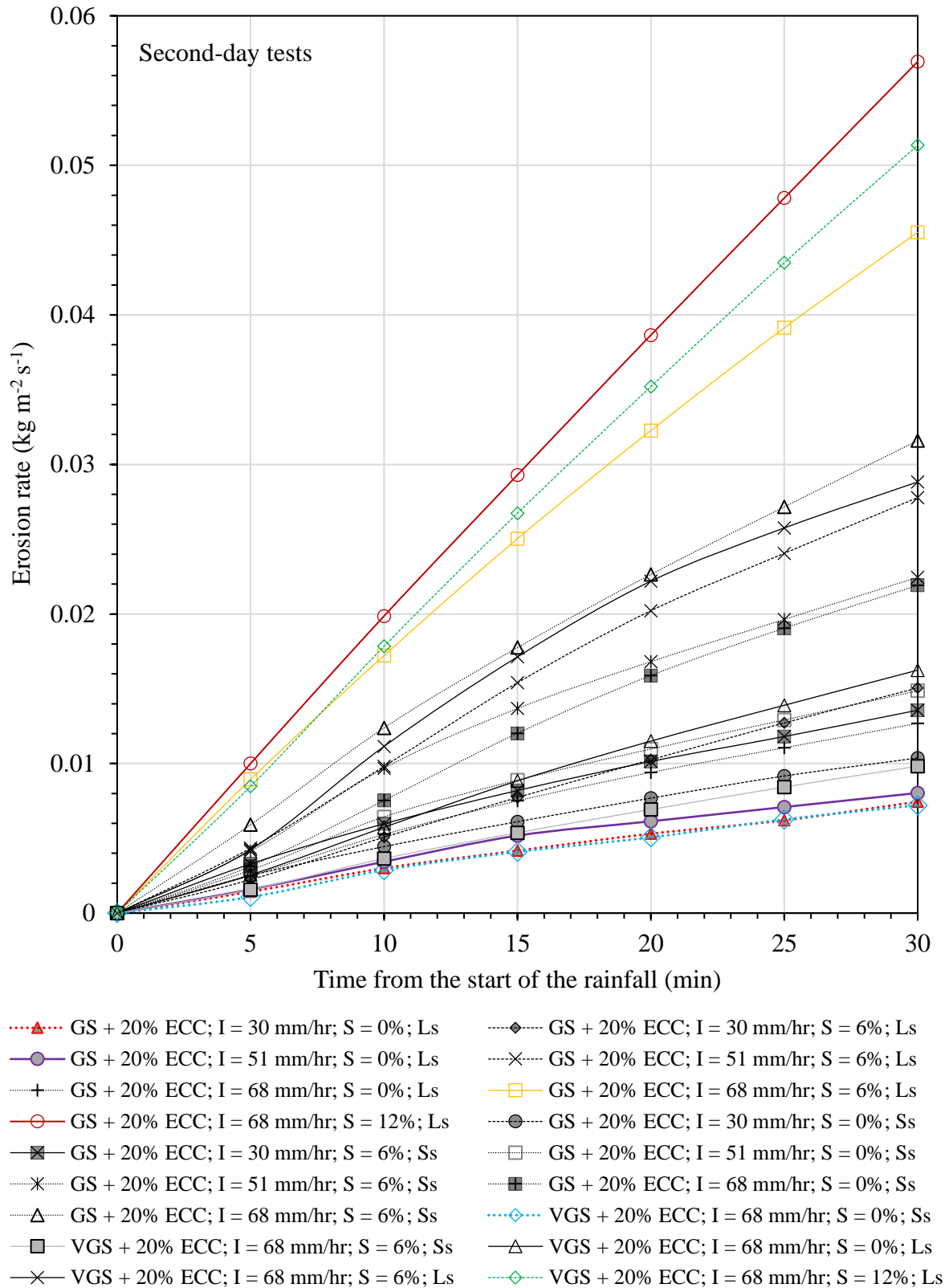


Figure 4. 25. Erosion rate from small- and large-scale second-day experiments for GS + 20% ECC and VGS + 20% ECC

#### 4.11.2. Erosion Rate for GS and VGS mixed with 15% ECC

The highest erosion rate for the first-day tests was obtained from a large-scale test on GS + 15% ECC tested using 68 mm/hr at a 6% slope reaching 0.067 kg/m<sup>2</sup>/s. Erosion during this test was runoff dependent due to the large testing box, higher rainfall intensity and greater gradient. The next higher rates were the small-scale test results on GS + 15% ECC, tested using 68 mm/hr and 51 mm/hr at a 6% slope, and GS + 15% ECC tested using 68 mm/hr at a 0% slope, which were controlled by the raindrops due to limited runoff because of the shorter testing box. The erosion rates were 0.054 kg/m<sup>2</sup>/s, 0.053 kg/m<sup>2</sup>/s and 0.049 kg/m<sup>2</sup>/s, respectively. On the other hand, the lower erosion rates were from the small-scale tests on GS + 15% ECC tested using 30 mm/hr at a 0% slope, and on VGS + 15% ECC tested using 68 mm/hr at 0% and 6% slopes, respectively at 0.017 kg/m<sup>2</sup>/s, 0.019 kg/m<sup>2</sup>/s and 0.023 kg/m<sup>2</sup>/s. The lower erosion rate was due to the lack of enough flow caused by a lower rainfall intensity and slope gradient, and a greater infiltration rate. Detailed results are shown in Figure 4.26.

In contrast, the second-day tests showed higher erosion rates from a small-scale test on GS + 15% ECC, tested using 51 mm/hr at a 6% slope, and 68 mm/hr at 0% and 6% slopes, amounting to 0.045 kg/m<sup>2</sup>/s, 0.05 kg/m<sup>2</sup>/s and 0.044 kg/m<sup>2</sup>/s, respectively. The erosion rate was 0.44 kg/m<sup>2</sup>/s for a large-scale test on GS + 15% ECC using 68 mm/hr at a 6% slope. The flow thickness reduced due to improved infiltration following removal of finer particles by the first-day rainfall. This reduced the sediment from the large-scale tests and gave an advantage to the small-scale tests which relied on detachment due to raindrops rather than the flow stresses. Thus, the lower erosion rates were from the large-scale tests on GS + 15% ECC using 30 mm/hr and 51 mm/hr at a 0% slope at 0.01 kg/m<sup>2</sup>/s and 0.012 kg/m<sup>2</sup>/s respectively. The small-scale tests on VGS + 15% ECC using 68 mm/hr at 0% and 6% slopes reached 0.013 kg/m<sup>2</sup>/s and 0.014 kg/m<sup>2</sup>/s, respectively. Details are shown in Figure 4.27.

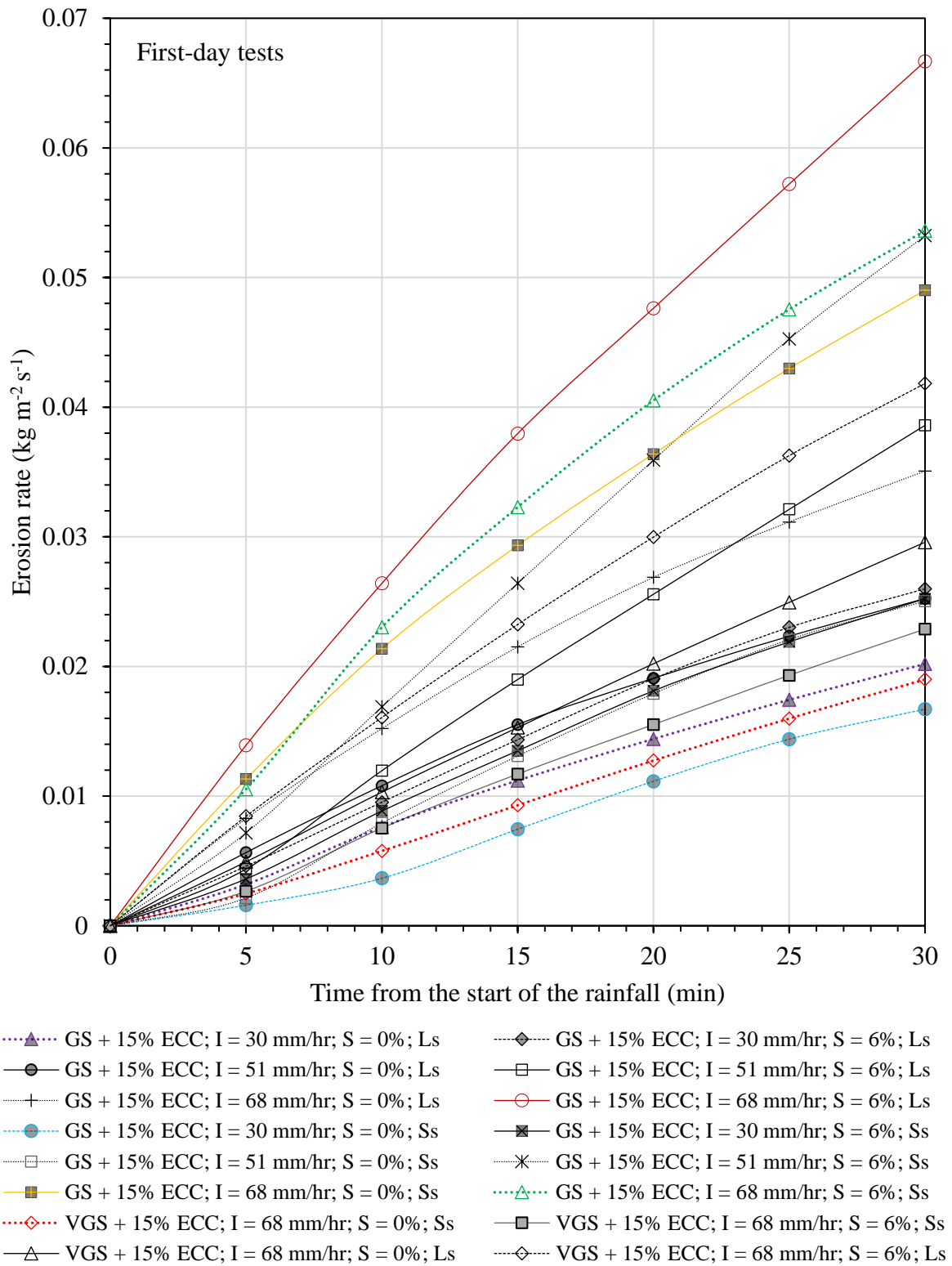


Figure 4. 26. Erosion rate from small- and large-scale first-day experiments for GS + 15% ECC and VGS + 15% ECC

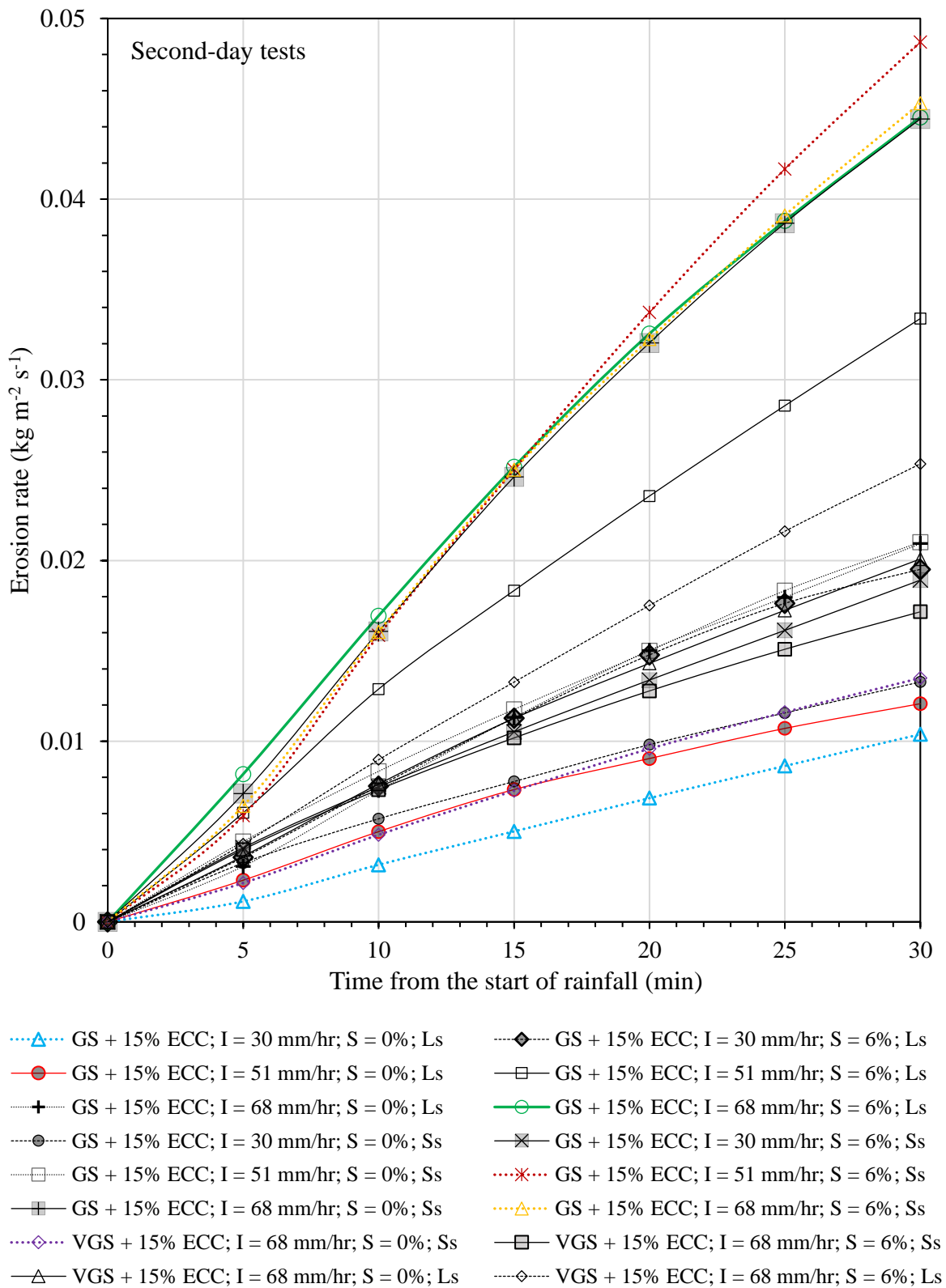


Figure 4. 27. Erosion rate from small- and large-scale second-day experiments for GS + 15% ECC and VGS + 15% ECC

#### 4.11.3. Erosion Rate for GS and VGS mixed with 10% ECC

The higher erosion rates for the first-day tests were noted from the small-scale tests on: GS + 10% ECC using 68 mm/hr and 51 mm/hr at a 6% slope reaching 0.09 kg/m<sup>2</sup>/s and 0.065 kg/m<sup>2</sup>/s, respectively. The other higher erosion rates were from the large-scale tests on GS + 10% ECC and VGS + 10% ECC using 68 mm/hr at a 6% slope, reaching 0.07 kg/m<sup>2</sup>/s and 0.067 kg/m<sup>2</sup>/s, respectively. Higher erosion rate was mainly due to a higher rainfall intensity and a greater slope gradient. One of the lower erosion rates was from a the small-scale test on GS + 10% ECC, tested using 30 mm/hr at a 0% slope at 0.024 kg/m<sup>2</sup>/s. Further lower erosion rates were from the large-scale tests on GS + 10% ECC using 30 mm/hr and 51 mm/hr at a 0%, and 30 mm/hr at a 6%; reaching 0.023 kg/m<sup>2</sup>/s, 0.025 kg/m<sup>2</sup>/s and 0.03 kg/m<sup>2</sup>/s, respectively. Lower erosion rates were essentially due to lower rainfall intensities and slope gradients. Details are shown in Figure 4.28.

The second-day results showed higher erosion rates from the small-scale tests on GS + 10% ECC using 68 mm/hr and 51 mm/hr at a 6% slope; and 68 mm/hr at a 0% slope at 0.089 kg/m<sup>2</sup>/s, 0.06 kg/m<sup>2</sup>/s and 0.043 kg/m<sup>2</sup>/s, respectively. It was due to higher rainfall intensities and greater slope gradients. Other higher erosion rates were from the large-scale tests on GS + 10% ECC and VGS + 10% ECC using 68 mm/hr at a 6% slope, eroding at 0.053 kg/m<sup>2</sup>/s and 0.045 kg/m<sup>2</sup>/s, respectively. In contrast, the lower erosion rates were from the small-scale tests on GS + 10% ECC using 30 and 51 mm/hr at a 0% slope and VGS + 10% ECC using 68 mm/hr at a 0% slope, respectively eroding at 0.0147 kg/m<sup>2</sup>/s, 0.019 kg/m<sup>2</sup>/s and 0.024 kg/m<sup>2</sup>/s. This was due to lower rainfall intensity and slope gradient, and greater infiltration capacity. Also, lower erosion rates were found from the large-scale tests on VGS + 10% ECC using 68 mm/hr at a 0% and GS + 10% ECC using 30 mm/hr at a 6%, eroding at 0.019 kg/m<sup>2</sup>/s and 0.021 kg/m<sup>2</sup>/s, respectively. Detailed results are shown in Figure 4.29.

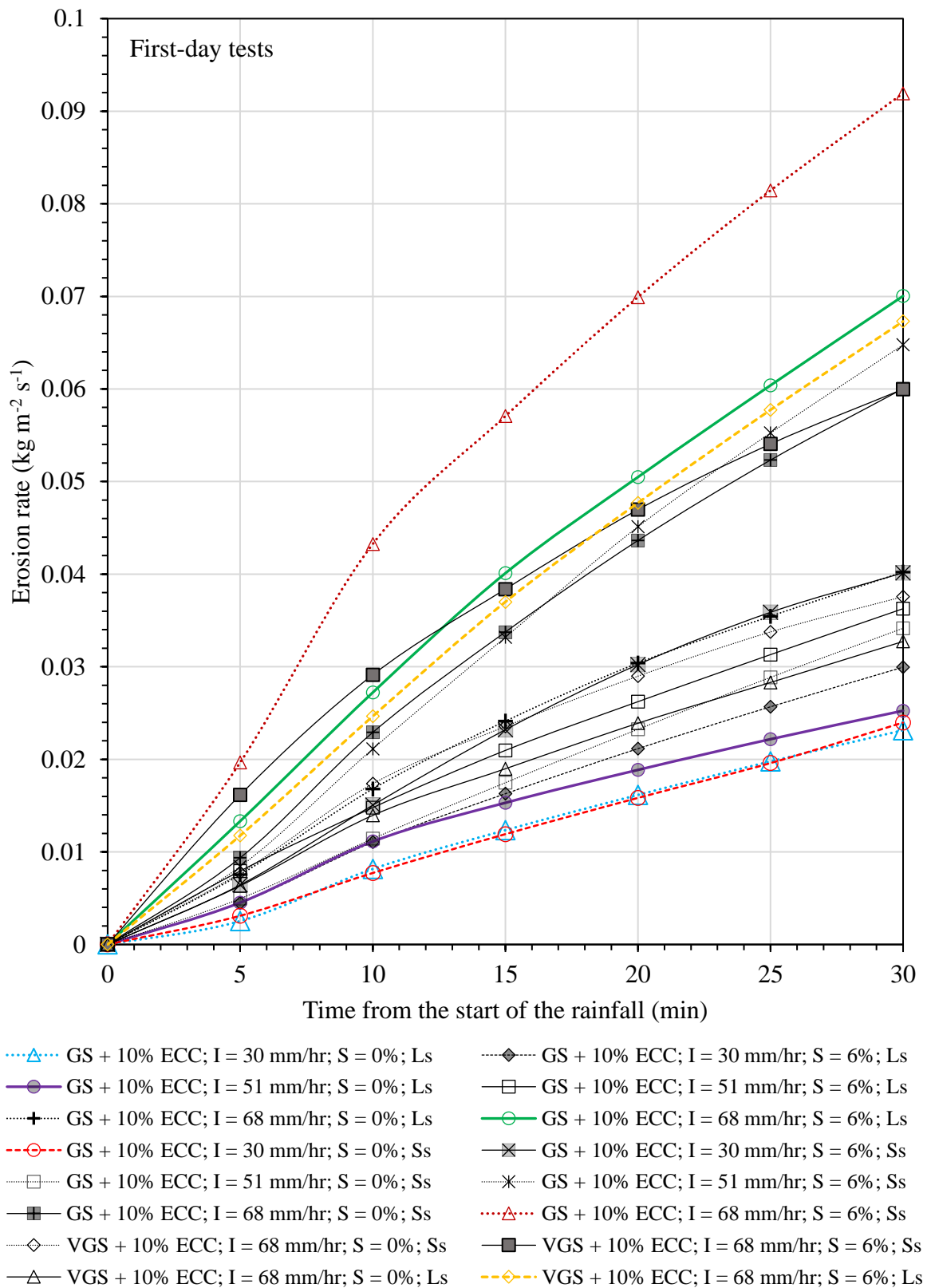


Figure 4. 28. Erosion rate from small- and large-scale first-day experiments for GS + 10% ECC and VGS + 10% ECC

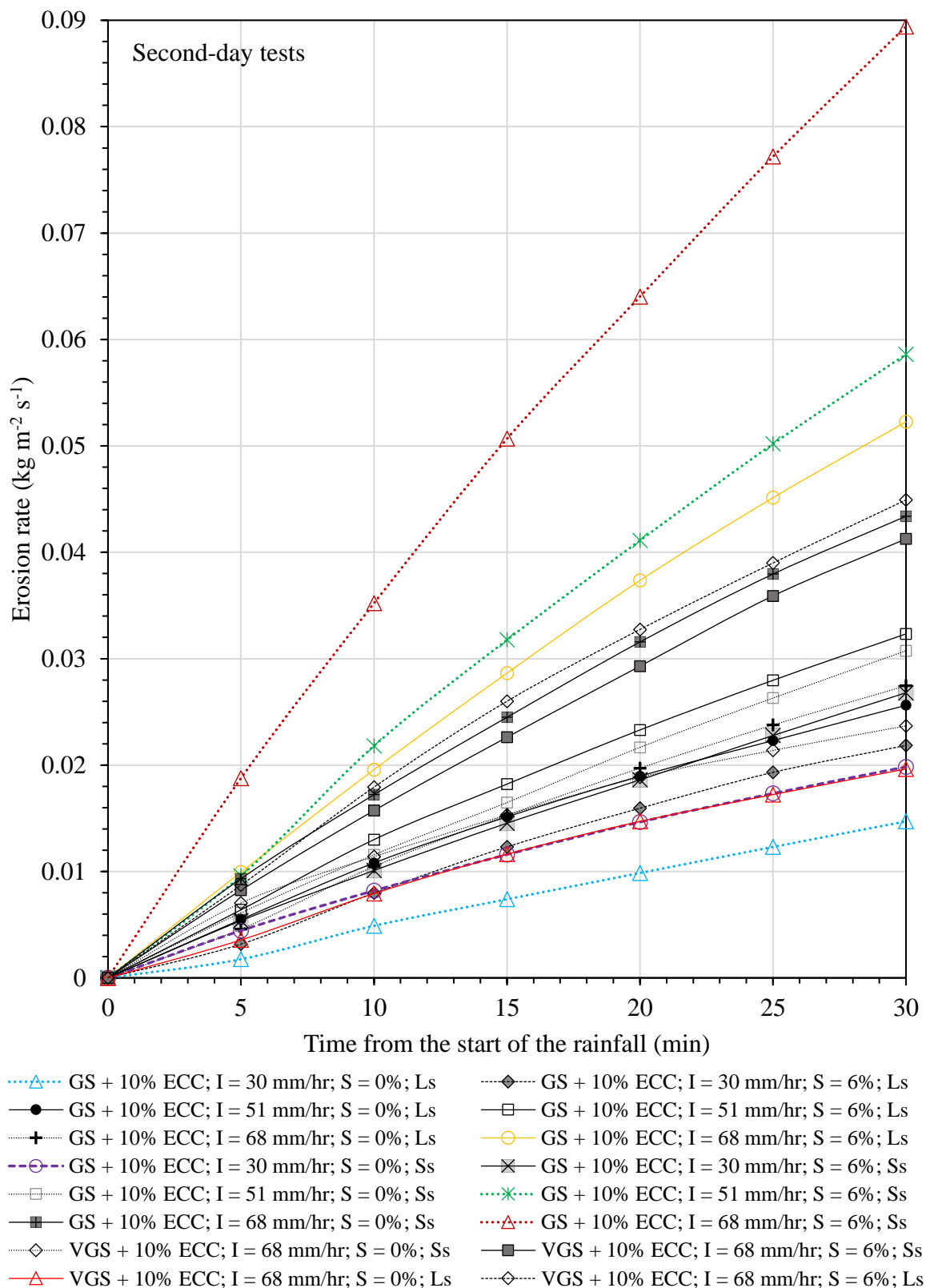


Figure 4. 29. Erosion rate from small- and large-scale second-day experiments for GS + 10% ECC and VGS + 10% ECC

#### 4.11.4. Erosion Rate for GS and VGS mixed with 5% ECC

The soils containing 5% ECC eroded significantly due to less clay content. For the first-day tests, erosion rates were higher from the small-scale tests on: GS + 5% ECC and VGS + 5% ECC, using 68 at a 6% slope; and GS + 5% ECC, using 68 mm/hr at a 0% slope; eroding at 0.097 kg/m<sup>2</sup>/s, 0.079 kg/m<sup>2</sup>/s and 0.066 kg/m<sup>2</sup>/s, respectively. The other higher erosion rates were from the large-scale tests on: GS + 5% ECC and VGS + 5% ECC, using 68 mm/hr at a 6% slope, reaching 0.084 kg/m<sup>2</sup>/s and 0.08 kg/m<sup>2</sup>/s, respectively. Higher rainfall intensities and greater slope gradients were the main causes for higher erosion rates. The lowest erosion rate was from the small-scale test on GS + 5% ECC tested using 30 mm/hr at a 0% slope reaching 0.029 kg/m<sup>2</sup>/s. Other lower erosion rates were from the large-scale tests on GS + 5% ECC using 30 mm/hr at a 0% and 6% slopes, GS + 5% ECC using 51 mm/hr at a 0% slope and VGS + 5% ECC using 68 mm/hr at a 0% reaching 0.017 kg/m<sup>2</sup>/s, 0.036 kg/m<sup>2</sup>/s, 0.037 kg/m<sup>2</sup>/s and 0.041 kg/m<sup>2</sup>/s, respectively. Lower rainfall intensities and slope gradients were the key causes for lower erosion rates. Detailed results are shown in Figure 4.30.

For second-day tests, higher erosion rates were obtained from the small-scale tests on: GS + 5% ECC using 68 at a 6% slope; GS + 5% ECC using 51 mm/hr at a 6% slope; and GS + 5% ECC using 68 mm/hr at a 0% slope; respectively at 0.095 kg/m<sup>2</sup>/s, 0.078 kg/m<sup>2</sup>/s and 0.057 kg/m<sup>2</sup>/s. Also, the erosion rates from the large-scale tests on: GS + 5% ECC and VGS + 5% ECC, using 68 mm/hr at a 6% slope; respectively at 0.058 kg/m<sup>2</sup>/s and 0.054 kg/m<sup>2</sup>/s. The lower erosion rates were from the large-scale tests on: GS + 5% ECC, tested using 30 mm/hr at 0% and 6% slopes; and VGS + 5% ECC, using 68 mm/hr at a 0% slope, respectively eroding at 0.01 kg/m<sup>2</sup>/s, 0.023 kg/m<sup>2</sup>/s and 0.03 kg/m<sup>2</sup>/s. Other lower erosion rates were from small-scale tests on: VGS + 5% ECC, using 68 mm/hr at a 0% slope and GS + 5% ECC, using 30 mm/hr at a 6% slope; respectively at 0.028 kg/m<sup>2</sup>/s and 0.029 kg/m<sup>2</sup>/s, as shown in Figure 4.31.

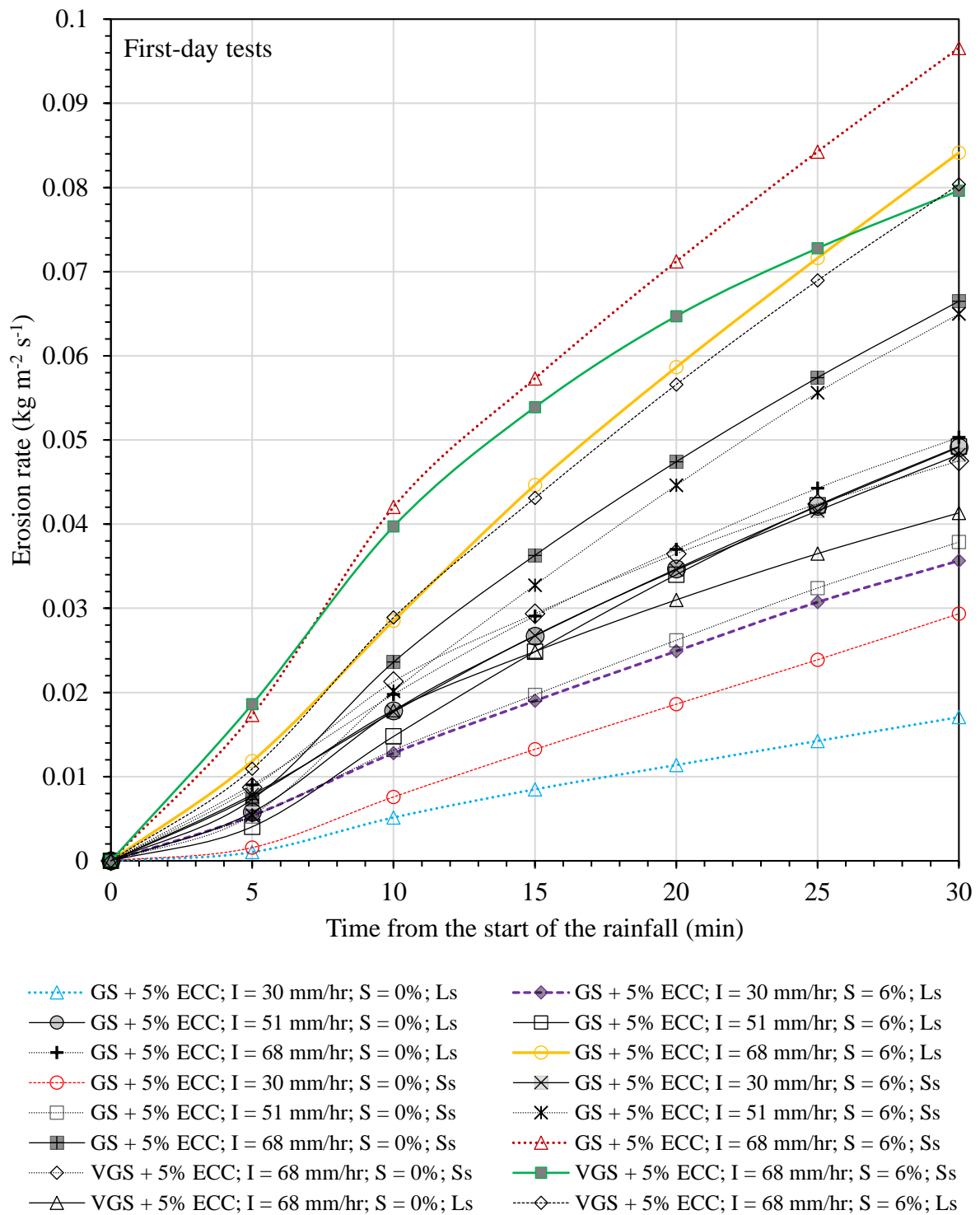
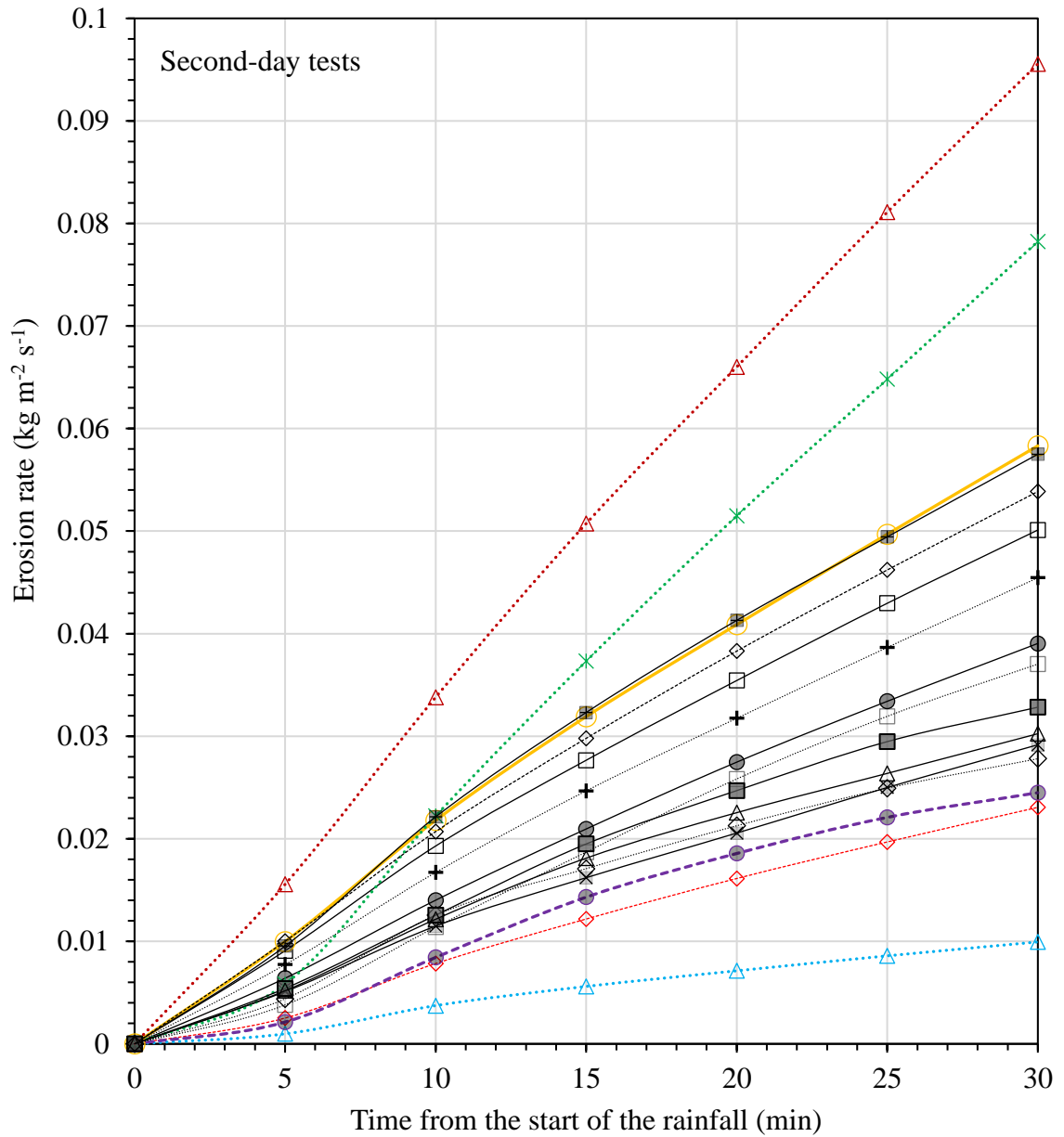


Figure 4. 30. Erosion rate from small- and large-scale second-day experiments for GS + 5% ECC and VGS + 5% ECC



- GS + 5% ECC; I = 30 mm/hr; S = 0%; Ls
- GS + 5% ECC; I = 51 mm/hr; S = 0%; Ls
- GS + 5% ECC; I = 68 mm/hr; S = 0%; Ls
- GS + 5% ECC; I = 30 mm/hr; S = 0%; Ss
- GS + 5% ECC; I = 51 mm/hr; S = 0%; Ss
- GS + 5% ECC; I = 68 mm/hr; S = 0%; Ss
- VGS + 5% ECC; I = 68 mm/hr; S = 0%; Ss
- VGS + 5% ECC; I = 68 mm/hr; S = 0%; Ls
- GS + 5% ECC; I = 30 mm/hr; S = 6%; Ls
- GS + 5% ECC; I = 51 mm/hr; S = 6%; Ls
- GS + 5% ECC; I = 68 mm/hr; S = 6%; Ls
- GS + 5% ECC; I = 30 mm/hr; S = 6%; Ss
- GS + 5% ECC; I = 51 mm/hr; S = 6%; Ss
- GS + 5% ECC; I = 68 mm/hr; S = 6%; Ss
- VGS + 5% ECC; I = 68 mm/hr; S = 6%; Ss
- VGS + 5% ECC; I = 68 mm/hr; S = 6%; Ls

Figure 4. 31. Erosion rate from small- and large-scale second-day experiments for GS + 5% ECC and VGS + 5% ECC

#### 4.11.5. Erosion Rate for GS and VGS mixed with 0% ECC

These soils were with highest amount of eroded soils, thus, with the highest erosion rates. The main cause for this was that the soils did not have some clay content, therefore, there was no cohesion to improve binding forces between particles, which would lead to greater resistance to erosive stresses. The erosion rates' results showed that for the first-day tests, they were higher for the small-scale tests on: GS + 0% ECC using 68 mm/hr at a 6% slope; VGS + 0% ECC using 68 mm/hr at a 6% slope; GS + 0% ECC using 51 mm/hr at a 6% slope; and GS + 0% ECC using 68 mm/hr at a 0% slope. These reached 0.105 kg/m<sup>2</sup>/s, 0.094 kg/m<sup>2</sup>/s, 0.069 kg/m<sup>2</sup>/s and 0.067 kg/m<sup>2</sup>/s, respectively. Also, a large-scale test on GS + 0% ECC using 68 mm/hr at a 6% achieved 0.077 kg/m<sup>2</sup>/s. The main causes for the higher erosion were higher rainfall intensities and greater slope gradients. Furthermore, the lower erosion rates were from the large-scale tests on GS + 0% ECC tested using 30 mm/hr at 0% and 6% slopes, and VGS + 0% ECC using 68 mm/hr at a 6% slope; and small-scale tests on GS + 0% ECC using 30 mm/hr and 51 mm/hr at a 0% slope. The erosion rates were 0.027 kg/m<sup>2</sup>/s, 0.041 kg/m<sup>2</sup>/s, 0.043 kg/m<sup>2</sup>/s, 0.033 kg/m<sup>2</sup>/s and 0.051 kg/m<sup>2</sup>/s respectively. Contrary to the soils with higher clay contents, the lines of the erosion rates showed concavity around five minutes from the start of the rainfall due to higher infiltration which caused less erosion. Detailed results are shown in Figure 4.32.

For the second-day tests, the higher erosion rates were from the small-scale tests on GS + 0% ECC using 68 mm/hr at 6% and 0% slopes, GS + 0% ECC using 51 mm/hr at 6% and 0% slopes, and a large-scale test on GS + 0% ECC using 68 mm/hr at a 6% slope. These were respectively 0.1 kg/m<sup>2</sup>/s, 0.081 kg/m<sup>2</sup>/s, 0.068 kg/m<sup>2</sup>/s, 0.056 kg/m<sup>2</sup>/s and 0.065 kg/m<sup>2</sup>/s. Similarly, lower erosion rates came from the small-scale tests on VGS + 0% ECC using 68 mm/hr at 0% and 6% slopes, and from the large-scale tests on GS + 0% ECC using 30 mm/hr at 0% and 6% slopes, and on VGS + 0% ECC using 68 mm/hr at a 6% slope; resulting in 0.014

kg/m<sup>2</sup>/s, 0.026 kg/m<sup>2</sup>/s, 0.018 kg/m<sup>2</sup>/s, 0.03 kg/m<sup>2</sup>/s and 0.033 kg/m<sup>2</sup>/s, respectively. As with the first-day tests, and for the same reasons, the lines of the erosion rates show concavity after around five minutes of the rainfall. Detailed results are shown in Figure 4.33.

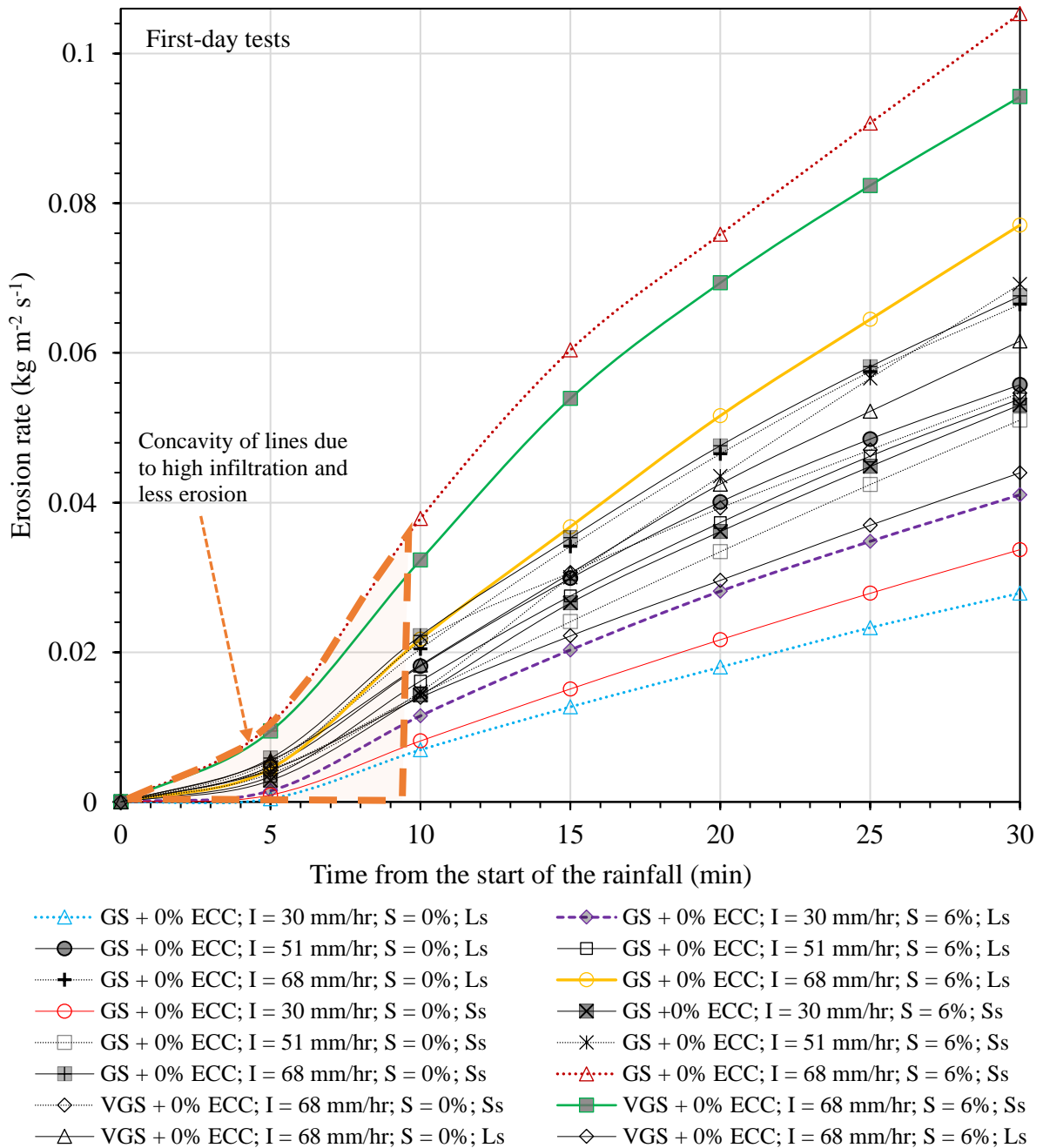
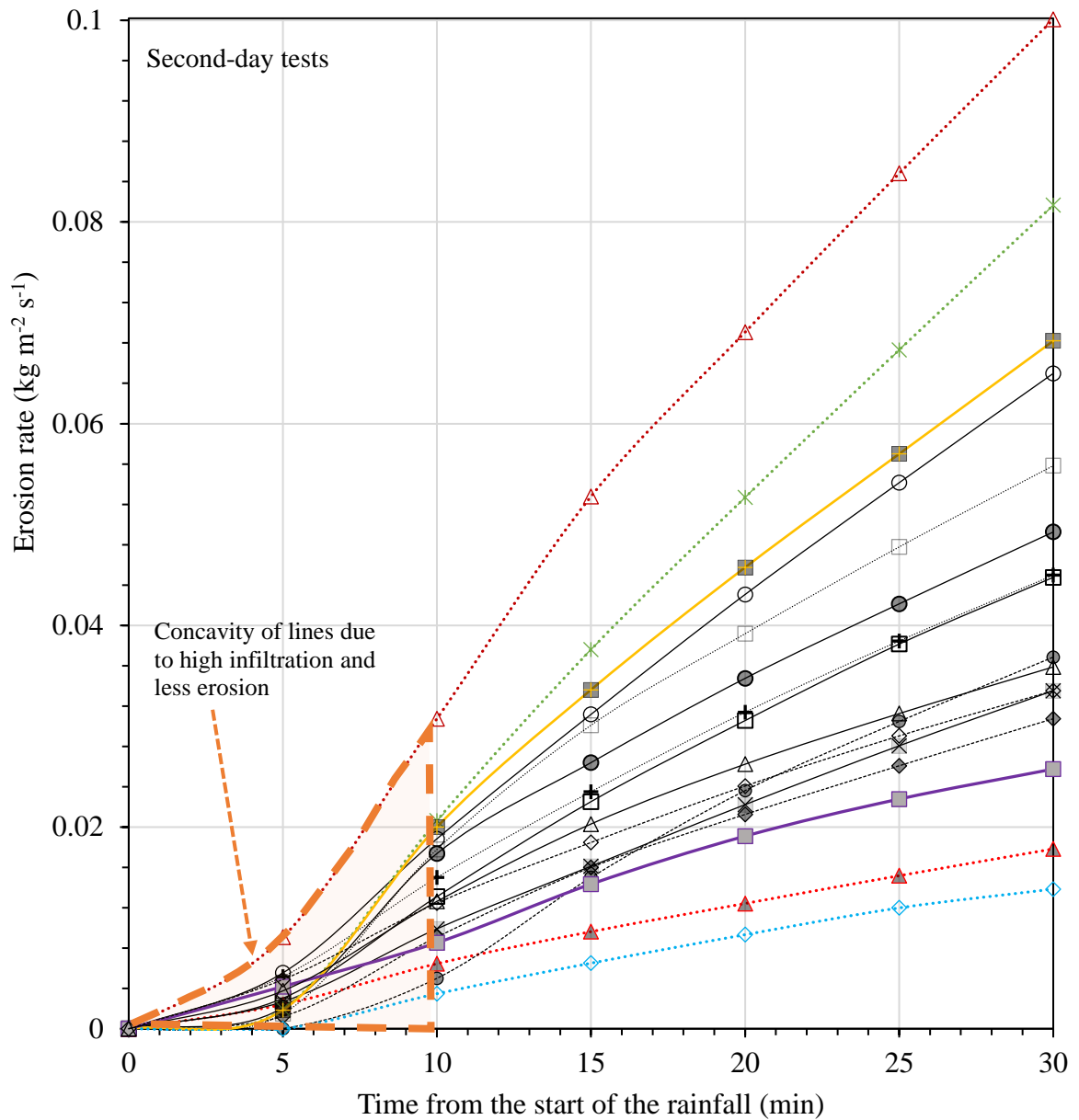


Figure 4. 32. Erosion rate from small- and large-scale first-day experiments for GS + 0% ECC and VGS + 0% ECC



- GS + 0% ECC; I = 30 mm/hr; S = 0%; Ls
- GS + 0% ECC; I = 51 mm/hr; S = 0%; Ls
- GS + 0% ECC; I = 68 mm/hr; S = 0%; Ls
- GS + 0% ECC; I = 30 mm/hr; S = 0%; Ss
- GS + 0% ECC; I = 51 mm/hr; S = 0%; Ss
- GS + 0% ECC; I = 68 mm/hr; S = 0%; Ss
- ◇ VGS + 0% ECC; I = 68 mm/hr; S = 0%; Ss
- △ VGS + 0% ECC; I = 68 mm/hr; S = 0%; Ls
- ◇ GS + 0% ECC; I = 30 mm/hr; S = 6%; Ls
- GS + 0% ECC; I = 51 mm/hr; S = 6%; Ls
- GS + 0% ECC; I = 68 mm/hr; S = 6%; Ls
- × GS + 0% ECC; I = 30 mm/hr; S = 6%; Ss
- ◇ GS + 0% ECC; I = 51 mm/hr; S = 6%; Ss
- △ GS + 0% ECC; I = 68 mm/hr; S = 6%; Ss
- ◇ VGS + 0% ECC; I = 68 mm/hr; S = 6%; Ss
- ◇ VGS + 0% ECC; I = 68 mm/hr; S = 6%; Ls

Figure 4. 33. Erosion rate from small- and large-scale second-day experiments for GS + 0% ECC and VGS + 0% ECC

#### 4.11.6. Erosion Rate for Subbase

The subbase soil significantly resisted detachment due to both raindrops and subsequent flow, and thus showed the smallest erosion rates. For the first-day tests, the higher erosion rates were from the large-scale tests using 68 mm/hr at a 6% slope, 30 mm/hr at a 6% slope, 68 mm/hr at a 0% slope, and 51 mm/hr at a 6% slope. These were respectively 0.0089 kg/m<sup>2</sup>/s, 0.0083 kg/m<sup>2</sup>/s, 0.008 kg/m<sup>2</sup>/s and 0.0074 kg/m<sup>2</sup>/s. Also, the lower erosion rates were from the small-scale tests using 30 mm/hr at 6% and 0% slopes, using 68 mm/hr at a 0% slope, and 51 mm/hr at a 6% slope with respectively 0.0025 kg/m<sup>2</sup>/s, 0.0027 kg/m<sup>2</sup>/s, 0.0031 kg/m<sup>2</sup>/s and 0.0032 kg/m<sup>2</sup>/s. Details are shown in Figure 4.34.

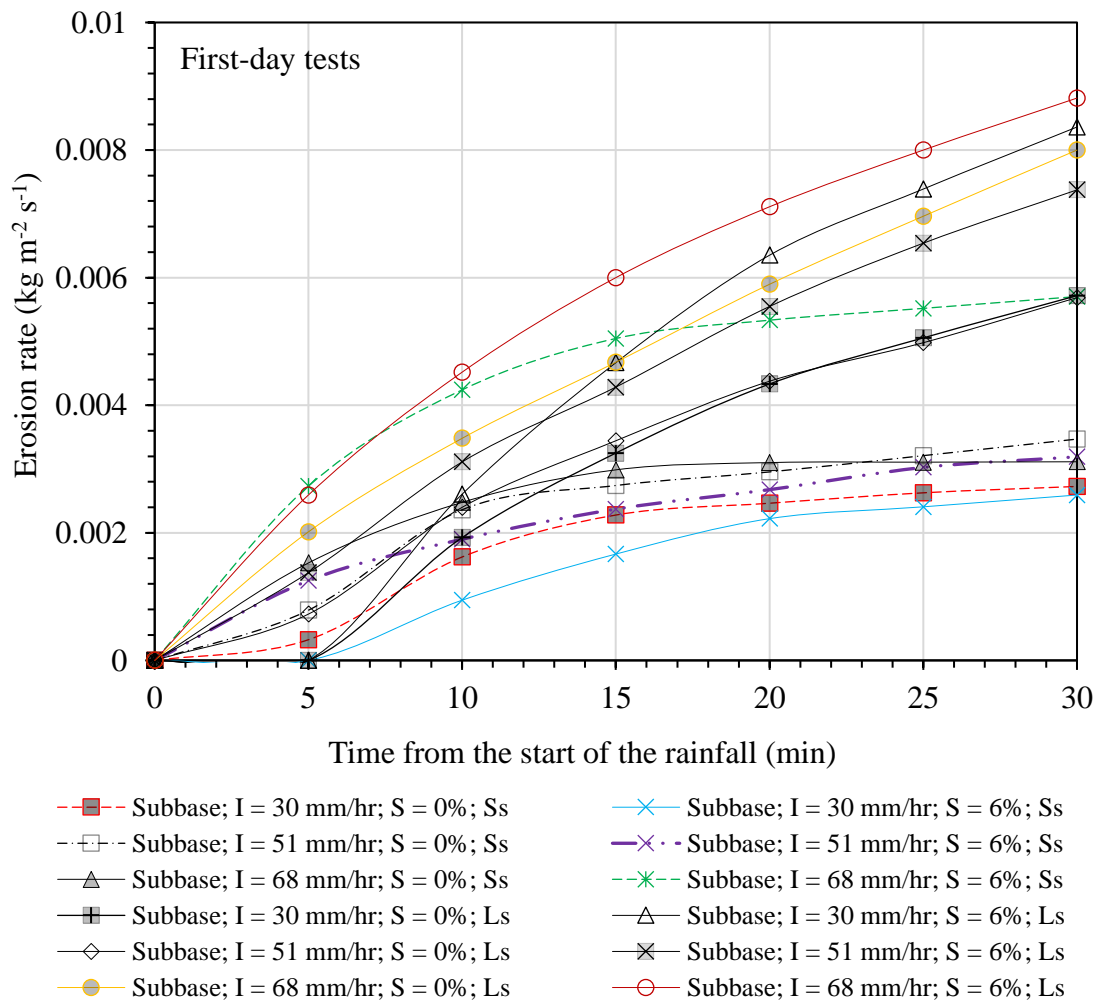


Figure 4. 34. Erosion rate from small- and large-scale first-day experiments for subbase

On the other hand, the higher erosion rates for the second-day tests on the subbase were obtained from the large-scale tests using 68 mm/hr at 6% and 0% slopes reaching 0.0088 kg/m<sup>2</sup>/s and 0.0064 kg/m<sup>2</sup>/s, respectively. Furthermore, the lower erosion rates were from the small-scale test using 68 mm/hr at a 6% slope and from the large-scale test using 51 mm/hr at 0% and 6% slopes resulting in 0.0008 kg/m<sup>2</sup>/s, 0.0036 kg/m<sup>2</sup>/s, and 0.0055 kg/m<sup>2</sup>/s, respectively. Detailed results are shown in Figure 4.35.

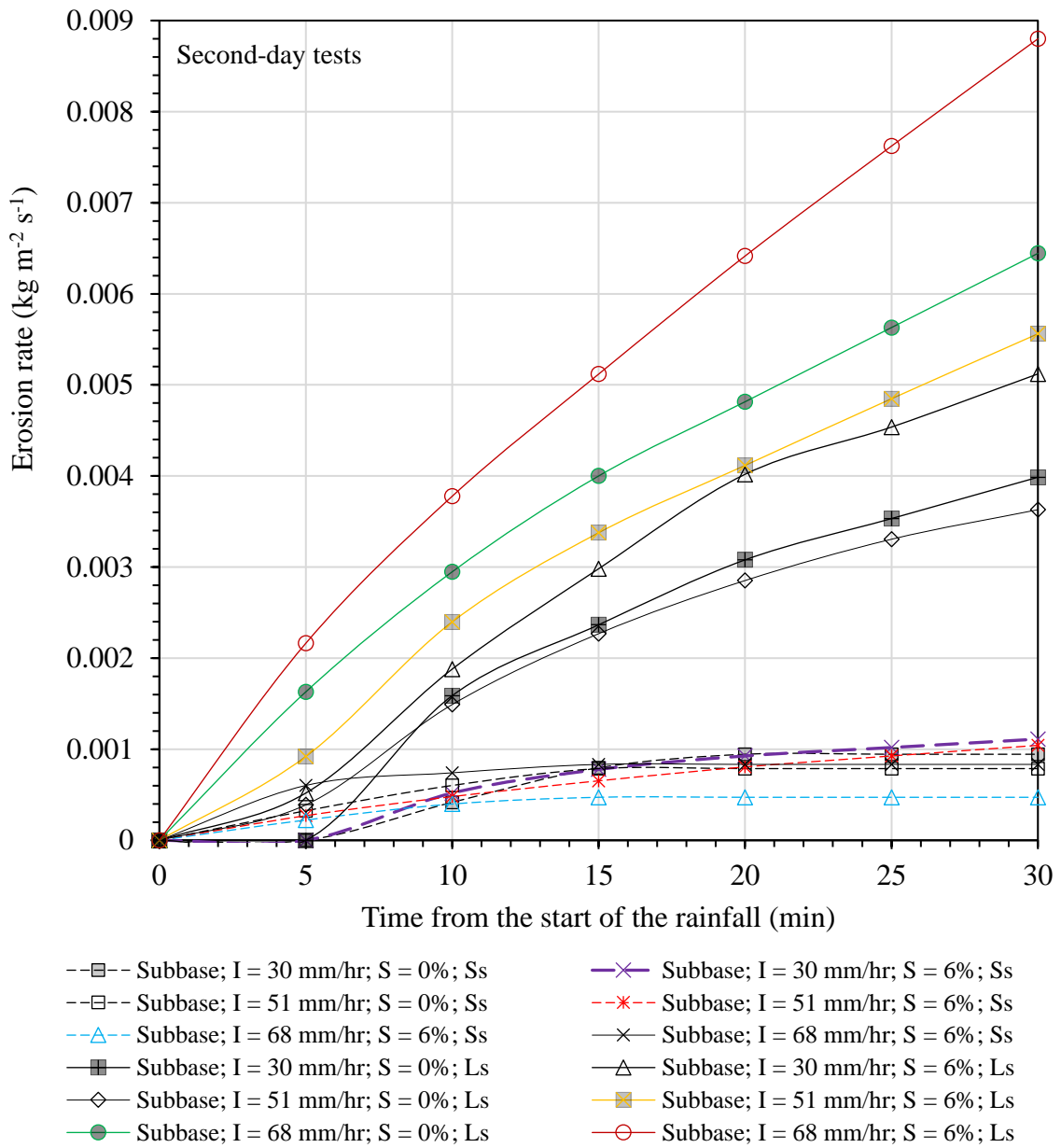


Figure 4. 35. Erosion rate from small- and large-scale first-day experiments for subbase

#### 4.12. Eroded Soil Materials Particle Size Distribution Changes

The erodibility tests showed that the particle size distribution of the eroded soils increased with the increasing time of the rainfall. Figure 4.36 shows that the sediment collected after the first 5 min of the rainfall plotted to the left of the control soil; while the sediment collected at 30 min plotted to the right of the control GS + 5% ECC soil tested with 30 mm/hr at a 0% slope. This showed that finer particles erode faster than coarser granular particles (Salles et al., 2000).

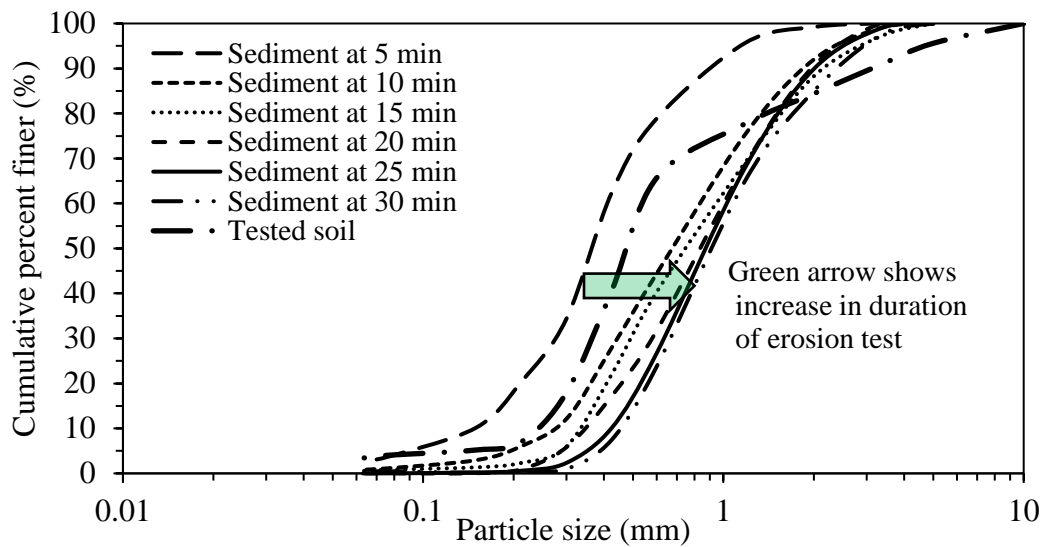


Figure 4. 36. PSD of the sediment from a GS + 5% ECC soil (Ngezahayo et al., 2019a, e)

Based on the trend of erodibility in Figure 4.36, envelopes for soils eroded for every ten minutes of the rainfall were plotted for soils containing up to 20% ECC. The envelopes are shown in Figure 4.37 and Figure 4.38 respectively for the first- and second-day tests. For the first-day erodibility tests, the envelope for soils eroded in the first 10 min plotted to the left; while the envelope for soils eroded in the last 10 min plotted to the right. Between the two envelopes, there is an envelope for soils eroded between 10 and 20 min. The  $D_{50}$  of the eroded soils ranged from about 0.15 mm to 0.3 mm in the first 10 min, 0.3 mm to 0.42 mm in the second 10 min; and 0.42 mm to 0.55 mm in the last 10 min of the erodibility tests, as shown in Figure 4.37. The smaller  $D_{50}$  in the first 10 min shows that the smaller particles eroded faster than larger particles.

For the second-day erodibility tests, the  $D_{50}$  of the eroded material ranged from about 0.23 mm to 0.36 mm in the first 10 min; 0.36 mm to 0.5 mm in the second 10 min; and 0.5 mm to 0.75 mm in the last 10 min of the erodibility tests, as shown in Figure 4.38. Expectedly, the  $D_{50}$  ranges show that generally larger soil particles were eroded during the second-day erodibility tests due to the smaller particles being eroded by the first-day rainfall events. Figure 4.38 shows that the 10 to 20 min and the 20 to 30 min envelopes tend to mix up in the bottom right hand for the particles smaller than 0.2 mm; which can be due to the particles detached and splashed on the walls of the testing box, and joining the flow later due to gravity and/or further splashes. In the first-day tests, particles were more bound by clay particles and eroded together in a more turbid flow. The second-day tests' flow was clearer due to the reduced surface clay content, and smaller sand-sized particles, which were seen splashed by raindrops or floating into the flow.

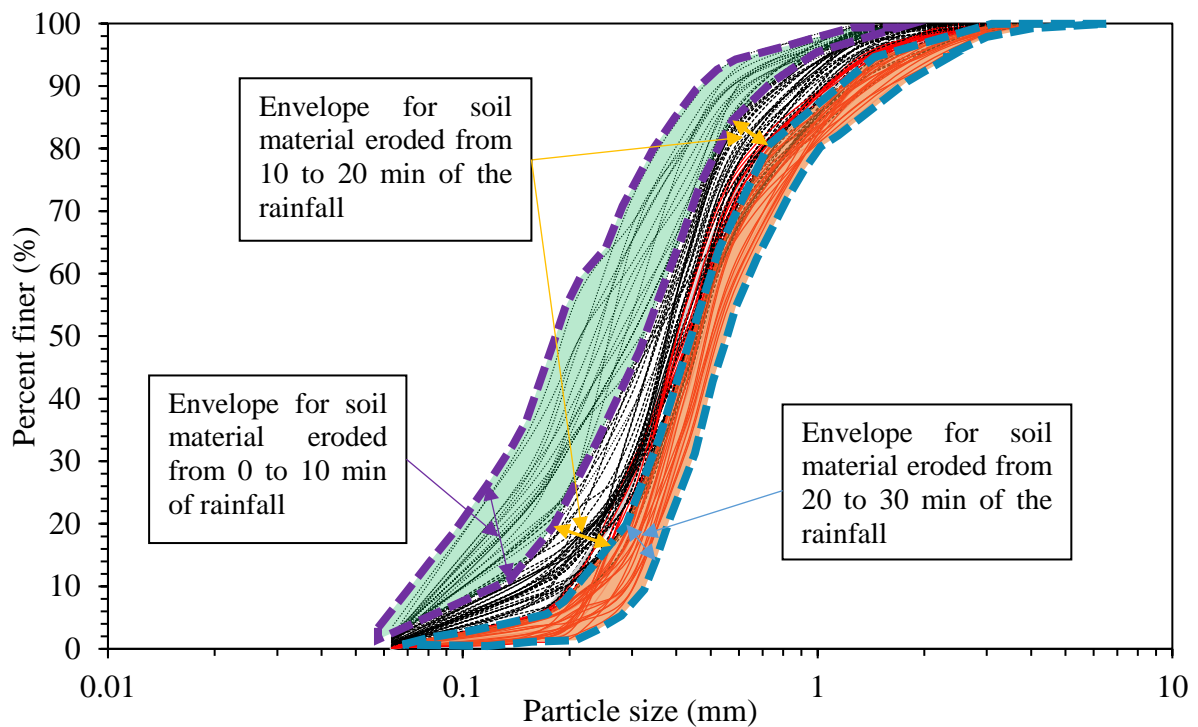


Figure 4. 37. PSD and envelopes for the sediment eroded from 0 to 30 min of the rainfall for the first-day erosion experiments

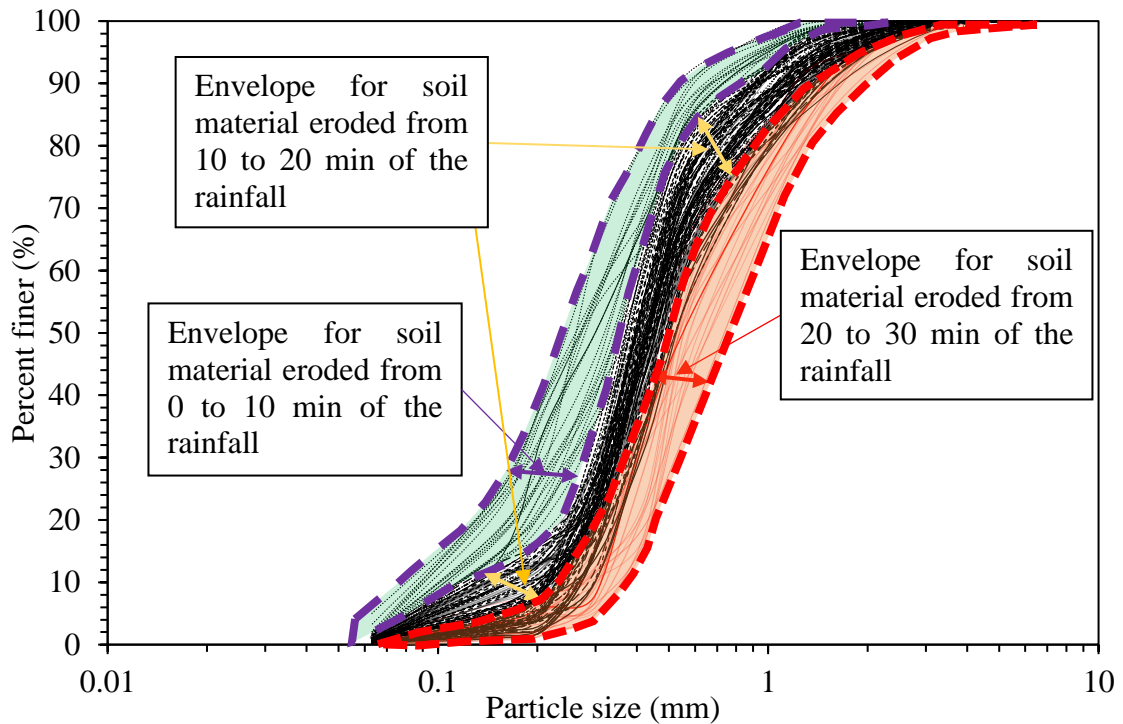


Figure 4. 38. PSD and envelopes for the sediment eroded from 0 to 30 min of the rainfall for the second-day erosion experiments

#### 4.13. Surface Particle Size Changes

As described in section 3.11, ImageJ software was used to analyse photographs taken during the erodibility tests. It was shown that the size of the particles at the surface increased as their number reduced with the increased duration of the rainfall. Using erodibility tests on GS + 5% ECC using a 30 mm/hr rainfall intensity, the photographs taken at the 10<sup>th</sup> min and 25<sup>th</sup> min were analysed for a 20 cm x 20 cm square in the middle of the tested soil surface. The number of particles reduced from 18,554 to 5,803 between the 10<sup>th</sup> and the 25<sup>th</sup> min of the rainfall as shown in Figures 4.39 and 4.40.

Figure 4.39 shows that at the 10<sup>th</sup> min, more particles were smaller than the biggest sand size (2 mm), as indicated by the darkness caused by the packing together of the particles. Only three particles were greater than 6 mm, including the biggest particle which was 7 mm. On the other

hand, Figure 4.40 shows that at the 25<sup>th</sup> min, the number of particles smaller than 2 mm reduced, as shown by the reduced darkness caused by the packing together of the particles. The particles greater than 6 mm increased to thirty-six, including the biggest particle which was 9.6 mm. During this time, the D<sub>50</sub> of the surface particles increased from 1.6 mm to 2.9 mm. This confirmed that smaller particles eroded before larger particles, which agreed with the particle size distribution of the eroded soil materials, as shown in Figures 4.37 and 4.38. Due to the large number of photographs, only the photographs from large-scale, first-day experiments are analysed as they were deemed enough to provide information on the surface particle changes.

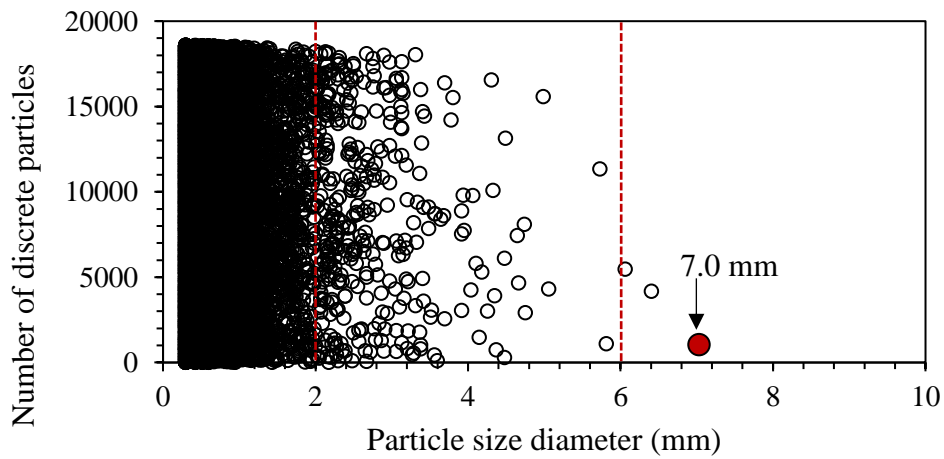


Figure 4. 39. Surface particle size analysis during erodibility test at 10<sup>th</sup> min of rainfall

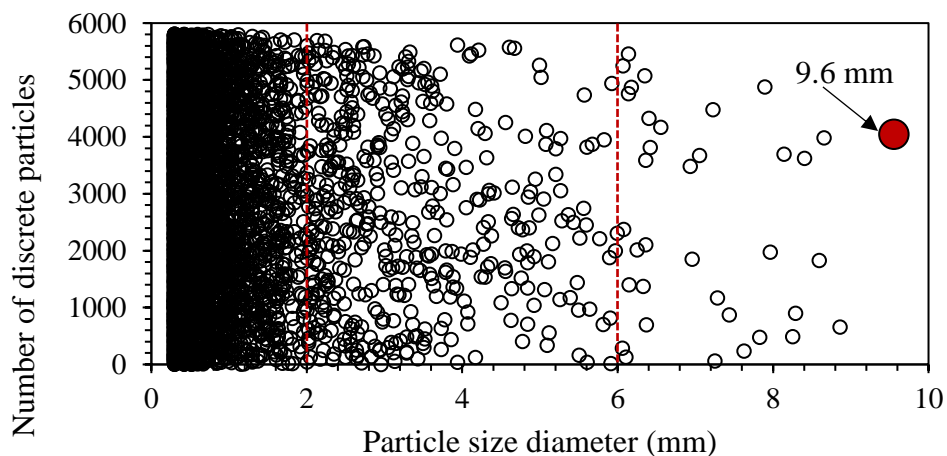


Figure 4. 40. Surface particle size analysis during erodibility test at 25<sup>th</sup> min of rainfall

#### 4.13.1. Surface Particle Size Changes Due to a 30 mm/hr Rainfall on GS + ECC mixes

The data from the ImageJ analysis of a 20 cm x 20 cm portion of the photographs (in the centre of the samples) shows that the number of particles at the surface reduced from about 27000, 24500, 23000, 21000 and 18000 particles before rainfall to about 8083, 7078, 6682, 5670 and 4671 after 30 min of rainfall respectively for GS + 20% ECC, GS + 15% ECC, GS + 10% ECC, GS + 5% ECC and GS + 0% ECC. On the other hand, the  $D_{50}$  increased from about 0.4 mm, 0.44 mm, 0.46 mm, 0.5 mm and 0.52 mm of diameter before rainfall to about 1.95 mm, 2.1 mm, 2.3 mm, 2.9 mm and 3.1 mm after 30 min of rainfall respectively for GS + 20% ECC, GS + 15% ECC, GS + 10% ECC, GS + 5% ECC and GS + 0% ECC, as shown in Figure 4.41.

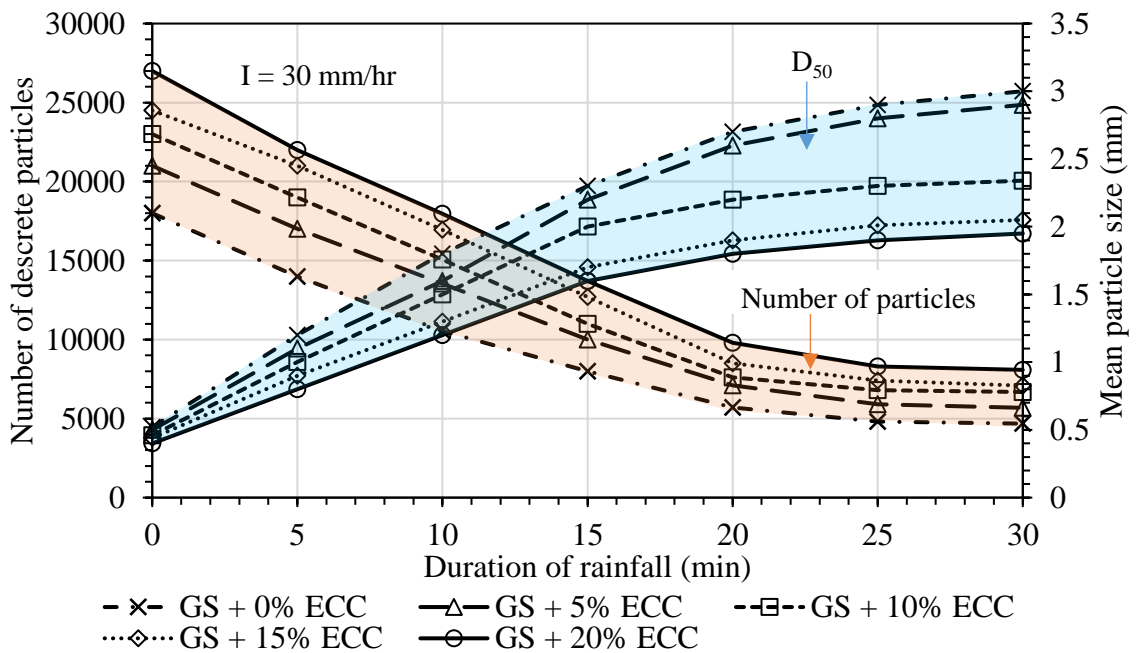


Figure 4. 41. Surface particles reduction and increase in  $D_{50}$  with increased 30 mm/hr rainfall duration for GS + ECC mixes based on image analysis

#### 4.13.2. Surface Particle Size Changes Due to a 51 mm/hr Rainfall on GS + ECC mixes

The data from the photographs analysis using ImageJ for a 20 cm x 20 cm portion of the samples shows that the number of surface particles reduced from about 26898, 24200, 22500, 21000 and 18200 before rainfall to about 7083, 6779, 6382, 5770 and 5671 after 30 min of rainfall,

respectively for GS + 20% ECC, GS + 15% ECC, GS + 10% ECC, GS + 5% ECC and GS + 0% ECC. Meanwhile, the  $D_{50}$  increased from about 0.4 mm, 0.44 mm, 0.46 mm, 0.5 mm and 0.52 mm to about 2.32 mm, 2.35 mm, 2.49 mm, 2.95 mm and 3.05 mm of diameter, respectively for GS + 20% ECC, GS + 15% ECC, GS + 10% ECC, GS + 5% ECC and GS + 0% ECC, as shown in Figure 4.42.

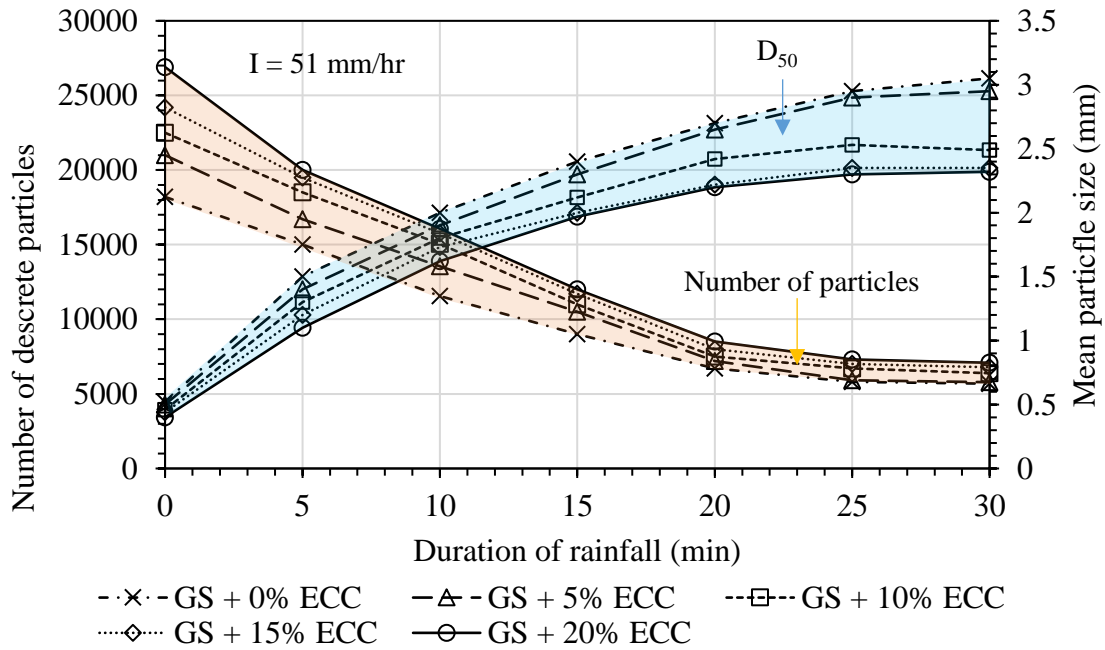


Figure 4. 42. Surface particles reduction and increase in  $D_{50}$  with increased 51 mm/hr rainfall duration for GS + ECC mixes based on image analysis

#### 4.13.3. Surface Particle Size Changes Due to a 68 mm/hr Rainfall on GS + ECC mixes

The data from the ImageJ analysis of a 20 cm x 20 cm portion of the photographs shows that the number of particles at the surface reduced from about 26002, 24099, 22496, 22000 and 20198 particles before rainfall to about 8406, 8113, 7968, 7783 and 7434 after 30 min of rainfall respectively for GS + 20% ECC, GS + 15% ECC, GS + 10% ECC, GS + 5% ECC and GS + 0% ECC. Meanwhile, the  $D_{50}$  increased from about 0.4 mm, 0.44 mm, 0.46 mm, 0.5 mm and 0.52 mm of diameter to about 2.15 mm, 2.19 mm, 2.22 mm, 2.41 mm and 2.55 mm diameter, respectively for GS + 20% ECC, GS + 15% ECC, GS + 10% ECC, GS + 5% ECC and GS +

0% ECC. The  $D_{50}$  increase was rapid in the first 5 min due to the finer particles being eroded quickly and reduced gradually up to the end of the experiment, as shown in Figure 4.43.

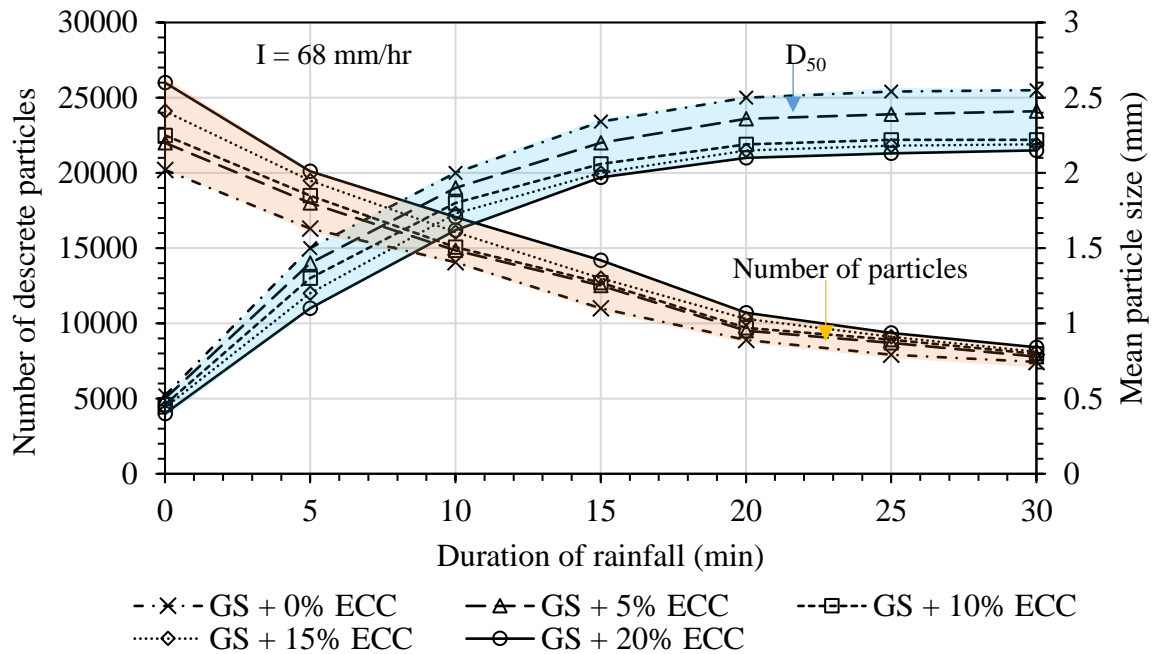


Figure 4. 43. Surface particles reduction and increase in  $D_{50}$  with increased 68 mm/hr rainfall duration for GS + ECC mixes based on image analysis

#### 4.13.4. Surface Particle Size Changes Due to a 68 mm/hr Rainfall on VGS mixes and Subbase

The data from the ImageJ analysis of a 20 cm x 20 cm portion of the photographs shows that the number of particles at the surface reduced from about 19333, 18100, 17999, 16012 and 15196 particles before rainfall to about 9823, 8512, 8479, 7778 and 6867 after 30 min of rainfall respectively for VGS + 20% ECC, VGS + 15% ECC, VGS + 10% ECC, VGS + 5% ECC and VGS + 0% ECC. Unlike with the GS + ECC mixes, there was a slow decrease of the number of particles between consecutive times of the photographs being taken. This was due to the ability of the larger particles of the VGS mixes to resist the raindrops' kinetic energy. This ability of the larger particles was highlighted more in the experiments on the subbase, as the surface particles reduced only from about 3814 to 2181 particles, which was the smallest reduction observed in all the tests. In contrast, the  $D_{50}$  increased from about 0.8 mm, 0.9 mm,

1.1 mm, 1.6 mm, and 1.2 mm of diameter before rainfall to about 1.95 mm, 2.1 mm, 2.3 mm, 2.9 mm and 3.1 mm after 30 min of rainfall respectively for VGS + 20% ECC, VGS + 15% ECC, VGS + 10% ECC, VGS + 5% ECC and VGS + 0% ECC. The  $D_{50}$  for the subbase increased from about 6.4 mm to about 7.2 mm, which was the smallest change observed in all the tests. No change of the  $D_{50}$  occurred after 20 min of rainfall, as shown in Figure 4.44.

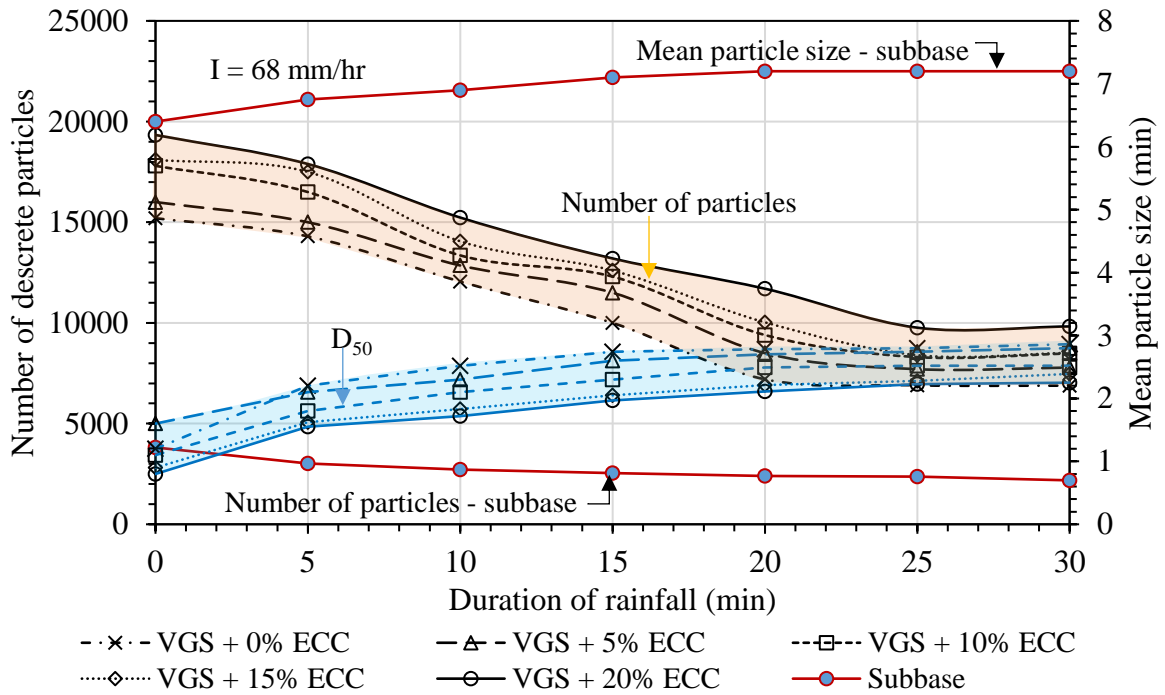


Figure 4. 44. Surface particles reduction and increase in  $D_{50}$  with increased 68 mm/hr rainfall duration for VGS + ECC mixes and subbase based on image analysis

#### 4.14. Runoff Coefficients

According to Thomas (2017), the runoff coefficient helps to transform rainfall into surface flow. Subsequently, the runoff coefficient mainly depends on rainfall intensity, porosity, surface level of compaction, degree of saturation and slope gradients. The magnitude of the runoff coefficient ranges from 0 to 1 respectively for very loose surfaces that allow all the rainfall to infiltrate to very dense surfaces and be converted into runoff. The runoff coefficients for compacted road

surfaces range from 0.7 to 0.95 (Mutreja, 1990; Karamage et al., 2017; Thomas, 2017). The rational method relationship was used to estimate the runoff coefficient (Thomas, 2017):

$$C_{\text{run}} = \frac{Q}{IA} \quad (\text{Eq. 4.9})$$

where  $C_{\text{run}}$  is the dimensionless runoff coefficient,  $Q$  is the discharge rate (l/s),  $I$  is the rainfall intensity in (l/s.m<sup>2</sup>) and  $A$  is area of the tested surface (m<sup>2</sup>). The estimated runoff coefficients added more understanding of the behaviour of particles at the surface of the tested soils with respect to the rainfall intensities used in this study.

#### 4.14.1. Influence of Various Rainfall Events on Runoff Coefficients

Using Eq. 4.9, it was found that runoff coefficients increased with the increase of rainfall intensity, which agrees with Mu et al., 2015. As shown in Figure 4.45, runoff coefficients were greater for 68 mm/hr rainfall intensity and smaller for 30 mm/hr rainfall intensity for the same soil type. These coefficients reduced with the reduction of clay content due to increased infiltration rate. For example, for the first-day experiments, the runoff coefficients on GS + 20% ECC at a 6% slope gradient were about 0.91, 0.87 and 0.84 for 68 mm/hr, 51 mm/hr and 30 mm/hr respectively. For the same slope gradient of 6%, the runoff coefficients reduced to about 0.79, 0.76 and 0.70 for GS + 10% ECC, and 0.71, 0.68 and 0.67 for GS + 5% ECC, respectively for 68 mm/hr, 51 mm/hr and 30 mm/hr rainfall intensities. Furthermore, the higher slope gradients increase the runoff coefficients due to increased flow velocity, hence reduced infiltration (Mu et al., 2015; Karamage et al., 2017). For example, for the first-day experiments on GS + 20% ECC, the runoff coefficients at a 6% slope were 0.91, 0.87 and 0.84 for 68 mm/hr, 51 mm/hr and 30 mm/hr respectively, and reduced to about 0.89, 0.84 and 0.8 at a 0% slope. Similarly for the same order of rainfall intensities, these reduced from about 0.79, 0.76 and 0.7 at 6% to about 0.76, 0.74 and 0.7 at 0% for GS + 10% ECC.

The coefficients of runoff were higher for the first-day than for the second-day erodibility tests due to reduced surface cohesion caused by the erosion of the finer particles by the first-day rainfall events, leading to increased infiltration and reduced thickness of the flow. Mu et al. (2015) reported that runoff coefficients reduce with rainfall duration and repeated rainfall events. For the first-day tests on GS + 20% ECC, the runoff coefficients at the 6% slope were about 0.91, 0.87 and 0.84 for 68 mm/hr, 51 mm/hr and 30 mm/hr respectively and reduced to about 0.89, 0.84 and 0.80 for the second-day tests. Similarly for the same rainfall intensities, the runoff coefficients which were about 0.79, 0.76 and 0.70 at 6% reduced to about 0.77, 0.74 and 0.72 for GS + 10% ECC. These reduced from about 0.71, 0.68 and 0.67 at 6% to about 0.69, 0.66 and 0.64 at 0% for GS + 5% ECC. Detailed data is shown in Figure 4.45.

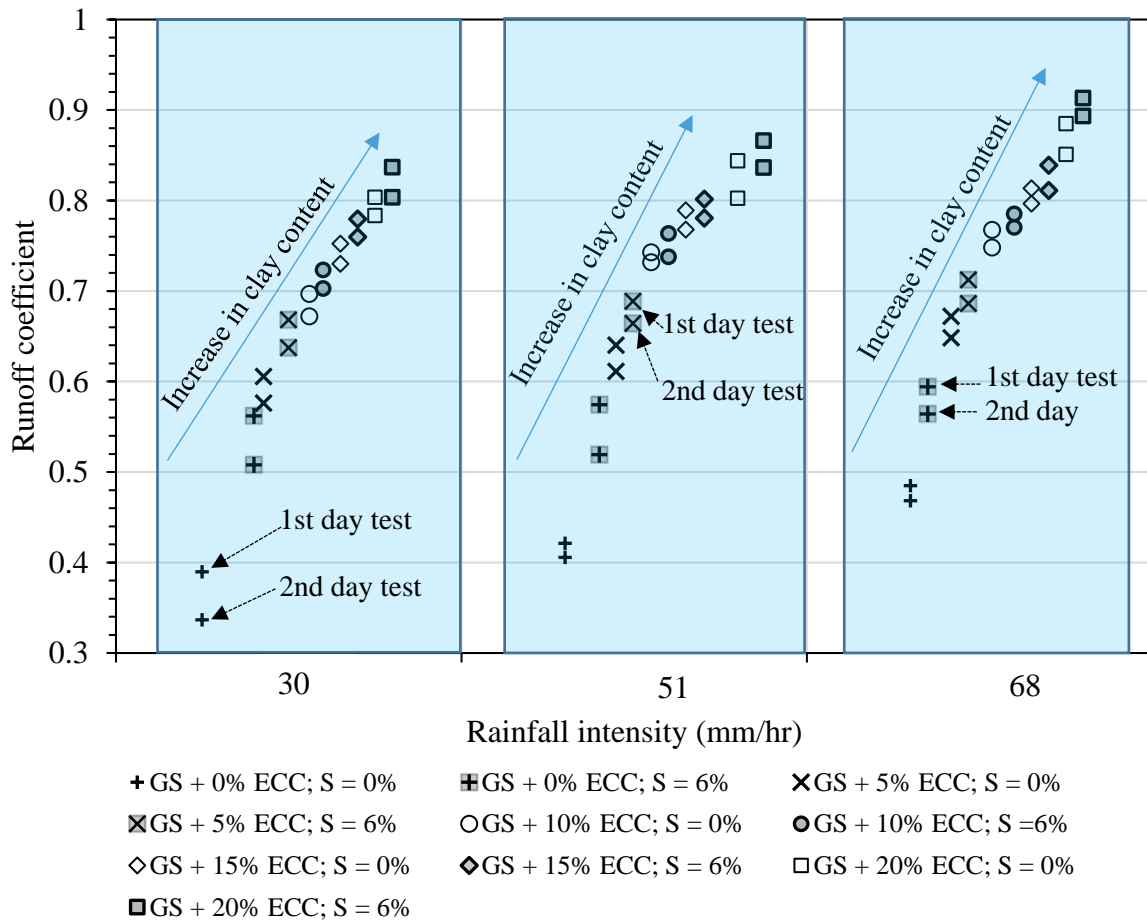


Figure 4. 45. Runoff coefficients, rainfall intensities and clay content

#### 4.15. Summary

The infiltration rate reduced with increases in ECC content. The results from the crumb and the double hydrometer tests proved that the selected soils ranged from non-dispersive to slightly dispersive, which may not pose any significant problems if used in the construction of unpaved roads. HET test showed that erosion rate reduced with increasing ECC content in samples. An efficient rainfall simulator was designed. It provided simulated rainfall energy of 193.5  $\mu\text{J}$ , 244  $\mu\text{J}$  and 301.1  $\mu\text{J}$  respectively for 30 mm/hr, 51 mm/hr and 68 mm/hr rainfall intensities. During rainfall erosion, there was lower moisture content in the lower layers of the sample containing higher ECC due to lessened infiltration. When plotted in the South African diagram of soils' performance in unpaved roads shown in Figure 4.6, five soils (GS, VGS, VGS + 5% ECC, VGS + 10% ECC and subbase) fell in the zone of corrugates and ravel; one soil (GS + 5% ECC) fell in the erodible zone; while the remaining five soils (GS + 10% to 20% ECC; VGS + 15% to 20% ECC) fell in the good zone. When plotted in the envelope of thresholds KE of raindrops and  $D_{50}$  of the soils, as shown in Figure 4.7, only the subbase was found non-detachable by target rainfall intensities. Sheet erosion tests showed that larger particles at the surface may cause erosion to expand over a wider area but shallowly while smaller particles may promote the formation of potholes in unpaved roads. The erosion damage for the tested soils was mainly located on the downslope due to increasing flow velocities with the increasing length of the bed slope, as shown in Figure 4.13. Furthermore, section 4.10 and its sub-sections give the results of the collected sediment; section 4.11 and its sub-sections shows the erosion rates from the tested soils; section 4.12 described the particle size distribution of the eroded soils; section 4.13 and its sub-sections described the changes in the number and the mean size of the particles at the surface during erodibility tests; while the section 4.14 gives the results on the estimated runoff coefficients during erodibility tests.

## 5. DISCUSSION

### 5.1. Introduction

This chapter contains the discussion of the results from laboratory tests to investigate the erodibility of soils in unpaved roads due to both rainfall and the subsequent flow. The purpose of this discussion is to have deep understanding about the parameters that accelerate erosion of unpaved roads' soils, and the ways to combat it so that these roads contribute effectively to the well-being of rural communities and to the achievement of the SDGs. An investigation was carried out using both small-scale and large-scale tests, as described in sections 3.8 and 3.9 respectively. Each of the tests was conducted for thirty minutes and for two successive days to assess the effect of repeated rainfall events on erodibility. The small-scale (Ss) and large-scale (Ls) experiments helped to assess the effect of the size of the soil testing boxes (scale factor) on erodibility. During the tests, data regarding the runoff (surface water) and sediment content was measured, and the change in the sizes of the particles exposed at the surface was estimated during rainfall events, as described in Chapter 3. Results have been presented in Chapter 4, while correlations between pertinent factors affecting erodibility are discussed in Chapter 6.

### 5.2. Erodibility Due to Simulated Rainfall

This part presents the discussion of the data for both small-and large-scale erodibility tests due to simulated rainfall. In section 5.2.1, the trends of erodibility (eroded soils) with respect to five-minute intervals of rainfall duration for both the first- and second-day erodibility tests are discussed. The erosion rate from the tested soils is discussed in section 5.2.2, with emphasis on the influence of parameters such as the clay content, the plasticity index and the maximum dry density of the tested soils on the erosion rate. The influence of the size of the soil testing box (scale factor) on the erosion rate is discussed herein. The section 5.3 discusses the behaviour of the eroded soil materials; section 5.4 discusses the behaviour of particles exposed at the surface

during erodibility tests, while section 5.5 discusses the effects of soil type ( $D_{50}$ , clay content, coefficient of uniformity, coefficient of gradation, percentage of fines, and maximum dry density), slope gradient, rainfall intensity, and rainfall events on runoff coefficients estimated during rainfall erosion.

#### 5.2.1. Eroded Soil Materials (Sediment) Collection

The simulated rainfall intensities of 30 mm/hr, 51 mm/hr and 68 mm/hr were used for all the experiments. The results for both small- and large-scale tests, first- and second-day rainfall events are discussed based on the amount of collected sediment during erodibility tests.

The results showed that soils tested at greater slope angles and higher rainfall intensities result in more sediment than soils tested at lower slope angles and rainfall intensities. In this study, the amount of eroded soils was generally smaller for a 0% slope gradient than for a 6% slope gradient; while it was always greater for a 12% slope gradient. This finding agrees with Petts et al. (2006), who argued that unpaved roads constructed at slope gradients smaller than 6% and with appropriate soils are not excessively eroded. For example, Cao et al. (2013) used simulated rainfall intensities ranging from 43.8 mm/hr to 142.2 mm/hr on a compacted silty loam road surface and found average erosion rates of about 0.00022 kg/m<sup>2</sup>/s, 0.00028 kg/m<sup>2</sup>/s and 0.00043 kg/m<sup>2</sup>/s; respectively for 10.5%, 17.6% and 26% slope gradients. Thus, the greater the slope, the higher the amount of eroded sediment and average erosion rate. Similarly, between 10.5% and 26.8% slopes, erosion rates ranged from 0.00015 kg/m<sup>2</sup>/s to 0.0025 kg/m<sup>2</sup>/s and 0.0002 kg/m<sup>2</sup>/s to 0.0004 kg/m<sup>2</sup>/s respectively for 43.8 mm/hr and 68.4 mm/hr. Also, the greater the rainfall intensity, the higher the erosion rate. Furthermore, Arnaez et al. (2007) studied erodibility of loamy soils with various gravel cover percentages using 30 min simulated rainfall intensities ranging from 30 mm/hr to 117.5 mm/hr on the test plots of about a 6.5%

slope. They reported increases of soil loss due to increasing rainfall intensity and proposed the following relationship between soil loss and rainfall intensity:

$$\text{Soil loss} = 0.668(R_i) - 11.98 \quad (\text{Eq. 5.1})$$

In this study, the average soil loss was related to the rainfall intensities by the following relation:

$$\text{Soil loss} = 24.01(R_i) + 205.16 \quad (\text{Eq. 5.2})$$

where  $R_i$  = rainfall intensity (mm/hr) and soil loss expressed in  $\text{g m}^{-2} \text{h}^{-1}$ .

From Eq. 5.1 and 5.2, the smaller soil loss reported by Arnaez et al. (2007) could be due to the lower antecedent moisture content of the field test plots (about 4.5%), and thus the higher strength of the soils when compared to the optimum moisture content ranging from 8.4% to 10.3% used in this study, as shown in Table 3.3. Also, the presence of surface gravel cover of about 13% not only resisted detachment due to both raindrops and surface flow stresses, but also increased the infiltration rate of the soils due to reduction of the flow velocities, hence reducing the erodibility of the soils tested by Arnaez et al. (2007).

The small-scale tests produced less sediment than the large-scale tests, which agrees with El-Swaify (1997) and Walling and Probst (1997). El-Swaify (1997) and Al-Madhhachi et al. (2013) said that soil loss increases with increasing shear stress due to surface flow, which is directly linked to the slope length, and that the erosion varies with slope length to the power 0.6. Walling and Probst (1997) modelled the soil loss from 70-m and 125-m silty loam slopes due to a 10 mm/hr natural rainfall intensity for 15 years. The slope gradients were about 35%. The soil loss from the 125-m slope ranged from 1.54 to 1.7 times the soil loss from the 70-m slope every year with an average of 1.6 times for 15 years.

For the tested soils, VGS + ECC mixes produced less sediment than GS + ECC mixes, which also agrees with the literature. Salles et al. (2000) used rainfall intensities ranging from 10 mm/hr to 140 mm/hr to study the detachment of sandy and silty loam soils. They concluded that for granular soils, the smaller the  $D_{50}$ , the higher the soil's detachment and erosion rate. The  $D_{50}$  values were smaller for GS + ECC mixes than for VGS + ECC mixes, as shown in Table 3.3; which justifies higher detachment of the former soils when the two are subjected to the same testing conditions. Furthermore, the erodibility increased with reduction in clay content, which also agrees with the literature (Carey and Simon, 1984; Salles et al., 2000; Briaud, 2008; Haghighi et al., 2013) and was due to a reduction of cohesion as clay content reduces. Knapen et al. (2007) said that when cohesion reduces, it becomes easier for both raindrops and shear stresses to detach discrete particles. Although the trends of erodibility by the findings of this study agree with the findings of the above mentioned researchers, it was not possible to directly compare the results of this study with the results of previous researches due to differences in the soils, slopes, rainfall intensities and other factors considered during investigations.

This study showed that erosion reduced with the second-day erodibility tests. This is normal in unpaved roads since the first rainfall events remove most of surface particles loosened by traffic passes during the dry season (Iverson, 1980; Ziegler et al., 2004; Foltz et al., 2008). However, the traffic was not considered in this laboratory investigation; thus, the reduction of erodibility could be due to the fact that smaller particles had been eroded by the first-day rainfall, leaving larger particles exposed at the surface. For the same rainfall intensities, slope length and gradient; larger surface particles of the second-day tests offered more resistance to the detachment due to raindrops and flow stresses. Those particles further promoted infiltration and for all these reasons reduced erosion.

### 5.2.2. Erosion Rate

Erosion rate is the measure of the amount of erosion that help to compare erodibility between different soils by relating the amount of eroded soils to the size of the eroded areas. To this fact, the results of erosion rate from erodibility tests on a variety of soils can help engineers to decide which soils are appropriate for both construction and maintenance of unpaved roads. Since these roads are severely deteriorated by surface water erosion (Paige-Green, 2006, 2008; Cao et al., 2009; Paige-Green et al., 2015; Ngezahayo et al., 2019a, b, f), appropriate soils for use in their construction must be less detachable by raindrops and surface flow. Results showed that erosion rate increased with increases in rainfall intensity. Moreover, effects of clay content and plasticity index, maximum dry density, slope length and particle size on erosion rate are discussed herein.

#### 5.2.2.1. Effect of ECC Content and Plasticity Index on Erosion Rate

The erosion rates estimated after 30 min of rainfall for all the slopes used, in the first- and second-day tests, and on small- and large-scale tests showed that for GS + ECC soils, the highest erosion rate was about 0.11 kg/m<sup>2</sup>/s for GS + 0% ECC ( $I_p = 0\%$ ); while the lowest was about 0.007 kg/m<sup>2</sup>/s for GS + 20% ECC ( $I_p = 12.2\%$ ). Similarly, for VGS + ECC soils, the highest erosion rate was about 0.095 kg/m<sup>2</sup>/s for VGS + 0% ECC ( $I_p = 0\%$ ); while the lowest was about 0.007 kg/m<sup>2</sup>/s for VGS + 20% ECC ( $I_p = 9.1\%$ ). These results agree with researchers such as Briaud (2008) and Haghghi et al. (2013) who said that erosion rates reduce with increasing clay content and plasticity index. Figures 5.1 and 5.2 show erosion rates against the English china clay content and plasticity of the soils, respectively. The weaker correlations are due to a combination of data for different rainfall intensities and slope gradients, but the trend of erodibility reduction due to increased clay content and increased plasticity was maintained.

Practically, reduced erosion rate due to increases in clay content suggests the need for some clay content in the soils used on the surface of unpaved roads. This improves the plasticity of those soils and therefore more cohesion which acts as binding property between the granular particles of the road material. The literature suggested an ideal plasticity index of 6%, and an acceptable range of about 2% to 12% (Gidigas, 1972; Keller and Sherar, 2003; ASANRA, 2013; Shearer et al., 2013; Paige-Green et al., 2015). However, no detailed data by these or other studies that substantiates the suitability of this range of plasticity has been found, and this study is the only one with robust and rigorous data that compares erodibility of soils of different plasticity indices.

Apart from erodibility (potholes, rills, surface loss) due to both water and wind erosion, lower plasticity of the surface soils may lead to unpaved road defects such as corrugates and raveling mainly due to soil loss and traffic loadings. Contrary, excessive plasticity may lead to a slippery surface in rainy seasons and dust in dry seasons (Paige-Green, 2006). By comparing the data in Figure 5.2 and Figure 2.21 (Chapter 2); and based on their plasticity; the soils used in this study can erode at critical shear stresses close to zero and up to about 100 N/m<sup>2</sup>. A wide range of shear stresses was probably due to the wide range of the plasticity index (0% to 12.2%) of the soils used. Since the soils used were appropriate for the construction of unpaved roads, these findings reflect the necessity to have the unpaved roads constructed so that shear stresses caused by runoff are minimized. This can be achieved by selecting the road alignment that allows lower slope gradients, and thus, reduces surface flow velocities. It can also be achieved by providing efficient cross-drainages at appropriate distances to remove water from the road' surface as quick as possible.

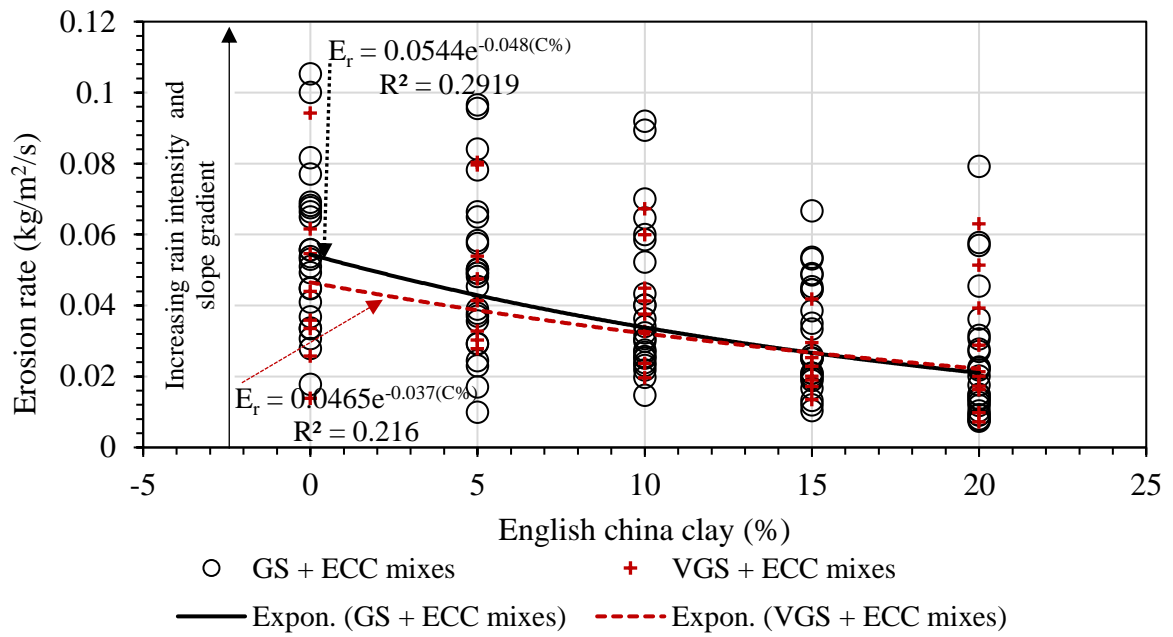


Figure 5. 1. Effect of ECC percentages on erosion rate

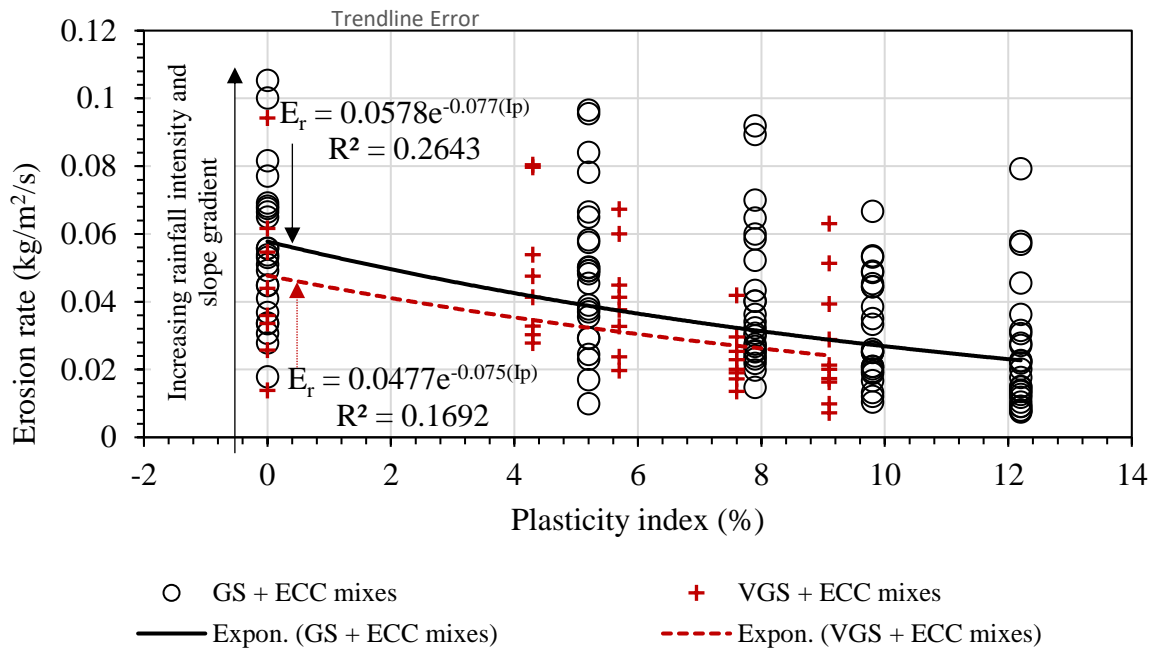


Figure 5. 2. Effect of plasticity on erosion rate

#### 5.2.2.2. Effect of Maximum Dry Density on Erosion Rate

The results from erodibility tests showed that erosion rate reduces with increasing maximum dry density of the soils, as shown in Figure 5.3. The weaker trends are due to the combination of data from different rainfall intensities, slope gradients and this time, different soils. These

results agree with both Hanson and Hunt (2007) and Al-Madhhachi et al. (2013) who argued that erodibility reduces with increasing compaction levels, with the lowest erosion rate occurring at the maximum dry density (optimum moisture content) of a given soil. In this study, the decrease of erodibility due to the increasing maximum dry density makes sense, since the latter increased with the increases of both the plasticity index and the added English china clay (Table 3.3); and thus the cohesion between particles. The effect of both higher plasticity and clay content in reducing erodibility was discussed in detail in the previous section. Thus, it is important to perform the compaction of unpaved roads satisfactorily to enhance the bearing capacity of the road and to avoid quicker deterioration through soil loss by water erosion.

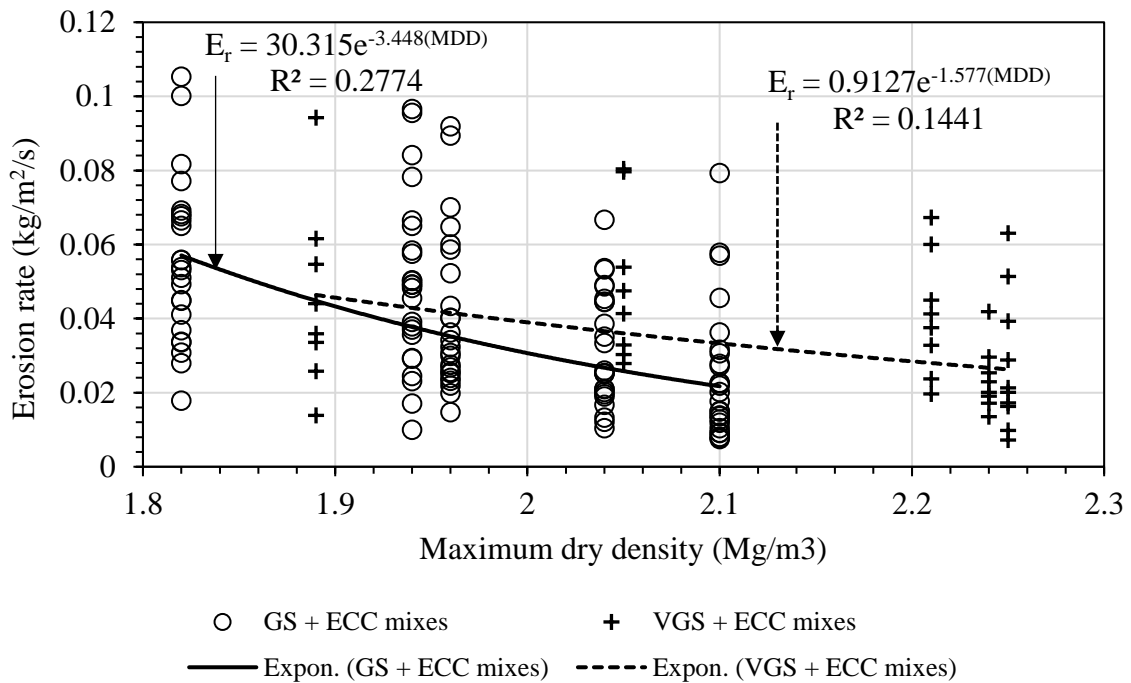


Figure 5. 3. Effect of maximum dry density on erosion rate

### 5.2.2.3. Scale Factor for Erodibility Tests

A scale factor or the effect of the size of the soil testing box on the interpretation of the results was shown by comparing the cumulative sediment and the erosion rate from the small- and large-scale tests, and the first- and second-day tests undertaken using the same testing criteria.

Figure 5.4 shows the equations that can help to convert the results of the eroded soil from one scale of the soil testing box to the other, with meaningful correlations between small- and large-scale tests. These are Equations 5.3 and 5.4 for the first- and second-day tests, respectively.

$$L_s = 6.7486(S_s)^{0.7766}; \quad R^2 = 0.768 \quad (\text{Eq. 5.3})$$

$$L_s = 2.9326(S_s)^{0.8815}; \quad R^2 = 0.7851 \quad (\text{Eq. 5.4})$$

Similarly, Figure 5.5 shows the relationships of erosion rates between the small- and large-scale tests, as shown in equations 5.5 and 5.6 respectively for the first- and second-day tests.

$$L_s = 0.1982(S_s)^{0.7766}; \quad R^2 = 0.768 \quad (\text{Eq. 5.5})$$

$$L_s = 0.326(S_s)^{0.8815}; \quad R^2 = 0.7851 \quad (\text{Eq. 5.6})$$

Although the effect of slope length on erodibility was less studied compared to slope steepness, Al-Madhhachi et al. (2013) reported that the unit area of the tested plot, thus, the slope length of the plot influences erodibility to a power of 0.6. Wischmeier and Smith (1965) suggested the power 0.5 as the influence of the slope length to the erosion rate for slope gradients greater than 6%. Generally, an exponent ranging from 0 to 0.9 can justify the effect of the slope length on the erodibility of soils (El-Swaify, 1997). In this study, the exponents in the power relation between small- and large-scale test results are about 0.78 and 0.88 respectively for the first- and second-day erodibility tests, as shown in Eq. 5.3 to Eq. 5.6. These exponents seem to be higher when compared to the exponents in agricultural soils by Wischmeier and Smith (1965) and Al-Madhhachi et al. (2013) due to differences in the soils and soil properties such as compaction considered in this study. However, this study's exponents agree with a range of exponents suggested by El-Swaify (1997). Therefore, exponents ranging from 0.7 to 0.9 can help to accurately relate and compare erosion rates from unpaved roads of different slope lengths.

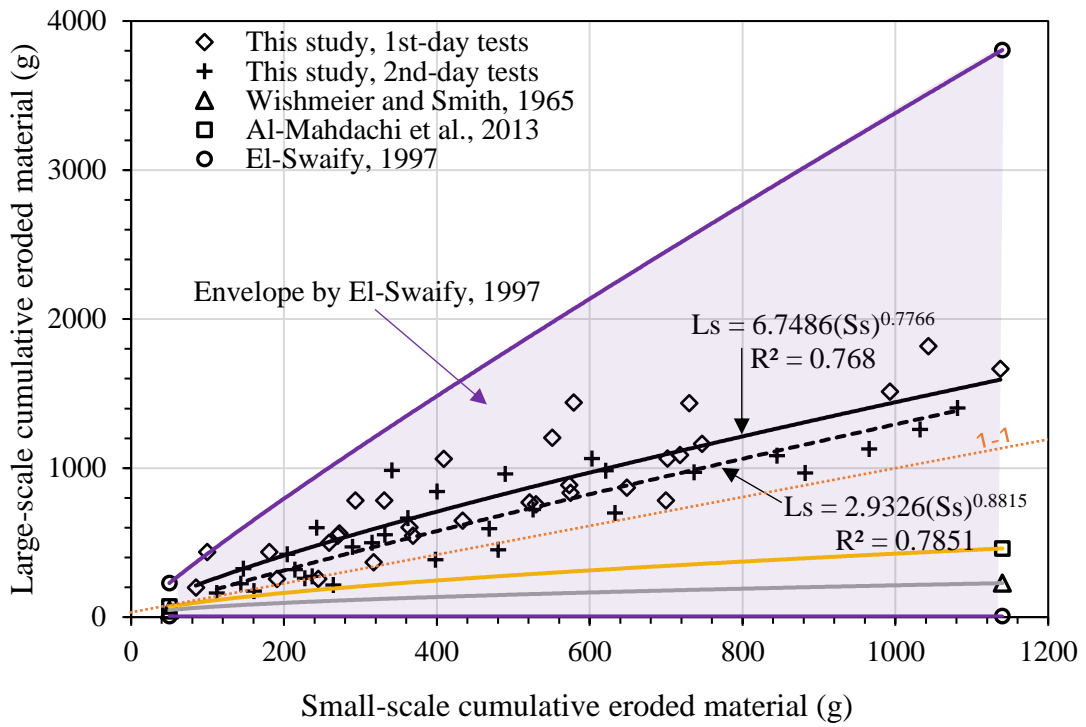


Figure 5. 4. Scale factor for eroded sediment

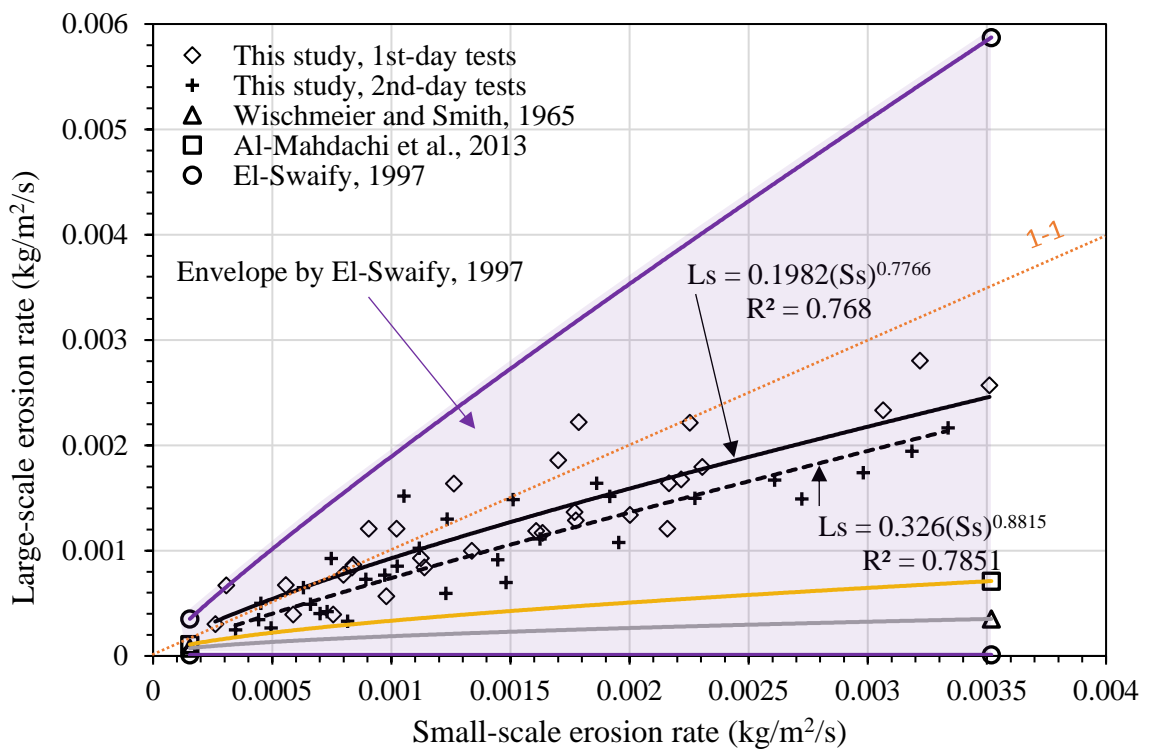


Figure 5. 5. Scale factor for erosion rate

#### 5.2.2.4. Effect of Particle Size on Erosion Rate

The results of this study showed that generally gravely SAND mixed with English china clay ( $D_{50}$  ranging from 0.4 to 0.52 mm) eroded more than very gravely SAND mixed with English china clay ( $D_{50}$  ranging from 0.8 to 1.6 mm). The only factor behind this difference was the particle size distribution, with the latter soil being with larger particles than the former soil. Salles et al. (2000) said that due to gravity effect, larger soil particles resist detachment by raindrops' kinetic energy. This suggests that when two soils satisfy the requirements (well-graded soil, required plasticity) for the construction of unpaved roads, the soil with larger particles could be better in terms of resisting erosion due to rainwater.

To advance the understanding of the effect of particle size, a subbase soil was tested. The subbase granular soil was selected because of its wide use in the lower layers of roads. Although this soil was not suitable for erosion investigation (ASTM, 2015), it helped to illustrate what may happen if it is left exposed at the surface because of erosion of the surface layer in unpaved roads. Due to higher infiltration, this soil can lead to the softening of the subgrade, with consequences including surface deflexion and subgrade soil mass movement which can lead to complete road destruction in prolonged rainy seasons.

Theoretically, the subbase's larger particle sizes ( $D_{50} = 6$  mm) cannot be detached by the kinetic energy of the raindrops (Salles et al., 2000), as shown in Figure 4.7. A higher infiltration rate ( $k = 7 \times 10^{-2}$  cm/s) discouraged formation of the surface flow, which in many cases prevented the collection of sediment in the first five minutes of the rainfall. Initially, the rainfall infiltrated and it was only upon saturation or filling up of the test box that the smaller particles were moved by water and collected. The subbase soil's erosion was far less than that observed in the other soils; which agrees with the literature as erosion reduces with increasing particle size of the granular soils (Carey and Simon, 1984; Salles et al., 2000; and Briaud, 2008).

The results proved that the subbase soil rarely respected the trends of erodibility with regard to slope length and gradient, rainfall intensity, and first- and second-day tests, as was observed for the other tested soils. This trend of erosion was not surprising since the subbase does not meet the requirements for the soils suitable for erosion studies, as shown in Table 3.1. The subbase case showed that unpaved roads with excessive rough surfaces can be subjected to weaker subgrades due to infiltrated water. Thus, it is necessary to keep their surfaces to appropriate standard through regravelling, preferably after each rainy season since finer particles are likely to have been eroded, leaving larger particles that form the rougher road' surfaces.

### 5.3. Particle Size Distribution of Eroded Soils

According to Salles et al. (2000) and based on the kinetic energy of the rainfall intensities used in this study, as shown in Table 3.9, the mean grain size of the eroded soils should be in the range of  $0.0007 \text{ mm} \leq D_{50} \leq 2.8 \text{ mm}$ ;  $0.0002 \text{ mm} \leq D_{50} \leq 3.2 \text{ mm}$ ; and  $0.0003 \text{ mm} \leq D_{50} \leq 4 \text{ mm}$ , respectively for the 30 mm/hr, 51 mm/hr, and 68 mm/hr rainfall intensities. The results of the laboratory tests showed that the mean grain size of the eroded soils ranged from about 0.15 mm to 0.55 mm and 0.23 mm to 0.75 mm; respectively for the first- and second-day tests, as shown in Figures 4.37 and 4.38.

Only about 2% of the eroded soils (both first- and second-day tests) was greater than 4 mm in size, which was the biggest  $D_{50}$  of the detachable soils by the rainfall intensities used in this study. This shows the limited role of flow in the detachment of particles due to the shortness of the investigated slopes. About 98% of particles could be detached by raindrops, while only the detachment of about 2% of eroded soils may have required the cumulative effect of raindrops and subsequent flow.

These results show that raindrops are the main cause of detachment in unpaved roads, and agree with Ziegler et al. (2000) who said that about 45% of sediment from these roads is due to raindrops kinetic energy, while the remainder 55% is due to a combination of raindrops energy, flow shear stresses, soil type, and road geometry among other factors. This suggests that during the selection of appropriate soils for the construction of unpaved roads, it is worth thinking about the range of rainfalls in the area in order to keep the soils easily detachable by this range of rainfalls to a minimum possible; considering the other factors contributing to the selection.

For all the tested soils, more sediment was eroded in the first 15 minutes of the rainfall, with a peak erosion delivery at about 10 min to 15 min from the start of the rainfall, as discussed in section 4.10. After this time of more sediment delivery, erosion due to a certain rainfall intensity tends to reach an equilibrium; which was because of finer particles being eroded faster and the remaining coarser materials significantly resisting the detachment due to both the raindrops' kinetic energy and flow velocity. This observation agrees with the literature (Knapen et al., 2007; Foltz et al., 2008; Cao et al., 2009; Liu et al., 2010; Cao et al., 2013), and reflects that the time for investigating the erodibility of soils suitable for unpaved roads should be at least 20 min to ensure that the peak sediment delivery and erosion equilibrium are included in the analysis of the erodibility trends.

#### 5.4. Surface Particle Size Changes

The raindrops and the surface flow affect the behaviour of the surface particles during erodibility tests. Based on the results from all the rainfall intensities used in this study, it was found that there was a decrease in the number of particles and an increase in the size of these particles at the surface with an increasing rainfall duration. Both the decrease in the number of particles and the increase in the mean particle size seemed to be linear in the first 15 min whereas they almost leveled after 20 min of rainfall. This was because of the increase in

sediment delivery up to about 15 min, and the tendency to reach the erosion equilibrium after about 20 min, from the start of the rainfall, as shown in Figures 4.18 and 4.19. The increase of the mean particle size and the decrease of the overall number of particles at the surface with increasing rainfall duration was due to most of the finer particles being eroded rapidly, leaving coarser particles which resisted detachment by the raindrops at the surface, as shown in Figures 4.39 to 4.43. However, the subbase soil showed a slow decrease in the number of particles leading to slow increase in the mean size of particles at the surface during rainfall due to the soil's overall lower erodibility, as shown in Figure 4.44.

While the common methods of investigating erodibility have focused on measuring the amount of collected sediment, decrease of surface elevation, and width and depth of created erosion rills (Stroosnider, 2005); this study has shown that erodibility of soils can be understood by assessing the changes in the surface particles number and mean grain size. To achieve this, ImageJ software was used to analyse photographs taken at the surface at different times during rainfall erosion. The results discussed in the previous paragraph agree with the findings obtained by measuring and analysing the particle size distribution of the eroded soils. Both methods show that finer particles erode faster than coarser particles, with the tendency of the erodibility to reach an equilibrium in about 20 min from the start of the rainfall.

### 5.5. Runoff Coefficients

The runoff coefficients are a measure of converting the rainfall into surface flow. Runoff coefficients are greatly affected by the surface soils' clay content, particle size and particle size distribution, infiltration capacity of the soil, bedslope, compaction levels, and the amount of rainfall (Mutreja, 1990; Thomas et al., 2017). The effect of the rainfall was shown in Figure 4.45, with generally higher rainfall intensities leading to higher runoff coefficients.

### 5.5.1. Effect of Clay Content and Particle Size on Runoff Coefficients

The runoff coefficient increased with the increase in clay content which improves particle packing, resulting in the increased dry density leading to a reduction of permeability, as shown in Table 3.3. The results from this study agree with other researchers' findings: Mutreja (1990), Mu et al. (2015), Karamage et al. (2017) and Thomas et al. (2017) said that runoff coefficients in unpaved roads may range from 0.5 to 0.9 depending on surface conditions.

For example, first-day experiments at a 6% slope, showed that runoff coefficients were about 0.59, 0.71, 0.78, 0.84 and 0.91 for GS + 0% ECC, GS + 5% ECC, GS + 10% ECC, GS + 15% ECC and GS + 20% ECC, respectively. Similarly, these were about 0.36, 0.57, 0.68, 0.76 and 0.82 for VGS + 0% ECC, VGS + 5% ECC, VGS + 10% ECC, VGS + 15% ECC and VGS + 20% ECC, respectively.

For the experiments undertaken at a 0% slope, the runoff coefficients reduced to about 0.48, 0.67, 0.77, 0.81 and 0.88 for GS + 0% ECC, GS + 5% ECC, GS + 10% ECC, GS + 15% ECC and GS + 20% ECC, respectively. Similarly, these reduced to about 0.29, 0.51, 0.65, 0.72 and 0.8 for VGS + 0% ECC, VGS + 5% ECC, VGS + 10% ECC, VGS + 15% ECC and VGS + 20% ECC, respectively. The second-day experiments also respected the increase runoff coefficients due to increasing clay content. However, these were smaller for VGS + ECC mixes than for GS + ECC mixes, which was due to higher infiltration in the former mixes related to larger soil particles. Also, the influence of particle sizes can be observed from the runoff coefficients of GS + 0% ECC, VGS + 0% ECC and the subbase which were 0.59, 0.35 and 0.2 at the 6% slope and 0.48, 0.29 and 0.1 at the 0% slope, respectively, as shown in Figure 5.6.

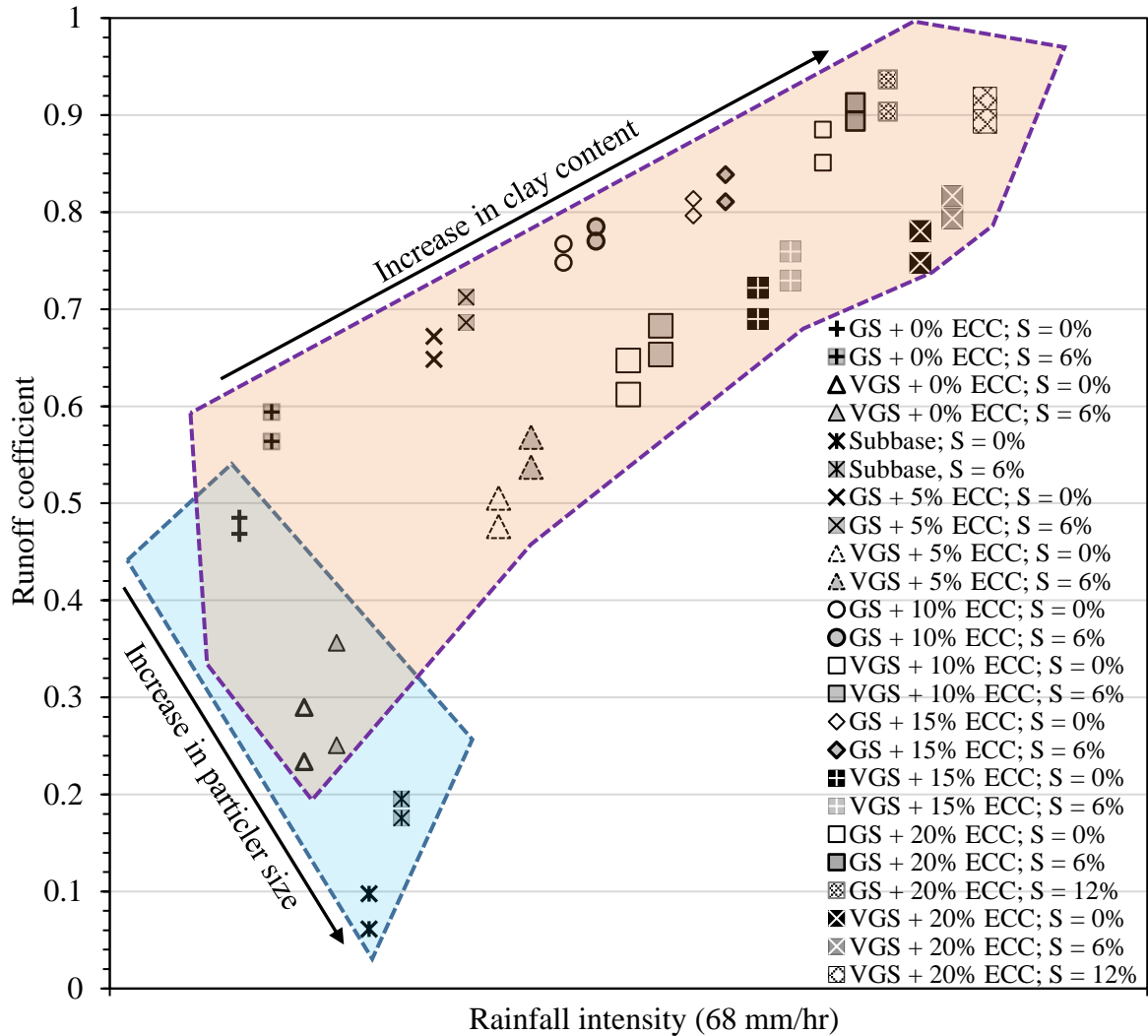


Figure 5. 6. Runoff coefficients, clay content and particle size

### 5.5.2. Effect of Clay Content and Slope on Runoff Coefficients

The data from erodibility tests using a rainfall intensity of 68 mm/hr was used to study the trends of the runoff coefficients for GS + ECC and VGS + ECC mixes tested at 0% and 6% slopes. The envelope for GS + ECC is above the envelope for VGS + ECC due to the higher runoff coefficients in the former soils. The polynomial relationship between the coefficients of runoff for the soils containing different clay contents at 0% and 6% slopes are the lower and upper bounds, respectively for the two envelopes. The combination of the two envelopes constitutes a third envelope with the upper and lower bounds being the polynomial correlation

of runoff coefficients for GS + ECC mixes tested at a 6% slope and for VGS + ECC mixes tested at a 0% slope, respectively. Meaningful correlations between the runoff coefficients for different clay contents range from  $R^2 = 0.9649$  to  $R^2 = 0.9856$ . The increase in the clay content and slope gradient result in the increase of the runoff coefficients, as shown in Figure 5.7.

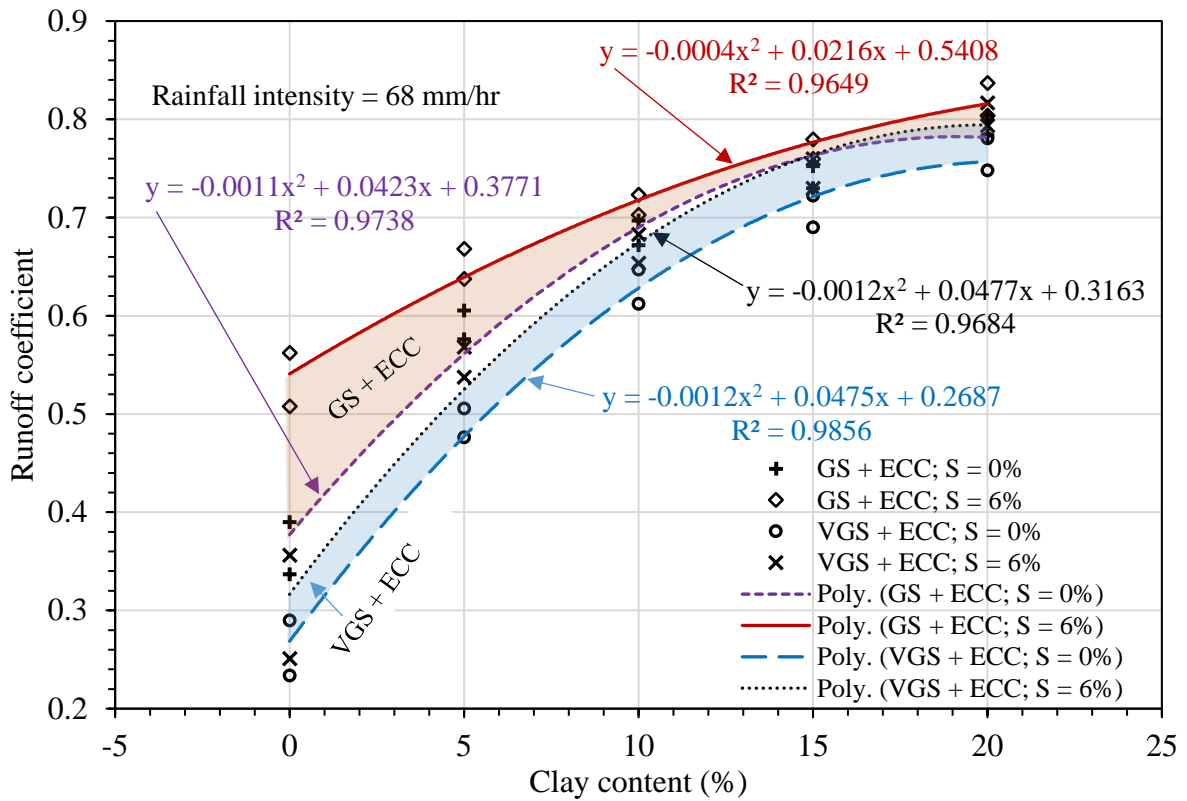


Figure 5. 7. Runoff coefficients and clay content

### 5.5.3. Effect of Mean Particle Size on Runoff Coefficient

The runoff coefficients are higher for the soils with smaller  $D_{50}$  and reduce exponentially with the increasing  $D_{50}$  because of the increasing infiltration. An envelope is conceived using the  $D_{50}$  of the soils used in this study, ranging from about 0.4 mm for GS + 20% ECC to about 6 mm for the subbase. The correlation strength is such that  $R^2 = 0.7803$ . Although there was a wide gap between the biggest  $D_{50}$  for VGS + ECC mixes (1.6 mm) and the  $D_{50}$  for the subbase (6 mm), as shown in Figure 5.8, this should not affect the trend of correlation, but the correlation strength can probably change if soils of closer  $D_{50}$  are tested.

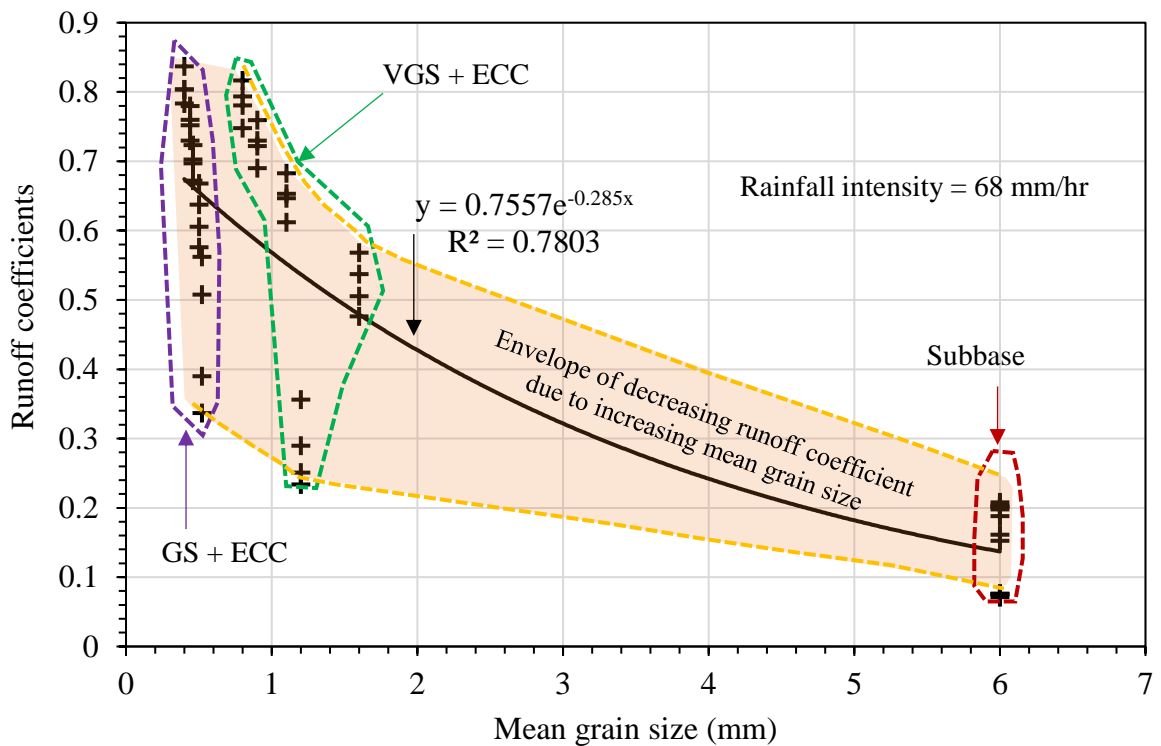


Figure 5. 8. Runoff coefficients and mean grain size

#### 5.5.4. Effect of Cu and Cc on Runoff Coefficients

The runoff coefficients increased exponentially with the increasing coefficient of uniformity (Cu) and coefficient of gradation (Cc) of the tested soils. By increasingly adding ECC contents to both GS and VGS soils, most of soils' coefficients of uniformity became greater than 6 while the coefficient of curvature ranged from 1 to 3. Since these are the conditions for the well-graded sand soils, they increased the maximum dry density and reduced infiltration of the soils; leading to more flow at the surface. Therefore, this study showed that runoff coefficients increase with increases in both the coefficient of uniformity and the coefficient of curvature, as shown in Figures 5.9 and 5.10.

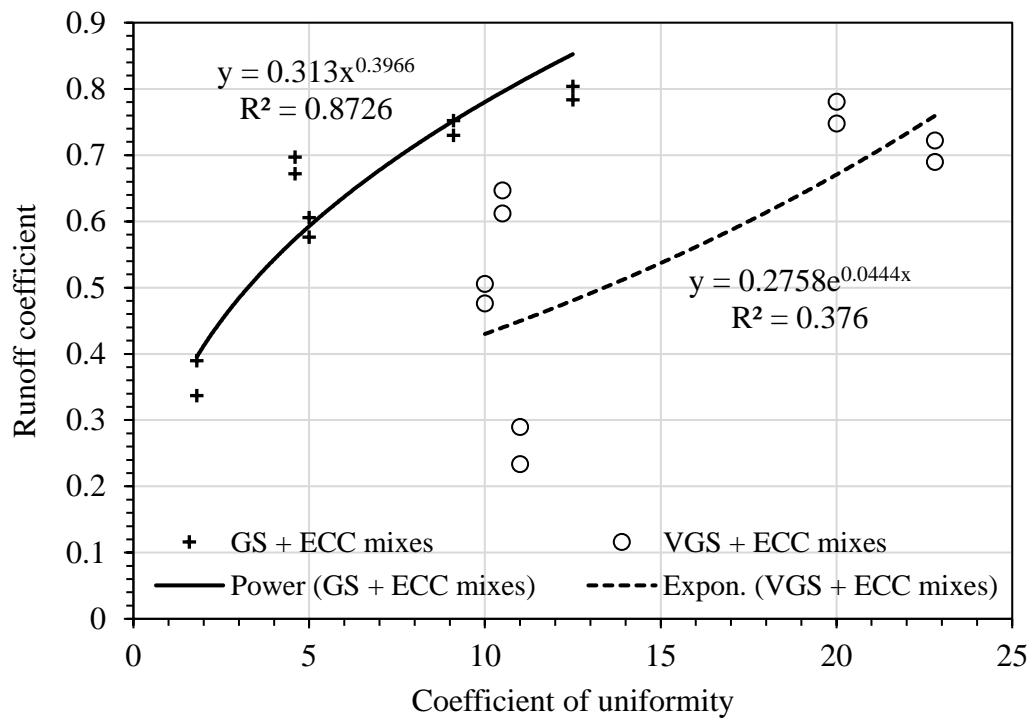


Figure 5. 9. Runoff coefficients and coefficient of uniformity

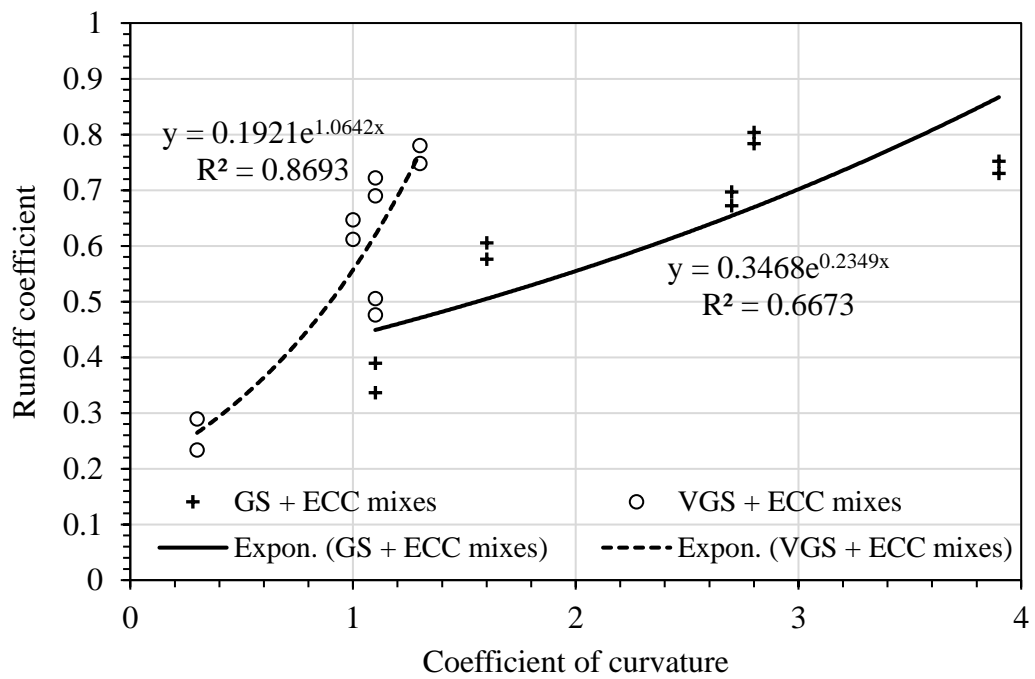


Figure 5. 10. Runoff coefficients and coefficient of gradation

### 5.5.5. Effect of Percent of Fines and Density on Runoff Coefficients

The additions of ECC to GS and VGS have increased the fraction of fines (< 63 microns) of the soil mixes. This reduced the porosity, improved the dry density, and reduced the infiltration of the soils, therefore increasing the runoff coefficients, as shown in Figures 5.11 and 5.12.

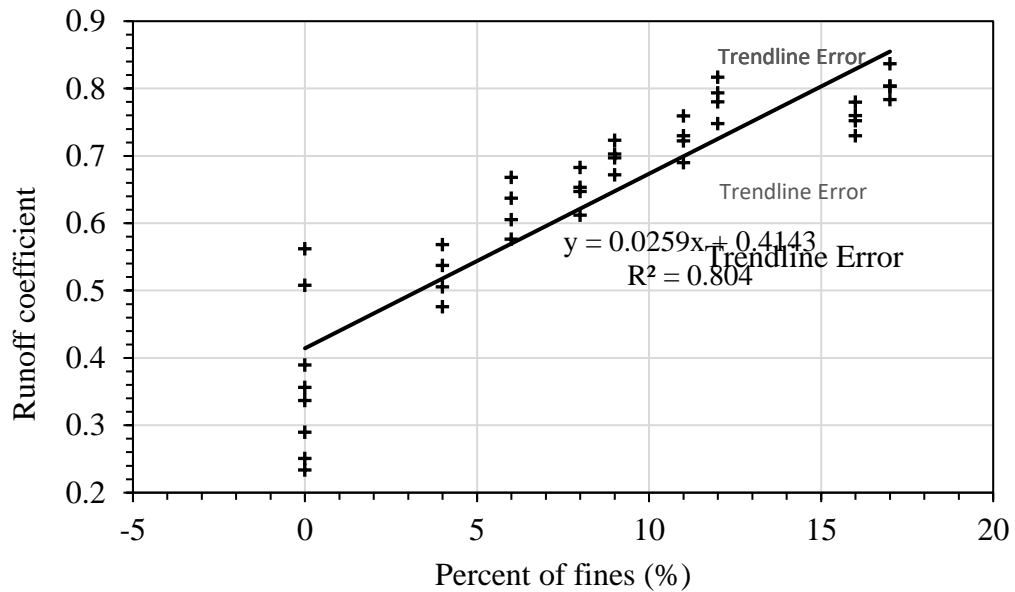


Figure 5. 11. Runoff coefficients and percent of fines in GS and VGS soils

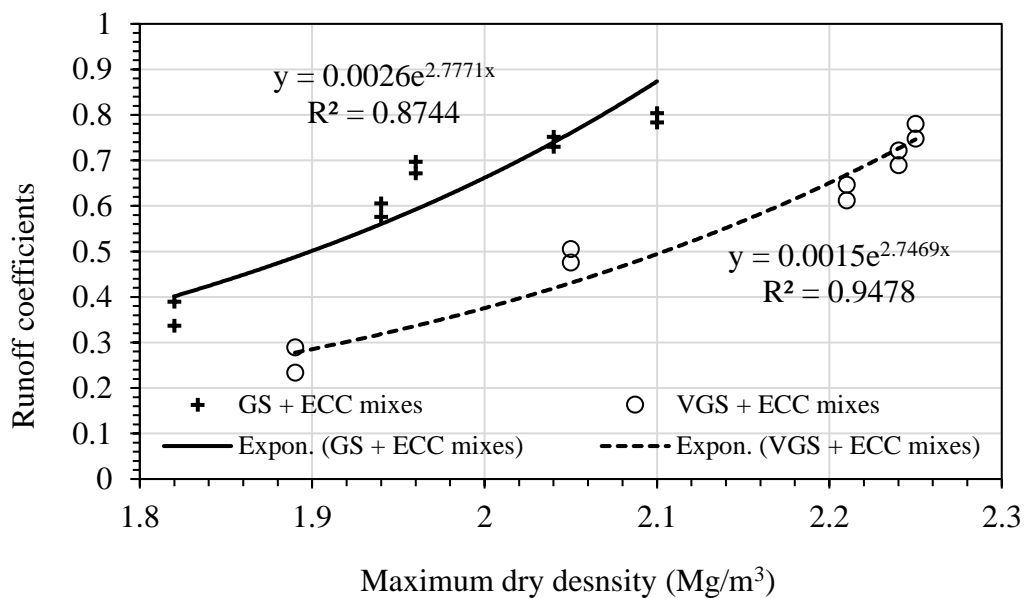


Figure 5. 12. Runoff coefficients and maximum dry density

## 5.6. Summary

The laboratory experiments to investigate erodibility due to rainfall on GS and VGS soils containing up to 20% ECC and on the subbase soil were undertaken. The first- and second-day experiments were conducted on the small- and large-scale settings based on the sizes of the soil testing box and the rainfall simulator. The slopes of 0%, 6% and 12% and the rainfall intensities of 30 mm/hr, 51 mm/hr and 68 mm/hr were used. The data for analysis and discussion regarded the eroded soils, the runoff and the surface photographs collected at 5-minute intervals of time during a 30 minutes rainfall. The results showed that erosion peak occurred between the 5<sup>th</sup> and 15<sup>th</sup> minute from the start of rainfall, and that erosion reached equilibrium after 20 minutes of rainfall. Erodibility decreased with the increases in the clay content and mean grain size, shorter slope, lower gradients, and rainfall intensity. Furthermore, the erosion rate decreased with the increasing clay content, plasticity index and mean grain size. The effects of the clay content, plasticity index and maximum dry density in reducing the erosion rate were discussed. The erosion rate was affected by the area of the soil testing box and generally the small-scale tests showed higher erosion rate. Sediment from the small-scale box was greater than half of the sediment from the large-scale box which was twice in size. This is was discussed herein as the scale factor which needs to be considered when comparing erodibility from unpaved roads of different slope lengths. The sediment particle size distribution showed that the finer particles eroded faster than the larger particles. Similarly, the number of the surface particles reduced while their mean particle size increased with the rainfall duration. The runoff coefficients were estimated and increased with the increases in the rainfall intensity, clay content, coefficients of uniformity and gradation, percentage of fines and maximum dry density, while these decreased with the second-day tests and increasing mean particle size.

## 6. CORRELATION OF FACTORS affecting ERODIBILITY IN UNPAVED ROADS

### 6.1. Introduction

This chapter describes the work to investigate the presence of correlations amongst the factors that affect erodibility of soils due to rainfall. It was based on the data collected from the 192 laboratory experiments. About 1152 test results were used to model the contribution of the factors controlled during erodibility tests to the quantity of the eroded soils. These were the small-scale test results, the large-scale test results and, for the robustness of modelling, the combined small- and large-scale test results. The data was treated as the first- and second- day tests data. The RapidMiner studio software (RapidMiner GmbH, 2019) was used to correlate the factors based on the linear regression analysis and create predictive models. The data preparation and model process were shown in Table 3.12 and Figure 3.20. The developed erosion predictive models can help to estimate the soil loss and enable to identify significant factors that affect erodibility in unpaved roads.

### 6.2. Validation of the Predictive Models

The predictive models' results were compared with the soil loss using Water Erosion Prediction Project (WEPP), Universal Soil Loss Equation (USLE) and Revised Universal Soil Loss Equation (RUSLE) on twenty USLE type plots, as reported by Laflen et al. (2004), and with the correlation between the observed and predicted soil loss in both graded and ungraded roads (Ramos-Scharrón and McDonald, 2005). Both the USLE and RUSLE are empirical models while the WEPP is a physical model which applies the (R)USLE principles with an embedded digital technology. It should be noted that these models are widely used in water erosion studies (Nearing et al., 1989; Laflen et al., 2004; Aksoy and Kavvas, 2005; Nearing et al., 2005; Ramos-Scharrón and McDonald, 2005; Brooks et al., 2006; Beskow et al., 2009). Furthermore, some of the factors used in this study were similar to those used by the (R)USLE equation:

$$A = R * K * L * S * C * P \quad (\text{Eq. 6.1})$$

where A is the mean annual soil loss (ton ha<sup>-1</sup>yr<sup>-1</sup>), R is the rainfall and runoff factor (MJ mm ha<sup>-1</sup>hr<sup>-1</sup>yr<sup>-1</sup>), K is the soil erodibility factor (ton hr MJ<sup>-1</sup>mm<sup>-1</sup>), L is the slope length factor, S is the slope gradient factor, C is the cover and management factor and P is the support practice factor. L, S, C and P, are dimensionless.

The (R)USLE (Eq. 6.1) is considered as the champion of erosion modelling successes for the last century, which resulted from intensive research on the erodibility of soils. The pertinent studies and models that led to the development of the (R)USLE are shown in Table 6.1.

Table 6. 1. Evolution of modelling in developing the USLE (Laflen and Flanagan, 2013)

Researchers	Developed model
Zingg (1940)	$A = C' L^{0.6} S^{1.4}$
Smith (1941)	$A = C'' L^{0.6} S^{1.4} P$
Browning et al. (1947)	$A = C''' L^{0.6} S^{1.4} P$
Musgrave (1947)	$A' = (P_{30}/1.25)^{1.75} K' (L/72)^{0.35} (S/10)^{1.35} C^*$
Wischmeier and Smith (1965) -USLE	$A = RK(L/72.6)^{0.5} (0.065 + 0.045S + 0.0065S^2) CP$
Wischmeier and Smith (1978) – USLE	$A = RK(L/72.6)^{0.5} (65.4 \sin^2 \Phi + 4.56 \sin \Phi + 0.065) CP$
Renard et al. (1997) – RUSLE	$A = RK(L/72.6)^M (a \sin \Phi + b) CP$

A- Soil loss in tons/acre; A' - Soil loss in inches of depth  
C', C'', C''' -Coefficients and C\* - Vegetative cover  
P<sub>30</sub>-Maximum precipitation amount (inches) falling in 30 minutes in a storm  
R – Rainfall and runoff erosivity factor =  $\sum EI_{30}$  in hundreds ft-tons inch/acre hour  
E – Storm rainfall energy in hundreds of ft-tons per acre  
I<sub>30</sub>- Maximum rainfall intensity in a 30-minute period within a storm in inches per hour  
K' - Musgrave equation soil erodibility factor (in/yr)  
K – USLE soil erodibility factor in (0.01-ton acre hour/ acre ft-ton inch)  
L – Slope length in inch, S – Slope gradient in percent  
Φ – Slope angle in degrees, C – Cropping management factor  
P – Conservation practice factor  
M – Exponent on length term-values depend on slope or slope and rill/interrill ratio  
a, b – Coefficients in function making up slope term-values depend on slope  
USLE standard plot – 72.6 ft long x 6 ft wide

Moreover, the efficiency of the predictive models was checked using the Nash and Sutcliffe (1970)' s method (Tawari et al., 2000; Cao et al., 2013). The method described below showed that all the predictive models have a coefficient of efficiency (ME) ranging from 0.62 to 0.74 compared to the coefficients of efficiency for USLE with 0.80, RUSLE with 0.72 and WEPP with 0.71 (Tawari et al., 2000).

$$ME = 1 - \frac{\sum(Q_{mi} - Q_{ci})^2}{\sum(Q_{mi} - Q_m)^2} \quad (\text{Eq. 6.2})$$

where ME is the efficiency of the model,  $Q_{mi}$  is the measured value of event “i”,  $Q_{ci}$  is the predicted value of event “i”, and  $Q_m$  is the mean of the measured values. ME ranges from 0 to 1; the greater the value, the better the model.

After designing the model process, and processing the data, the results which include the linear regression statistics, model performance and the table of data with an additional column of predicted eroded soil mass were generated. The columns of “eroded mass” and “predicted mass” were used in the calculation of the coefficient of efficiency, as shown in Figure 6.1. This data was also used to present the relationship between measured and predicted soil loss graphically, and thus, allow comparison between different models and different rainfall events, as shown in Figures 6.2 to 6.7. In total, six models were produced and validated. These were models for the first-and second-day tests; for each of the small- and large-scale tests, and for the combination of small- and large-scale tests data. In addition to the predictive equations and resulting graphs, Table 6.2 shows the level of the factors' contribution to the erodibility models, with four stars showing the most contribution, whilst a - indicates no significant contribution to the modelling or to the erodibility.

//Trials w/ht zeros/Process/Large scale 1st test - RapidMiner Studio Educational 9.2.000 @ DESKTOP-11526LS

File Edit Process View Connections Cloud Settings Extensions Help

Views: Design Results Turbo Prep Auto Model Find data, operators... etc

ExampleSet (//My large scale predictions [...] ditrial sand-gravel-1st test large scale)

Result History ExampleSet (Apply Model) LinearRegression (Linear Regression) PerformanceVector (Performance)

Open in Turbo Prep Auto Model Filter (88 / 88 examples): all

Row No.	Eroded mas...	prediction(E...	Clay content...	Plasticity (%)	D50 (mm)	Dry density (...)	Slope length...	Slope gradie...	Rain intensit...	Rain duratio...
1	51.940	57.803	0	0	0.410	1.820	1.200	0	30	5
2	87.360	60.295	0	0	0.410	1.820	1.200	0	30	10
3	183.400	104.835	0	0	0.410	1.820	1.200	0	51	20
4	159.600	107.327	0	0	0.410	1.820	1.200	0	51	25
5	170.100	109.281	0	0	0.410	1.820	1.200	6	30	10
6	149.100	111.773	0	0	0.410	1.820	1.200	6	30	15
7	113.400	114.265	0	0	0.410	1.820	1.200	6	30	20
8	100.800	119.248	0	0	0.410	1.820	1.200	6	30	30
9	217.840	148.838	0	0	0.410	1.820	1.200	6	51	10
10	287.360	180.860	0	0	0.410	1.820	1.200	6	68	10

Figure 6. 1. Typical results from the processed data

### 6.3. Regression Equations

The regression equations generated by the RapidMiner software show contributions of different factors controlled during erodibility tests to the quantity of predicted (label attribute) eroded soil mass ( $E_{MP}$ ). Those factors (regular attributes) include clay content (C), plasticity index ( $I_p$ ), mean particle size ( $D_{50}$ ), maximum dry density (MDD), optimum moisture content (OMC), slope length ( $S_L$ ), slope gradient ( $S_G$ ), rainfall intensity ( $R_I$ ) and rainfall duration ( $R_D$ ). The significance of the correlations was indicated by the root mean square (RMS) and the squared correlations ( $R^2$ ), as shown in Equations 6.3 to 6.8. The graphs of the predicted eroded mass against the measured eroded mass, and the validation graphs are shown in Figures 6.2 to 6.7.

#### 6.3.1. Small-scale, First-day Erodibility Tests

$$E_{MP} = 29431.3 + 260.9(C) - 45.5(I_p) - 14334.3(D_{50}) - 13086.6(MDD) + 20.9(S_L) + 6.03(R_I) + 16.9(R_D); \text{RMS} = 98.75; R^2 = 0.837 \quad (\text{Eq. 6.3})$$

#### 6.3.2. Small-scale, Second-day Erodibility Tests

$$E_{MP} = 6844.5 + 31.1(C) - 21.9(I_p) - 1975.8(D_{50}) - 4784.1(MDD) + 87.8(OMC) + 17.8(S_G) + 5.9(R_I) + 16.2(R_D); \text{RMS} = 117.62; R^2 = 0.79 \quad (\text{Eq. 6.4})$$

The models given by the Eq. 6.3 and 6.4 show that there may be an over-prediction for the soil loss up to  $3000 \text{ g/m}^2$ , followed by an under-prediction, for both the first- and second-day rainfall events on the small-scale experiments. This was due to cumulative eroded soils used, whilst it was noted that erosion was higher in about the first 15 minutes and reduced in the last 10 minutes during the 30 minutes of rainfall. However, the correlation strengths were good for both the first- and second-day tests ( $R^2 = 0.795$  and  $0.757$ ), as shown in Figure 6.2.

The validation process showed that although the trend of the results of this study agrees with Laflen et al. (2004) and Ramos-Scharrón and McDonald (2005), the values of the measured and predicted erosion were smaller; which could affect the visualisation of the comparison graph. For this reason, the coefficient of efficiency (Eq. 6.2) for each model was used to estimate additional data for this study. The estimated data was less than 5% of the measured data but of the same magnitude with Laflen et al. (2004) and Ramos-Scharrón and McDonald (2005) data to allow the plotting of the comparative graphs. The results of this study are plotted below the results by Laflen et al. (2004), which could be due to the fact that generally (R)USLE and WEPP models are suitable for bed slopes longer than 4 m, while this study used shorter slopes of 0.6-m and 1.2-m length. Also, this study's data plotted above the data for erodibility of both graded and ungraded existing roads with greater resistance to detachment, due to lower field moisture and higher densities (Ramos-Scharrón and McDonald, 2005), as shown in Figure 6.3.

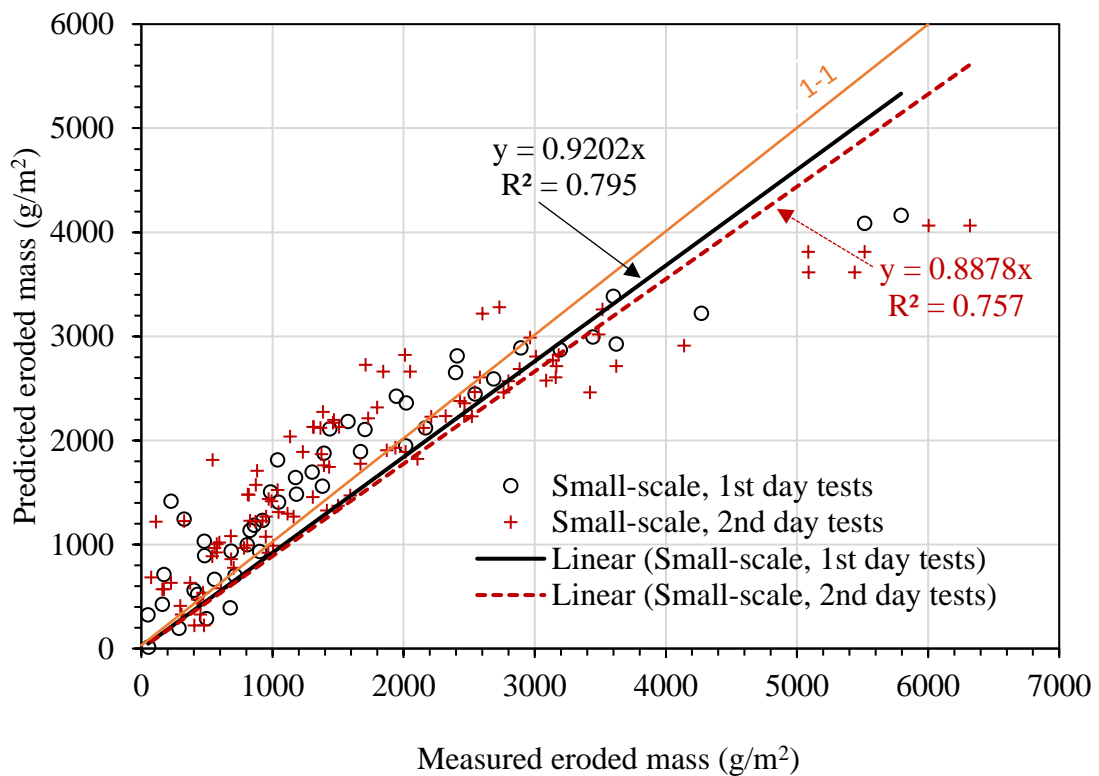


Figure 6. 2. Small-scale testing correlation between measured and predicted eroded mass

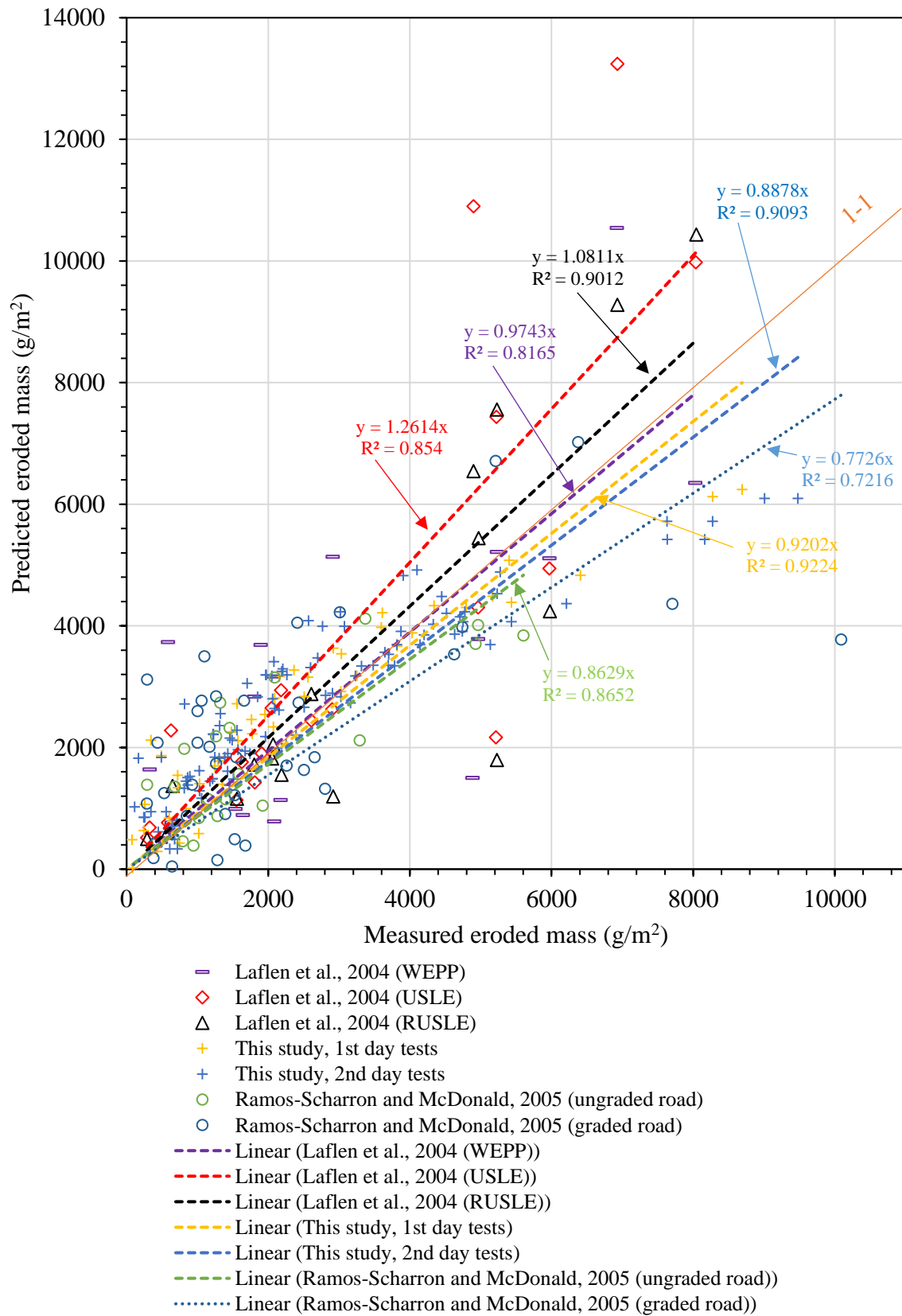


Figure 6. 3. Validation of the small-scale testing correlations between measured and predicted eroded mass

### 6.3.3. Large-scale, First-day Erodibility Tests

$$E_{MP} = 122.7 - 8.97(C) + 6.4(I_p) - 30.1(D_{50}) + 19.9(MDD) - 10.9(OMC) + 10.1(S_G) \\ + 2.65(R_I) - 1.27(R_D); \text{RMS} = 50.678; R^2 = 0.66 \quad (\text{Eq. 6.5})$$

### 6.3.4. Large-scale, Second-day Erodibility Tests

$$E_{MP} = 166.4 - 4.94(C) + 4.5(I_p) - 5.2(D_{50}) - 84.5(MDD) + 8.7(S_G) + 1.8(R_I) \\ + 0.8(R_D); \text{RMS} = 34.26; R^2 = 0.681 \quad (\text{Eq. 6.6})$$

The large-scale models showed a generalised over-prediction of the data up to about 500 g/m<sup>2</sup>, followed by the under-prediction, as shown in Figure 6.4. The strength of correlation between the factors that affect erodibility was better than for the small-scale tests, with R<sup>2</sup> = 0.832 and 0.878, respectively for the first- and second-day tests. This was because of the increased scale of the bed slope that provides more consistency in the data collection. Similar to the small-scale tests, the model efficiency (Eq. 6.2) was used to estimated less than 5% of the measured data as additional data to increase the visibility of the comparative graph. Since the purpose of the estimated data was only to allow visualization when comparing the trend of this study's results with data of larger values reported in the literature; the estimated data was kept to such a small value to minimize its effect on the measured data, hence keep the originality of the trends. The comparison of the this study's large-scale trends with (R)USLE, WEPP and erodibility from graded and ungraded roads are shown in Figure 6.5. Similarly, this study's models agree and plotted below the results reported by Laflen et al. (2004) using (R)USLE and WEPP, but below the results from both the graded and ungraded roads reported by Ramos-Scharrón and McDonald (2005).

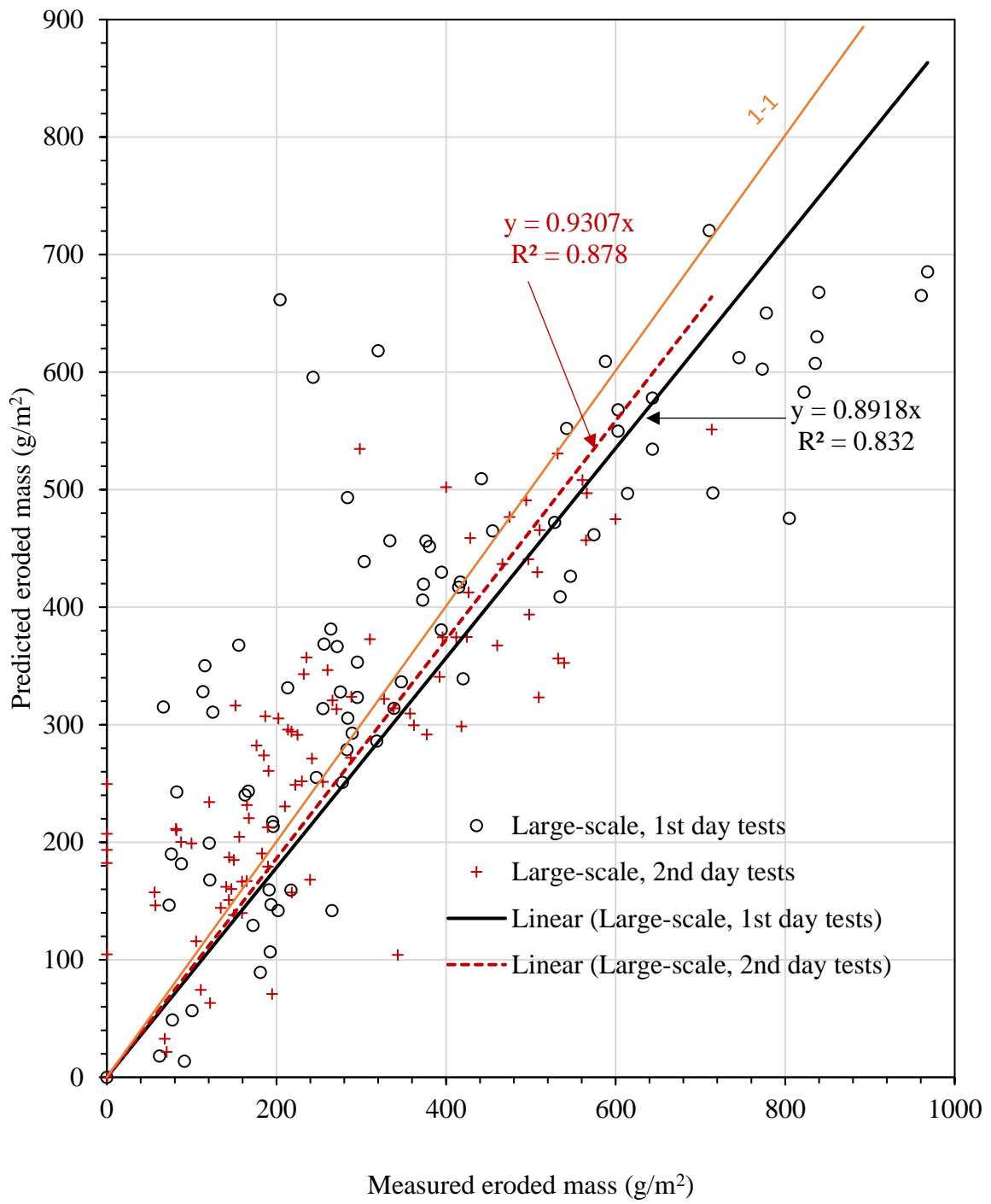
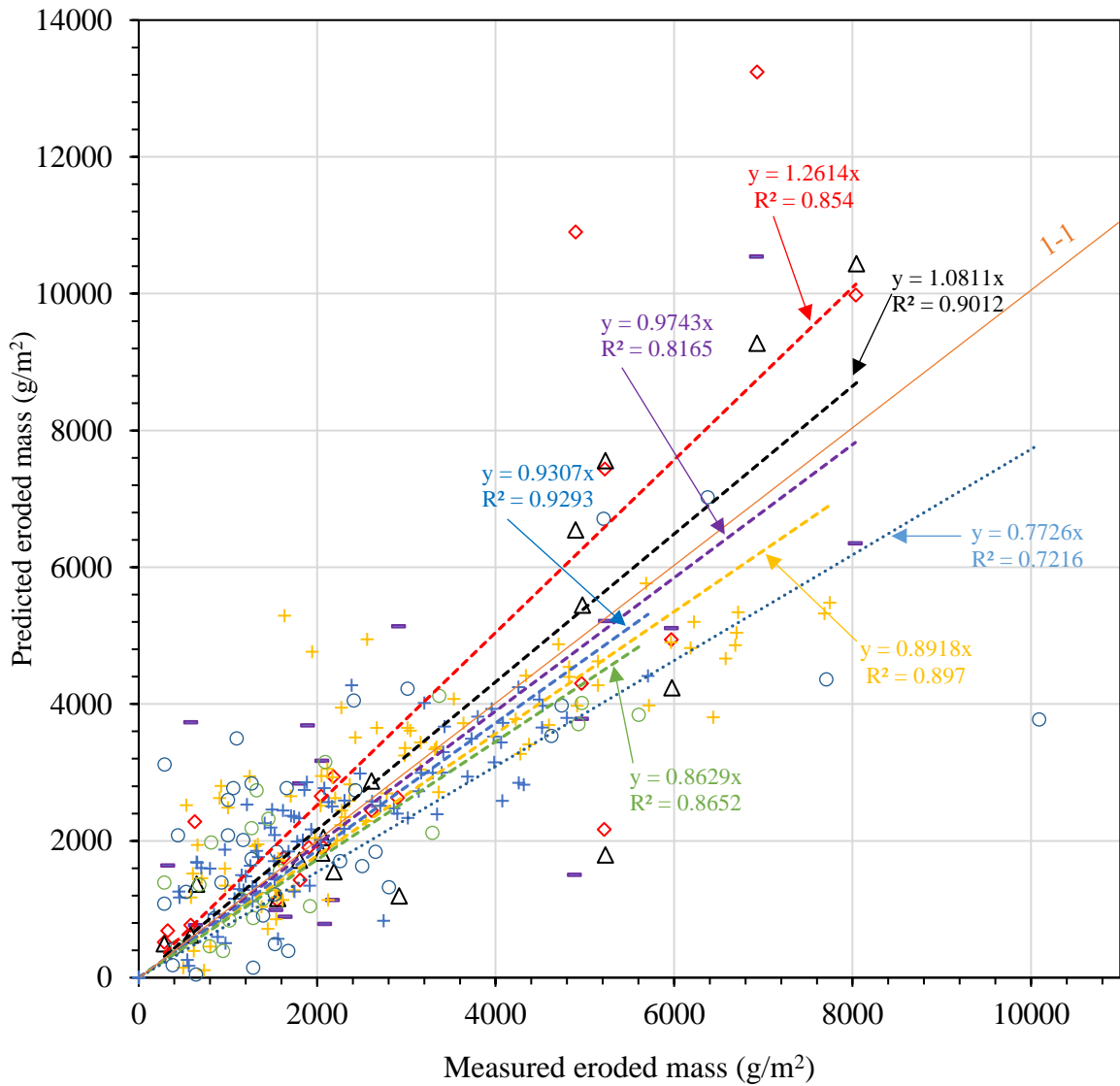


Figure 6. 4. Large-scale testing correlations between measured and predicted eroded mass



- Laflen et al., 2004 (WEPP)
- ◇ Laflen et al., 2004 (USLE)
- △ Laflen et al., 2004 (RUSLE)
- + This study, 1st day tests
- + This study, 2nd day tests
- Ramos-Scharron and McDonald, 2004 (ungraded road)
- Ramos-Scharron and McDonald, 2005 (graded road)
- - - Linear (Laflen et al., 2004 (WEPP))
- - - Linear (Laflen et al., 2004 (USLE))
- - - Linear (Laflen et al., 2004 (RUSLE))
- - - Linear (This study, 1st day tests)
- - - Linear (This study, 2nd day tests)
- - - Linear (Ramos-Scharron and McDonald, 2004 (ungraded road))
- ⋯ Linear (Ramos-Scharron and McDonald, 2005 (graded road))

Figure 6. 5. Validation of the large-scale testing correlations between measured and predicted eroded mass

### 6.3.5. Combined Small- and Large-scale, First-day Erodibility Tests

$$E_{MP} = 243.98 - 4.5(C) - 164.93(I_p) - 23.32(OMC) - 265.7(S_L) + 13.5(S_G) + 3.64(R_I) + 6.2(R_D); \text{RMS} = 91.55; R^2 = 0.623 \quad (\text{Eq. 6.7})$$

### 6.3.6. Combined Small- and Large-scale, Second-day Erodibility Tests

$$E_{MP} = 437.34 - 6.1(C) + 0.68(I_p) - 206.5(MDD) + 10.6(OMC) - 275.6(S_L) + 11(S_G) + 4.3(R_I) + 7.1(R_D); \text{RMS} = 114.63; R^2 = 0.558 \quad (\text{Eq. 6.8})$$

Similar to both the small- and large-scale models, the combined small- and large-scale models showed an over-prediction of the data up to about 1100 g/m<sup>2</sup>, and then an under-prediction, as shown in Figure 6.6. The strength of correlation between the factors of erodibility reduced, compared to the separate small- and large-scale correlation strengths, with  $R^2 = 0.586$  and  $0.549$  respectively for the first- and second-day tests. This was because of the scale factor effect on the erodibility, as reported in section 5.2.5. For example, the fact that erodibility of longer slopes was hugely affected by runoff and slope gradient, while the shorter slope was essentially affected by the detachment due to the raindrops. In the comparison graph, the combined small- and large-scale tests' data plotted only above the data of erodibility for the graded earth roads (Ramos-Scharrón and McDonald, 2005), and below the other data used for comparison, as shown in Figure 6.7.

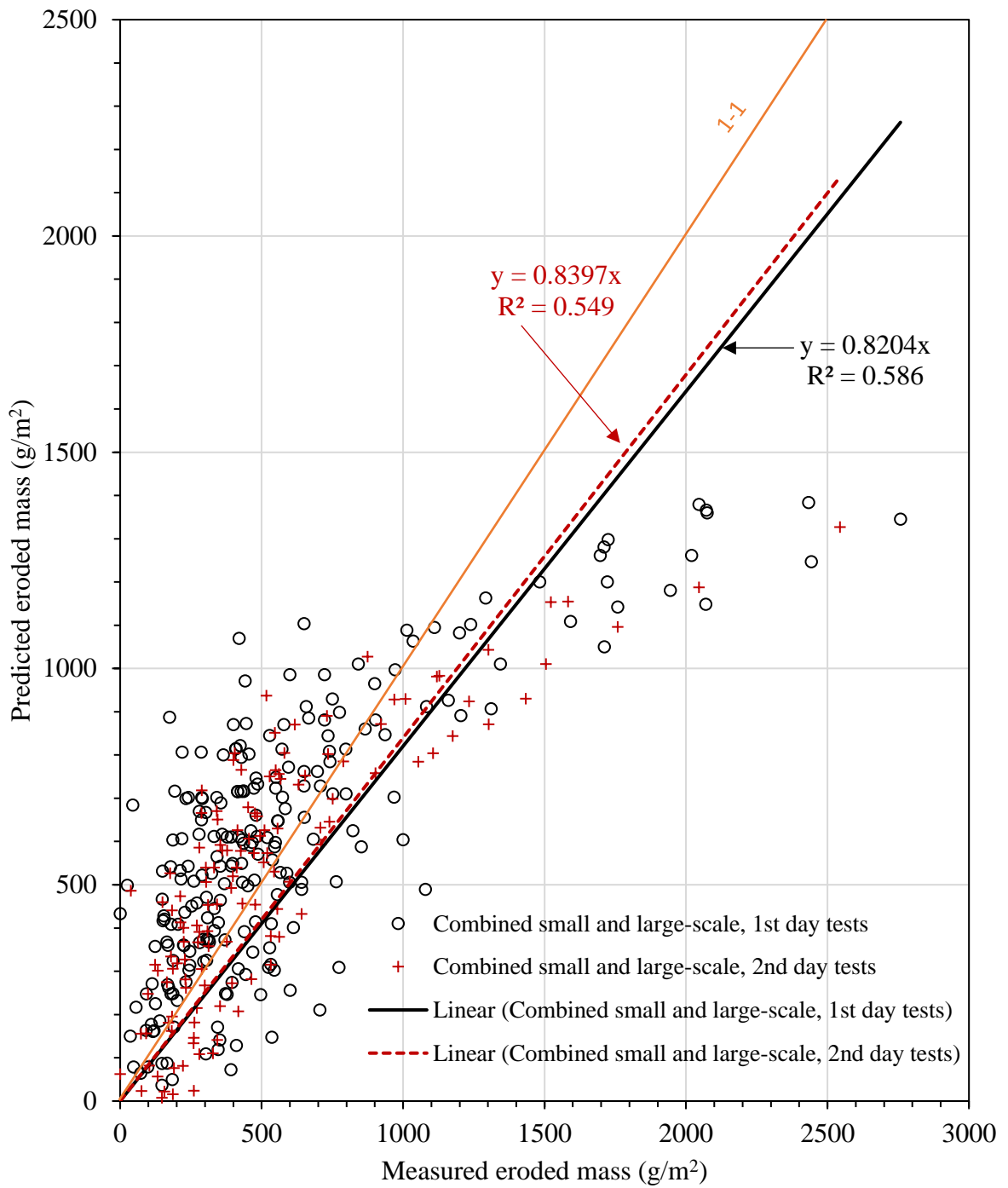


Figure 6. 6. Small- and large-scale combined tests correlation between measured and predicted eroded mass

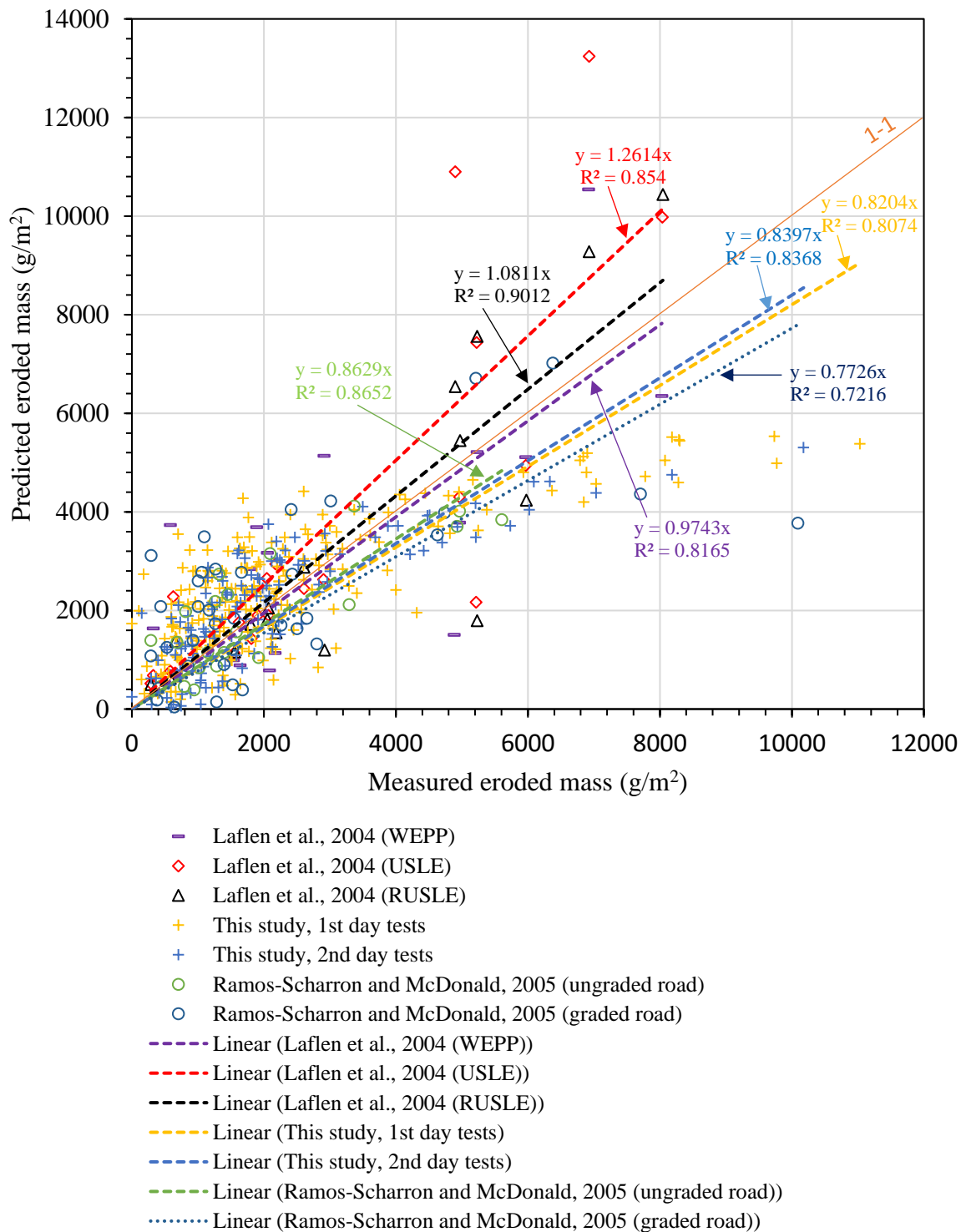


Figure 6. 7. Validation of small- and large-scale combined tests correlation between measured and predicted eroded mass

Table 6. 2. Rating of the factors' contribution to the predictive erosion model

Contributing factors	Small-scale tests		Large-scale tests		Combined small- and large-scale tests	
	1 <sup>st</sup> day (Eq.6.3)	2 <sup>nd</sup> day (Eq.6.4)	1 <sup>st</sup> day (Eq.6.5)	2 <sup>nd</sup> day (Eq.6.6)	1 <sup>st</sup> day (Eq.6.7)	2 <sup>nd</sup> day (Eq.6.8)
Clay content (%)	****	-	****	**	****	**
Plasticity index (%)	****	-	*	-	-	-
D <sub>50</sub> (mm)	****	-	****	-	-	-
OMC (%)	-	-	-	-	**	***
MDD (Mg/m <sup>3</sup> )	****	-	-	-	**	****
Slope length (m)	-	-	-	-	****	****
Slope gradient (%)	****	****	****	****	****	****
Rainfall intensity (mm/hr)	****	****	****	****	****	****
Rainfall duration (min)	****	****	***	**	****	****
Model efficiency (ME)	0.74	0.62	0.69	0.67	0.72	0.73

#### 6.4. Summary

Six erosion predictive models detailing the correlations between nine factors of erodibility were developed. This was the first attempt at correlating many erodibility factors. The developed models are simple and can offer the room for improvement if more results from laboratory and field tests become available. The contribution of different factors to the quantity of the eroded soils for both the small- and large-scale tests shows that the first-day test results are highly affected by the clay content, plasticity index, mean particle size, maximum dry density, slope gradient, and rainfall intensity and duration. In contrast, the second-day test results are mainly affected by the slope gradient, and rainfall intensity and duration. The differences in the contribution of various factors between small- and large-scale tests was because of the difference in the slope length. Longer slope causes more runoff flow with greater transport capacity of the eroded soils. The combined small- and large-scale test results improved robustness of modelling. Like separate tests, results show that for the first-day tests, the clay content, slope length, slope gradient, rainfall intensity and rainfall duration are the main factors that influence the erodibility. Furthermore, second-day tests results show that the slope length,

slope gradient, rainfall intensity and rainfall duration have more effect on the surface erosion in unpaved roads. Generally, the predictive models show that the slope length, slope gradient, rainfall intensity and rainfall duration are the factors which hugely affect erosion in unpaved roads, regardless of the soil type, composition, and compaction efforts. Therefore, in addition to the selection of good soils for construction, the best way to combat erosion in unpaved roads requires the best construction and management practices. These include informed decisions on slope length and gradient, provision of adequate drainage systems, and proper maintenance to limit the growth of erosion features at the early stages of development. Finally, although the models have the under- and over-prediction character, this was because of the other factors of erodibility (Figure 2.14) which were not controlled during laboratory tests. To some extent, this character of under- and over-prediction seems to be common in erosion models (Laflen et al., 2004; Ramos-Scharrón and McDonald, 2005).

## 7. CONCLUSIONS AND RECOMMENDATIONS

The aim of this research was to investigate erodibility of soils in unpaved rural roads. It was achieved by clearly introducing the problem of the erodibility of soils in unpaved roads and setting specific objectives (Chapter 1). Then Chapter 2 gathered a systematically detailed review of the literature. Moreover, an experimental study based on various soil specimens subjected to a range of rainfall intensities and durations subsequently followed. One hundred and ninety-two erosion tests were conducted over a period of twenty months (Chapter 3). For results, surface water was collected and analysed to ascertain the eroded materials. In addition to this, photographic images were analysed to study the change in the sizes and numbers of the soil particles at the surface during the rainfall events (Chapter 4). The results of the work done in Chapters 3 and 4 were discussed in Chapter 5 with supporting pieces of evidence from Chapter 2. Chapter 6 correlated the key factors that affect erodibility and helped to develop predictive equations for erosion in unpaved roads. The conclusions drawn from this study are described whilst the recommendations for further work are also suggested (Chapter 7). The overall goal was to improve the sustainability of unpaved roads and the unparalleled impact of these roads on development, particularly in rural areas. The findings of this study have been published in a conference proceeding, three journal and four conference papers, whilst one paper is under review process (Appendix 4). Another six journal papers are under preparation.

### 7.1. Conclusions

#### 7.1.1. Rainfall Erosion

The main objective of the rainfall erosion tests was to assess the erodibility of soils due to raindrops and subsequent surface flow. Three rainfall intensities of 30 mm/hr, 51 mm/hr and 68 mm/hr, representing typical rainfall intensities were used. Their average drop sizes were 3 mm, 3.2 mm, and 3.5 mm, respectively. Three slope gradients of 0%, 6% and 12% were

considered during the erosion tests. Two soil testing boxes were used: the small-scale testing box (0.6 m x 0.3 m x 0.17 m) and the large-scale testing box (1.2 m x 0.3 m x 0.17 m). The units for the testing boxes are respectively the length x width x depth. The tests were undertaken for a thirty-minute period for two successive days and the data for both eroded sediment and surface photographs was collected at five-minute intervals. Eleven soil types were tested. These were five mixes of a gravelly SAND and English china clay percentages, five mixes of a very gravelly SAND and English china clay, a Subbase soil. Based on the analysis of both the sediment contained in the runoff and changes in the particle sizes and numbers at the surface during rainfall events, the following conclusions have been drawn:

For cumulative eroded sediment:

- The results from the erodibility experiments due to rainfall confirmed that the quantities of eroded soils increase with the increase in both rainfall intensity and duration.
- The quantities of eroded soils increase with increases of both the slope length and the slope gradient of the tested soil samples.
- This study confirmed that the quantities of eroded soils reduce with both an increase in clay content and an increase in particle size.
- This study revealed that the peak sediment delivery in unpaved roads happens between five and fifteen minutes from the start of the rainfall, whilst erosion tends to reach equilibrium after twenty minutes.
- This study revealed that the quantities of eroded soils from unpaved roads may be larger for the first rainfall event and smaller for the subsequent rainfall events.
- Since this study used two different sizes (scales) of soil testing boxes (small- and large-scale), it was found that generally the larger the scale, the more the eroded soils due to increasing runoff with the increase in slope length, and thus more transported sediment.

For erosion rate:

- The longer slopes may not necessarily have greater erosion rates than the shorter slopes. Generally, the shorter slope (small-scale) experiments showed a greater erosion rate than the longer slope (large-scale) experiments. Although the area of the large-scale soil testing box was twice the area of the small-scale soil testing box, the former produced less than twice the quantity of the eroded soil from the latter. This was due to some of the particles being deposited halfway along the increased slope length leading to a reduced erosion rate when applied to the area of the larger scale box. Ideally, the net erosion is the difference between detachment and deposition occurring in a specific land area during the rainfall event.

Behaviour of surface particles during rainfall events:

- From the analysis of both the eroded soils and the change in particle size at the surface; the larger granular soils better resisted both the rainfall drops and the surface flow than the smaller granular soils. Smaller particles eroded faster than larger particles. The number of the soil particles reduced, whilst the mean grain size increased at the surface with the increase in the duration of the rainfall.

The runoff coefficients:

- This study revealed that runoff coefficients on the tested soils reduced with the reduction in clay content and increased with the increasing rainfall intensity. Smaller runoff coefficients were also found for soils with larger particles due to increased infiltration and surface roughness. Greater slope gradients lead to greater runoff coefficients due to increased flow velocity. Moreover, runoff coefficients increase with an increasing coefficient of uniformity, coefficient of curvature, and percentage of fines, which increase compaction levels and thus, reduce the infiltration rate.

Correlating the factors affecting erodibility in unpaved roads:

- RapidMiner studio software was used to correlate the factors controlled during the rainfall erosion tests based on the quantities of the eroded soils. Six predictive equations that can help to estimate the quantity of the eroded soils were developed. The factors used to generate these equations are clay content, mean particle size, maximum dry density, optimum moisture content, plasticity index, slope length, slope gradient, rainfall intensity, and rainfall duration.

#### 7.1.2. Sheet Erosion

The sheet erosion experiments were conducted on soils with/without buried glass marbles and with exposed glass marbles to simulate larger particle sizes. The main goal was to check the effect of larger soil particles at the surface of unpaved roads on the formation of potholes and the overall loss of surface soils. The major findings were that the depth of erosion was greater in the soil with smaller particle sizes (GS + 20% ECC); whereas the soil with larger particle sizes (VGS + 20% ECC) eroded shallowly but over a greater area due to better resistance to runoff velocities. The exposed glass marbles promoted both the formation of potholes and the widening of the eroded area.

#### 7.1.3. Practical Implication of the Study

This study showed that the soils at the surface of unpaved roads need careful selection to avoid unacceptable soil losses due to rainwater erosion. The construction and maintenance of these roads needs soils which contain an ideal plasticity index and particle size distribution to effectively resist detachment due to both the raindrops and the flow's shear stress. To achieve this, different graphs of direct use have been developed. These include graphs relating: the rainfall's threshold kinetic energy (critical flow velocity) to the mean particle size of the soil (soil particle size distribution); erosion rate to both plasticity index and shear stress; and critical

shear stress to mean particle size. Moreover, an envelope for appropriate soil selection was developed to avoid slippery, raveling, corrugations, and soil loss at the surface of unpaved roads. Furthermore, based on the properties of the soils used for the erosion experiments and the quantities of sediment eroded from these soils, this study helps to define suitable soils for the construction and maintenance of unpaved roads. Also, the soil properties, rainfall and road geometry characteristics helped to develop predictive equations for soil loss in unpaved roads. Overall, the study provides ways in which the appropriate soils can be selected for both construction and maintenance activities, to achieve the sustainability of unpaved roads. This can help to preserve the quarries of the already scarce suitable soils and to save money that would be used for recurrent and unplanned maintenance works. Importantly, the sustainability of these roads in rural areas improves the rural transport systems and the well-being of communities through poverty reduction, access to education and health services, and access to workplaces and markets.

## 7.2. Recommendations for Further Work

The main goal of this study was to investigate the erodibility of soils in unpaved roads due to rainfall and subsequent surface flow. This work was undertaken on only 11 soil types. These soils were synthesised in a laboratory. Whilst the trends identified are relevant for understanding erodibility of soils, it is suggested that further work may be undertaken to improve the understanding of the topic. The following areas should be given emphasis:

- Undertake both laboratory and field rainfall erosion studies on soils used in unpaved roads. These studies should include the following:
  - The impact of traffic of various types and volumes in accelerating erodibility of soils in unpaved roads
  - A range of representative soil types like the soils used in this study

- Different climatic regions to assess the effect of climate changes such as dry-wet cycles on erosion processes
  - A range of construction and road operation scenarios related to the main and secondary unpaved roads
  - A range of soil improvement techniques such as erosion control products and geotextiles to assess how these can reduce erosion in unpaved roads
  - Modes of failure to relate the formation of potholes, rills and ephemeral gullies to both water erosion and soil particles at the surface in unpaved roads.
- Undertake more laboratory and field sheet erosion studies on the soils used in unpaved roads, with focus on the impact of larger soil particles at the surface on the formation of potholes and the expansion of the eroded area.
  - Enrich and improve the predictive equations by incorporating the data obtained from field erosion experiments on the same soils and using the same methods as those used in this laboratory study.
  - Since this PhD has focused on the rainwater erosion in unpaved roads, it is suggested that (natural and mechanical) wind erosion be a topic for future work. The wind erosion not only causes soil loss in unpaved roads, but also subsequent dust may cause air pollution which can be associated with many negative health and socio-economic effects.

## REFERENCES

- Abd Elbasit MAM, Yasuda H, Salmi A and Anyoji H (2010). Characterization of rainfall generated by dripper-type rainfall simulator using piezoelectric transducers and its impact on splash soil erosion. *Earth Surf. Processes and Landforms*, 35: 466–475.
- Abdullah ME, Jaya RP, Shahafuddin MNA, Yaacob H, Ibrahim WMH, Nazri FM, Ramli NI and Mohammed AA (2017). Performance of Kaolin Clay on the Concrete Pavement. *IOP Conf. Series: Materials Sc. Eng.* 358 (2018) 012049.
- Agassi M and Bradford JM (1999). Methodologies for interrill soil erosion studies. *Soil and Tillage R.*, 49: 277 - 287.
- Aggregates Advisory Survey (1999). Department of the Environment, Transport, and the Regions Research Contract MP0623 Symonds, Digest no. 055 (2):1-99.
- Akbulut H and Gürer C (2007). Use of aggregates produced from marble quarry waste in asphalt pavements. *Building and Environment*, 42: 1921 - 1930.
- Aksoy H and Kavvas ML (2005). A review of hillslope and watershed scale erosion and sediment transport models. *Catena*, 64: 247 - 271.
- Aksoy H, Unal E, Cogkor S, Gedikli S, Yoon J, Koca K, Inci Boran S and Eris E (2012). A rainfall simulator for laboratory-scale assessment of rainfall-runoff-sediment transport processes over a two-dimensional flume. *Catena*, 98: 63-72.
- Aksoy H, Eris E and Tayfur G (2017). Empirical Sediment Transport Models Based on Indoor Rainfall Simulator and Erosion Flume Experimental Data. *Land Degradation and Development*, 28: 1320-1328.
- Alfsen KH, De Franco MA, Glomsrød S and Torgeir J (1996). The cost of soil erosion in Nicaragua. *Ecological Economics*, 16: 129 - 145.

- Ali M and Sterk G (2015). Availability and performance of sediment detachment and transport functions for overland flow conditions. *Hydrol. Sc.*, 60(9): 1550 - 1565.
- Allen PM, Arnold J and Jakubowski Ed (1997). Design and Testing of a Simple Submerged Jet Device for Field Determination of Soil Erodibility. *Env. Eng. Geosc.*, 3 (4): 579 - 584.
- Al-Madhhachi AT, Hanson GJ, Fox GA, Tyagi AK and Bulut R (2013). Measuring Soil Erodibility Using a laboratory "Mini" -Jet. *Trans. ASABE*, 56(3): 901 - 910.
- Al-Riffai M and Nistor I (2013). Influence of Boundary Seepage on the Erodibility of Overtopped Embankments: A Novel Measurement and Experimental Technique. *Proceedings of the 35<sup>th</sup> IAHR Congress, Beijing*.
- Alzubaidi H (1999). Operation and maintenance of gravel roads. A literature study. Swedish National Road and TRI. VTI Meddelande 85A.
- Anderson DM and MacDonald LH (1998). Modelling Road Surface Sediment Production Using a Vector Geographic Information System. *Earth Surf. Proc. Landf.*, 23: 95 - 107.
- Archwichai L, Youngme W, Somphadung S, Changsuwan S, Wannakao P, Hokjaroen S, and Wannakao L (1993). Engineering properties of lateritic soils from Khom Kaen and its vicinity, Thailand. *J. Southeast Asian E. Sc.*, 8(1 - 4): 549 - 556.
- Arnaez J, Lasanta T, Ruiz-Flaño P and Ortigosa L (2007). Factors affecting runoff and erosion under simulated rainfall in Mediterranean vineyards. *Soil & Tillage Res.*, 93:324 - 334.
- Arnáez J and Larrea V (1995). Erosion Processes and Rates on Road-Sides of Hill-Roads (Iberian System, La Rioja, Spain). *Phys. Chem. Earth*, 20(3-4): 395 - 401.
- Arthur E, Cornelis WM, Vermang J and De Rocker E (2011). Effect of compost on erodibility of loamy sand under simulated rainfall. *Catena*, 85: 67 - 72.
- Arulanandan K and Perry EB (1983). Erosion in Relation to Filter Design in Earth Dams. *J. Geotec. Eng.*, 109 (5): 682 - 698.

- ASANRA-Association of Southern African National Road Agencies (2013). Guidelines for Use of Sand in Road Construction in the SADC Region.
- Assouline S (2009). Drop size distributions and kinetic energy rates in variable intensity rainfall. *Water Resources Research*, vol. 45, W11501.
- ASTM (2015). Standard Test Method for Determination of Rolled Erosion Control Product Performance in Protecting Hillslopes from Rainfall-Induced Erosion. ASTM: West Conshohocken, PA, USA.
- Asselman NEM, Middelkoop H and van Dijk PM (2003). The impact of changes in climate and land use on soil erosion, transport and deposition of suspended sediment in the River Rhine. *Hydrological Processes*, 17: 3225 - 3244.
- Aziz MA and Ramaswamy SD (1992). Incinerator Residue for Roads. *J. Geotechnical Testing*, 15(3): 300 - 304.
- Barthès B and Roose E (2002). Aggregate stability as an indicator of soil susceptibility to runoff and erosion; validation at several levels. *Catena*, 47: 133-149.
- Bediako M, Gawu SKY, Adjaottor AA and Ankrah JS (2016). Early and Late Strength Characterization of Portland Cement Containing Calcined Low-Grade Kaolin Clay. *Journal of Engineering*, volume 2016, article ID 7210891: 1-5.
- Behak L (2011). Performance of Full-Scale Test Section of Low-Volume Road with Reinforcing Base Layer of Soil–Lime. *Journal of TRB*, 2204:158 - 164.
- Behiry AEA El-Maaty (2013). Utilization of cement treated recycled concrete aggregates as base or subbase layer in Egypt. *Ain Shams Eng. J.*, 4:661 - 673.
- Benahmed N and Bonelli S (2012). Investigating concentrated leak erosion behaviour of cohesive soils by performing hole erosion tests. *Europ. J. Env. Civ. Eng.* 16(1): 43 - 58.

- Bernal SA, Mejia de Gutierrez R and Provis JL (2012). Engineering and durability properties of concretes based on alkali-activated granulated blast furnace slag/metakaolin blends. *Construction and Building Materials*, 33: 99-108.
- Beskow S, Mello CR, Norton RD, Curi N, Viola MR and Avanzi JC (2009). Soil erosion prediction-Grande River Basin, Brazil using distributed modelling. *Catena*, 79: 49-59.
- Boardman J (1983). Soil erosion at Albourne, West Sussex, England. *App. Geo.*, 3: 317 - 329.
- Boardman J and Favis-Mortlock DT (1993). Climate Change and Soil Erosion in Britain. *Geographical J.*, 159 (2): 179 - 183.
- Boardman J and Robinson DA (1985). Soil erosion, climatic vagary and agricultural change on the Downs around Lewes and Brighton, autumn 1982. *Applied Geography*, 5: 243 - 258.
- Bohlin I (2012). Formalizing Syntheses of Medical Knowledge: The Rise of Meta-Analysis and Systematic Reviews. *Perspectives on Sciences*, 20: 273 – 309.
- Bonelli S, Brivois O, Borghi R and Benahmed N (2006). Observation, analysis and modelling in complex fluid media on the modelling of piping erosion. *C. R. Mec.*, 334: 555 – 559.
- Brandt CJ (1988). The Transformation of Rainfall Energy by a Tropical Rain Forest Canopy in Relation to Soil Erosion. *Journal of Biogeography*, 15(1):41-48.
- Briaud JL (2006). Erosion Tests on New Orleans Levee Samples, Internal Report, Zachry Dpt. of Civil Engineering, Texas A&M University, College Station, pp107, 2006
- Briaud JL (2008). Case Histories in Soil and Rock Erosion: Woodrow Wilson Bridge, Brazos River Meander, Normandy Cliffs, and New Orleans Levees. The 9th Ralph B. Peck Lecture, Reston, Virginia, USA. *J. Geot. and Geoenvironmental Eng.*, 134 (10):1 - 27.
- Briaud JL, Chen, HC, Kwak K, Han SW, Ting F (2001). Multiflood and Multilayer Method for Scour Rate Prediction at Bridge Piers. *J. Geot. and Geoenv. Eng.*, 127(2):114-125.

- British Geological Survey (2009). Kaolin - Mineral Planning Factsheet for Construction Aggregates. British Geological Survey.
- Brooks ES, Boll J, Elliot WJ and Dechert T (2006). Global Positioning System/GIS-Based Approach for Modeling Erosion from Large Road Networks. *Journal Hydrological Engineering*, 11(5): 418 - 426.
- Brouwers HJH and Radix HJ (2005). Self-Compacting Concrete: The Role of the Particle Size Distribution. First Internat. Symposium on Design, Performance and Use of Self-Consolidating Concrete. 26-28 May 2005, Changsha, Hunan, China.
- Browning GM, Parish CI and Glass G (1947). A method of determining the use and limitations of rotation and conservation practices in the control of soil erosion in Iowa. *Journal of American Society of Agronomy*, 39(1): 65 – 73.
- Brunori F, Penzo MC and Firenze DT (1989). Soil Shear Strength: Its Measurement and Soil Detachment. *Catena*, 16: 59 - 71.
- Bryan RB (2000). Soil erodibility and processes of water erosion on hillslope. *Geomorphology*, 32: 385 - 415.
- Bryan RB, Govers G, and Poesen J (1989). The Concept of Soil Erodibility and Some. Problems of Assessment and Application. *Catena*, 16: 393 - 412.
- BS 1377-2 (1990). Methods of test for Soils for civil engineering purposes. Classification tests.
- BS 1377-3 (1990). Methods of test for Soils for civil engineering purposes. Chemical and electrochemical tests.
- BS 1377-4 (1990). Methods of test for Soils for civil engineering purposes. Compaction tests.
- BS 1377-5 (1990). Methods of test for Soils for civil engineering purposes. Compressibility, permeability and durability tests.
- BS 1377-7 (1990). Methods of test for Soils for civil engineering purposes. Shear strength tests.

- BS 1377, Test 16 (1990). Methods of test for Soils for civil engineering purposes. CBR Test.
- BS 5930 (2015). Code of practice for ground investigations.
- BS 7291-3 (2010). Thermoplastics pipe and fitting systems for hot and cold water for domestic purposes and heating installations in buildings. Specifications for cross linked polyethylene (PE-X) pipes and associated fittings.
- Burns B, Barker R and Ghataora GS (2006). Investigating internal erosion using a miniature resistivity array. *NDT&E Internat.*, 39: 169 - 174.
- Burrow MPN, Evdorides H, Ghataora GS, Petts R and Snaith MS. (2016). The evidence for rural road technology in low-income countries. *Proc. ICE*, 169, Issue TR6, 366 - 377.
- Burrow MPN, Petts RC, Snaith MC, Evdordes H, Ghataora GS (2014). Technology selection and its sustainability for low volume, rural roads in low income countries: protocol for a systematic review (Protocol). London: EPPI Centre, University of London.
- Cantón Y, Solé-Benet A, Asensio C, Chamizo S and Puigdefábregas J (2009). Aggregate stability in range sandy loam soils Relationships with runoff and erosion. *Catena*, 77: 192- 199.
- Cantón Y, Solé-Benet A, de Vente J, Boix-Fayos C, Calvo-Cases A, Asensio C and Puigdefábregas J (2011). A review of runoff generation and soil erosion across scales in semiarid south-eastern Spain. *J. Arid Environments*, 75: 1254 - 1261.
- Cao CS, Chen L, Gao W, Chen Y and Maochao Y (2006). Impact of planting grass on terrene roads to avoid soil erosion. *Landscape & Urban Plan.* 78: 205 -216.
- Cao L, Zhang K and Zhang W (2009). Detachment of road surface soil by flowing water. *Catena*, 76:155 - 162.
- Cao L, Zhang K, Dai H and Liang Y (2013). Modelling Interill Erosion on Unpaved Roads in the Loess Plateau of China. *Land Degradation and Development*.

- Cao L-X, Zhang K-L, Dai H-L and Guo Z-L (2011). Modelling Soil Detachment on Unpaved Road Surfaces on the Loess Plateau. *Trans. ASABE*, 54 (4): 1377 - 1384.
- Carey WP and Simon A (1984). Physical basis and potential estimation techniques for soil erosion parameters in the Precipitation-Runoff Modelling System (PRMS). U.S. Geological Survey, Water Resources Investigations Report 84 - 42 18.
- Cerdà A (2001). Effects of rock fragment cover on soil infiltration, interrill runoff and erosion. *European J. Soil Sc.*, 52: 59 - 68.
- Cerdan O, Govers G, Le Bissonnais Y, Van Oost K, Poesen J, Saby N, Gobin A, Vacca A, Quinton J, Auerswald K, Klik A, Kwaad FJPM, Raclot D, Ionita I, Rejman J, Rousseva S, Muxart T, Roxo M J and Dostal T (2010). Rates and spatial variations of soil erosion in Europe: A study based on erosion plot data. *Geomorphology*, 122: 167 - 177.
- Cerdan O, Le Bissonnais Y, Souchère V, Martin P and Lecomte V (2002). Sediment concentration in interrill flow: interactions between soil surface conditions, vegetation and rainfall. *Earth Surface Processes and Landforms*, 27: 193 - 205.
- Chang DS and Zhang LM (2011). A Stress-controlled Erosion Apparatus for Studying Internal Erosion in Soils. *Geotechnical Testing J.*, 34(6): 1 - 11.
- Chang DS and Zhang LM (2010). Simulation of the erosion process of landslide dams due to overtopping considering variations in soil erodibility along depth. *Natural Hazards Earth System Science*, 10: 933 - 946.
- Chen YH and Cotton GK (1988). Design of Roadside Channels with Flexible Linings. Report FHWA-IP-87-7, Hydraul. Eng. Circ. No.15 (HEC-15), Washington, DC.
- Choi ECC (2002). Modelling of wind-driven rain and its soil detachment effect on hill slopes. *J. Wind Eng. Industrial Aerodynamics*, 90: 1081 - 1097.

- Choudhary MA, Lal R and Dick WA (1997). Long-term tillage effects on runoff and soil erosion under simulated rainfall for a central Ohio soil. *Soil & Tillage R.*, 42: 175-184.
- Chowdary V, Ramulu G, Shankar S and Prasad CSRK (2012). Influence of unbound material properties on rutting potential of low volume roads. *Elixir Cement and Concrete Composites*, 42: 6377 - 6382.
- Cochrane TA and Flanagan DC (1996). Detachment in a Simulated Rill. *American Society of Agricultural Engineers*, 40(1): 111 - 119.
- Comino JR, Iserloh T, Lassu T, Cerdà A, Keestra SD, Prosdocimi M, Brings C, Marzen M, Ramos MC, Senciales JM, Sinoga JDR, Seeger M and Ries JB (2016). Quantitative comparison of initial soil erosion processes and runoff generation in Spanish and German vineyards. *Science of the Total Environment*, 565: 1165 - 1174.
- Cook JR, Petts R and Rolt J (2013). *Low Volume Rural Road Surfacing and Pavements: A Guide to Good Practice*. OTB Engineering, UK LLP 2013.
- Cook JR, Petts R and Tam DM (2005). The Performance of Low-Volume Unsealed Rural Roads in Vietnam. *Sustainable Access and Local Resource Solutions*, Sept. 28<sup>th</sup> – 30<sup>th</sup>.
- Cook J, Petts R, Visser C and Yiu A (2017). *The Contribution of Rural Transport to Achieve the Sustainable Development Goals*. Research for Community Access Partnership.
- Crim SH Jr, Parker F Jr, Melville J G, Curry JE and Güven O (2003). *Erosion Characteristics of Alabama Soils Obtained with the Erosion Function Apparatus and Correlations with Classification Properties*. ALDOT Highway Research Centre, Project 930-490, Harbert Engineering Center, Auburn University, Alabama 36849.
- Croke J and Mockler S (2001). Gully Initiation and Road to Stream Linkage in a Forested Catchment, South-eastern Australia. *Earth Surface Proc. Landforms*, 26: 205 - 217.

- Croke J, Mockler S, Fogarty P and Ingrid T (2005). Sediment concentration changes in runoff pathways from a forest road network and the resultant spatial pattern of catchment connectivity. *Geomorphology*, 68: 257 - 268.
- De Figueredo T and Poesen J (1998). Effects of surface rock fragment characteristics on interrill runoff and erosion of a silty loam soil. *Soil and Tillage Research*, 46: 81 - 95.
- Demarée GR and Van de Vyver H (2013). Construction of Intensity-Duration-Frequency (IDF) curves for precipitation with annual maxima data for Rwanda, Central Africa. *Advanced Geosciences*, 35, 1–5.
- Dickey EC, Shelton DP, Jasa PJ and Peterson T (1984). Tillage, Residue and Erosion on Moderately Sloping Soils. *Biological Systems Eng.: Papers and Publ.*, Paper 288.
- Dotterweich M (2008). The history of soil erosion and fluvial deposits in small catchments of central Europe: Deciphering the long-term interaction between humans and the environment. A review. *Geomorphology*, 101: 192 - 208.
- Dubé KV, Megahan WF and McCalmon M (2004). *Washington Road Surface Erosion Model: State of Washington: DNR.*
- Durnford D and King JP (1993). Experimental Study of Processes and Particle Size Distributions of Eroded Soils. *J. Irrigation and Drainage Eng.*, 119(2): 383 - 398.
- Edvardsson K (2009). Gravel Roads and Dust Suppression. *Road Materials and Pavement Design*, 10(3): 439 - 469.
- Edwards L, Burney JR, Richter G and MacRae AH (2000). Evaluation of compost and straw mulching on soil-loss characteristics in erosion plots of potatoes in Prince Edward Island, Canada. *Agr., Ecosystems and Environment*, 81: 217 - 222.
- Eigel JD and Moore ID (1983). A Simplified Technique for Measuring Raindrop Size and Distribution. *Trans. Am. Soc. Agric. Biol. Eng.*, 26(4), 1079-1084.

- Ekern PC and Muckenhirn RJ (1947). Water drop impact as a force in transport sand. *Soil Sci. Soc. Am. Proc.*, 12: 441-444.
- Ekwue EI (1990). Effects of Organic Matter on Splash Detachment and the Processes Involved. *Earth Surface Processes and Landforms*, 15: 175 – 181.
- Ekwue EI (1991). The Effects of Soil Organic Matter Content, Rainfall Duration and Aggregate Size on Soil Detachment. *Soil Technology*, 4: 197 - 207.
- Ekwue EI and Stone RJ (1995). Organic Matter Effects on the Strength Properties of Compacted Agricultural Soils. *Trans. ASAE*, 38(2): 357 - 365.
- Ekwue EI, Ohu JO and Wakawa IH (1993). Effects of Incorporating Two Organic Materials at Varying Levels on Splash Detachment of Some Soils from Borno State, Nigeria. *Earth Surface Processes and Landforms*, 18: 399 - 406.
- Elliot WJ (1988). "A process-based rill erosion model", PhD thesis, Iowa State University.
- El-Swaify SA (1997). Factors affecting soil erosion hazards and conservation needs for tropical steep lands. *Soil Technology*, 11: 3 - 16.
- Elwell HA and Stocking MA (1976). Vegetal cover to estimate soil erosion hazard in Rhodesia. *Geoderma*, 15: 61 - 70.
- Erpul G, Gabriels D and Janssens D (1998). Assessing the drop size distribution of simulated rainfall in a wind tunnel. *Soil and Tillage Research*, 45:455 - 463.
- Erpul G, Gabriels D, Cornelis WM, Samray HN and Guzelordu, T (2008). Sand detachment under rains with varying angle of incidence. *Catena*, 72: 413 - 422.
- Erpul G, Gabriels, D and Norton, LD (2005). Sand detachment by wind-driven raindrop. *Earth Surface Processes and Landforms*, 30: 241- 250.
- Erpul G, Norton LD and Gabriels D (2002). Raindrop-induced and wind-driven soil particle transport. *Catena*, 47: 227 - 243.

- Evans, R (2010). Runoff and soil erosion in arable Britain: changes in perception and policy since 1945. *Environmental Science and Policy*, 13: 141 - 149.
- Faiz A (2012). The Promises of Rural Roads. Review of the Role of Low-Volume Roads in Rural Connectivity, Poverty Reduction, Crisis Management and Livability. TRB Low Volume Roads Committee. Circular Number E-C 167.
- Favis-Mortlock D and Boardman J (1995). Nonlinear responses of soil erosion to climate change: a modelling study on the UK South Downs. *Catena*, 25: 365 - 387.
- Fell R, Wan CF, Cyganiewicz J and Foster M (2003). Time for Development of Internal Erosion and Piping in Embankment Dams. *J. Geot. Geoenviron. Eng.*, 129(4): 307 - 314.
- Fernandez-Illescas CP, Porporato A, Laio F and Rodriguez-Iturbe I (2001). The ecohydrological role of soil texture in a water-limited ecosystem. *Water Resources Research*, 37: 2863 - 2872.
- Ferreira T and Rasband W (2012). ImageJ User Guide. <https://imagej.nih.gov/ij/docs/guide>.
- Finnie I (1960). Erosion of Surfaces by Solid Particles. *Wear*, 3: 87 - 103.
- Fitzjohn C, Ternan JL and Williams AG (1998). Soil moisture variability in a semi-arid gully catchment: implications for runoff and erosion control. *Cat.*, 32: 55 - 70.
- Flores-Berrones R, Ramírez-Reynaga M and Macari EJ (2011). Internal Erosion and Rehabilitation of an Earth-Rock Dam. *J. Geot. Geoenviron. Eng.*, 137(2): 150 - 160.
- Foltz RB and Burroughs ER (1990). Sediment production from forest roads with wheel ruts. In *Proceedings from Watershed Planning and Analysis in Action*, ASCE, Durango, CO, July 9–11, 1990. ASCE: Reston, VA pp. 266–275.
- Foltz RB, Copeland NS and Elliot WJ (2009). Reopening abandoned forest roads in northern Idaho, USA: Quantification of runoff, sediment concentration, infiltration, and interrill erosion parameters. *Journal of Environment Management*, 90: 2542 - 2550.

- Foltz RB, Rhee H and Elliot WJ (2008). Modeling changes in rill erodibility and critical shear stress on native surface roads. *Hydrological Processes*, 22: 4783 - 4788.
- Fox DM, Bryan RB and Price AG (1997). The influence of slope angle on final infiltration rate for interrill conditions. *Geoderma*, 80: 181 - 194.
- Fujisawa K, Murakami A and Nishimura S (2010). Numerical Analysis of the Erosion and the Transport of Fine Particles within Soils Leading to the Piping Phenomenon. *Soils and Foundations*, 50(4): 471 - 482.
- Fukubayashi Y and Kimura M (2014). Improvement of rural access roads in developing countries with initiative for self-reliance of communities. *Soils & Found.*, 54(1): 23- 35.
- Fullen MA (1998). Effects of grass ley set-aside on runoff, erosion and organic matter levels in sandy soils in east Shropshire, UK. *Soil and Tillage Research*, 46: 41 - 49.
- Gabet EJ and Sternberg P (2008). The effects of vegetative ash on infiltration capacity, sediment transport, and the generation of progressively bulked debris flows. *Geomorphology*, 101: 666 - 673.
- García-Ruiz JM, Teodoro L and Francisco A (1997). Soil erosion by piping in irrigated fields. *Geomorphology*, 20: 269 - 278.
- Gidigasu MD (1972). Mode of Formation and Geotechnical Characteristics of Laterite Materials of Ghana in Relation to the Soil Forming Factors. *Eng. Geology*, 6: 79 - 150.
- Giménez R and Govers G (2002). Flow Detachment by Concentrated Flow on Smooth and Irregular Beds. *Soil Science Society American J.*, 66: 1475 - 1483.
- Gomes KC, Rocha BD, Ferreira DTA, Lira EC, Torres SM, De Barros SR and Barbosa NB (2012). Activation alkaline waste kaolin for fabrication of building blocks. *Key Eng. Materials*, 517: 622 - 627.

- Gough D, Oliver S, and Thomas J (2017). An introduction to systematic reviews. London: SAGE Publications Ltd.
- Govers G (1985). Selectivity and Transport Capacity of Thin Flows in Relation to Rill Erosion. *Catena*, 12: 35 - 49.
- Greene RSB and Hairsine PB (2004). Elementary Processes of Soil - Water Interaction and Thresholds in Soil Surface Dynamics: A Review. *E. Sur. Proc. Land.*, 29: 1077 - 1091.
- Griesmer ME, Ellis AL and Fristensky A (2008). Runoff Particle Sizes Associated with Soil Erosion in the Lake Tahoe Basin, USA. *Land Degradat. Dev.*, 19: 331–350.
- Grimm M, Jones RJA, Rusco E and Montanarella L (2003). Soil Erosion Risk in Italy: a revised USLE approach. European Soil Bureau Research Report No.11, EUR 20677 EN. Office for Official Publications of the European Communities, Luxembourg.
- Haghighi I, Chevalier C, Duc M, Guédon S and Reiffsteck P (2013). Improvement of Hole Erosion Test and Results on Reference Soils. *J. Geot. Geoenviron. Eng.*, 139(2): 330 - 339.
- Hanson GJ and Hunt SL (2007). Lessons Learned Using Laboratory Jet Method to Measure Soil Erodibility of Compacted Soils. *App. Eng. Agricult.*, 23(3): 305 - 312.
- Henning TF, Alabaster, Arnold G and Liu W (2014). Relationship between Traffic Loading and Environmental Factors and Low-Volume Road Deterioration. *Transp. Res. Record*, No. 2433, pp. 100 - 107.
- Henning TFP, Giummarra GJ, and Roux DC (2008). The development of gravel deterioration models for adoption in a New Zealand gravel road management system (GRMS). *Land Transport NZ Research Report 348*, 96 p.
- Hine J (2014). Promoting the Adoption of Good Policies and Practices on Rural Transport in Africa. *The Planning and Prioritisation of Rural Transport Infrastructure and Services, Sub-Saharan Africa Transport Policy*, Working Paper.

- Horne MA (2017). Design and Construction of a Rainfall Simulator for Large-scale Testing of Erosion Control Practices and Products. Master's Thesis. Auburn University.
- Hossain A (2011). Stabilized Soils Incorporating Combinations of Rice Husk Ash and Cement Kiln Dust. *J. Materials in Civil Eng.*, 23(9): 1320 - 1327.
- Ismail F, Mohamed Z and Mukri M (2008). A Study on the Mechanism of Internal Erosion Resistance to Soil Slope Instability. *Internat. J. Geot. Eng.*, Vol. 13, Bund. A.
- Issa OM, Le Bissonnais Y, Planchon O, Favis-Mortlock D, Silvera N and Wainwright J (2006). Soil detachment and transport on field- and laboratory-scale interrill areas: erosion processes and the size-selectivity of eroded sediment. *E. Sur. Proc. Land.*, 31: 929 - 939.
- Istanbulluoglu E, Bras RL and Homero F-C (2005). Implications of bank failures and fluvial erosion for gully development: Field observations and modeling. *J. Geographic. Res.*, 110: 1 - 2.
- Iverson RM (1980). Processes of Accelerated Pluvial Erosion on Desert Hillslopes Modified by Vehicular Traffic. *Earth Surface Proc.*, 5: 369 - 388.
- Jayawardena AW and Rezaur RB (2000). Drop size distribution and kinetic energy load of rainstorms in Hong Kong. *Hydrological Processes*, 14: 1069-1082 (2000)
- Johnson AI (1963). A field method for measurement of infiltration, US Govern. Printing Office.
- Jordán A, Zavala LM and Gil J (2010). Effects of mulching on soil physical properties and runoff under semi-arid conditions in southern Spain. *Catena*, 81: 77 - 85.
- Jungerius PD, Matundura J and Van de Ancker JAM (2002). Road Construction and Gully Erosion in West Pokot, Kenya. *Earth Surf. Proc. Land.*, 27: 1237 - 1247.
- Karamage F, Zhang C, Fang X, Liu T, Ndayisaba F, Nahayo L, Kayiranga A and Nsengiyumva JB (2017). Modeling Rainfall-Runoff Response to Land Use and Land Cover Change in Rwanda (1990–2016). *Water*, 9: 147.

- Kathiravelu G, Lucke T and Nichols (2016). Rain Drop Measurement Techniques: A Review. *Water* 8(29): 1 - 20.
- Katz HA, Daniels JM and Ryan SE (2011). Rates of gully erosion along Pikes Peak Highway, Colorado, USA. *Landform Analysis*, 17: 75 - 80.
- Katz HA, Daniels JM and Ryan SE (2013). Slope-area thresholds of road-induced gully erosion and consequent hillslope–channel interactions. *Earth Surf. Proc. Landforms*.
- Kelkar, VN (1959). Size distribution of raindrops - Part II. *Indian J. Meteo. Geoph.*, 4: 323-330
- Keller G and Sherar J (2003). *Low-Volume Roads Engineering. Best Management Practices Field Guide*. US Agency for International Development.
- Kerényi A (1981). A study of dynamics of drop erosion under laboratory conditions, in *Erosion and Sediment Transport Measurement*. IAHS Publ., 133: 365 - 372.
- Kinnell PIA (2005). Raindrop-impact-induced erosion processes and prediction: a review. *Hydrological Pr.*, 19: 2815 - 2844.
- Knapen A, Poesen J, Govers G, Gyssels G and Nachtergaele J (2007). Resistance of soils to concentrated flow erosion: A review. *Earth-Science Rev.*, 80: 75 - 109.
- Kukul SS, Sur HS and Gil SS (1991). Factors responsible for soil erosion hazard in submontane Punjab, India. *Soil Use and Management*, 7 (1): 38 - 44.
- Kuliffayova M, Krajci L, Janotka I and Šmatko V (2012). Thermal behaviour and characterization of cement composites with burnt kaolin sand. *J. Thermal Analysis and Calorimetry*, 108: 425-432.
- Lachouette D, Gola F and Bonelli S (2008). One-dimensional modeling of piping flow erosion. *C. R. Mecanique*, 336: 731 - 736.
- Laflen JM and Flanagan DC (2013). The development of U.S soil erosion prediction and modelling. *International Soil and Water Conservation Research*, 1(2): 1 - 11.

- Lafren JM, Elliot WJ, Simanton JR, Holzhey CS and Kohl KD (1991). WEPP: Soil Erodibility Experiments for Rangeland and Cropland Soils. *J. Soil Water Cons.*, 46(1): 39 - 44.
- Lafren, JM., Flanagan DC and Bernard AE (2004). Soil Erosion and Sediment Yield Prediction Accuracy Using WEPP. *J. Am. Water Res. Ass.*, 40(2):289 - 297.
- Lal R (1994). *Soil Erosion Research Methodology*. Soil Cons. Soc. Am., Ankeny, IA.
- Lane PNJ and Sheridan GJ (2002). Impact of an Unsealed Forest Road Stream Crossing: Water Quality and Sediment Sources. *Hydrological Processes*, 16: 2599 - 2612.
- Laws JO and Parson DA (1943). The relation of raindrop-size to intensity. *Transactions of the American Geographical Union, Papers Hydrology*, 453 - 460.
- Le Bissonnais Y, Cerdan O, Lecomte V, Benkhadra H, Souchère V, Martin M (2005). Variability of soil surface characteristics influencing runoff and interrill erosion. *Catena*, 62: 111 - 124.
- Leguédou S and Le Bissonnais Y (2004). Size Fractions Resulting from an Aggregate Stability Test, Interrill Detachment and Transport. *Earth Sur. Pro. Landforms*, 29: 1117 - 1129.
- Li Z-W, Zhang G-H, Geng R, and H Wang (2015). Rill erodibility as influenced by soil and land use in a small watershed of the Loess Plateau, China. *Biosys. Eng.*, 129: 248 - 257.
- Lili M, Bralts VF, Yinghua P, Han L, Tingwu L (2008). Methods for measuring soil infiltration: State of the art. *International Journal of Agricultural and Biological Eng.*, 1(1): 22 - 30.
- Liu G, Tian FX, Warrington DN, Zheng SQ and Zhang Q (2010). Efficacy of Grass for Mitigating Runoff and Erosion from an Artificial Loessial Earthen Road. *J. Am. Society Agricultural Biological Eng.*, 53 (1): 119 - 125.
- Liu Y-J, Hu J-M, Wang T-W, Cai Ch-F, Li Z-X and Zhang Y (2016). Effects of vegetation cover and road-concentrated flow on hillslope erosion in rainfall and scouring simulation tests in the Three Gorges Reservoir Area, China. *Catena*, 136: 108 -117.

- Liu, G. and Zheng, S. (2010). Impact of Planting Grass on Loessial Earthen Road with Different Slope Gradients to Avoid Runoff and Erosion. The 2010 WASE Int. Conference on Information Eng., p. 171 - 176.
- Loch RJ, Slater BK and Devoil C (1998). Soil erodibility (Km) values for some Australian soils. Australian J. Soil Research, 36: 1045 - 1055.
- Lotfy A, Karahan O, Ozbay E, Hossain KMA and Lachemi M (2015). Effect of kaolin waste content on the properties of normal-weight concretes. J. Construction and Building Materials, 83: 102-107.
- Lu J, Zheng F, Li G, Bian F and An J (2016). The effects of raindrop impact and runoff detachment on hillslope soil erosion and soil aggregate loss in the Mollisol region of Northeast China. Soil and Tillage Research, 161: 79 - 85.
- Luce CH and TA Black (1999). Sediment Production from Forest Roads in Western Oregon. Water Resources Research, 36(8): 2561-2570.
- Luk SH (1979). Effect of Soil Properties on Erosion by Wash and Splash. Earth Surface Processes, 4: 241 - 255.
- Luo H, Zhao T, Dong M, Gao J, Peng X, Guo Y, Wang Z and Liang C (2013). Field studies on the effects of three geotextiles on runoff and erosion of road slope in Beijing. Catena, 109: 150 - 156.
- Lye C, Dhir R and Ghataora G (2015). Elastic modulus of concrete made with recycled aggregates. Institution of Civil Engineers, Structures and Buildings, 169 (5): 314-339.
- Lyles L, Dickerson JD and Schmeidler NF (1974). Soil Detachment from Clods by Rainfall: Effects of Wind, Mulch Cover, and Initial Soil Moisture. ASAE, 17(4): 697 - 700.
- MacDonald LH, Anderson DM, Dietrich WE (1997). Paradise Threatened: Land Use and Erosion on St John Virgin Island. Environmental Manag., 21(6): 851 - 863.

- MacDonald LH, Sampson RW and Anderson DM (2001). Runoff and Road Erosion at the Plot and Road Segment Scales, St John, US Virgin Islands. *E. Sur. Pr. L.*, 26: 251 - 272.
- McCarthy CJ (1980). Sediment transport by rain splash. Ph.D. thesis. University of Washington, Seattle, USA.
- Maharaj A (2011). The Use of the Crumb Test as a Preliminary Indicator of Dispersive Soils. Proceedings of the 15th African Regional Conference on Soil Mechanics and Geotechnical Engineering. C. Quadros and S.W. Jacobsz (Eds.) IOS Press, 299 - 306.
- Maharaj, A and Paige-Green, P (2013). The SCS Double Hydrometer Test in dispersive Soil identification. Proceedings of the 18th International Conference on Soil Mechanics and Geotechnical Engineering. Paris, France, pp. 389 - 392.
- Masannat YM (1980). Development of piping erosion conditions in the Benson area, Arizona, U.S.A. *Quarterly J. of Eng. Geology*, 13: 53 - 61.
- Meyer LD and Harmon WC (1984). Susceptibility of agricultural soils to inter-rill erosion. *Soil Science Society American J.*, 48: 1152 - 1157.
- MLRRB-Minnesota Local Road Research Board (2003). Erosion Control Handbook for Local Roads. Manual No, 2003 - 08.
- Mizugaki S, Nanko K and Onda Y (2010). The effect of slope angle on splash detachment in an unmanaged Japanese cypress plantation forest. *Hydrological Proc.*, 24: 576 - 587.
- Mohyont B, Demarée GR, Faka DN (2004). Establishment of IDF-curves for precipitation in the tropical area of Central Africa - comparison of techniques and results. *Natural Hazards and Earth System Science*, 4 (3): 375 - 387.
- Moore ID and Burch GJ (1986). Sediment Transport Capacity of Sheet and Rill Flow: Application of Unit Stream Power Theory. *Water Resources Res.*, 22(8): 1350 - 1360.

- Moore ID, Hirschi MC and Barfield BJ (1983). Kentucky Rainfall Simulator. *Trans. Am. Society of Agricultural and Biological Eng.*, 26(4): 1085 - 1089.
- Moore JS (2001). Predicting Interparticle Bond Shear Strength Number of the Headcut Erodibility Index from Soil Index Tests. *Proceedings of the Seventh Federal Interagency Sedimentation Conference, March 25 - 29, 2001, Reno, NV*, pp 9 - 14.
- Morgan RPC (1978). Field Studies of Rainsplash Erosion. *Earth Surface Proc.*, 3: 295 - 299.
- Morgan RPC, Morgan DDV and Finney HJ (1984). A Predictive Model for the Assessment of Soil Erosion Risk. *J. Agricultural Eng. Research*, 30: 245 - 253.
- Morgan RPC, Quinton JN, Smith RE, Govers G, Poesen JWA, Auerswald K, Chisci G, Torri D, Styczen ME and Folly AJV (1998). The European soil erosion model (EUROSEM): documentation and user guide. Silsoe College, Cranfield University.
- Morin J and Benyamin Y (1977). Rainfall Infiltration into Bare Soils. *Water Resources Research*, 13(5): 813 - 817.
- Mu W, Yu F, Li C, Xie Y, Tian J, Liu J and Zhao N (2015). Effects of Rainfall Intensity and Slope Gradient on Runoff and Soil Moisture Content on Different Growing Stages of Spring Maize. *Water*, 7: 2990 - 3008.
- Musgrave GW (1947). The quantitative evaluation of factors in water erosion- a first approximation. *Journal of Soil and Water Conservation*, 2(3): 133 – 138.
- Mutreja KN (199). *Applied Hydrology*. New Delhi: Tata McGraw-Hill.
- Nagy G and Nagy L (2015). Identification and Treatment of Erodible Clays in Dikes. *Geotechnical Safety and Risk*, V.T. Schweckendiek et al. (Eds.), 535 - 539.
- Nanko K, Mizugaki S and Onda Y (2008). Estimation of soil splash detachment rates on the forest floor of an unmanaged Japanese cypress plantation based on field measurements of throughfall drop sizes and velocities. *Catena*, 72: 348 - 361.

- Nearing MA and Bradford JM (1985). Single Waterdrop Splash Detachment and Mechanical Properties of Soils. *Soil Science Society American J.*, 29: 547 - 552.
- Nearing MA, Bradford JM and Parker SC (1991). Soil Detachment by Shallow Flow at Low Slopes. *Soil Science Society American J.*, 55: 339 - 344.
- Nearing MA, Foster GN, Lane LJ and Finkner SC (1989). A Process - Based Soil Erosion Model for USDA-Water Erosion Prediction Project Technology. *American Society of Agricultural Engineers*, 32 (5): 1587 - 1593.
- Nearing MA, Jetten V, Baffaut C, Cerdan O, Couturier A, Hernandez M, Le Bissonnais Y, Nichols MH, Nunes JP, Renschler CS, Souchère V and van Oost K (2005). Modeling response of soil erosion and runoff to changes in precipitation and cover. *Catena*, 61: 131- 154.
- Nearing MA, Simanton JR, Norton LD, Bulyigin SG and Stone J (1999). Surface Erosion by Surface Water Flow on a Stony Semi-Arid Hillslope. *E. Sur. Proc. Land.*, 24: 677 - 684.
- Ngezahayo E, Burrow MPN and Ghataora GS (2019a). Rainfall Induced Erosion of Soils Used in Earth Roads. In Tarantino, A & Ibraim, E (Eds), 7th Int. Symposium on Deformation Characterisation of Geomaterials, ISBN 978-2-7598-9064-4, Vol. 92 (17006), EDP Sc.
- Ngezahayo E, Burrow MPN and Ghataora GS (2019b). The Advances in Understanding Erodibility of Soils in Unpaved Roads. *Int. Journal of Civil Infrastructure*, 2: 18-29.
- Ngezahayo E, Ghataora G and Burrow M (2019c). Evaluation of the influence of geotechnical, environmental and road aspects on erodibility of rural roads. *Int. Journal of Latest Engineering and Management Research (IJLEMR, ISSN: 2455-4847)*, 04 (11): 29-54.
- Ngezahayo E, Burrow M and Ghataora G (2019d). Rural Roads –roles, challenges and solutions for Sub-Saharan Africa’s sustainable development. *Int. Journal of Latest Engineering and Management Research (IJLEMR, ISSN: 2455-4847)*, 04 (10): 70-79.

- Ngezahayo E, Burrow MPN and Ghataora GS (2019e). Rainfall Induced Erosion of Soils Used in Earth Roads. Proceedings of the 7th Int. Symposium on Deformation Characteristics of Geomaterials, IS- Glasgow, UK, 26th – 28th June, E3S Web of Conferences 92: 17006, 2019. Available at <https://doi.org/10.1051/e3sconf/20199217006>.
- Ngezahayo E, Ghataora GS and Burrow MPN (2019f). Factors Affecting Erosion in Unpaved Roads. Proceedings of the 4th World Congress on Civil, Structural and Environmental Engineering (CSEE'19), Rome, Italy, April 7 – 9. Paper No. ICGRE 108. Available at [http://avestia.international-aset.com/CSEE2019\\_Proceedings](http://avestia.international-aset.com/CSEE2019_Proceedings).
- Noble Christine A and Morgan RPC (1983). Rainfall Interception and Splash Detachment with a Brussels sprouts plant: A laboratory Simulation. *Earth Sur. Pro. Land.*, 8: 569 - 577.
- Nwankwor GI, Udoka UP, Egboka BC and Opara AI (2015). The Mechanics of Civil –Works Induced Gully Erosion: Applications to Development of Preventive Measures in South Eastern Nigeria. *Applied Ecology and Environmental Sciences*, 3 (2): 60 - 65.
- Obi ME and Salako FK (1995). Rainfall parameters influencing erosivity in Southeastern Nigeria. *Catena*, 24: 275- 287.
- Paige-Green P (1999). Geological Factors Affecting Performance of Unsealed Road Materials. *J. Transport Research Board*, 1652: 10 - 15.
- Paige-Green P (2003). Strength and Behavior of Materials for Low-Volume Roads as Affected by Moisture and Density. 8th International Conference on Low-Volume Roads, Reno, Nevada, June 22 -25. *Transportation Res. Record* 1819(2): 104 - 109.
- Paige-Green P (2006). Appropriate Roads for Rural Access. Third Gulf Conf. on Roads (TGCR06), March 6 – 8. Pretoria, South Africa: CSIR Built Environ.
- Paige-Green P (2008). Dispersive and erodible soils - fundamental differences. Problem soils in SA conference, Midrand, Gauteng, Nov. 3 – 4, Pretoria, CSIR Built Environment.

- Paige-Green P, Pinard M and Netterberg F (2015). A review of specifications for lateritic materials for low volume roads. *Transportation Geotechnics*, 5: 86 - 98.
- Parker DB, Michel TG and Smith JL (1995). Compaction and Water Velocity Effects on Soil Erosion in Shallow Flow. *J. Irrigation and Drainage Eng.*, 121(2): 170 - 178.
- Pedersen HS and Hasholt B (1995). Influence of wind speed on rain-splash erosion. *Catena*, 24: 39 - 54.
- Pelletier JD (2011). Fluvial and slope-wash erosion of soil-mantled landscapes: detachment- or transport-limited? *Earth Surface Processes and Landforms*.
- Petts R (2013). How much should developing countries spend on road maintenance? Briefing Note. Intech Asset Management, UK&AFCAP Steering Group, pp. 1 - 10.
- Petts R, Cook J, Tuan PG, Dzung BT and Kackada H (2006). Rural Road Surfacing Research for Sustainable Access and Poverty Reduction in South East Asia. Indian Roads Congress. International Seminar on "Innovations in Construction and Maintenance of Flexible Pavements", Agra, Sept. 1 - 4, Construction and Maintenance of LV Roads.
- Pham TL (2008). Erosion et dispersion des sols argileux par un fluide. *Sciences de l'ingénieur [physics]*. These de Doctorat. Ecole des Ponts ParisTech. Français.
- Poesen J and Savat J (1981). Detachment and Transport of Loose Sediment by Raindrop Splash. Part 2: Detachability and Transportability Measurements. *Catena*, 8: 19 - 41.
- Poesen J, Nachtergaele J, Verstraeten G and Valentin C (2003). Gully erosion and environmental change: importance and research needs. *Catena*, 50: 91 - 133.
- Powledge GR, Ralston DC, Miller P, Chen YH, Clopper PE and Temple DM (1989). Mechanics of Overflow Erosion on Embankments. II: Hydraulic and Design Considerations. *J. Hydraulic Eng.*, 115 (8): 1056 - 1077.

- Quansah C (1981). The Effect of Soil Type, Slope, Rain Intensity, and their Interactions on Splash Detachment and Transport. *Journal of Soil Science*, 32: 215 - 224.
- Ramos–Scharrón CE and MacDonald LH (2005). Measurement and Prediction of Sediment Production from Unpaved Roads. *Earth Surf. Proc. Landforms*, 30: 1283 - 1304.
- RapidMiner GmbH (2019). RapidMiner 9. Operator Reference Manual. Available at [www.rapidminer.com](http://www.rapidminer.com).
- Rashad AM (2013). Alkali-activated metakaolin: A short guide for civil Engineer-An overview. *Construction and Building Materials*, 41: 751-765.
- Rashad AM (2015). Metakaolin: Fresh properties and optimum content for mechanical strength in traditional cementitious materials - A comprehensive overview. *Reviews on Advanced Materials Science*, 40: 15-44.
- Rauws G and Govers G (1988). Hydraulic and Soil Mechanical Aspects of Rill Generation on Agricultural Soils. *Journal of Soil Science*, 39: 111 - 128.
- Reichert JM, Schafer MJ, Cassol EA and Norton LD (2001). "Interrill and rill erosion on a tropical sandy loam soil affected by tillage and consolidation". The 10th Int. Soil Conservation Organization Meeting, Purdue University and the USDA-ARS Nat. Soil Erosion Lab., May 24 - 29, 1999.
- Renard KG, Foster GR, Weesies GA, McCool DK and Yoder DC (1997). Predicting soil erosion by water. A guide to conservation planning with the Revised Universal Soil Loss Equation (RUSLE). *Agricultural Handbook No. 703*, USDA, Washington, pp. 384.
- Ricks MD, Horne MA, Faulkner B, Zech C, Fang X, Donald WN and Perez MA (2019). Design of a Pressurized Rainfall Simulator for Evaluating Performance of Erosion Control Practices. *Water* 2019, 11, 2386.

- Rienzi EA, Fox JF, Grove JH, Matocha CJ (2013). Interrill erosion in soils with different land uses: The kinetic energy wetting effect on temporal particle size distribution. *Catena*, 107: 130 - 138.
- Riezebos, H TH and Epima, GF (1985). Drop Shape and Erosivity, Part 2: Splash Detachment, Transport and Erosivity Indices. *E. Surf. Proc. Land.*, 10: 69 - 74.
- Rijsdijk A, Bruijnzeel LAS and Sutoto C K (2007). Runoff and sediment yield from rural roads, trails and settlements in the upper Konto catchment, East Java, Indonesia. *Geomorphology*, 87: 28 - 37.
- Riverson J, Gaviria J and Thriscutt S (1991). Rural Roads in Sub-Sahara Africa: Lessons from World Bank Experience. The WB Tech. Paper 141. Africa Techn. Department Series.
- Robinson KM and Hanson GJ (2001). Headcut Erosion Research. Proceedings of the 7th Federal Interagency Sedimentation Conference, March 25 - 29, Reno, Nevada.
- Sabir BB, Wild S and Bai J (2001). Metakaolin and calcined clays as pozzolans for concrete: a review. *Cement and Concrete Composites*, 23: 441 - 454.
- Salles C and Poesen J (2000). Rain properties controlling soil splash detachment. *Hydrological Processes*, 14: 271 - 282.
- Salles C, Poesen J and Govers G (2000). Statistical and physical analysis of soil detachment by raindrop impact: Rain erosivity indices and threshold energy. *Water Resources Research*, 36 (9): 2721 - 2729.
- Savat J and Poesen J (1981). Detachment and Transportation of Loose Sediment by Raindrop Splash, Part 1: The Calculation of Absolute Data on Detachability and Transportability. *Catena*, 8: 1 - 17.
- Shao Y and Lu H (2000). A simple expression for wind erosion threshold friction velocity. *Journal of Geophysical Research*, 105(17): 22437 - 22443.

- Sharma PP and Gupta SC (1989). Sand detachment by single raindrops of varying kinetic energy and momentum. *Soil Sci. Soc. Am. J.*, 53: 1005 - 1010.
- Sharma PP, Gupta SC and Rawls WJ (1991). Soil detachment by single raindrops of varying kinetic energy. *Soil Sci. Soc. Am. J.*, 55: 301 - 307.
- Shearer D, Ziegler T and Nevel E (2013). What is new with driving surface aggregates? Potential upcoming additions to specification information for pavement management field trip. Centre for Dirt and Gravel Road Studies, Pennsylvania State, USA.
- Sheppard DM, Bloomquist D and Slagle PM (2006). Rate of Erosion Properties of Rock and Clay. UF Project 00030890 (4554013-12), Final Report, Department of Civil and Coastal Engineering, University of Florida, Gainesville, Florida 32611.
- Sheridan GJ, Noske PJ, Lane PNJ and Sherwin CB (2008). Using rainfall simulation and site measurements to predict annual interrill erodibility and phosphorus generation rates from unsealed forest roads: Validation against in-situ erosion measurements. *Catena*, 73: 49 - 62.
- Siegrist S, Schaub D, Pfiffner L and Mäder P (1998). Does organic agriculture reduce soil erodibility? The results of a long-term field study on loess in Switzerland. *Agric. Ecosystems and Environment*, 69: 253 - 264.
- Smith DD (1941). Interpretation of soil conservation data for field use. *Agricultural Engineering*, 22(5): 173 – 175.
- Smith JA, Hui E, Steiner M, Baeck ML, Krajewski WF and Ntelekos AA (2009). Variability of rainfall rate and raindrop size distributions in heavy rain. *Water Resources Research*, vol. 45, W04430.

- Smith V, Devane D, Begley CM and Clarke M (2011). Methodology in conducting a systematic review of systematic reviews of healthcare interventions. *BMC Medical Research Methodology*, 11(15): 1 – 6.
- Soroush A, Shourijeh, PT and Mohammadinia A (2011). Controlling internal erosion in earth dams and their foundations: case studies. *Pr. Indian Geot. Conf.*, Dec. 15 - 17, 2011.
- Sperinck S, Raiteri P, Marks N and Wright K (2011). Dehydroxylation of kaolinite to metakaolin-a molecular dynamics study. *J. Materials Chemistry*, 21: 2118 - 2125.
- Stroosnijder L (2005). Measurement of erosion: Is it possible? *Catena*, 64: 162 - 173.
- Sugden BD and Scott WW (2007). Sediment Production from Forest Roads in Western Montana. *J. American Water Resources Association*, 43(1): 193 - 206.
- Sutherland RA and Ziegler AD (1998). The influence of the soil conditioner ‘Agri-SC’ on splash detachment and aggregate stability. *Soil and Tillage Research*, 45: 373 - 387.
- Svoray T and Markovitch H (2009). Catchment scale analysis of the effect of topography, tillage direction and unpaved roads on ephemeral gully incision. *Earth Surface Processes and Landforms*, 34: 1970 - 1984.
- Swift LW, Jr (1984). Gravel and Grass Surfacing Reduces Soil Loss from Mountain Roads. *Forestry Sciences*, 30: 657 - 670.
- Swift LW, Jr (1985). Soil Losses from Roadbeds and Cut and Fill Slopes in the Southern Appalachian Mountains. *Southern Journal of Applied Forestry*, 8(4): 209 - 213.
- Temple DM and Hanson GJ (1994). Headcut Development in Vegetated Earth Spillways. *Applied Engineering in Agriculture*, 10 (5): 677 - 682.
- Tengbeh GT (1993). The Effect of Grass Roots on Shear Strength Variations with Moisture Content. *Soil Technology*, 6: 287 - 295.

- Thomas Christine (2017). A case study of runoff coefficients for urban areas with different drainage systems. Master's Thesis. Water and Envir. Eng., Lund University, Sweden.
- Tiwari AL, Risse LM and Nearing MA (2000). Evaluation of WEPP and its comparison with USLE and RUSLE. *Trans. Amer. Soc. Agric. Eng.*, 4(5): 129 – 1135.
- Torfs H, Mitchener H, Huysentruyt H, and Toorman, E (1996). Settling and consolidation of mud/sand mixtures. *Coastal Engineering*, 29: 27 - 45.
- Torero M and Chowdhury S (2005). Increasing access to infrastructure for Africa's rural poor, IFPRI: 2020 Africa Conference Brief. Workshop 16.
- Torri D and Poesen J (1992). The Effect of Soil Surface Slope on Raindrop Detachment. *Catena*, 19: 561 - 578.
- Torri D, Sfalanga M and Firenze MDS (1987). Splash Detachment: Runoff Depth and Soil Cohesion. *Catena*, 14: 149 - 155.
- Tossell RW, Dickinson WT, Rudra RP and Wall GJ (1987). A Portable Rainfall Simulator. *Canadian Agricultural Engineering*, 29(2):155 - 162.
- Usman LS (2011). Systematic Reviews and Meta-Analyses. *J. Canadian Academy Child and Adolescent Psychiatry*, 20 (1): 57 – 59.
- Van der Knijff JM, Jones RJA and Montanarella L (1999). Soil Erosion Risk Assessment in Italy. Eur. Comm. Directorate General Joint Res. Centre, Space Applications Institute.
- Van Dijk AIJM, Meesters AGCA and Bruijnzeel LA (2002). Exponential distribution theory and the interpretation of splash detachment and transport experiment. *Soil Sc. Society of America J.*, 66(5): 1466 - 1474.
- Van Klaveren RW and McCool DK (2010). Freeze–Thaw and Water Tension Effects on Soil Detachment. *Soil Science Society American J.*, 74 (4): 1327 - 1338.

- Wagesho N and Claire M (2016). Analysis of Rainfall Intensity-Duration-Frequency Relationship for Rwanda. *Journal of Water Resource and Protection*, 8: 706 - 723
- Walling DE and Probst J-L (1997). Human Impact on Erosion and Sedimentation, Proceedings of Rabat Symposium S6, April 1997. IAHS Publ. No. 245.
- Wan CF and Fell R (2004). Laboratory Tests on the Rate of Piping Erosion of Soils in Embankment Dams. *Geotechnical Testing Journal*, 27(3): 1 - 9.
- Wang B, Zhang G-H, Shi Y-Y, Zhang XC (2014). Soil detachment by overland flow under different vegetation restoration models in the Loess Plateau of China. *Cate.*, 116: 51-59.
- Wang B, Zheng F, Römken JM Mathias and Darboux F (2013). Soil erodibility for water erosion: A perspective and Chinese experiences. *Geomorphology*, 187:1 - 10.
- Wilson MJ (1999). The Origin and Formation of Clay Minerals in soils: Past, Present and Future Perspectives. *Clay Minerals* 34, 735. Macaulay Land Use Research Inst., Aberdeen, UK.
- Wischmeier WH and Mannering JV (1969). Relation of Soil Properties to its Erodibility. *Soil Science Society of America Proc.*, 33: 131 - 137.
- Wischmeier WH and Smith DD (1965). Predicting rainfall-erosion losses from cropland east of the Rocky Mountains. *Agric. Handbook 282*, USDA, Agric. Res. Services.
- Wischmeier WH and Smith DD (1978). Predicting Rainfall Erosion Losses – a guide to conservation planning. US Department of Agriculture. *Agriculture Handbook No 537*.
- World Bank (2008). Safe, Clean and Affordable Transport for Development. The World Bank Group's Transport Business Strategy 2008 - 2012.
- World Factbook (2017). Listing Roadways Field [Online, Accessed on 27<sup>th</sup> September 2018]. <https://www.cia.gov/library/publications/the-world-factbook/rankorder/2085rank.html>

- Wuddivira MN, Stone RJ and Ekwue EI (2009). Clay, Organic Matter, and Wetting Effects on Splash Detachment and Aggregate Breakdown under Intense Rainfall. *Soil Science Society American Journal*, 73: 226 - 232.
- Yarbařt N, Kalkan E, and Akbulut S (2007). Modification of the geotechnical properties, as influenced by freeze–thaw, of granular soils with waste additives. *Cold Regions Science and Technology*, 48: 44 - 54.
- Yariv S (1976). Comments on the Mechanism of Soil Detachment by Rainfall. *Geoderma*, 15: 393 - 399.
- Yu Y-C, Zhang G-H, Geng R and Sun L (2014). Temporal variation in soil detachment capacity by overland flow under four typical crops in the Loess Plateau of China. *Biosystems Engineering*, 122: 139 - 148.
- Zanchi C and Torri D (1980). Evaluation of rainfall energy in central Italy. In *Assessment of Erosion*, De Boodt M, Gabriels D (eds), Wiley: Chichester; 133-142
- Zhang G–H, Liu B–Y, Nearing MA, Huang C–H and Zhang K L (2001). Soil Detachment by Shallow Flow. *Trans. ASAE*, 45 (1): 1 - 8.
- Zhang G-H, Liu G-B, Tang KM, Zhang XC (2008). Flow Detachment of Soils under Different Land Uses in the Loess Plateau of China. *Trans. ASABE*, 51 (3): 883 - 890.
- Zhang G-H, Liu Y-M, Han Y-F and Zhang XC (2009). Sediment Transport and Soil Detachment on Steep Slopes: I. Transport Capacity Estimation. *Soil Science Society America J.*, 73 (4): 1291 - 1297.
- Zhang LT, Gao ZL, Li ZB and Tian HW (2016). Downslope runoff and erosion response of typical engineered landform to variable inflow rate patterns from upslope. *Natural Hazards*, 80: 775 - 796.

- Zhang L-T, Gao Z-L, Yang S-W, Li Y-H and Tiand H-W (2015). Dynamic processes of soil erosion by runoff on engineered landforms derived from expressway construction: A case study of typical steep spoil heap. *Catena*, 128:108 - 121.
- Zhang XC and Nearing MA (2005). Impact of climate change on soil erosion, runoff, and wheat productivity in central Oklahoma. *Catena*, 61: 185 - 195.
- Zhu TX (2012). Gully and tunnel erosion in the hilly Loess Plateau region, China. *Geomorph.*, 153 - 154: 144 - 155.
- Ziegler AD, Giambelluca TW, Nullet MA, Sutherland RA, Yarnasarn S, Pinthong J, Preechapanya P and Jaiaree S (2004). Towards understanding the cumulative impacts of roads in upland agricultural watersheds of northern Thailand. *Agr. Ecosystems Environment*, 104: 145 - 158.
- Ziegler AD, Giambelluca TW, Sutherland RA, Vana, TT and Nullet MA (2001). Horton overland flow contribution to runoff on unpaved mountain roads: A case study in northern Thailand. *Hydrology Processes*, 15: 3203 - 3208.
- Ziegler AD, Sutherland RA and Giambelluca TW (2000). Partitioning total erosion on unpaved roads into splash and hydraulic components: The roles of interstorm surface preparation and dynamic erodibility. *Water Resources Research*, 36(9): 2787 - 2791.
- Ziegler AD, Sutherland RA and Giambelluca TW (2001). Interstorm Surface Preparation and Sediment Detachment by Vehicle Traffic on Unpaved Mountain Roads. *Earth Surface Processes and Landforms*, 26: 235-250.
- Zingg AW (1940). Degree and length of land slope as it affects soil loss in runoff. *Agricultural Engineering*, 21(2): 59 – 64.
- Zuazo VHD and Pleguezuelo CRR (2008). Soil-erosion and runoff prevention by plant covers. A review. *Agronomy Sustainable Development*, 28: 65 – 86.

APPENDICES

Appendix 1

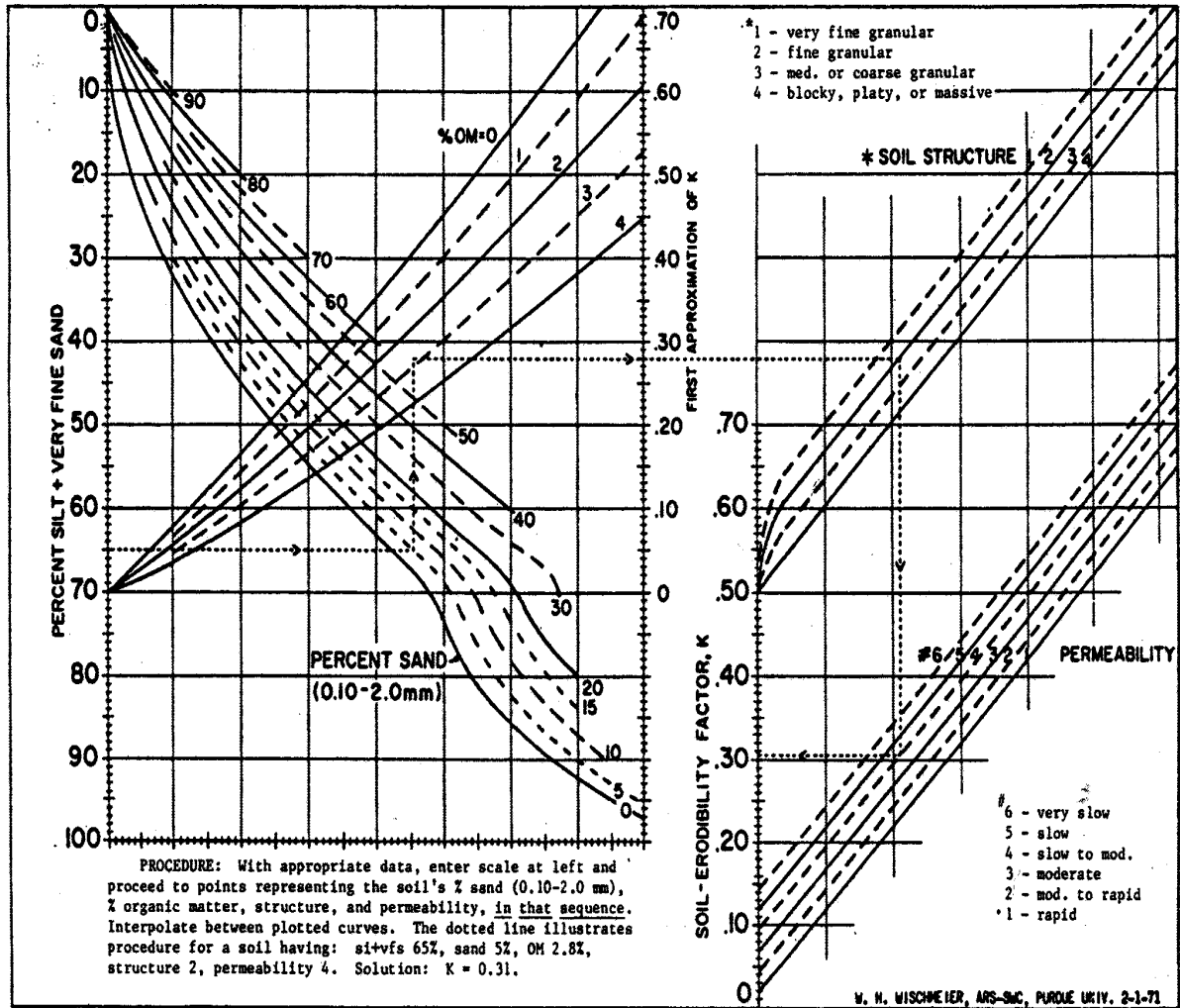


Figure 1. Soil-erodibility nomograph (after Wischmeier and Smith, 1978). For conversion to SI, divide K values of this nomograph by 7.59. K is in U.S. customary units.

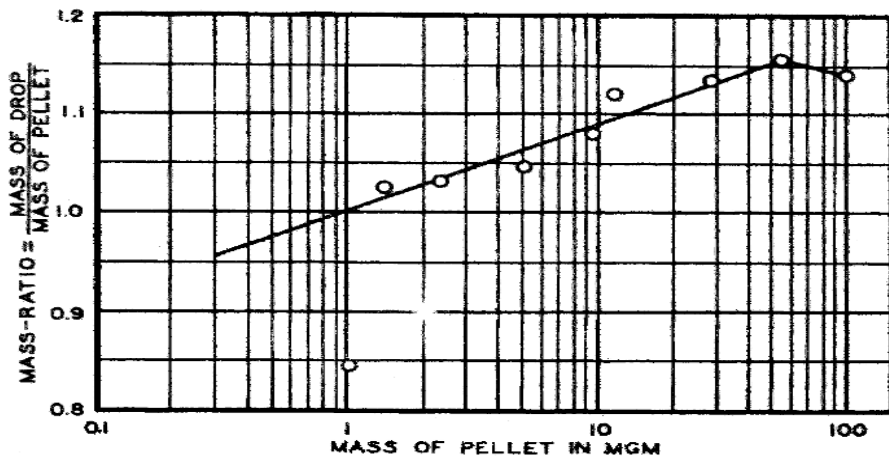
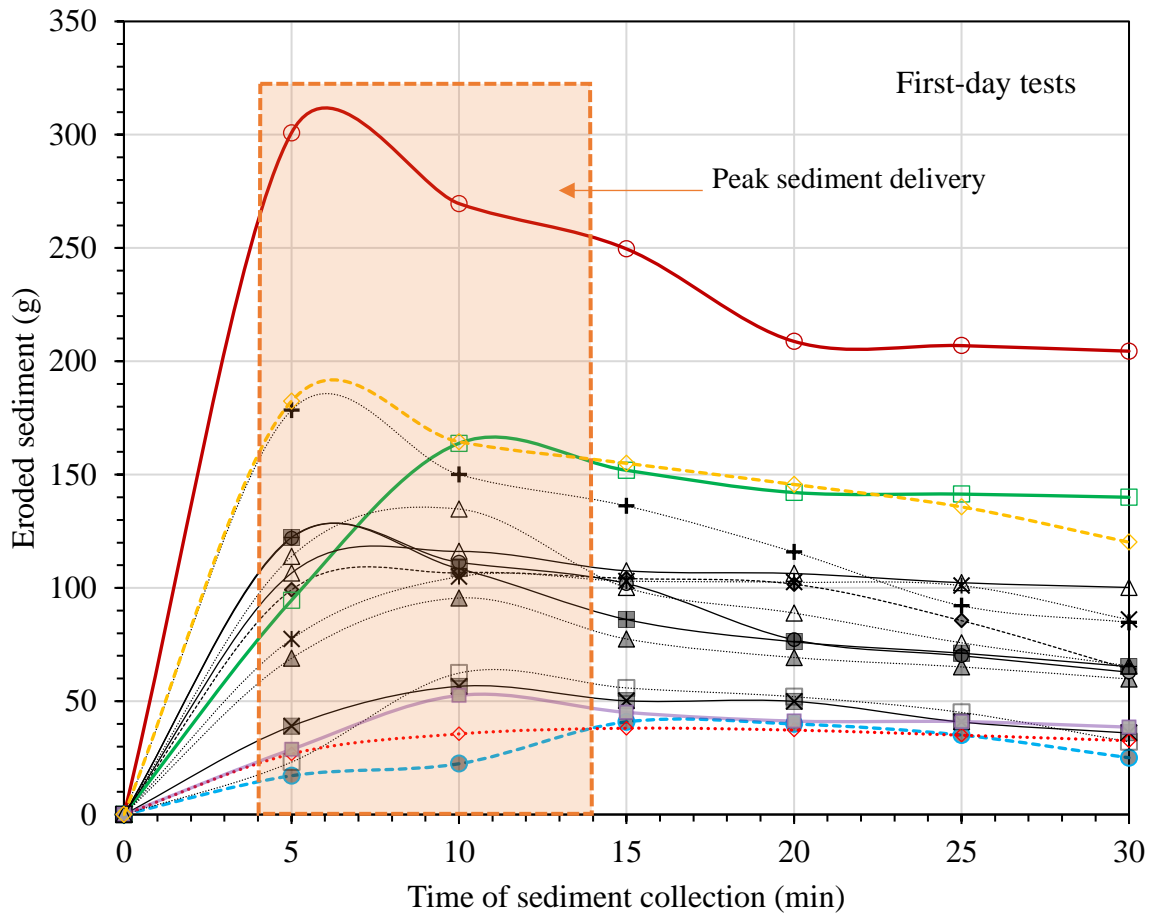


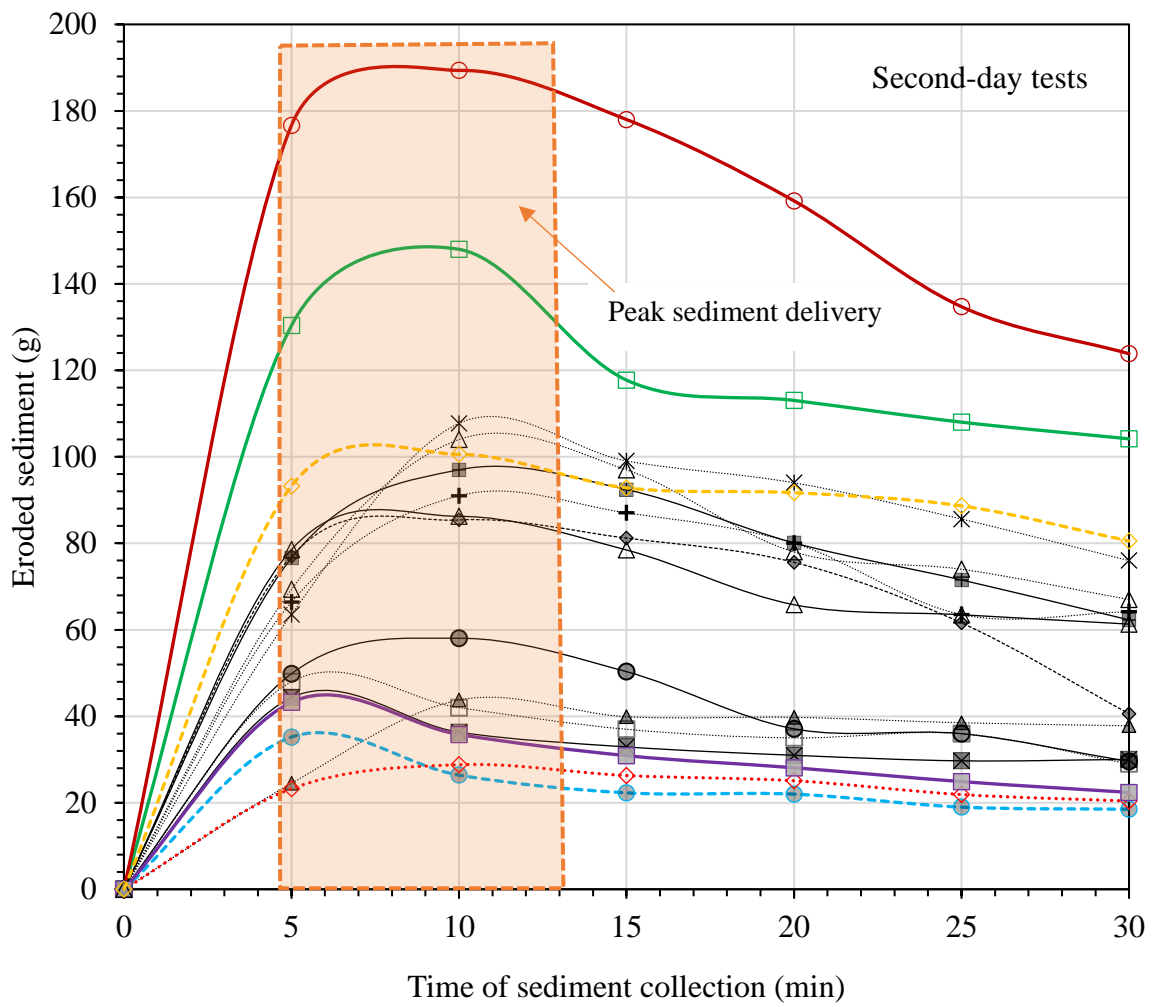
Figure 2. Flour method calibration curve (Laws and Parsons, 1943)

Appendix 2



- |   |   |
|---|---|
| —△— GS + 15% ECC; I = 30 mm/hr; S = 0%; Ls  | —◇— GS + 15% ECC; I = 30 mm/hr; S = 6%; Ls  |
| —○— GS + 15% ECC; I = 51 mm/hr; S = 0%; Ls  | —□— GS + 15% ECC; I = 51 mm/hr; S = 6%; Ls  |
| —+— GS + 15% ECC; I = 68 mm/hr; S = 0%; Ls  | —○— GS + 15% ECC; I = 68 mm/hr; S = 6%; Ls  |
| —●— GS + 15% ECC; I = 30 mm/hr; S = 0%; Ss  | —×— GS + 15% ECC; I = 30 mm/hr; S = 6%; Ss  |
| —□— GS + 15% ECC; I = 51 mm/hr; S = 0%; Ss  | —*— GS + 15% ECC; I = 51 mm/hr; S = 6%; Ss  |
| —■— GS + 15% ECC; I = 68 mm/hr; S = 0%; Ss  | —△— GS + 15% ECC; I = 68 mm/hr; S = 6%; Ss  |
| —◇— VGS + 15% ECC; I = 68 mm/hr; S = 0%; Ss | —■— VGS + 15% ECC; I = 68 mm/hr; S = 6%; Ss |
| —△— VGS + 15% ECC; I = 68 mm/hr; S = 0%; Ls | —◇— VGS + 15% ECC; I = 68 mm/hr; S = 6%; Ls |

Figure 1. Sediment from small- and large-scale first-day experiments for GS + 15% ECC and VGS + 15% ECC



- |   |   |
|---|---|
| —▲— GS + 15% ECC; I = 30 mm/hr; S = 0%; Ls  | —◆— GS + 15% ECC; I = 30 mm/hr; S = 6%; Ls  |
| —●— GS + 15% ECC; I = 51 mm/hr; S = 0%; Ls  | —□— GS + 15% ECC; I = 51 mm/hr; S = 6%; Ls  |
| —+— GS + 15% ECC; I = 68 mm/hr; S = 0%; Ls  | —○— GS + 15% ECC; I = 68 mm/hr; S = 6%; Ls  |
| —●— GS + 15% ECC; I = 30 mm/hr; S = 0%; Ss  | —■— GS + 15% ECC; I = 30 mm/hr; S = 6%; Ss  |
| —□— GS + 15% ECC; I = 51 mm/hr; S = 0%; Ss  | —*— GS + 15% ECC; I = 51 mm/hr; S = 6%; Ss  |
| —■— GS + 15% ECC; I = 68 mm/hr; S = 0%; Ss  | —△— GS + 15% ECC; I = 68 mm/hr; S = 6%; Ss  |
| —◇— VGS + 15% ECC; I = 68 mm/hr; S = 0%; Ss | —■— VGS + 15% ECC; I = 68 mm/hr; S = 6%; Ss |
| —△— VGS + 15% ECC; I = 68 mm/hr; S = 0%; Ls | —◇— VGS + 15% ECC; I = 68 mm/hr; S = 6%; Ls |

Figure 2. Sediment from small- and large-scale first-day experiments for GS + 15% ECC and VGS + 15% ECC

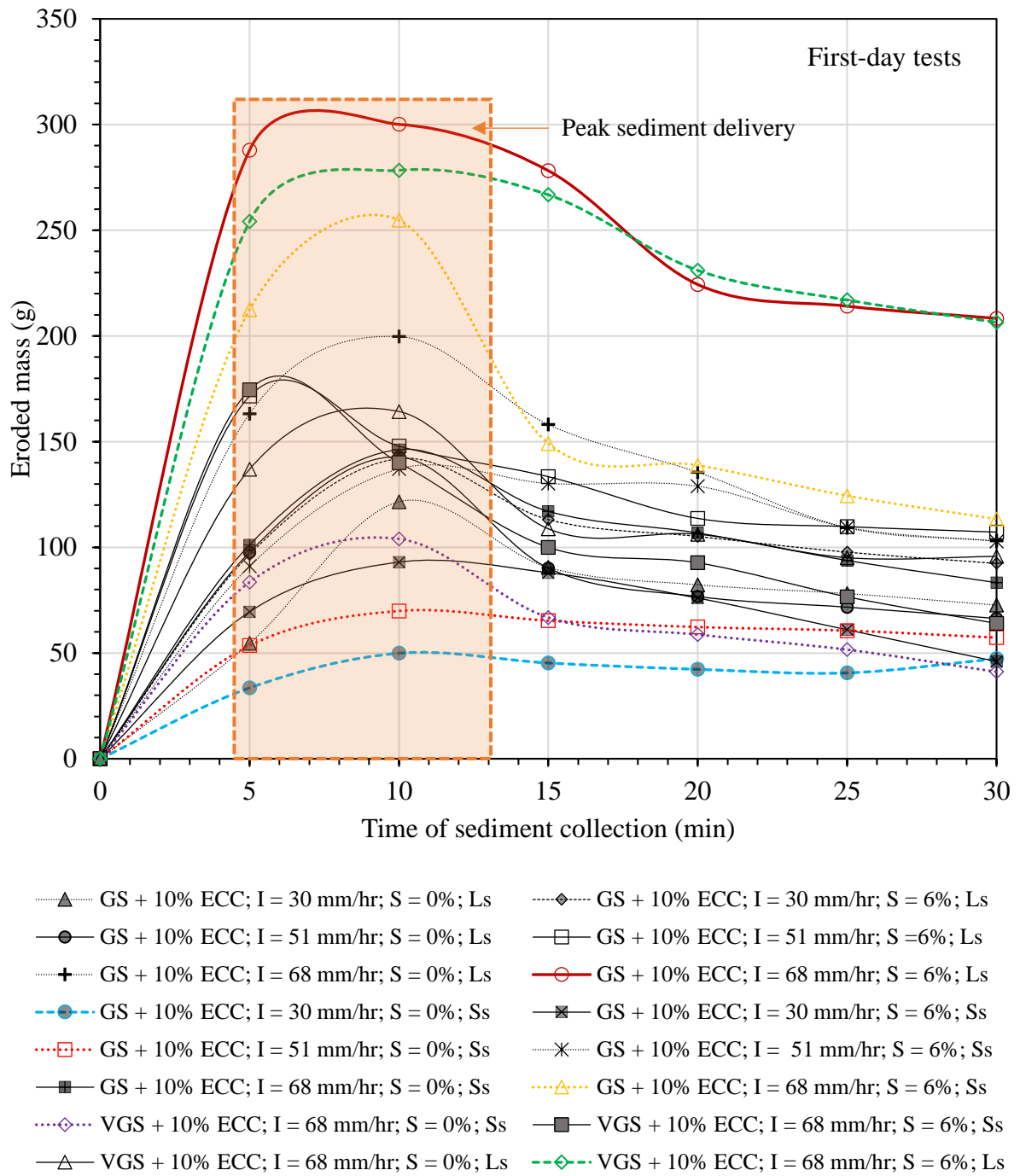
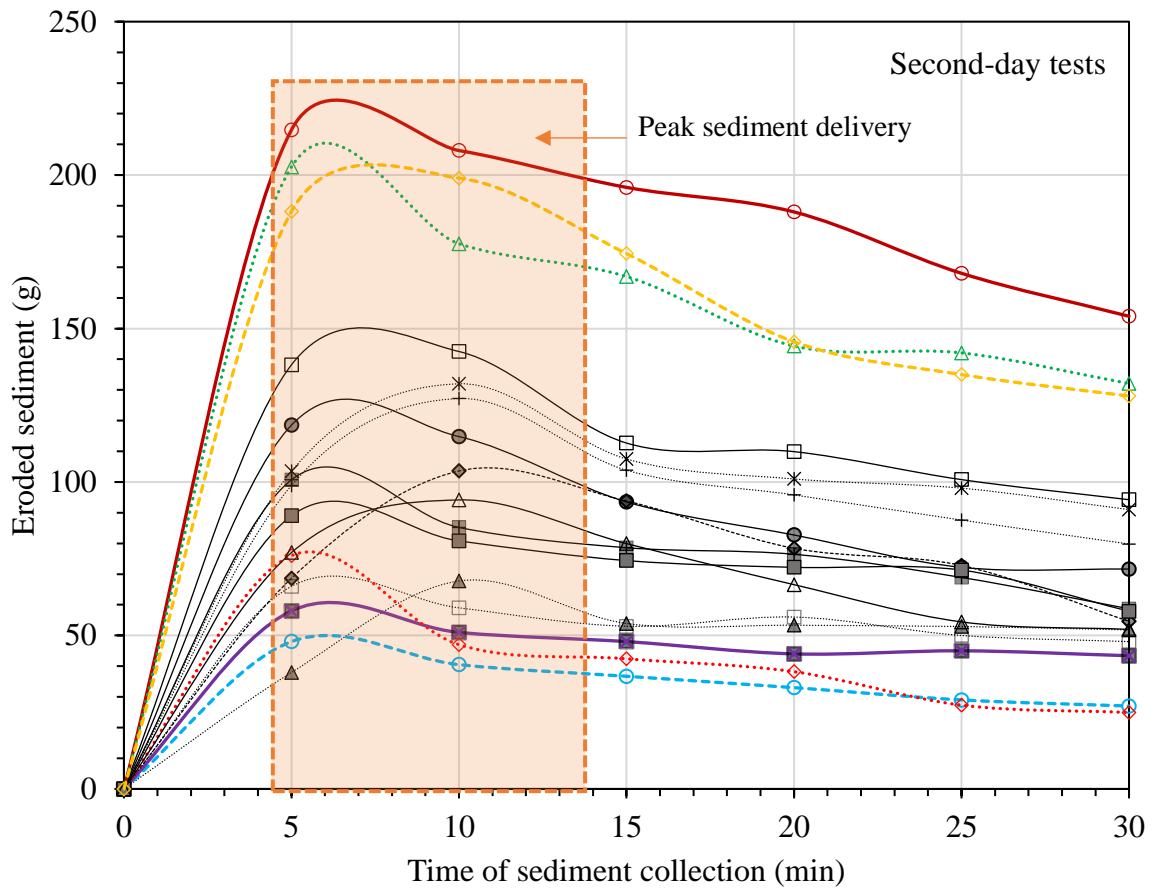
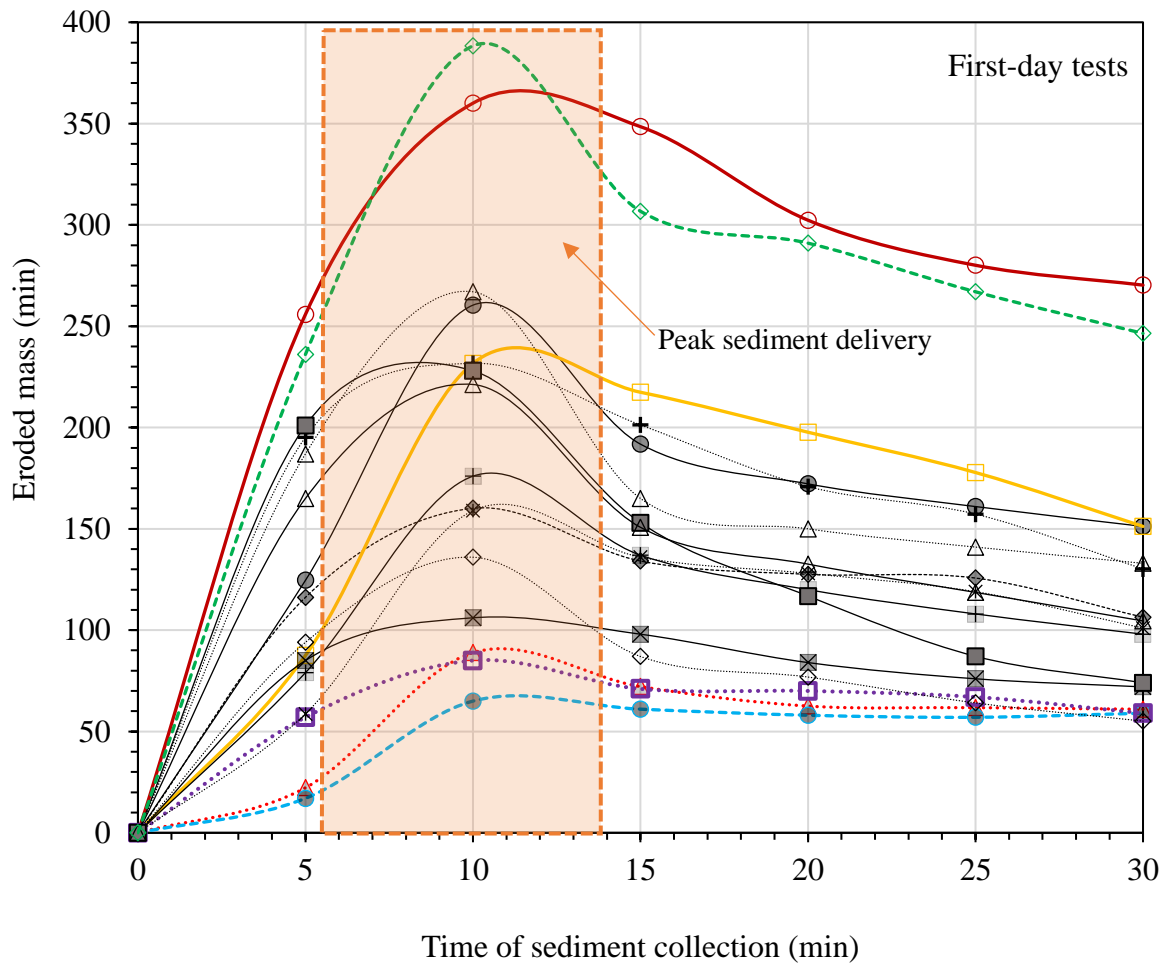


Figure 3. Sediment from small- and large-scale first-day experiments for GS + 10% ECC and VGS + 10% ECC



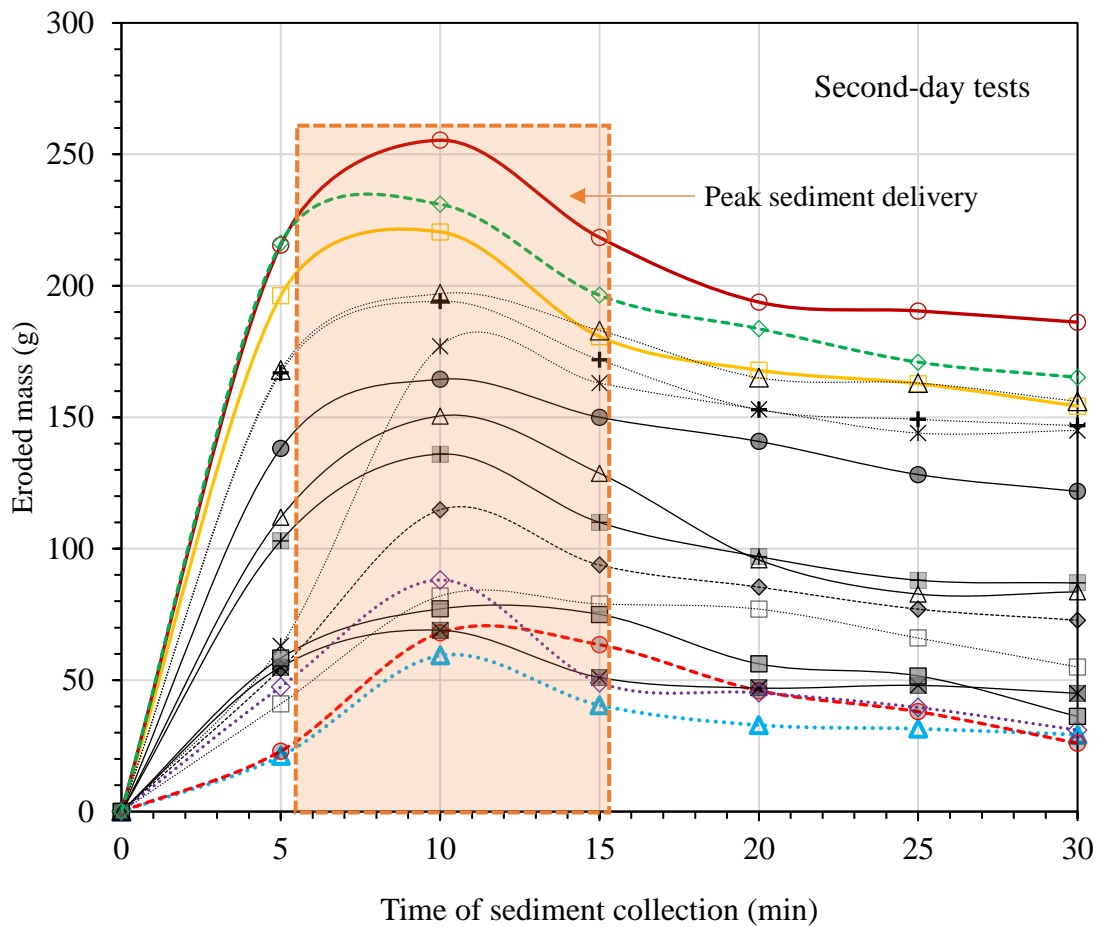
- |   |   |
|---|---|
| —▲— GS + 10% ECC; I = 30 mm/hr; S = 0%; Ls  | —◆— GS + 10% ECC; I = 30 mm/hr; S = 6%; Ls  |
| —●— GS + 10% ECC; I = 51 mm/hr; S = 0%; Ls  | —□— GS + 10% ECC; I = 51 mm/hr; S = 6%; Ls  |
| —+— GS + 10% ECC; I = 68 mm/hr; S = 0%; Ls  | —○— GS + 10% ECC; I = 68 mm/hr; S = 6%; Ls  |
| —○— GS + 10% ECC; I = 30 mm/hr; S = 0%; Ss  | —■— GS + 10% ECC; I = 30 mm/hr; S = 6%; Ss  |
| —□— GS + 10% ECC; I = 51 mm/hr; S = 0%; Ss  | —*— GS + 10% ECC; I = 51 mm/hr; S = 6%; Ss  |
| —■— GS + 10% ECC; I = 68 mm/hr; S = 0%; Ss  | —△— GS + 10% ECC; I = 68 mm/hr; S = 6%; Ss  |
| —◇— VGS + 10% ECC; I = 68 mm/hr; S = 0%; Ss | —■— VGS + 10% ECC; I = 68 mm/hr; S = 6%; Ss |
| —△— VGS + 10% ECC; I = 68 mm/hr; S = 0%; Ls | —◇— VGS + 10% ECC; I = 68 mm/hr; S = 6%; Ls |

Figure 4. Sediment from small- and large-scale second-day experiments for GS + 10% ECC and VGS + 10% ECC



- |  |  |
|--|--|
| .....▲..... GS + 5% ECC; I = 30 mm/hr; S = 0%; Ls  | .....◇..... GS + 5% ECC; I = 30 mm/hr; S = 6%; Ls  |
| .....●..... GS + 5% ECC; I = 51 mm/hr; S = 0%; Ls  | .....□..... GS + 5% ECC; I = 51 mm/hr; S = 6%; Ls  |
| .....+..... GS + 5% ECC; I = 68 mm/hr; S = 0%; Ls  | .....○..... GS + 5% ECC; I = 68 mm/hr; S = 6%; Ls  |
| .....●..... GS + 5% ECC; I = 30 mm/hr; S = 0%; Ss  | .....×..... GS + 5% ECC; I = 30 mm/hr; S = 6%; Ss  |
| .....□..... GS + 5% ECC; I = 51 mm/hr; S = 0%; Ss  | .....*..... GS + 5% ECC; I = 51 mm/hr; S = 6%; Ss  |
| .....+..... GS + 5% ECC; I = 68 mm/hr; S = 0%; Ss  | .....△..... GS + 5% ECC; I = 68 mm/hr; S = 6%; Ss  |
| .....◇..... VGS + 5% ECC; I = 68 mm/hr; S = 0%; Ss | .....■..... VGS + 5% ECC; I = 68 mm/hr; S = 6%; Ss |
| .....△..... VGS + 5% ECC; I = 68 mm/hr; S = 0%; Ls | .....◇..... VGS + 5% ECC; I = 68 mm/hr; S = 6%; Ls |

Figure 5. Sediment from small- and large-scale first-day experiments for GS + 5% ECC and VGS + 5% ECC



- ⋯ ▲ GS + 5% ECC; I = 30 mm/hr; S = 0%; Ls
 ⋯ ◆ GS + 5% ECC; I = 30 mm/hr; S = 6%; Ls
- ● GS + 5% ECC; I = 51 mm/hr; S = 0%; Ls
 — □ GS + 5% ECC; I = 51 mm/hr; S = 6%; Ls
- ⋯ + GS + 5% ECC; I = 68 mm/hr; S = 0%; Ls
 — ○ GS + 5% ECC; I = 68 mm/hr; S = 6%; Ls
- - ⊖ GS + 5% ECC; I = 30 mm/hr; S = 0%; Ss
 — ⊠ GS + 5% ECC; I = 30 mm/hr; S = 6%; Ss
- ⋯ □ GS + 5% ECC; I = 51 mm/hr; S = 0%; Ss
 ⋯ \* GS + 5% ECC; I = 51 mm/hr; S = 6%; Ss
- ■ GS + 5% ECC; I = 68 mm/hr; S = 0%; Ss
 ⋯ △ GS + 5% ECC; I = 68 mm/hr; S = 6%; Ss
- ⋯ ◇ VGS + 5% ECC; I = 68 mm/hr; S = 0%; Ss
 — ■ VGS + 5% ECC; I = 68 mm/hr; S = 6%; Ss
- △ VGS + 5% ECC; I = 68 mm/hr; S = 0%; Ls
 - - ◇ VGS + 5% ECC; I = 68 mm/hr; S = 6%; Ls

Figure 6. Sediment from small- and large-scale second-day experiments for GS + 5% ECC and VGS + 5% ECC

### Appendix 3. Laboratory and field erosion key considerations

Laboratory and field experiments have used different settings and parameters depending on the objectives of the studies. Knapen et al. (2007) summarised the main parameters for field plots and laboratory experiments in which concentrated flow erosion was measured. These are shown in Tables 2.13 and 2.14 for field and laboratory studies respectively. As indicated by the column headings, the parameters were essentially the following: Soils (number of soil types tested), ST (number of soil treatment types), Slope (slope of soil surface),  $Q_{inflow}$  (simulated concentrated flow discharge),  $I_{rainfall}$  (simulated rainfall intensities),  $\tau$  (range of applied flow shear stresses), Flow (origin of flow. R: Rainfall simulation, I: Inflow), Rill plot dimensions (length  $\times$  width), flume dimensions (length  $\times$  width  $\times$  depth), flume sample dimensions (length  $\times$  width  $\times$  depth), Mc (moisture condition and treatment of the soil prior to testing), Surface condition (S: Smoothened, I: Irregular). The n.a. was used for not available or not applicable.

Table (a). Summary of field erodibility tests (Knapen et al., 2007)

Country	Soils (#)	ST (#)	Slope (%)	$Q_{inflow}$ (l/min)	$I_{rainfall}$ (mm/h)	$\tau$ (Pa)	Flow	Rill plot dim. (m $\times$ m)	Mc	Surface condition	Source
Iran	1	3	n.a.	132–1693	/	2.2–13.2	<i>I</i>	15 $\times$ 0.3	actual natural conditions	<i>I</i> , varying vegetation cover	Adelpour et al. (2004)
Brazil	1	1	n.a.	n.a.	n.a.	n.a.	<i>I + R</i>	9 $\times$ 0.5	actual natural conditions	<i>I</i> , residue removed and tilled	Braida and Cassol (1996)
Brazil	1	1	6.7	0–50	74	n.a.	<i>I + R</i>	n.a.	prewetted with rainfall sim.	n.a.	Cantalice et al. (2005)
USA	2	3	3–15	96–768	/	4.0–37.3	<i>I</i>	10 $\times$ 0.75	actual natural conditions	<i>I</i> , residue removed and tilled	Franti et al. (1985,1999)
Brazil	1	1	n.a.	0	60	n.a.	<i>I + R</i>	9 $\times$ 0.5	actual natural conditions	<i>I</i> , residue removed and tilled	Giasson and Cassol (1996)
USA	30	1	4–13	7–35	62	n.a.	<i>I + R</i>	9 $\times$ 0.46	actual natural conditions	<i>I</i> , residue removed and tilled	Gilley et al. (1993)
USA	4	1	0.5–3	n.a.	/	1–36	<i>I</i>	30.5 $\times$ 0.91	actual natural conditions	<i>I</i> , no cover	Hanson (1989,1990a,b)
USA	1	1	1–3	4–17.10 <sup>4</sup>	/	12–55	<i>I</i>	29 $\times$ 1.8	actual natural conditions	<i>I</i> , no cover	Hanson and Cook (1999)
USA	2	9	5–11	n.a.	/	n.a.	<i>I</i>	10.7 $\times$ 3	actual natural conditions	<i>I</i> , varying canopy cover	Hussein and Laflen (1982)
USA	2	6	4	11–189	64	0.7–14	<i>I + R</i>	4 $\times$ 0.2	prewetted with rainfall sim.	<i>I</i> , varying tillage practices	King et al. (1995)
USA	2	2	3–15	n.a.	/	n.a.	<i>I + R</i>	n.a.	actual natural conditions	n.a.	Laflen (1987)
USA	56	1	2–13	0.1–0.6	63	0–22	<i>I + R, R, I</i>	9–11 $\times$ 0.5–3	actual natural conditions	<i>I</i> , residue removed and tilled	Laflen et al. (1991); Elliot et al. (1989)
USA	1	1	3–6	8–38	/	2–10	<i>I</i>	5.5 $\times$ 2	sprinkling of the soil	<i>I</i> , residue removed and tilled	Mamo and Bubbenzer (2001b)
Canada	3	1	12–14	/	25–30	n.a.	<i>R</i>	10 $\times$ 0.8	n.a.	<i>I</i> , vegetation free, seedbed conditions	Merz and Bryan (1993)
USA	1	1	4–6	8–38	51	1.3–6.1	<i>I, I + R</i>	68.6 $\times$ 6.1	actual natural conditions	<i>I</i> , tilled and all residue buried	Morrison et al. (1994)
USA	2	3	3–5	8–53	64	0–6	<i>I + R</i>	6.1 $\times$ 0.76	actual natural conditions	<i>I</i> , residue removed and tilled	Norton and Brown (1992)
USA	1	4	27	16–23	/	24–192	<i>I</i>	6 $\times$ 0.3	actual natural conditions	<i>I</i> , vegetation clipped to various heights	Prosser et al. (1995)
Australia	1	1	1–12.7	1.7–8	/	n.a.	<i>I</i>	20 $\times$ 1	actual natural conditions	<i>I</i> , vegetation clipped to various heights	Prosser (1996)
Brazil	1	4	10	12–120	65	2.5–19	<i>I + R</i>	6 $\times$ 0.2	prewetted with rainfall sim.	n.a.	Reichert et al. (2001)
USA	1	5	2–31	8–60	60	2–7	<i>I + R</i>	4.6 $\times$ 0.3	prewetted with rainfall sim.	<i>I</i> , residue removed and plants clipped	West et al. (1992)

Table (b). Summary of laboratory erodibility tests (Knapen et al., 2007)

Country	Soils (#)	Slope (%)	$Q_{inflow}$ (l/min)	$I_{rainfall}$ (mm/h)	$\tau$ (Pa)	Flow	Flume dim. (m×m×m)	Sample dim. (m) or (m × m)	Mc	Soil sample type	SS	Source
Italy	6	10–40	2.4–18	/	1–12	<i>I</i>	1.5 × 0.2	0.025–0.1 × 0.14	saturated or sprinkled	<i>R</i> (sieved at 2 mm)	<i>I</i>	Ciampallini and Torri (1998)
Australia	1	2–7	2.5–40	/	n.a.	<i>I</i>	1.8 × 0.6 × 0.2	1.8 × 0.6	saturated without subsequent drain.	<i>R</i> (sieved at 10 mm)	<i>S</i>	Crouch and Novruzi (1989)
Mexico	1	0	n.a.	/	1.1–38.2	<i>I</i>	4.9 × 0.3 × 2.5	0.102	certain tension level after saturation	<i>R</i> (sieved at 2 mm)	<i>S</i>	Ghebreyessus et al. (1994)
Belgium	2	5–21	3.3–60	/	1–24	<i>I</i>	4 × 0.4 × 0.45	4.5 × 0.4	air-dried	<i>R</i> (sieved at 20 mm)	<i>I</i>	Giménez and Govers (2002)
Belgium	2	9–21	6.7–60	/	1–16	<i>I</i>	2 × 0.10 × 0.09	0.39 × 0.098	saturated and drained to field cap.	<i>R</i> (sieved at 20 mm)	<i>S</i>	Giménez and Govers (2002)
Belgium	2	1.5–7	0.7–10.4	/	0.1–1.3	<i>I</i>	6 × 0.12	6 × 0.116	moist/saturated	<i>R</i>	<i>S</i>	Govers (1985)
Belgium	1	20–30	18–114	/	4.4–22.4	<i>I</i>	2 × 0.10 × 0.09	0.388 × 0.096	saturated and drained for 24 h	<i>U</i>	<i>I</i>	Gyssels et al., 2006
Canada	5	n.a.	n.a.	/	n.a.	<i>I</i>	9.1 × 0.15	0.15 × 0.6	saturated	<i>R</i>	n.a.	Kamphuis and Hall (1983)
USA	5	0.2	n.a.	/	n.a.	<i>I</i>	18.3 × 0.77 × 0.46	n.a.	saturated and drained for 18 h	<i>R</i> (sieved at 20 mm)	n.a.	Lafren and Beasley (1960)
USA	7	0.2	n.a.	/	n.a.	<i>I</i>	22 × 0.4 × 0.76	5.5 × 0.4	n.a.	n.a.	<i>I</i>	Lyle and Smerdon (1965)
USA	1	3–5	7.6–37.9	/	n.a.	<i>I</i>	4 × 0.2 × 0.05	0.1	saturated and drained for 12 h	<i>R</i> (sieved at 4.8 mm)	<i>I</i>	Mamo and Bubenzer (2001a)
Canada	1	14	/	34	n.a.	<i>R</i>	10 × 0.8 × 0.2	10 × 0.8	n.a.	<i>R</i>	<i>I</i>	Merz and Bryan (1993)
USA	8	n.a.	6.1–30.3	/	0–3.2	<i>P*</i>	1.84 × 0.10 × 0.19	0.02 × 0.09	after fire	<i>U</i>	<i>I</i>	Moody and Smith, (2005)
Belgium	1	10–35	5.6–11.5	/	1.6–5.7	<i>I</i>	2 × 0.10 × 0.09	0.05	actual natural conditions	<i>U</i>	<i>S</i>	Nachtergaele and Poesen (2002)
USA	1	n.a.	n.a.	/	0.1–1.3	<i>P*</i>	18.3 × 0.30 × 0.38	18.3 × 0.30	actual natural conditions	<i>R</i>	<i>S</i>	Partheniades (1965)
S-Africa	12	2–20	0.08–0.32	/	0.2–4.9	<i>I</i>	0.5 × 0.05 × 0.13	0.5 × 0.05	Saturated	<i>R</i> (sieved at 2 mm)	<i>S</i>	Rapp (1998)
Israel	3	2–20	0.08–0.32	/	0.2–4.9	<i>I</i>	0.5 × 0.05 × 0.13	0.5 × 0.05	Saturated	<i>R</i> (sieved at 2 mm)	<i>S</i>	Rapp (1998)
Belgium	1	2.6–14	n.a.	/	n.a.	<i>I</i>	2 × 0.4	2 × 0.4	n.a.	n.a.	<i>S</i>	Rauws (1987)
Belgium	1	3–33	n.a.	20	n.a.	<i>II + R</i>	2.5 × 0.6	2.5 × 0.6	n.a.	n.a.	<i>I</i>	Rauws and Govers (1988)
USA	1	2–20	0.04–0.2	/	0.4–4.8	<i>I</i>	0.5 × 0.05 × 0.12	0.5 × 0.046	air-dried	<i>R</i> (sieved at 2 mm)	<i>S</i>	Shainberg et al. (1994)
Israel	3	5	0.04–0.32	/	0.8–1.8	<i>I</i>	0.5 × 0.05 × 0.12	0.5 × 0.046	air-dried	<i>R</i> (sieved at 2 mm)	<i>S</i>	Shainberg et al. (1996)
Australia	16	5–30	0.1–1.8	100	n.a.	<i>I + R</i>	3 × 0.8 × 0.15	3 × 0.8	air-dried	<i>R</i> (sieved at 50 mm)	<i>S</i>	Sheridan et al. (2000a,b)
Canada	1	9	n.a.	30–35	n.a.	<i>R</i>	15 m long	n.a.	air-dried	<i>R</i> (sieved at 8 mm)	<i>S</i>	Slattery and Bryan (1992)
USA	11	0–1	n.a.	/	n.a.	<i>I</i>	18.3 × 0.77 × 0.46	5.5 × 0.77	n.a.	<i>R</i>	n.a.	Smerdon and Beasley, (1959)
USA	5	0.1–0.2	n.a.	0–127	n.a.	<i>I + R</i>	22 × 0.8	5.5 × 0.8	saturated and drained for 24 h	<i>R</i> (sieved at 5 mm)	<i>I</i>	Smerdon (1964)
Italy	4	1–31	n.a.	15–110	0–3.3	<i>I + R</i>	2 × 0.5 × 0.1	2 × 0.5	air-dried	<i>R</i> (sieved at 4 mm)	<i>S</i>	Torri et al. (1987)
USA	1	7	2–4	/	1.9–3.9	<i>I</i>	2.73 × 0.46 × 0.88	2.73 × 0.46	different tension levels	<i>R</i> (sieved at 6.4 mm)	<i>S</i>	Van Klavem and McCool (1998)
USA	5	1.5–5	3.8–15.1	/	0.5–2.5	<i>I</i>	6.4 × 0.15 × 0.05	1 × 0.15	saturated without subsequent drain.	<i>R</i> (sieved at 4 mm)	<i>S</i>	Zhu et al. (1995)
USA	5	0–5.5	n.a.	/	0.5–2.5	<i>I</i>	6.4 × 0.15 × 0.05	1 × 0.15	saturated	n.a.	n.a.	Zhu et al. (2001)

#### Appendix 4. List of Publications

##### Contribution to Conference Proceedings (book):

1. Ngezahayo E, Burrow MPN and Ghataora GS (2019a). Rainfall Induced Erosion of Soils Used in Earth Roads. In Tarantino, A & Ibraim, E (Eds), *7th Int. Symp. on Deformation Characteristics of Geomaterials*, ISBN 978-2-7598-9064-4, Vol. 92 (17006), EDP Sc.

##### Journal Papers:

2. Ngezahayo E, Burrow MPN and Ghataora GS (2019b). The Advances in Understanding Erodibility of Soils in Unpaved Roads. *Int. J. Civil Infrastructure*, 2(2019): 18-29.
3. Ngezahayo E, Ghataora G and Burrow M (2019c). Evaluation of the influence of geotechnical, environmental and road aspects on erodibility of rural roads. *Int. J. of Latest Engineering and Management Research (IJLEMR, ISSN: 2455-4847)*, 04 (11): 29-54.
4. Ngezahayo E, Burrow M and Ghataora G (2019d). Rural Roads –roles, challenges and solutions for Sub-Saharan Africa’s sustainable development. *Int. J. of Latest Engineering and Management Research (IJLEMR, ISSN: 2455-4847)*, 04 (10): 70-79.

##### Conference Papers:

5. Ngezahayo E, Burrow MPN and Ghataora GS (2019e). Rainfall Induced Erosion of Soils Used in Earth Roads. *Proc. 7<sup>th</sup> Int. Symposium on Deformation Characteristics of Geomaterials*, IS - Glasgow, UK, 26<sup>th</sup> – 28<sup>th</sup> June, E3S Web of Conferences 92: 17006, 2019, <https://doi.org/10.1051/e3sconf/20199217006>.
6. Ngezahayo E, Ghataora GS and Burrow MPN (2019f). Factors Affecting Erosion in Unpaved Roads. *Proc. of the 4<sup>th</sup> World Congress on Civil, Structural and Environmental Engineering (CSEE'19)*, Rome, Italy, 7<sup>th</sup> – 9<sup>th</sup>, April 2019. Paper No. ICGRE 108, Doi: 10.11159/icgre19.108, [http://avestia.international-aset.com/CSEE2019\\_Proceedings](http://avestia.international-aset.com/CSEE2019_Proceedings).
7. Ngezahayo E, Ghataora G and Burrow M (2018). Rural Roads Place for Africa’s Sustainable Development. *Int. Conf. African Studies Ass. UK (ASAUK18)*, Birmingham, Sept. 11-13, [https://coms.events/ASAUK2018/data/abstracts/en/abstract\\_0451.html](https://coms.events/ASAUK2018/data/abstracts/en/abstract_0451.html).

##### Technical and Helpdesk Reports:

8. Sasidharan M, Usman K, Ngezahayo E and Burrow MPN (2019). Evidence on impact evaluation of transport networks using network theory. K4D Helpdesk Report. Brighton, UK: Institute of Development Studies.

##### Submitted for Publication:

9. Ngezahayo E, Ghataora G and Burrow M (2020). Using ImageJ Software for Investigating Surface Particles Behaviours during Rainfall Erosion on Unsurfaced Roads. *Rwanda Journal of Science, Engineering, Technology, and Environment*. [Under Review].